1999

Investigation and analysis of lubricant effects on the performance of an HFC-134a refrigeration system

Predrag Popovic
Iowa State University

INFORMATION TO USERS

This manuscript has been reproduced from the microfilm master. UMI films the text directly from the original or copy submitted. Thus, some thesis and dissertation copies are in typewriter face, while others may be from any type of computer printer.

The quality of this reproduction is dependent upon the quality of the copy submitted. Broken or indistinct print, colored or poor quality illustrations and photographs, print bleedthrough, substandard margins, and improper alignment can adversely affect reproduction.

In the unlikely event that the author did not send UMI a complete manuscript and there are missing pages, these will be noted. Also, if unauthorized copyright material had to be removed, a note will indicate the deletion.

Oversize materials (e.g., maps, drawings, charts) are reproduced by sectioning the original, beginning at the upper left-hand corner and continuing from left to right in equal sections with small overlaps.

Photographs included in the original manuscript have been reproduced xerographically in this copy. Higher quality 6" x 9" black and white photographic prints are available for any photographs or illustrations appearing in this copy for an additional charge. Contact UMI directly to order.

Bell & Howell Information and Learning
300 North Zeeb Road, Ann Arbor, MI 48106-1346 USA

UMI®
800-521-0600

Investigation and analysis of lubricant effects on the performance of an HFC-134a refrigeration system

by

Predrag Popovic

A dissertation submitted to the graduate faculty

in partial fulfillment of the requirements for the degree of

DOCTOR OF PHILOSOPHY

Major: Mechanical Engineering

Major Professor: Michael B. Pate

Iowa State University

Ames, Iowa

1999

Graduate College

Iowa State University

This is to certify that the Doctoral dissertation of

Predrag Popovic

has met the dissertation requirements of Iowa State University

Signature was redacted for privacy.

Major Professor

Signature was redacted for privacy.

For the Major Program

Signature was redacted for privacy.

For the Graduate College

TABLE OF CONTENTS

LIST OF FIGURES

LIST OF TABLES

ACKNOWLEDGMENTS

This work was sponsored by the lubricant manufacturer, Henkel Corporation. Especially, I wish to thank Bruce Beimisch for his support and technical advice throughout the project. In addition, Mr. Nicholas Schnur was very cooperative and he greatly aided the completion of the project.

Tecumseh Products was very generous in providing especially designed equipment. Particularly, Mr. Ronald Shimon was very helpful and supportive of the project.

CHAPTER 1

INTRODUCTION

Ozone safe HFC refrigerants, such as HFC-134a, are accepted alternatives to a number of CFC and HCFC refrigerants, which have been systematically phased out in refrigeration applications. Since new refrigerants have shown poor miscibility with conventional mineral oils, namely an inability to mix well when in the liquid phase, new synthetic lubricants such as polyol esters (POEs) and polyalkylene glycols (PAGs) have been developed. The development of new lubricants is driven by a belief that refrigerant/lubricant miscibility extends refrigeration system (i.e., compressor) life, especially, since widely used CFC-12 and mineral oils were miscible with each other. However, there are some existing refrigeration applications in which operating refrigerants and lubricants have poor miscibility characteristics. In addition to the question of reliability, the question of what are the effects of new miscible lubricants on system efficiency compared to the immiscible mineral oils also needs addressing. The answer to this latter question is the focus of the study reported herein.

In refrigeration systems with reciprocating compressors, it is inevitable that a small amount of lubricant, usually less than one percent of the refrigerant mass, leaves the compressor with refrigerant vapor. Even such a small amount of lubricant has to be recirculated, since the lubricant could start accumulating in some part of the system, eventually leading to the loss of lubricant from the compressor which could result in damage to compressor parts. If the refrigerant and lubricant are miscible, the lubricant trapped in the system could be diluted with a low viscosity refrigerant, which, in turn, reduces lubricant viscosity and enhances the lubricant return to the compressor. However, refrigeration systems have achieved oil return and operated reliably in the past with partial miscibility conditions (e.g. HCFC-22 and mineral oil) or total immiscibility conditions (e.g. R-502 and mineral oil or ammonia and mineral oil), and thus, as a result the need of miscibility for a reliable compressor operation in the HFC-134a systems has been questioned.

Besides compressor reliability and, hence, system reliability, it is important to understand the effect of the lubricant on system performance. The effects on system performance due to a particular lubricant/refrigerant mixture could be the result of changes in evaporator performance, compressor performance, or the performance of other components (e.g. piping, valves, etc.).

It should be emphasized that the refrigerant and lubricant in a refrigeration system constitute a mixture with characteristics different from those of pure substances. Hence, it is essential to recognize that system performance must be analyzed from the point of view of real mixtures rather than the common approach of analyzing pure refrigerants with negligible amounts of lubricant. For example, even a small amount of circulating lubricant in the refrigeration system affects the refrigerant's primary function of effective evaporation heat transfer, while the addition of the refrigerant in the compressor crankcase affects the lubricant's primary function of lubrication.

1.1 Miscibility

As described in the ASHRAE Refrigeration Handbook (1998), two major issues related to miscibility are the lubricant return from the evaporator and flooded startups in the compressor. Since some amount of lubricant always leaves the compressor with the discharged refrigerant vapor, it is considered important to eventually circulate the lubricant back to the compressor. Thus, the existence of miscibility in the evaporator reduces the lubricant viscosity, and, therefore, promotes lubricant return. If the lubricant is not returned to the compressor crankcase, it remains in the evaporator and leads to oil-logging.

The flooded startup of the compressor refers to systems in which liquid refrigerant occupies the crankcase when the compressor or system is shut down. If a refrigerant/lubricant mixture is not miscible, then lubricant starvation of portions of the compressor crankcase during compressor startup may occur, thus increasing compressor wear. More details about this phenomenon will be presented in the next section.

According to the ASHRAE Refrigeration Handbook (1998), the miscibility of the refrigerant/lubricant mixture is perceived as the most important criterion for reliable compressor operation. However, as mentioned earlier, refrigeration systems have operated reliably with partial miscibility conditions (e.g. HCFC-22 and mineral oil) or total immiscibility conditions (e.g. R-502 and mineral oil or ammonia and mineral oil). In addition, there are several studies, such as Reyes-Gavilan et al. (1996), that indicate that a miscible refrigerant/lubricant mixture does not necessarily improve compressor reliability, and, thus, the miscibility criterion might be, in some cases, conservative.

1.2 Viscosity

The other prominent characteristic of a lubricant is its viscosity in that the lubricant needs to have sufficient viscosity to provide proper lubrication of compressor moving parts. Since refrigerant viscosity is only a fraction of a lubricant's viscosity, a mixture of lubricant and refrigerant has a substantially different viscosity than that of a pure lubricant. The dilution of a lubricant by a refrigerant, as mentioned earlier, is associated with improved lubricant return to the compressor.

In the compressor environment where a refrigerant exists in the vapor phase, some amount of a refrigerant is dissolved in the lubricant, diluting the pure lubricant, and, therefore, interfering with the lubricant's primary function. The characteristics of such a mixture (i.e., the amount of dissolved refrigerant) depend on the temperature, pressure, and other properties of the refrigerant/lubricant pair, and they are collectively known as the mutual solubility characteristics. These solubility characteristics can affect the viscosity of refrigerant /lubricant mixture, and also, the system performance and reliability.

Any lubricant mixed with a refrigerant alters the refrigerant-vapor liquid equilibrium and heat transfer characteristics. The effects of lubricants on the evaporation heat transfer rate are especially important, as they are directly proportional to the evaporator performance, and thus, the refrigerant's primary function. The fact that the evaporation heat transfer rate

could be significantly altered by lubricant properties, especially the viscosity and quantity of lubricant present, is important to the system performance study presented herein.

1.3 Reliability and Efficiency

The past research dealing with lubricant effects on refrigeration systems has primarily focused on system reliability. The approaches used to assess reliability have been

- testing the capability of a lubricant/refrigerant mixture to provide adequate lubrication,
- measuring the wear on compressor moving parts,
- checking the material compatibility of system components with refrigerant/lubricant mixtures, and
- investigating the chemical stability of refrigerant/lubricant mixtures.

Even though past studies investigated lubricant effects in HFC-134a refrigeration systems from the standpoint of compressor and system reliability, it is increasingly important today to improve the operating efficiency in order to contribute to demanding energy conservation regulations. Hence, it is essential to include the investigation of system performance when evaluating the use of lubricants. The effects of lubricants on system performance should be an integral part of the lubricant selection process. Specifically, if refrigerant/lubricant pairs have satisfied reliability tests, then the pair that shows the best system efficiency should be chosen.

Since the past studies reported in the literature have been concerned with compressor reliability, it is unknown whether the performances of HFC-134a systems are higher with an immiscible lubricant (i.e. mineral oil) or a miscible lubricant (i.e. POE). Also, the effects of lubricant viscosity values and partial miscibility characteristics are also of importance. Hence, the focus of the study reported herein is on the refrigeration system performance (i.e. efficiency) rather than on reliability

1.4 Objective

The objective of the work presented herein is to investigate the effects of lubricants on the performance of a vapor compression refrigeration system. This research focuses on system efficiency and performance rather than system reliability. The effect on system performance of lubricant characteristics such as the refrigerant miscibility and viscosity along with refrigerant charge and refrigerant heat transfer surface are emphasized in this study.

Refrigerant HFC-134a was selected as being representative of a new family of HFC refrigerants, and also, because it is fast becoming a widely used refrigerant for which lubricants are commercially available. The Henkel Corporation supplied all of the lubricants tested. An existing air conditioning test facility, which is approximately the size of a residential unit, was used to evaluate the refrigerant and lubricant mixtures used in the study. Tecumseh Products, a compressor manufacturer, supplied a specially designed HFC-134a reciprocating compressor.

Miscibility effects were investigated by testing and comparing two different lubricants, a miscible POE and an immiscible mineral oil. Since both lubricants have similar viscosity characteristics, their comparison put the focus of the analysis on the miscibility effects.

Since the effect on system performance of a lubricant may vary with the type of heat transfer surface in the evaporator coil, two coils with different heat transfer surfaces on the interior walls of the coil tubing, namely a conventional smooth type and an enhanced microfin type, were evaluated.

Partial miscibility effects on system performance were also evaluated by using a specially designed POE. Specifically, a partial miscibility condition for a refrigerant/lubricant mixture was achieved in the evaporator which then provided the focus of investigation.

The effect of lubricant viscosity on system performance was also measured and evaluated for miscible lubricants of different viscosity grades. While miscibility effects were analyzed by comparing the system performance of immiscible and miscible lubricants of

similar viscosity, the effects of viscosity were investigated by comparing the system performance of two miscible POEs with different viscosities.

In order to accomplish the above stated goals, it was essential to investigate the effects of refrigerant charge on system performance, so that these effects can be eliminated from biasing the investigation of lubricant effects. Finally, the lubricant test results were used to estimate lubricant effects on evaporation heat transfer.

1.5 Scope

The scope of the project was grouped into three major tasks, namely test facility development, data collection, and data analysis. Each task is not necessarily independent, and in many instances actual work in each category was overlapping. For example, it was possible to concurrently perform the data analysis with the data collection.

1.5.1 Test Facility Development

- Preliminary tests were run on an existing facility to determine the scope of changes needed in order to achieve the project objectives. Extensive testing was conducted to determine the capability, the operation, and the performance of the existing refrigeration system, instrumentation, and data acquisition system.
- The test facility was modified as follow
    - A new commercially available DX coil with a smooth-tube type surface was installed in order to use a coil that is widely used in refrigeration applications. Later, the DX coil was replaced with an enhanced surface microfin-tube type coil because of the increasing usage of this tube type.

- A specially designed HFC-134a, reciprocating compressor was added to the installation. The compressor has special plugs installed for easy lubricant changing, which was required in the project.
- A more accurate refrigerant flow meter, as well as a number of new thermocouples and pressure transducers, were added to the existing instrumentation. It was decided that the existing data acquisition system was appropriate for the project; however, the controlling program had to be modified for work with the new instruments. All instruments were calibrated prior to the first set of tests.

1.5.2 Data Collection

Each lubricant was tested at nine different points, which corresponded to a combination of three evaporator air and condenser water temperatures. The set of the standard test conditions was designed to cover a wide variety of operating conditions found in refrigeration applications. The number of data points that could be taken was limited by the time required to perform each test

Measurements were performed and data was collected in the following categories

- Smooth-tube Coil
  - Charge effects on system performance with miscible lubricant
  - Miscible POE and immiscible mineral oil lubricants with similar viscosity
- Microfin-tube Coil
  - Charge effects on system performance with miscible lubricant
  - Miscible POE and immiscible mineral oil with similar viscosity. These two lubricants are identical to those tested in the smooth-tube coil, thus allowing a comparison of two coil types.
  - Lower viscosity miscible POE lubricant
  - Partially miscible POE lubricant

1.5.3. Data Analysis

The analysis of the collected data focused on determining and comparing the refrigerant system performance for the above combinations of lubricant, refrigerant, and coil types. In order to accomplish this goal, the refrigeration system was run with the same set of operating parameters with the only change being the type of lubricant present in the system. The uncertainty in parameters was directly derived from the uncertainty in the measured parameters by utilizing a propagation-of-error approach.

Since the results suggested that lubricants have a major impact on evaporator performance, or more specifically evaporator heat transfer, a detailed model was developed to compare evaporation heat transfer for the different lubricant types.

CHAPTER 2

LUBRICANTS IN VAPOR COMPRESSION SYSTEMS

The primary function of lubricants in vapor compression refrigeration systems, as well as in other types of machinery, is to lubricate moving parts. In most types of compressors, the lubricant comes into direct contact with the operating refrigerant, and thus, the lubricant and the refrigerant form a mixture with properties different than those of pure substances. In the compressor, where most of the lubricant is stored, some amount of refrigerant dissolves in the lubricant altering the properties of lubricant, and thus, it can be thought of as the refrigerant affecting the lubricant's primary function. On the other hand, small amounts of the lubricant circulating through the system affects properties and functions of the refrigerant, such as heat transfer and refrigerant vapor-liquid equilibrium. Therefore, the lubricant which circulates through the system can be regarded as affecting the refrigerant's primary function.

Regardless of which component of the refrigeration system is analyzed, the refrigerant and lubricant constitute a complex mixture, with the lubricant being in the liquid phase and the refrigerant existing in the vapor, liquid, or vapor-liquid mixture phase. The properties of the refrigerant/lubricant mixture affect the performance of the entire system and, therefore, the presence of a lubricant in the refrigerant or the refrigerant in the lubricant must not be neglected.

The goal of this chapter is to characterize both lubricants and refrigerant/lubricant mixtures. The appearance of new refrigerants, such as HFC-134a, has forced industry to consider the use of new synthetic lubricants as opposed to the conventional mineral oils that have been widely used in the past. New refrigerant/lubricant mixtures have properties that are different from those of conventional refrigerant/lubricant mixtures, and hence, they have a different impact on the system performance, which has not been investigated to date.

This chapter contains a broad presentation of both lubricant and refrigerant/lubricant characteristics, specifically emphasizing HFC-134a and synthetic POE lubricants, which were utilized in this study.

2.1 Lubricant Chemical Composition

There are two basic types of lubricants, namely mineral oils obtained from natural products (petroleum) and synthetic lubricants, which are obtained from controlled processes. Mineral oils are a mixture of a large number of organic compounds, in some instances more than a hundred, while on the other hand, synthetic lubricants are mixtures of fewer compounds, 10 to 15. Much of the information presented in this section was adopted from the AHSRAE Refrigeration Handbook (1998).

2.1.1 Mineral Oil

Mineral oil is made up of organic compounds obtained by processing petroleum products. These oils are mixtures of structural components which are depicted below:

- Paraffins (N-Penthane and isopenthane) are straight and branched carbon chain saturated hydrocarbons. They exhibit sound chemical stability, but poor solubility with HCFC-22 refrigerant and also indicate poor boundary lubrication characteristics. The straight chain paraffins tend to precipitate as wax crystals when cooled close to the pour point, and also they form flocs in certain solutions.
- Naphthenes (cycloparaffins as cyclo penhtane) are also saturated hydrocarbons but are contrary to paraffins of cyclic or ring structures.
- Aromatics (benzene) are unsaturated cyclic hydrocarbons of one or more rings with alternate double bonds. The aromatics are reactive, have good solubility with polar refrigerants, exhibit good boundary lubrication, and have higher viscosity than saturates.

- Nonhydrocarbons are carbon structures that contain sulfur, nitrogen, or oxygen in addition to carbon and hydrogen. Small amounts of nonhydrocarbons are good for boundary lubrication; however, they are highly reactive. (ASHRAE, 1998)

Since oil has a complex structure, its composition is described by carbon type and molecular analysis. The carbon type gives percentage of the fundamental structure by mass, for example, $\%C_P$ the percentage of carbon atoms having paraffinic structure. Molecular analysis determines the amount of saturates, aromatics, and nonhydrocarbons.

Each mineral oil consists of fundamental structures which all have different characteristics. The nature of a mineral oil is determined by a dominated fundamental structure, as for example, naphthenic mineral oil refers to a mixture of oil fundamental structures with the largest portion of naphthens. In practice, properties of mineral oils can be controlled to a certain extent by combining different portions of fundamental structures (ASHRAE, 1998).

2.1.2 Synthetic lubricants

A large number of synthetic lubricants are used in the refrigeration industry. In general, they are two- to three-times more expensive than mineral oils; moreover, they are highly hygroscopic requiring special care in handling. The synthetic lubricants are divided in several distinct groups and additional information can be found in ASHRAE Refrigeration Handbook (1998)

- **Alkylbenzenes** can be branched or linear. They are synthesized by reacting an olefin or chlorinated paraffin with benzene in the presence of a catalyst, AlCl or HF. They have better high temperature and oxidation stability than comparable mineral oils. These lubricants are recommended to be used in HCFC-22 systems.
- **Polyalkylene glycols** (PAGs) are derived from propylene or ethylene oxide. Polymerization is initiated with alcohol, resulting in monol or water, resulting in diol. Three distinct groups of PAGs are used in refrigeration applications: polypropylene

glycol, polypropylen-polyethylene glycol, and polypropylene-polyethylene ether. The glycols are classified as mono-, di-, or tri-functional, which is an indication of the number of terminal hydroxil groups that are involved in manufacturing. PAGs are increasingly used with HFC-134a in automotive applications. Good lubricity, low-temperature fluidity, and compatibility with elastomers are good characteristics, while concerns arise in their hygroscopicity, immiscibility with mineral oils, and the requirement of additives for thermal and chemical stability. In addition, some of the PAGs are even miscible with ammonia. Short et al. (1996) reported that by incorporation of ethylene in PAGs, the miscibility with HFCs can be improved, but also water solubility may be increased. Reduction in both miscibility with HFCs and water solubility are attained by making the product ether. PAGs exhibit inverse solubility.

- **Polyalphaolefins** (PAOs) are produced from linear α-olefins. They are not miscible with HCFC-22 and HFC-134a refrigerants. PAOs are commonly used as immiscible oil in ammonia systems, due to the excellent low temperature characteristics.
- **Polyol esters or POEs** are formed from reactions between alcohol (pentaerythritol, or trimethylopropane, or neopenhyl glycol) and a carboxylic (fatty) acids of 5-15 carbon atoms (Short and Rajewski, 1996). The acids can be classified as linear, branched, or mixed. POEs are used in HFC-134a systems for all applications except automotive. There are possibilities for controlling properties of POEs by combining different alcohols and acids as well as by blending different lubricants. Also, it is a common practice to add special-task additives to enhance particular lubricant functions as detailed in the next section. POEs, which are based on lower molecular weight alcohols, such as neopentyl glycols, tend to be more miscible than those based on higher molecular weight alcohols. This fact is an important characteristic with regards to their use with HFC-134a refrigerant, which is highly insoluble with most lubricants. A POE utilizing linear acids becomes less miscible when manufactured in higher viscosity grades, due to the use of higher molecular weight acids. Short et al. (1996) also reports that the addition of branched acids help improve miscibility.

- **Other Synthetic Lubricants** are also in the developing phase. For example, Short et al. (1996) reports on developments of three other types of lubricants that are entering the market and are currently being experimentally evaluated:
    1. Carbonates are esters or diesters of carbonica acid, usually made through the transeterification of dimethyl carbonate.
    2. Complex esters utilize malonate-acrylate chemistry.
    3. Modified PAGs combine short chain acids with the standard type of PAG to form an ester.

2.2 Lubricant Functions

The essential function of a lubricant is to lubricate compressor moving parts. In addition, depending on compressor design, the lubricant can also perform other secondary functions, such as

- Sealing in order to maintain pressure or to keep out contaminants. Krause and Schroeder (1985) reported that a non-lubricated reciprocating compressor has a lower efficiency than a lubricated compressor.
- Reducing Noise
- Removing Heat
- Inhibiting corrosion
- Carrying debris

The lubrication of sliding or moving parts in a compressor is the essential oil function. Properly lubricated surfaces are supported on a thin lubricant film, which is known as hydrodynamic lubrication.

Hydrodynamic lubrication

Hydrodynamic lubrication is present in a normal mode of operation, characterized by the formation of a lubricant film between moving parts. In order to achieve and maintain surface separation, the lubricant must have a minimum dynamic viscosity.

Boundary lubrication

Boundary lubrication occurs at abnormal conditions, such as starting-up, stopping, and overloading due to inadequate amount of lubricants. In each of the three above cases, the mating surfaces are in contact when a lubricant film is not thick enough to separate surfaces. Lubricants for refrigeration systems have no additives for enhancement of boundary lubrication, as it is believed that these additives would react with refrigerants (Krause and Schroeder 1985). It is standard practice to investigate a lubricant for sufficient boundary lubrication by standardized tests, such as

- Four-ball extreme-pressure method
- Falex
- Timken
- Alpha LFW-1 machine

2.3 Lubricant Properties

The major lubricant characteristics are lubricity, stability, materials compatibility, mutual solubility with refrigerant, viscosity, and, finally, foamability. The lubricity or capability of a lubricant to provide adequate lubrication to compressor moving parts is the essential role of the lubricant in a compressor. This lubricant property is described in the previous section.

Once a lubricant with good lubricity, stability, material compatibility, and adequate viscosity is selected, the mutual solubility of the lubricant and refrigerant becomes the most prominent mixture characteristic, because it affects refrigeration system efficiency and reliability. Since the lubricant vapor pressure is negligible in comparison to the refrigerant vapor pressure, the lubricant in the refrigeration system exists only as liquid. In a compressor where the refrigerant is in the vapor phase and the bulk of the lubricant is stored, some amount of refrigerant gets dissolved in the lubricant, thus altering the properties of a pure lubricant, which in turn, affects lubricant functions. It is also important to note that any

lubricant that leaves the compressor and ends up in the condenser and evaporator blends with the refrigerant, thus affecting the properties of the pure refrigerant and altering the pure refrigerant heat transfer characteristics. The relationship between the refrigerant and lubricant which takes into account characteristics of their mixing is termed mutual solubility.

2.3.1 Stability and Material Compatibility

Lubricants must not decompose into undesirable products during the life of the refrigeration system in order to avoid the formation of any by-products which may induce an undesirable chemical reaction, thus leading to a reduction of the refrigeration system lifetime. An established test for compatibility is the sealed tube method in which steel, aluminum or copper strips are enclosed with a particular refrigerant/lubricant mixture. Visual and chemical changes are possible through the chemical reaction that takes place when a metal acts as a catalyst of refrigerant-lubricant reaction.

In general, the stability of POEs and PAGs deteriorates with the presence of moisture (Wu, and Thomas, 1997). The POEs undergo a hydrolysis process, which is opposite to the esterification. Short et al. (1996) reported that even a small amount of moisture may lead to the breakdown of some POEs, and it is recommended to limit the moisture level to 100 ppm and 250 ppm for POEs and PAGs, respectively. POEs, manufactured with a higher percentage of branched acids, are more stable in the presence of water than those with a high proportion of linear acids.

Wu, and Thomas (1997) reported that air as the contaminant usually has only a small effect on the stability of POEs. Contaminant metals, such as tin, must be avoided in refrigeration systems, since it is a catalyst for a chemical reaction between the refrigerant and lubricant.

Lubricants need to be compatible with components of the refrigeration system. The POEs show a somewhat different material compatibility to mineral oils. The Air-Conditioning and Refrigeration Technology Institute (ARTI) has conducted extensive studies

on material compatibility, and they can be found in the public domain (Short and Rajewski, 1996).

2.3.2 Miscibility

The homogeneity of a solution of substances in the liquid phase at a given pressure and temperature is known as the property miscibility. Applying this definition to the refrigeration field, miscibility refers to the property of a liquid lubricant to form a homogenous mixture by either dissolving or being dissolved in the liquid refrigerant. Miscibility depends on lubricant concentration and temperature, and if there are concentrations and temperatures at which the lubricant/refrigerant solution is not homogenous, the refrigerant-lubricant pair is said to be partially miscible. The characteristic of a partially miscible solution is that two distinct solutions or phases exist - an oil rich and a refrigerant rich. In the limiting case, the mixture could be totally immiscible, in which two pure substances, namely a refrigerant and a lubricant, would exist.

A typical miscibility chart of a partially miscible lubricant/refrigerant mixture is presented in Figure 2.1, with miscible and immiscible regions being clearly distinct. In this case an upper and a lower immiscibility region (dome) exists and as observed, the miscibility characteristics are a function of both temperature and concentration. The temperatures, which correspond to the peak points on the domes, are called upper and lower critical solution temperatures (CST), respectively. For example the upper CST is 19.3°C as indicated in Figure 2.1.

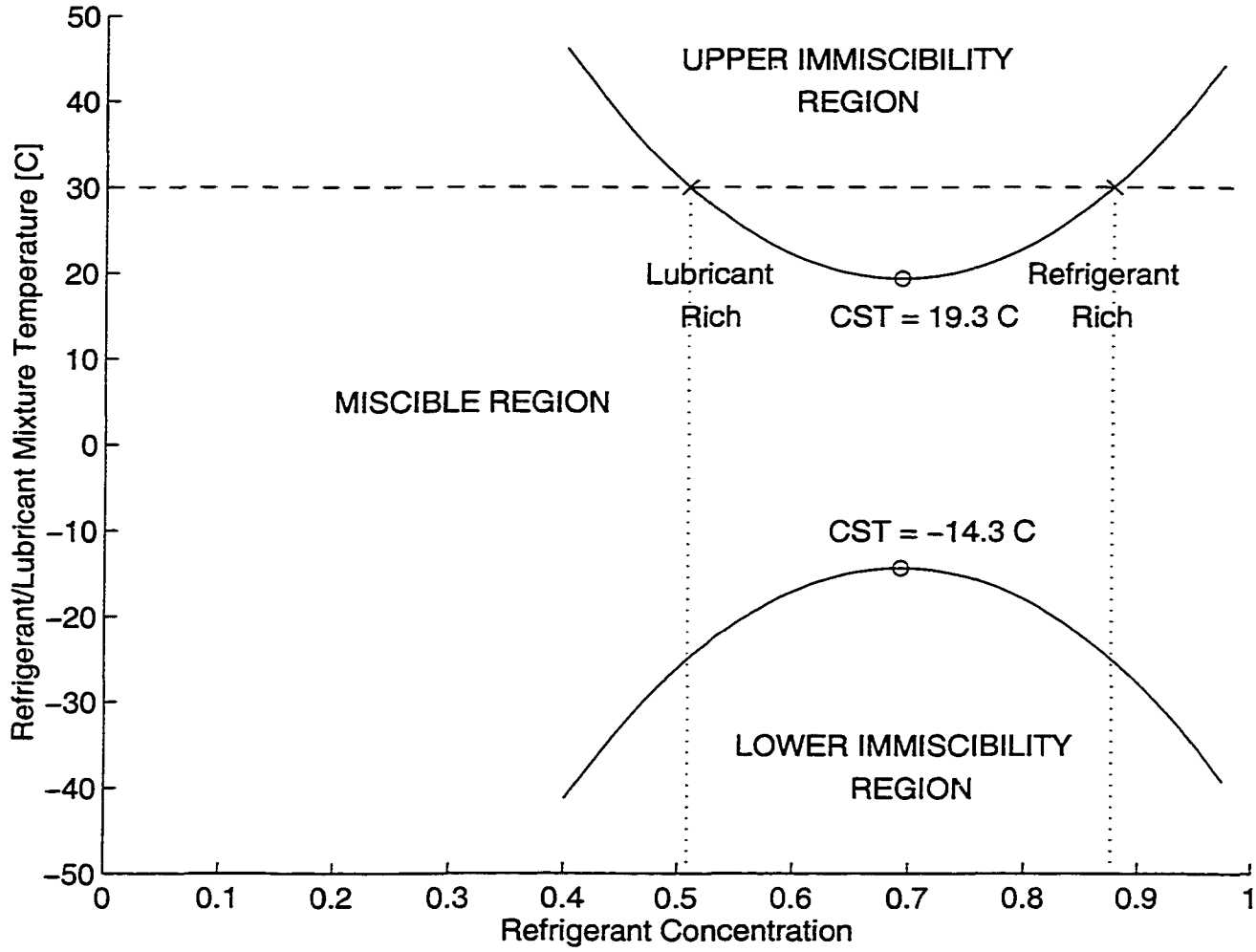

Figure 2.1. Typical miscibility chart with upper and lower immiscibility dome

The miscibility chart is just an example of a possible phase separation diagram for a lubricant/refrigerant mixture. The immiscibility dome can be wider or a mixture could be completely miscible or completely immiscible for all concentrations and temperatures. In the case when immiscibility and miscibility regions are clearly defined, such as the case presented in Figure 2.1, the lubricant refrigerant mixture is partially miscible with a refrigerant-rich phase and lubricant-rich phase. For example, at a temperature of 30°C the refrigerant/lubricant mixture is immiscible for all refrigerant concentrations larger than 51 percent and smaller than 88 percent. For any other concentration, i.e. smaller than 51 percent and larger than 88 percent, the mixture is miscible, if it is homogenous.

For a mixture with refrigeration concentrations between 51 and 88 percent at 30°C, the mixture would exist in two phases: a lubricant-rich phase and a refrigerant-rich phase. The composition of two phases of the immiscible solution is determined by the intersection of the 30°C temperature line with the miscibility dome, as marked with x's in Figure 2.1. The lubricant-rich phase has refrigerant concentration of 51 percent, while the refrigerant-rich phase has an 88 percent refrigerant concentration.

Referring again to Figure 2.1, if the refrigerant/lubricant mixture is at 0°C, the solution is miscible for all concentrations. If the temperature of the solution is reduced below -14.3°C which represents the lower CST, the lower immiscibility region is reached, and, therefore, the mixture is partially miscible for some solution concentration.

Miscibility is determined by observing whether a refrigerant/lubricant solution for any given temperature and concentration is homogenous, i.e. in one phase. It should be noted that the miscibility chart is constructed from experimental data, since accurate analytical tools have not been developed to model the miscibility behavior of a refrigerant/lubricant solution. For example one of the most extensive studies performed in the past was by Zoz et al. (1994) who measured miscibility of seven lubricants with ten non-CFC refrigerants.

Miscibility such as CFC-12 with mineral oil or HFC-134a with POE is usually perceived as the most important criterion for reliable oil return,. However, reliable operation of refrigeration systems are used with partial miscibility, e.g. HCFC-22 and a mineral oil mixture, or total immiscibility, e.g. R-502 and mineral oil or ammonia and mineral oil.

2.3.3 Solubility

The solubility of a refrigerant/lubricant mixture refers to the property of gaseous refrigerants to dissolve in a liquid lubricant. For these conditions, the refrigerant dissolved in a lubricant would exist in the vapor phase if no lubricant were present. This property is vital for the compressor environment, where the refrigerant exists in the vapor phase and considerable amount of refrigerant could be dissolved in the lubricant thus significantly affecting lubricant functions.

For a given temperature and pressure, a fixed amount of refrigerant is dissolved in the lubricant at equilibrium conditions. This is determined by the Gibbs phase rule (Moran and Shapiro, 1997)

$$\#\text{ of phases} + \#\text{ of variance} = \#\text{ of components} + 2 \qquad (2.1)$$

where the # of variance is the number of the intensive properties that must be specified to completely determine all other intensive properties.

Since there are two phases present, liquid and vapor, and two components, refrigerant and lubricant, the # of variance equals 2, if the phase rule given in Equation 2.1. is applied, thus, two intensive properties, e.g. pressure and temperature, are needed to determine the state of the mixture. It can be inferred that for a given temperature and pressure at equilibrium conditions, the concentration as well as other properties of a lubricant/refrigerant mixture are defined. Equilibrium solubility data is presented by a solubility plot, which is constructed from experimental data. A solubility plot, also known as the Daniel plot, taken from ASHRAE (1998), is given in Figure 2.2. The solubility data for a POE and HFC-134 refrigerant was generated by Cavestri et al. (1993).

The semi-logarithmic plot comprises concentration and viscosity information for the lubricant/refrigerant mixture. The solution temperature is on the abscissa, while kinematic viscosity is provided on the ordinant in the logarithmic scale. The lines of constant refrigeration concentration are presented with dashed lines starting with 0 percent, i.e. pure lubricant, increasing in steps of 10 percent up to 60 percent. Constant pressure lines are

plotted as solid lines for several pressures. For example, referring to the solubility plot in Figure 2.2, if the lubricant/refrigerant mixture is at 25°C and 550 kPa at equilibrium conditions, it must have an approximate refrigerant concentration of 30 percent and kinematic viscosity of 3 mm^2/s.

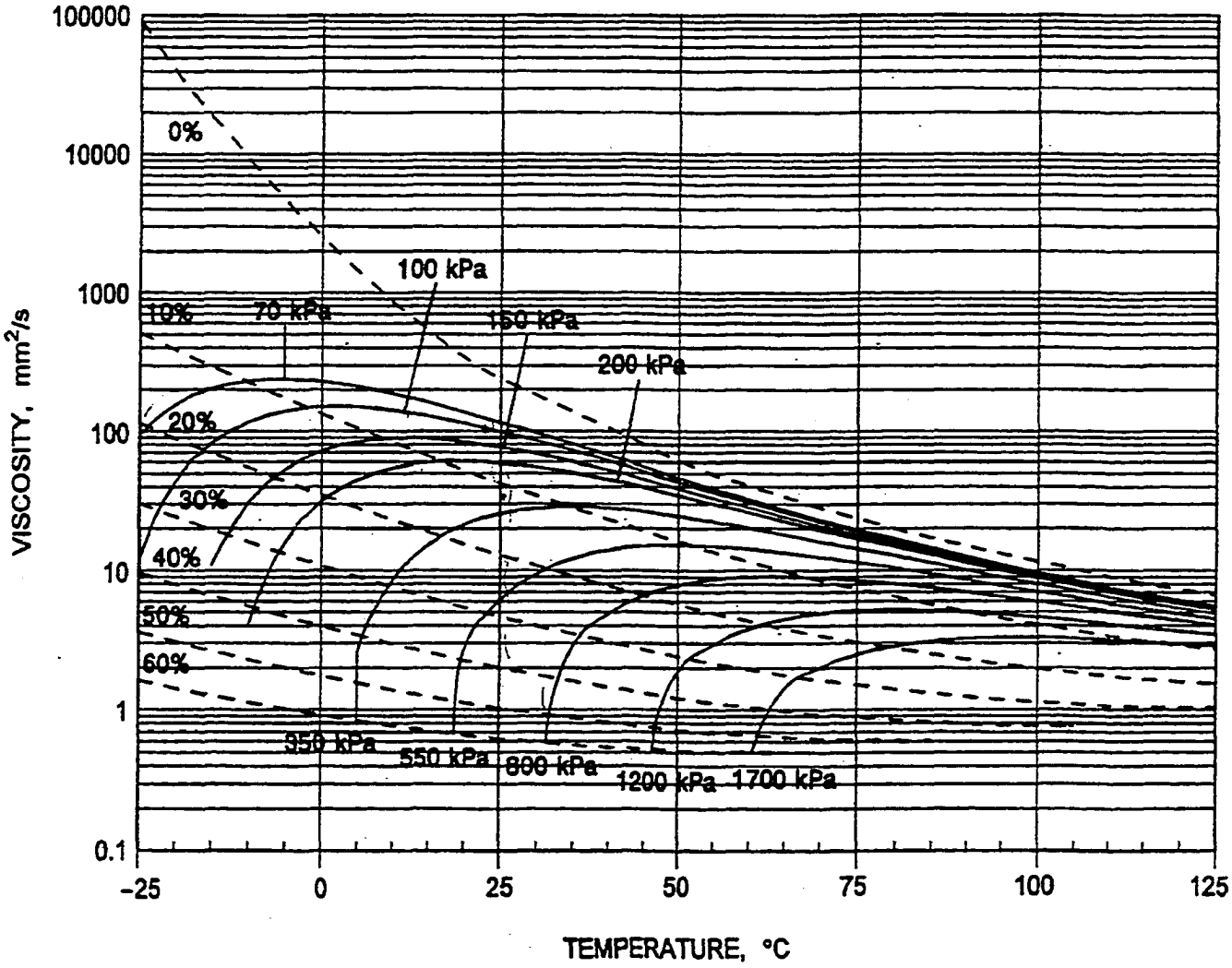

Figure 2.2. Solubility plot for 32 ISO VG branched acid POE with HFC-134a

It should be emphasized that the above solubility data is for equilibrium conditions, and it may not be relevant for an actual refrigeration system performance which is usually transient in nature. Leung et al. (1998) measured absorption rates of several HFC refrigerants and a POE lubricant, reporting that it takes approximately one hour for a POE

lubricant to reach equilibrium with refrigerant HFC-134a. In other words, this is the time required for a pure lubricant to absorb all of the refrigerant vapor that it can contain in equilibrium at a given temperature and pressure. Thus, absorption and desorption (outgassing) of a refrigerant vapor from a lubricant are processes which are on a time scale of approximately one to two hours long depending on other thermodynamic properties as well as the type of lubricant and refrigerant in the mixture (Leung et al., 1998).

Zoz (1991) measured solubility data of HFC-134 with two POE lubricants, and the data was correlated within a 5 percent error with the following analytical equations:

$$\log_{10}\mu = A_0 + A_1C + A_2\theta + A_3C\theta + A_4C^2 + A_5C^2\theta + \\ + A_6C\theta^2 + A_7\theta^2 + A_8C^2\theta^2 \qquad (2.2)$$

$$P = B_0 + B_1C + B_2\theta + B_3C\theta + B_4C^2 + B_5C^2\theta + \\ + B_6C\theta^2 + B_7\theta^2 + B_8C^2\theta^2 \qquad (2.3)$$

where:
μ is dynamic viscosity, centipoise [cp],
P is absolute pressure [MPa],
θ is the ratio of actual temperature [K] to reference temperature of 293.15 K, and
C is the mass fraction of refrigerant in lubricant.

This correlation is not based on any theoretical background, and it is valid for concentrations up to 40 percent, temperatures from 40°C to 120°C and pressures up to 3.5 MPa. The same format was used to curve-fit Cavestri (1993) solubility data for two POE lubricants of different viscosity grades with HFC-134a. The curve-fitted coefficients A and B are presented in Tables 2.1 through 2.2.

Table 2.1. Curve fitted coefficients for viscosity of POE/HFC-134a mixture

	A_0	A_1	A_2	A_3	A_4	A_5	A_6	A_7	A_8
32 VG POE branched (Zoz)	9.466	-4.543	-11.3	2.094	0	0	0	3.421	0
10 VG POE branched (Zoz)	11.79	-7.548	-14.25	3.853	1.22	0	0	4.423	0
32 VG POE branched (Cavestri)	12.82	1.436	-16.92	-17.93	-18.10	39.63	11.66	5.816	-19.06
10 VG POE branched (Cavestri)	10.52	14.39	-10.44	-47.45	-30.94	67.12	26.33	2.286	-32.02

Table 2.2. Curve fitted coefficients for pressure of POE/HFC-134a mixture

	B_0	B_1	B_2	B_3	B_4	B_5	B_6	B_7	B_8
32 VG POE branched (Zoz)	0	48.99	0	-109.8	21.71	-23.64	63.12	0	0
10 VG POE branched (Zoz)	0	23.08	0	-65.56	111.8	-179.9	44.39	0	67.21
32 VG POE branched (Cavestri)	4.709	18.72	-7.744	-64.92	-7.793	44.94	48.23	3.110	-39.22
10 VG POE branched (Cavestri)	-.420	49.38	0.483	-116.0	-35.51	89.50	68.75	0	-56.19

2.3.4. Viscosity

Viscosity is defined as a resistance to flow, and it is a fundamental lubricant property on which lubrication theory is founded. A lubricant needs to have an adequate viscosity in order to provide proper lubrication. In general, viscosity is very dependent on temperature with viscosity decreasing with an increase in temperature,.

The viscosity of a lubricant is 5,000 to 10,000 times greater than the viscosity of a halocarbon refrigerant, and, therefore, any refrigerant which is diluted in a lubricant significantly reduces its viscosity (Chang and Nagashima, 1993). Thus, a high degree of solubility of a refrigerant in a lubricant leads to large viscosity reduction. As a result, an

appropriate lubricant for a particular application must be cautiously selected in regard to its viscosity reduction. On the other hand, the selection of a lower viscosity of lubricant may result in a smaller energy consumption in the compressor due to less friction. In conclusion, lubricants should have a viscosity as low as possible, while still maintaining proper hydrodynamic lubrication, which includes possible viscosity reductions, due to refrigerant solubility. Short (1990) summarized the effects that can lead to an inadequate lubricant viscosity

- selection of lubricant with too low viscosity,
- over-dilution of the lubricant by the refrigerant,
- increase in lubricant temperature, and
- breakdown of the lubricant through loss of chemical or thermal stability.

Compared on a mass-basis, low-viscosity lubricants absorb more refrigerant than high-viscosity lubricants (ASHRAE, 1998).

The English system of units for viscosity are Saybolt Second Universal (SSU or SUS), which represents time in seconds for which specific amounts of lubricant flow through a Saybolt universal viscometer. SI units for kinematic viscosity are mm^2/s.

Viscosity Grade

The viscosity grades are standardized viscosity levels defined by the International Organization for Standardization (ISO). Standard ASTM D 2422 discusses this oil classification. The reference viscosity is reported at 40°C, so for example ISO VG 68 refers to a lubricant which has a kinematic viscosity of 68 mm^2/s, which approximately corresponds to a viscosity grade of 315 SUS at 100 °F in the English unit system.

Viscosity Index

The viscosity index is an empirical number which is related to the slope of temperature viscosity relationship. This number is determined from the standard ASTM D 2270. A lubricant with a high viscosity index shows less change in viscosity over a given temperature change (ASHRAE, 1998).

According to the standard ASTM D341, the relationship between temperature and kinematic viscosity can be represented by the following equation (ASHRAE, 1998):

$$\log\log(\nu + 0.7) = A + B\log T \tag{2.4}$$

where kinematic viscosity, ν, is in mm^2/s and temperature is in K.

The viscosity dependence on the temperature given in the above equation is the basis for viscosity-temperature charts in which the lubricant viscosity dependence on temperature is represented by two empirical numbers, A and B, appearing in Equation 2.4

2.3.5 Foamabiliy and Surface Tension

Oil foaming occurs when an oil/refrigerant mixture is exposed to a sudden pressure drop, such as occurs in the startup of a reciprocating compressor. The foaming is due to sudden outgassing of the refrigerant, and Swallow et al. (1995) reported that dense foam builds up if a halocarbon refrigerant is released from a mineral oil. It is also speculated by the same author that the amount of foaming is directly proportional to the desorption (outgassing) rate of refrigerant from lubricant. Reportedly, the desorption rate of a halocarbon refrigerant is slow and steady, resulting in a stable dense foam, while the desorption rate from synthetic lubricants is fast and violent, resulting in an unsteady large-bubble foam.

Foaming reduces noise and vibration in compressors. In experiments conducted by Sibley (1993) and Yanagisawa (1991) it was found that foam height depends on the concentration, with the maximum occurring around 50 percent refrigerant concentration (Sibley, 1993). Yanagisawa (1991) also reported that there is little foaming occurring between alternative HFC refrigerants and synthetic lubricants.

Foaming affects heat transfer characteristics in that it is believed that evaporation heat transfer of a two/phase refrigerant/lubricant mixture is somewhat enhanced by the foaming characteristics of a lubricant (Kruse and Schroeder, 1985).

Surface tension plays an important role in keeping lubricant between sliding surfaces under the prevailing pressure difference. Also, the oil foaming characteristic of a lubricant and the oil sealing function are affected by surface tension. The oil surface tension can be related to lubricant kinetic viscosity (Kruse and Schroeder, 1985) as follows.

$$\sigma_{40} = 10^{-3}\left(0.040x10^{-6}\ \nu_{40} + 27.03\right) \qquad \sigma = \sigma_{40} - a\left(t - 40^{o}C\right)$$
$$a = -0.082x10^{-3}\ N/(mK) \tag{2.5}$$

2.4 Refrigerant/Lubricant Mixture Thermodynamics Properties

Thermodynamic properties of refrigerant/lubricant mixtures must be evaluated and modeled as properties of mixtures and not of pure constituent components. The vapor pressure of oil is one millionth of refrigerant vapor pressure, and hence, the vapor phase of refrigerant/lubricant mixtures is regarded as pure refrigerant. Lubricant and refrigerant mixture properties are modeled on the principles of phase equlibria.

It should be noted that the phase diagram of a mixture is different from the phase diagram of a pure substance. A phase diagram of a binary mixture is given in Figure 2.3, and the saturation temperature of the mixture is a function of concentration. The dew point temperature is the temperature at which vapor begins to condense upon cooling, and the bubble temperature is the temperature at which evaporation starts occurring upon heating. The phase diagram presented is given for constant pressure.

One of the characteristics of a mixture phase diagram is that phases have different compositions. As shown in Figure 2.3 for a zeotropic binary mixture at a given temperature, there is a liquid phase with x composition and a vapor phase with y composition.
An actual HFC-134a/POE lubricant phase diagram for a constant pressure which was adopted from Thome (1995) is shown in Figure 2.4.

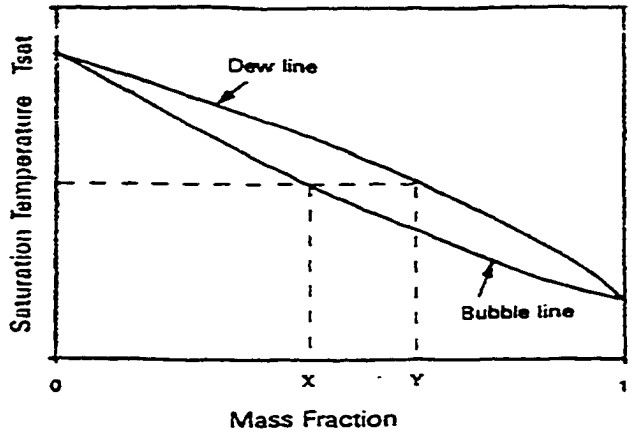

Figure 2.3. Phase diagram for a binary mixture

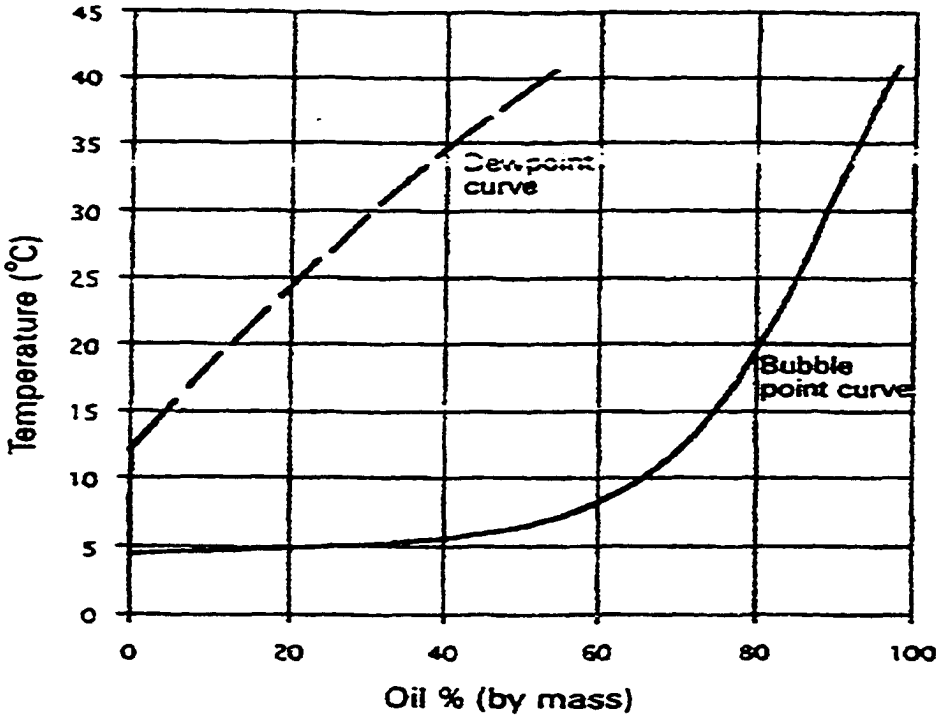

Figure 2.4. Phase diagram for HFC-134a/POE at 343 kPa (Thome, 1995)

Liquid refrigerant starts boiling at a bubble point temperature which differs from the saturation temperature of pure refrigerant depending on lubricant concentration. At large concentrations of oil, the bubble point temperature is significantly higher from the saturation temperature at the same pressure. As refrigerant evaporates through an evaporator the oil concentration increases and when the oil concentration is beyond 50 percent, the refrigerant/oil bubble point temperature sharply increases. It can be concluded that presence of oil increases the saturation temperature of the mixture and also prevents the evaporation of some amount of refrigerant in the evaporator.

Thome (1995) developed a generalized model for predicting bubble point temperature as a function of oil concentration and saturation pressure of pure refrigerant. The model is valid for oil concentrations up to 70 percent. This is an adequate model since 90 percent or more of evaporator would have oil concentrations which are lower than 50 percent.

It is essential to recognize that any lubricant present in the refrigeration system changes the bubble point temperature of the pure refrigerant. An alternative presentation to Figure 2.4 is given in Figure 2.5 where refrigerant/lubricant mixture vapor pressure is presented as a function of concentration for a completely miscible refrigerant/lubricant pair. As expected from the previous discussion, the vapor pressure decreases with an increase of lubricant concentration in the mixture, eventually reaching zero in the limiting case as the mixture approaches pure lubricant.

There have been several attempts to model vapor-liquid equilibria (VLE) for refrigerant/lubricant mixtures from experimental data. One such effort was made by Martz et al. (1996a) who measured and modeled (VLE) data for a POE lubricant and several refrigerants. The correlation was developed by using tools for modeling real multicomponent mixtures. Martz and his co-authors used vapor-phase fugacity to model the equation of state for real gases by using the Poynting effect, which accounts for vapor pressure effects of vapor pressure of liquid fugacities. The deviations from the Lewis-Randal rule (i.e. ideal mixture) were expressed in terms of activity coefficient behavior. The deviations are related to molecular size differences, intermolecular forces in the mixture, and other effects.

Martz et al. (1996b) reported several different equations that can be used to model VLE data of lubricant/refrigerant mixtures with the introduction of interaction parameters which must be derived from experimental data. Hewitt and McMullan (1997) used a modified Flory-Higgins equation to describe the solubility of miscible POE lubricants/HFC refrigerant mixtures. The Flory-Higgins equation is an useful parameter to depict phase immiscibility.

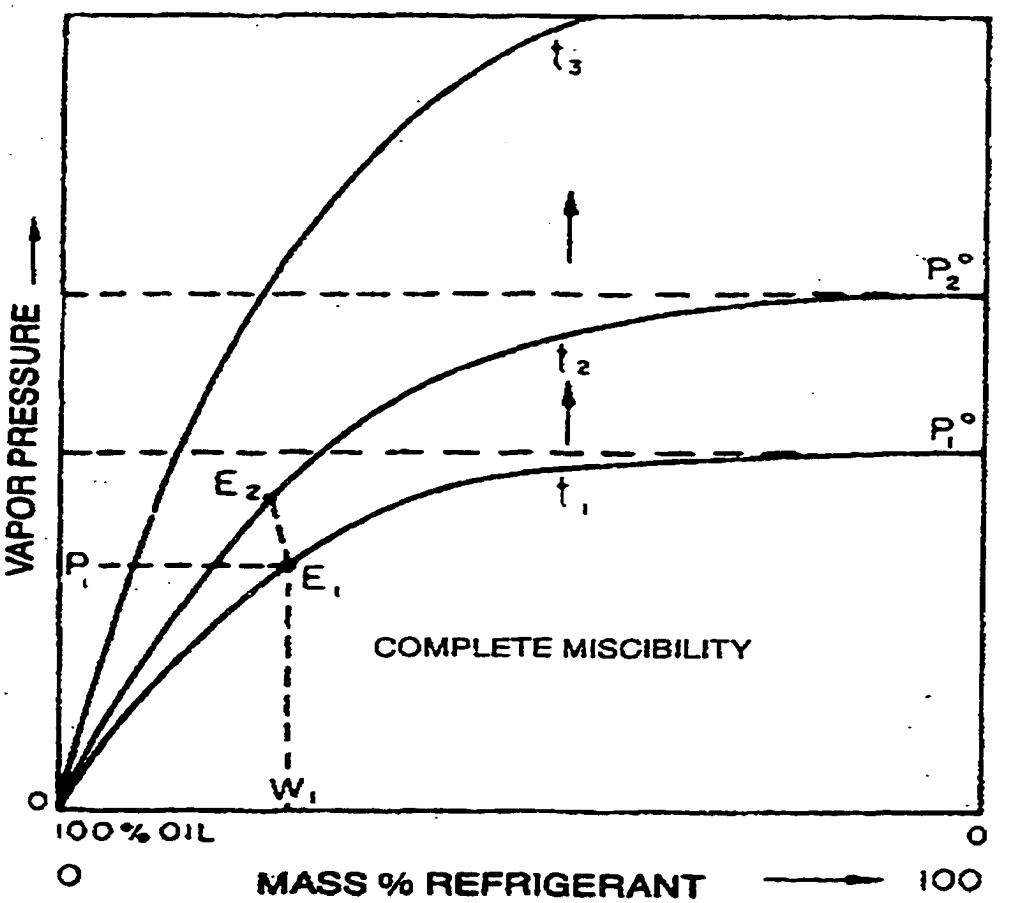

Figure 2.5. P-T-S diagram for completely miscible refrigerant lubricant mixture

2.5 Lubricants Effects on System Performance

As presented in previous sections, lubricants in vapor-compression refrigeration system affect system performance. Some small amount of oil usually enters the refrigeration system (i.e. leaves the compressor) and affects refrigerant properties and its primary functions. On the other hand, refrigerant vapor dissolves in the lubricant, which is stored in the compressor, and affects the properties and primary functions of the lubricant.

In this section, the effects of lubricant on the system performance are presented with a focus on refrigerant charge and the major components of the refrigeration system (i.e. compressor, evaporator, condenser, and expansion valve). Depending on the amount of refrigerant vapor dissolved in the lubricant, the effective viscosity of lubricant is reduced in the compressor and also a reduction in the refrigeration system charge exists. The presence of lubricant in the evaporator alters refrigerant properties, such as an increase in the evaporator temperature. In addition, the lubricant may enhance the refrigerant two-phase heat transfer in the evaporator, while always reducing the refrigerant heat transfer in the condenser. It is possible that the immiscibility of the refrigerant/lubricant mixture in the evaporator leads to a lubricant coating of the heat transfer surface area, thus deteriorating the heat transfer rate.

2.5.1 Refrigerant Charge

The correct amount of refrigerant required in a refrigeration system, i.e. optimum charge, is a charge which gives the best system performance. It was confirmed that the refrigeration system operates most efficiently if charged in the vicinity of the charge that results in a saturated liquid refrigerant leaving the condenser. This charge is hereafter called the cut-off charge. Any increase in charge from the cut-off charge leads to an increase in amount of subcooling, and usually the optimum charge has only a small amount of subcooling. Depending on the solubility characteristics of a refrigerant/lubricant pair, the actual charge may vary for the amount of lubricant dissolved. Distinction will be made

between the actual charge, which is the mass of refrigerant charged in the system, and the effective charge, which is the actual refrigerant charge reduced for the amount of refrigerant that is dissolved in the lubricant. For instance, the actual charge of a refrigeration system could be considerably different from the effective charge depending on the lubricant used. For example, an HFC-134a refrigeration system would have a larger effective charge if operated with mineral oil (poor solubility) than with a POE lubricant.

Due to the belief that charge effects on system performance are not substantial, there has been only a modest research effort directed to analyzing charge effects on system performance. Specifically, it has been widely accepted that the adequate charge is close to the cut-off charge with small amounts of subcooling. Farzad and O'Neal (1991) reported that a 5 percent overcharge results in a 5 percent decrease in seasonal energy efficiency ratio (SEER). Damasceno et al. (1990) noted that the charge affects the system performance considerably. Linton et al. (1991) found that the effects of subcooling are beneficial for tests that were conducted for fixed condenser refrigerant temperatures. However, it must be noted that their testing conditions were fundamentally different to those used in this study.

The amount of refrigerant dissolved in the lubricant in the crankcase sump can be considerable. Depending on the actual compressor used and the conditions that exist within the compressor environment, the effective charge can vary substantially. It is important to determine optimum charge for each refrigerant/lubricant pair, in order to prevent any system performance losses.

2.5.2 Compressor

Reciprocating compressors usually have oil reservoirs on the low-pressure (i.e. suction) side. On the other hand, rotating compressors normally have oil reservoirs on the discharge (high) pressure side in order to utilize pressure differences across the compressor for adequate sealing (Kruse and Schroeder, 1985). Refrigerant solubility increases with an increase in pressure and temperature, thus, compressors which have oil reservoirs on the high-pressure side of the compressor are more susceptible to inadequate lubrication.

A solubility chart can be utilized to approximate the amount of dissolved refrigerant. However, these curves need to be used cautiously, since they are generated for equilibrium conditions. The dynamic conditions in a compressor are less than equilibrium and viscosity estimates could be overly conservative, as there is usually less dilution of refrigerant in the lubricant than estimates show (Short, 1990). The solubility of the refrigerant in the lubricant leads to substantial reductions in viscosity, and this represents the critical condition that has to be considered in the selection of a refrigerant/lubricant pair. The lubricant/refrigerant mixture should have the lowest viscosity that can provide proper lubrication while still maintaining other secondary lubricant tasks.

During the startup of a reciprocating compressor, there is a sudden pressure drop which leads to outgassing of refrigerant from the lubricant. The outgassing in such instances can lead to vapor lock in systems with oil pumps resulting in compressor starvation of the lubricant, which can last for several minutes (Swallow, 1995). In addition, the outgassing may result in foam build up which may deteriorate the proper lubrication of compressor moving parts. Leung et al. (1998) studied refrigerant desorption rates and found that it takes approximately one hour for HFC-134a to reach equilibrium solubility conditions with a POE lubricant. The desorption (outgassing) rates are different for different refrigerant/lubricant pairs and Swalow (1995) reported that outgassing of refrigerants from POE lubricants is faster than from conventional mineral oils, thus leading in some instances to excessive foaming in the compressor sump.

The compressor can also have a flooded start which is the result of a large presence of liquid refrigerant in the lubricant sump. As the compressor is started, compressor parts can be exposed for extensive period of times to liquid refrigerant or refrigerant-rich liquid mixtures which may not provide proper lubrication. It is also recommended that refrigerants have good lubricity in order for the lubricant to have excellent boundary lubrication characteristics.

The temperature of lubricant/refrigerant mixtures in a compressor crankcase is relatively constant for different operating conditions as reported by Shimon (1998). Shimon (1998) measured the temperature of lubricant/refrigerant mixtures in a compressor sump by inserting a thermocouple. For wide variety of conditions, the temperature in the sump varied

between 40 and 60 °C, and it was adequately modeled as a function of compression ratio. Using this temperature, it is possible to estimate the amount of refrigerant dissolved in the lubricant by utilizing solubility data.

2.5.3 Evaporator

The effects of lubricant on the performance of the evaporator are twofold. Firstly, the lubricant, if miscible with the refrigerant, alters refrigerant properties thus resulting in an increase in evaporator temperature, and, secondly the lubricant affects the refrigerant evaporation heat transfer.

The dissolved lubricant in a refrigerant reduces the vapor pressure below that of a pure refrigerant (ASHRAE, 1998) at a given temperature. A lubricant that is miscible with a refrigerant may have unfavorable effects on system performance due to increases in evaporator temperature. Referring to Figure 2.4 at a given pressure, the saturation (i.e., the bubble point) temperature of refrigerant/lubricant mixtures increase as the lubricant concentration increases. The larger the amount of lubricant entrained in the system, the higher is the average temperature in the evaporator. An increase in the evaporator temperature results in a capacity reduction which was quantitatively assessed by Grebner and Crawford (1992). They recorded extensive pressure-temperature-solubility (PTS) data and, subsequently, generated relations for R-12/mineral oil mixtures and R-134a/POE mixtures. The authors used the generated PTS relations to determine the amount of capacity reduction due to the presence of lubricant and found that a R-12 mineral oil mixture reduces the capacity more than the R-134a/ synthetic lubricant case due to a higher solubility of mineral oil in R-12 compared to the solubility of R-134a in synthetic lubricant. Quantitatively, they found that for a lubricant circulation rate of 1 percent, there is a 4 percent capacity reduction for a CFC-12/napthenic oil mixture while a 2 percent capacity reduction was found for a HFC-134/POE mixture at given evaporator operating conditions. For larger lubricant concentrations, 5 percent leads to a capacity reduction of 30 percent for the CFC-12/napthenic oil mixture.

The presence of a miscible lubricant in the evaporator, up to 3 percent by mass, usually leads to heat transfer improvements. Kruse and Schroeder (1985) explained this by the presence of oil foaming effects. Oil concentrations larger than 3 percent usually lead to a deterioration in the heat transfer process.

Eckels (1991) studied the effects of lubricant on the two-phase heat transfer process, and it was found that the presence of up to 3 percent lubricant in some instances improves evaporation heat transfer compared to that of pure refrigerant. An improvement in the evaporation heat transfer leads to smaller temperature differences in the coil, and if the non-refrigerant side of the coil is fixed, then the evaporator temperature increases, thus improving the coil performance.

Since the refrigerant system performance is affected by the performance of the evaporator, reports in the literature comparing the heat transfer coefficients of miscible and immiscible lubricants mixed with refrigerants are also applicable to the performance study reported herein. The effects of lubricant miscibility on evaporator heat transfer coefficients were studied by Sundaresan et al. (1996b) who found that evaporation heat transfer coefficients of R-407C and R-410a mixed with a miscible POE lubricant were consistently higher, around 10 to 15 percent, compared to the refrigerants mixed with an immiscible mineral oil.

Of importance to the study reported herein, the viscosity of miscible lubricants may affect evaporation heat transfer and, hence, system performance. Eckels and Pate (1991) reported increases in the evaporation heat transfer coefficient as the viscosity of a miscible lubricant decreases. For example, for a 0.5 percent lubricant circulation rate, Eckels and Pate (1991) reported that the HFC-134a evaporation heat transfer coefficient was 16 percent larger with a lower viscosity POE (ISO VG 32) than with a higher viscosity POE (ISO VG 100).

2.5.4 Condenser and Expansion Valve

According to Eckels (1991) study, any lubricant present in the condenser reduces the condensation heat transfer rate and, consequently, the lubricant should be kept at a minimum in the condenser. The reduction in the condenser performance indirectly worsens the performance of a refrigeration system.

Lubricants probably do not affect the performance of an expansion valve, except that lubricants may start to solidify at lower temperatures which could eventually pose a possibility of expansion valve clogging (Kruse and Schroeder 1985).

2.6. Oil Return to Compressor

Proper oil return is the main concern in refrigeration operation, oil return is directly related to refrigerant/lubricant mixture miscibility and solubility characteristics. It is widely believed in the refrigeration industry that without significant refrigerant and lubricant miscibility and solubility then at evaporator temperatures the compressor would be starved of oil and eventually leads to compressor failure. Lubricants circulating through the system reach the coldest point in the evaporator which is also where the lubricant has the highest viscosity. If there is no refrigerant dissolved to reduce its viscosity, then the lubricant would start accumulating in the evaporator. The oil return is crucial for low-temperature refrigeration applications and, conversely, with higher application temperatures the oil return become less of an important issue.

Sundaresan and Radermacher (1996a) observed lubricant levels in an air-conditioning compressor operating with HCFC-22 and its alternatives, R-407C and R-410A. The authors utilized an immiscible mineral oil and a miscible POE lubricant, and they found that the oil level in the compressor was lower if the system was operated with the immiscible mineral oil. This oil level observation led the authors to conclude that the low oil level may shorten compressor life by inducing wear.

Reyes-Gavilan et al. (1996) investigated oil return of a miscible POE and immiscible naphthenic mineral lubricant in a household refrigerator operating with HFC-134a. Even though they modified the refrigerator configuration to eliminate any beneficial impacts of gravity to oil return, refrigerant vapor velocity was high enough to provide proper lubricant return. Reyes-Gavilan also proposed enhanced naphthenic mineral oils to be used in household refrigerators as these oils indicated good bench tests results as well as beneficial impact on system performance. A supermarket freezer operating with HFC-134 and an immiscible lubricant successfully worked for an extensive period of time (Reyes-Gavilan et al., 1997).

It appears that based on the work of Reyes-Gavilan and his co-workers oil return is not only dependent on oil viscosity but also on refrigeration vapor velocity in that high vapor momentum could provide adequate lubricant return to a compressor regardless of refrigeration system configuration. Since oil return is not only facilitated if a refrigerant and lubricant are miscible, the correlation between oil return and miscibility is not as critical as it appears from what has been suggested by refrigeration industry.

The miscibility of the refrigerant/lubricant mixture is perceived as the most important criterion for reliable compressor operation (ASHRAE Refrigeration Handbook, 1998). However, refrigeration systems have operated reliably in the past with partial miscibility conditions (e.g. HCFC-22 and mineral oil) or total immiscibility conditions (e.g. R-502 and mineral oil or ammonia and mineral oil) and, thus, the need for miscibility for reliable compressor operation in HFC-134a systems has been questioned.

2.7 Oil Circulation

The oil circulation rate is an important parameter as it indicates the extent to which refrigerant properties and refrigeration system operation is affected. The oil circulation rate measurement is expressed in fractions of refrigerant mass. The standard method of measuring the amount of circulation oil in a refrigeration system is to actually sample the refrigerant/oil mixture from the high-pressure refrigeration liquid line (i.e. condenser outlet).

Recently, accurate instruments for online measurements have been developed, but are not currently available as off-the-shelf devices for the refrigerant and lubricant pair in this study.

2.7.1 Oil Concentration Measurement Techniques

Newel (1996) used a refractometry method to develop an accurate instrument for the measurement of oil in refrigerants and concentrations of aqueous coolant brines.
There are two techniques that are based on the refractometry:

- difference between light beam incident angle of a substance with the known refractive index into a solution, and
- measurement of the "cut-off" angle as light passes from a medium of relatively high refractive index to a solution with a smaller refractive index.

This second technique was used by Newel as he developed an instrument with a sensitivity of 0.1 percent of PAG lubricants in the HFC-134a refrigerants.

Another method developed to measure oil circulation ratios is based on using differences in light absorption of different substances. Suzuki et al. (1993) developed procedures based on the property of lubricants to absorb light in the wavelength range of infrared rays. In contrast, at wavelengths of infrared light, refrigerants are light absorbers. Suzuki et al. (1993) reported that CFC-12 refrigerant absorbs none of the infrared light while HFC-134a absorbs some infrared light. For CFC-12/lubricant mixtures, the amount of light absorbed is directly proportional to the amount of oil in the mixture. Measuring the oil circulation rate with HFC-134a requires adjustments for the property of the refrigerant to absorb infrared light.

The speed of sound of an induced pressure wave through a liquid mixture of refrigerant and oil is different from the speed of sound of the induced wave through a pure refrigerant. This measurable difference is another technique which can be utilized to measure the oil circulation rate in refrigerants, and it was developed by Baustian et al. (1988c). Meyer and Jabardo (1994) developed an instrument based on the speed of sound

measurement technique and reported uncertainties in oil circulation rate of around 0.25 percent for refrigerants CFC-12 and HCFC-22.

Baustian et al. (1988b) used a unique in-line viscosimeter to measure oil circulation rate. Their measurements for CFC-12/napthenic oil mixtures were ±1 percent of oil circulation rate and ± 2 percent for HCFC-22/napthenic oil mixtures.

2.7.2 Measurement of Oil Concentration in Refrigerants with Densimeter

An accurate densimeter can be an appropriate tool to estimate oil concentrations since the liquid refrigerant and oil have different densities in the refrigerant high-pressure line. The simplest way to determine the refrigerant/oil circulation is by assuming a linear mixing law, or in other words, an ideal solution

$$\rho = \frac{\rho_{oil}}{1 + (1 - \omega_{oil})(\rho_{oil}/\rho_{ref} - 1)} \tag{2.6}$$

Liquid density is a function of oil concentration, temperature, and liquid compressibility. Liquid compressibility is not significant in the range from 0 to 6 percent. Hou et al. (1992) fitted the Tait equation and correlated HFC-134a liquid densities to about 0.3 percent error. Bayani et al. (1995) curve fitted Hou et al. (1992) data to obtain density functions which relate refrigerant density, ρ [kg/m^3] as function of pressure, P [MPa], and coefficients C, D, and E which are functions of temperature, T [K].

$$\rho_{ref} = [C - D\ln(P + E)]^{-1} \tag{2.7}$$

$$C = 1.649e-3 - 1.02105e-5T + 4.14318e-8T^2 - 4.70121e-11T^3 \tag{2.8}$$

$$D = 2.04e-4 - 1.90911e-6T + 7.4178e-9T^2 - 8.34015e-12T^3 \quad (2.9)$$

$$E = 7.09286e2 - 6.20421T + 1.9443e-2T^2 - 2.15073e-5T^3 \quad (2.10)$$

The oil density can be estimated from approximate function developed by Thome (1992) and provided in Baustian et al. (1995)

$$\rho_{oil} = \rho_{man}\left[\frac{T_{crit} - T}{T_{crit}\left(T_{man} + 273.15\right)}\right]^{0.29} \quad (2.11)$$

In actual refrigeration operation the density difference between pure refrigerant and lubricant in the high-pressure line is around 300 kg/m^3, and in order to estimate oil circulation with an accuracy of 0.1 % by mass, the density has to be measured with an accuracy of 0.30 kg/ m^3

Baustian et al. (1988a) used a commercially available U-tube densimeter. The U-tube flow channel was forced to vibrate at the natural frequency by using electromagnetic coils in the probe with. The vibrating frequency of the U-tube is correlated to the density of liquid within the sensor. Baustian et al. (1988a) measured oil circulation of CFC-12 /naphthenic oil within ± 1percent and HCFC-22/napthenic oil and CFC-502/alkylbenzyne within ± 2 percent.

Bayani et al. (1995) used a high accuracy, straight vibrating-tube density flowmeter. The density flowmeter had a calibrated accuracy of 0.1 kg/m^3. The meter is different from the well-known Corolius flowmeter, which measures the magnitude of the twist of a U-tube during oscillation while keeping a near constant vibrating frequency. The best accuracy of the Corolius flowmeter is around 1.5 kg/m^3. On the other hand, the Bayani et al. (1995) density meter measures the resonant frequency of vibration of the tube whose natural frequency changes with variations in the mass of tube.

2.7.3 Standard Measurement of Oil Concentration in Refrigerants

ANSI/ASHRAE Standard 41.4-1984 outlines a procedure for the determination of oil circulation by withdrawing samples. Three samples are required, and the sample are taken from the system and weighed. Then, the sampled refrigerant is evaporated as the pressure is reduced by using a vacuum pump. The sampling cylinder is then heated to 150 °C, so that all of the refrigerant dissolved in the lubricant evaporates. The sample is again weighed, with an accuracy of $\pm$ 0.01 g.

2.8. HFC-134a

HFC-134a is the refrigerant that has been accepted as the alternative to the banned CFC-12 refrigerant for a large number of applications. The refrigerant exhibits very poor mixing characteristics (i.e. miscibility and solubility) with conventional mineral oils (Short, 1990) which were previously used with CFC-12 refrigerant. Further, Short (1990) reported that HFC-134 is highly insoluble and immiscible with alkyl-benzenes, PAOs, and most diesters and poliolesters, and thus, a new family of miscible lubricants were introduced to operate in HFC-134a installations. The refrigeration industry has established that lubricants and refrigerants should be miscible over the entire temperature range of operation. Therefore, synthetic lubricants have been produced which are soluble with HFC-134a, specifically polyalkylene glycols (PAGs), used in automotive applications, and polyol esters (POEs), utilized for all other HFC-134a applications.

HFC-134a, as well as, other HFC refrigerants, indicate worse lubricity characteristics than those of CFC-12, and thus, special attention should be placed on the selection of a suitable lubricant. The lack of refrigerant lubricity is critical during the start-up operation of the compressor since it can be starved of lubricant at this time.

CHAPTER 3

EXPERIMENTAL FACILITY AND TEST PROCEDURE

The tests conducted in this study were performed on an air-conditioning test facility which is approximately the size of a residential air-conditioning unit. The facility had to be modified to meet the test requirements of the project. A number of instruments, which were operated by a data acquisition system, were used to measure and control performance parameters. All instruments were calibrated and the project was conducted following established laboratory testing procedures.

3.1 Experimental Facility

The test facility used in this project consists of an air flow loop and a refrigeration system in which the evaporator of the refrigeration system is also part of the air flow loop. Both, the air loop, and the refrigeration system are equipped with a large number of instruments which are used to control and evaluate system performance. The air loop was used to simulate the cooling load, and also to achieve precise control of air properties (i.e., temperature, humidity, and flow rate) entering the refrigeration system. The refrigeration system is a conventional vapor-compression system with a reciprocating compressor.

3.1.1 Air Side Loop

The air flowing through the evaporator coil was recirculated and conditioned in the air flow loop as shown in Figure 3.1. A variable-speed fan circulated the air while the temperature and humidity of the air was controlled by heat exchangers and an electric heater.

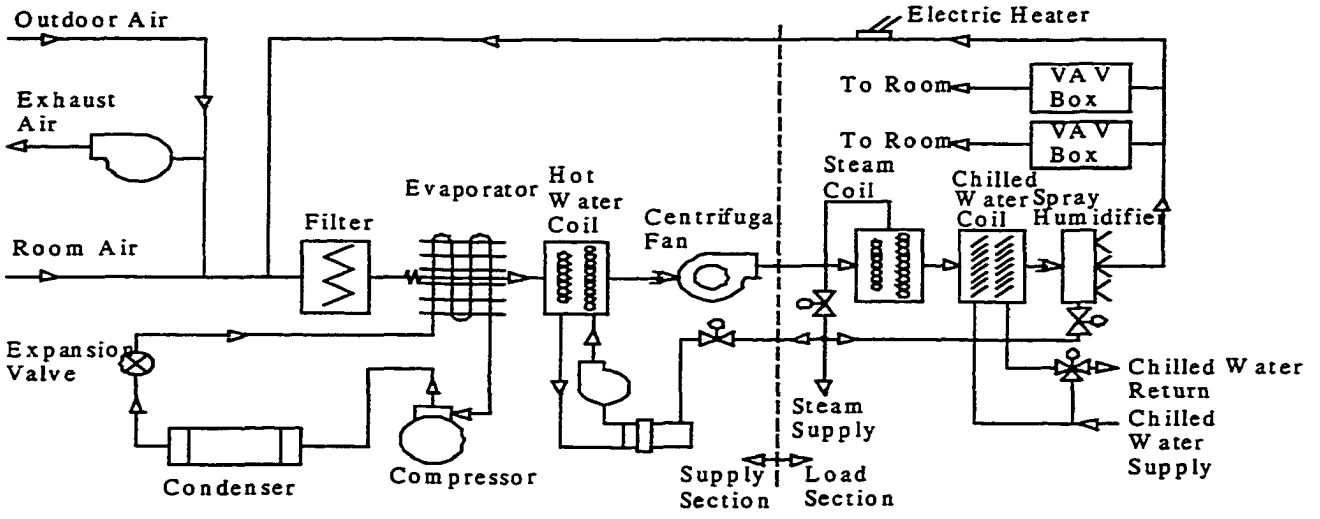

Figure 3.1. Schematic of the air side loop

The air was normally cooled down 6 to 10 °C as it flowed over the refrigerant coil, and then the air was reheated, simulating a cooling load, by a steam coil and an electric heater. The steam coil provided the bulk of the cooling load, while the electric heater was used to precisely control the air temperature.

The air humidity was kept at a low level so that the coating of evaporator fins with either condensation or frost did not become an unknown variable. The procedure for reducing the humidity in the air was to first recirculate the air over a chilled water coil in the tightly sealed air loop. As a result, the air humidity was reduced to the dew point of the chilled water coil. Then, as the refrigeration system was operated, the air humidity was further reduced to the dew point temperature of the evaporator. Before taking data, the system was operated until additional condensation had drained from the coil. In order to assure that there was no frost forming on the coil, the air flow rate was constantly monitored for flow path blockage, and the coil surface was regularly observed. In addition, the air temperature was always maintained above 6 °C, and for most tests the refrigerant temperature was greater than 0 °C.

3.1.2 Refrigeration System

The vapor-compression refrigeration system is rated at 3-ton (10.5 kW) capacity. The system operated with HFC-134a refrigerant, and a schematic indicating instruments is shown in Figure 3.2

Two types of direct expansion, DX, evaporator coils were utilized in the system for the testing of lubricants in this project. Both coils are crossflow-type heat exchangers with refrigerant flowing through copper tubes and air flowing across the tubes. Air-side heat transfer is enhanced with aluminum fins mounted on the copper tubes. Based on the internal surface of the tubes, the two coils tested are a smooth-tube coil and a microfin-tube coil. Specifications for the two coils are provided in Table 3.1.

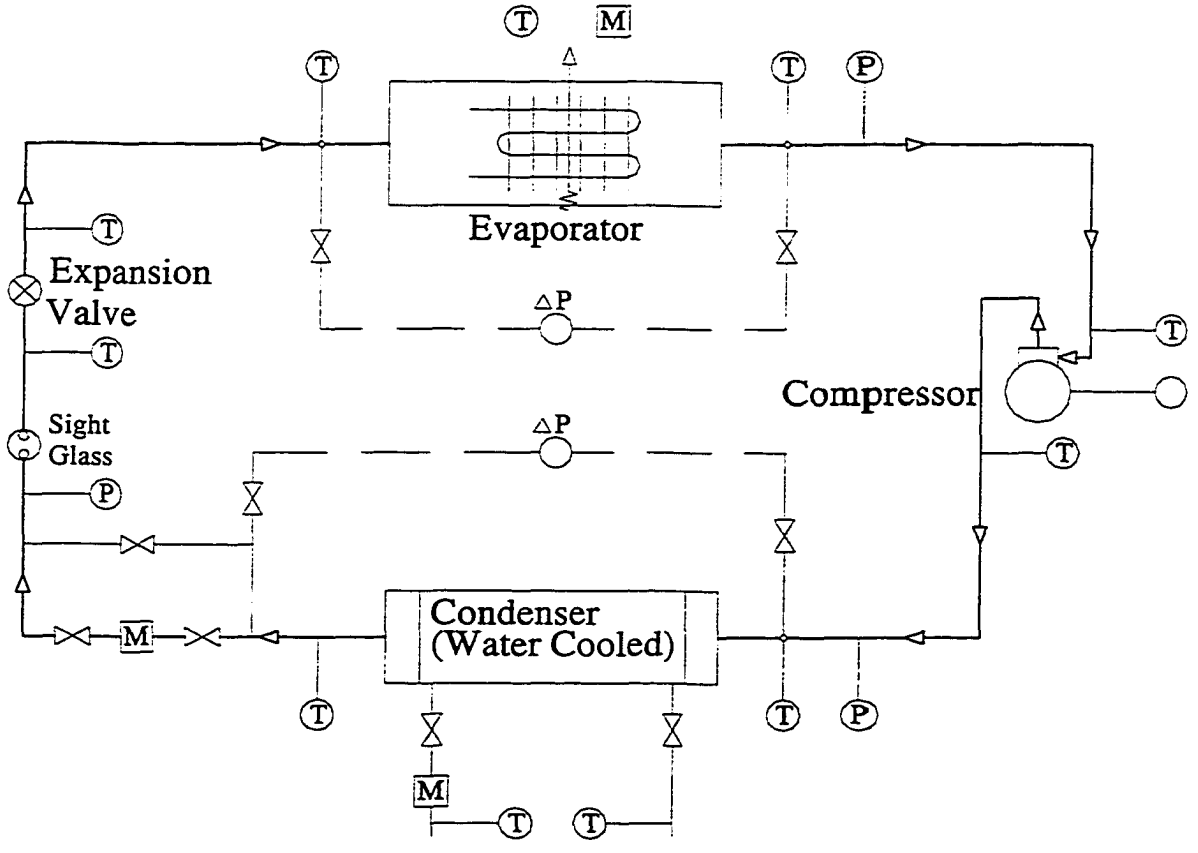

Figure 3.2. Schematic of the refrigeration test facility

Initially, a DX coil with 15.9 mm (5/8 in.) diameter copper tubes which are smooth on the inside (i.e. refrigerant side) was used. This coil is hereafter referred to as the smooth-tube coil. Later, a second coil was installed which has 9.5 mm (3/8 in.) copper tubes of the microfin tube type, consisting of 60 internal fins with spiral angles of 17 degrees and fin heights of 0.2 mm. The tubes are arranged in 10 passes and 4 rows with air flowing across a finned tube bank. The fins are flat in shape are made of aluminum with 15 fins per inch (fpi).

Table 3.1. Technical specifications of DX coils

	Tube Diameter mm (in.)	Number of Rows	Number of Passes	Fin Spacing Fins/cm (fpi)	Fin Type
Smooth	15.9 (5/8)	10	5	31 (12)	Al, Louvered
Microfin	9.52 (3/8)	12	4	38 (15)	Al, Flat

Both coils have the same design capacity of 10.5 kW (3 tons), but they differ in physical characteristics with the microfin-tube coil being smaller than the smooth-tube coil. For example, the microfin tube coil has around a 25 percent smaller cross-sectional area than the smooth-tube coil. Also, the volume of the microfin-tube coil on the refrigerant side is about 70 percent smaller than the inside volume of the smooth-tube coil.

The compressor is a hermetically-sealed, constant-speed reciprocating type with two cylinders, designed to operate with HFC-134a refrigerant. The compressor has specially designed connectors for easy charging and draining of the lubricant so that oil changes can be performed without removing the compressor.

The water-cooled condenser is a counter-flow heat exchanger. The refrigerant flows in the inner tube while water flows in the outer tube. The tube walls are enhanced on the water side to improve heat transfer. The condenser water supply was designed so that it can be maintained at a prescribed temperature by mixing the condenser return water with tap water.

There are two expansion devices installed in the refrigeration system, namely a thermostatic expansion valve and a needle valve. Since the thermostatic expansion valve has a slow response time, the needle valve is the preferred device for flow rate control as described in Crown (1992). In addition, the needle valve can be directly controlled by the data acquisition system. Thus, the expansion device consists of a needle valve controlled by the data acquisition system. A DC motor was used to finely adjust flow rates through the valve so that the desired amount of superheat at the compressor inlet could be achieved.

3.1.3 Instrumentation

A number of sensors installed on the refrigeration system are shown in Figure 3.2. Temperature measurements were obtained by utilizing thermocouple probes located before and after each of the components of the refrigeration system. In addition, thermocouple grids, consisting of 18 thermocouples each, were installed on the air flow side of the evaporator coil in order to accurately measure inlet and outlet air temperatures. Humidity was measured before and after the evaporator coil with dry bulb/wet bulb thermocouples and hygrometers. As shown in Figure 3.2, four absolute and two differential pressure transducers were used to measure refrigerant pressure throughout the refrigeration system. Additional intrumentation consisted of flowmeters and a watt transducer.

Accounting for the following three types of precision errors, measurement uncertainties were determined for all instruments:

1. Precision of devices used for instrumentation calibration.
2. Mean standard deviation of a curve-fitted calibration curve.
3. Random fluctuation of an instrument reading.

Thermocouples

Installed in both systems are 60 thermocouples, which were calibrated with precision thermometers over their anticipated operating ranges. The precision thermometers used in the calibration have a rated precision of ± 0.05 °C, which represents a source of uncertainty in temperature measurement. The thermocouples were calibrated by curve-fitting third-order polynomials, which on average yielded a standard mean deviation of approximately ± 0.2°C. The last source of temperature uncertainty comes from fluctuations in temperature readings as a steady state condition is being reached. Although these fluctuations differ among thermocouples, they are estimated to be around ± 0.05 °C based on the experimental observations. Combining these three error sources yields the temperature uncertainty of ± 0.21 °C.

Pressure transducers

Four absolute pressure transducers are installed in the system, and a dead weight tester of high precision, namely about ± 0.35 kPa, was used for their calibration. Besides the tester's precision, another source of error in the pressure measurements can be attributed to the curve-fit calibration data, which yielded a standard mean deviation of about ± 0.85 kPa. Average fluctuations in pressure readings as a steady state is reached were estimated to be around ± 0.5 kPa. A combination of the three error sources gives an uncertainty estimate in pressure readings of ± 1.05 kPa.

Water turbine flowmeter

A turbine flowmeter with an estimated precision of ± 0.04 kg/min is used to measure the flow rate of condenser water. In addition, the calibration data for the flowmeter has a curve-fit standard mean deviation of approximately ± 0.86 kg/min. Lastly, the fluctuations in the water flow rate reading as steady state is reached are estimated to be around ± 0.16 kg/min. Based on a combination of the three sources of errors, the overall water flow rate measurement uncertainty is ± 0.88 kg/min.

Air flow rate measurement

The air flow rate is calculated as the product of the air density, air velocity, and an appropriate cross-sectional area. A Pitot-tube station was used to measure the air velocity with an accuracy estimated of ± 0.13 m/s. The air density uncertainty was estimated from measurements of the air dry and wet bulb temperatures as ± 8.61×10^{-4} kg/m^3. The uncertainty in the measurement of cross-sectional area is neglected. The estimated uncertainty of the air flow rate was evaluated to be ± 0.029 kg/s with the velocity measurement uncertainty being the predominant source of error.

Other Instruments

The instrument manufacturer provided measurement uncertainties for the remaining measured parameters, namely refrigerant flow rate, refrigerant/oil density, and compressor power consumption. These instrument uncertainties along with the estimated uncertainties discussed previously are presented in Table 3.2.

Table 3.2. Instrumentation uncertainties

Measured parameter	Estimated uncertainty (±)	Average value in data set	Uncertainty in percentile of the average values.
Temperature	**0.21** °C		
Pressure	**1.05** kPa	750 kPa	0.15 %
Water Mass Flow Rate	**0.88** kg/min	78.50 kg/min	1.12 %
Air Flow Rate	**0.029** kg/s	1.340 kg/s	2.16 %
Refrigerant Flow Rate	**0.007** kg/min	3.786 kg/min	0.18 %
Refrigerant/oil density	**3** kg/m^3	1190 kg/m^3	0.25 %
Compressor Power	**0.02** kW	2.76 kW	0.55 %

The refrigerant flow rate was measured with a Coriolius type flowmeter that was precalibrated by the manufacturer. The flowmeter sensor is installed in a 3-foot long straight tube in order to increase the accuracy of the flow rate measurements. Even though the flowmeter sensor is equipped with a densimeter, the uncertainty in the measured density was too large to allow accurate estimates of oil circulation rates. Thus, the oil circulation rate was determined by sampling the liquid region downstream of the condenser, just prior to entering the expansion device and immediately after the sight glass as shown in Figure 3.2. More details about measuring oil circulation rates are given in Section 3.3.

Uncertainties for the operating parameters that are not directly measured were derived by utilizing the propagation-of-error theory. These uncertainties reported in Table 3.3 were calculated by using the measurement uncertainties provided in Table 3.2 and average absolute values in a data set. An example of derived uncertainty calculations as well as more details on the uncertainty analysis can be found in Appendix A.

Table 3.3. Derived uncertainties for performance parameters

Performance Parameter	Estimated uncertainty (±)	Average value in data set	Uncertainty in percentile of the average values.
Evaporator Capacity	**0.030** kW	10.426 kW	0.29 %
Coefficient Of Performance - COP	**0.030**	3.817	0.78 %
COP Percent Difference	**1.11 %**		
Capacity Percent Difference	**0.41 %**		
Power Percent Difference	**1.02 %**		
Isentropic Efficiency	**0.46 %**	50.12 %	
Volumetric Efficiency	**0.34 %**	80.53 %	
Overall Efficiency	**0.97 %**	99.89 %	
UA value	**8.97 W/K**	892 W/K	1.08 %
LMTD	**0.19 °C**	11.4 °C	

Data Acquisition System

The data acquisition system consists of a computer, an IEEE-488 GPIB (General Purpose Interface Bus) controller card, a computer addressable digital voltmeter, and two scanners. The GPIB controller card allowed for computer control of the scanners and the voltmeter. All of the instruments were connected to the data acquisition system, allowing constant updating of the system operating parameters and storing of the information in the computer memory.

3.2 Experimental Procedures

The data acquired in this study was for the steady state operation of the test facility. There were a number of independent parameters which had to be set to achieve one operating point. A short description of these independent parameters along with process of achieving the steady state is provided in this section.

3.2.1 Definition of Operating Point

In order to compare the refrigeration system performance for different types of lubricants, testing and data taking must be done at the same operating conditions. Therefore, it was necessary to define steady-state operating points by assigning values to the independent parameters. Six different parameters could be controlled during testing, and, as such, they are considered to be independent parameters. Four out of six independent parameters were kept constant for all tests:

1. **Superheat** at the compressor inlet was kept at 7.5 °C (13.5 °F) above the saturation temperature corresponding to the suction pressure. This is representative of the superheat used in the refrigeration industry.
2. Refrigerant **charge** was kept at an optimum value of 3.4 kg (7.5 lb) for all tests reported here. Charge effects on the system performance are discussed in more detail later in this paper.

3. Condenser **water flow rate** was kept constant at a maximum value, which corresponds to approximately 80 kg/min (175 lb/min). At high water flow rates, the condenser performance becomes independent of the water flow rate magnitude due to a negligible thermal resistance between the water and the tube wall. Thus, the water flow rate was removed as a variable during system testing and analysis, and as a result, the condenser performance is only a function of water inlet temperature, refrigerant flow rate, and refrigerant temperatures. This approach was successfully used in a previous study by Crown (1992).
4. **Air volumetric flow rate** was kept constant at approximately 1.3 m^3/sec (2400 CFM). This flow rate magnitude is close to the maximum achievable air flow rate in the test facility. The air flow rate was kept large compared to the actual practice not only to remove this parameter as a variable, but also to minimize flow maldistribution. It should be noted that minimizing flow maldistribution will minimize variations in air temperatures which may be unique to the duct geometry and other characteristics of the flow loop used in this study. One effect of higher flow rates is to reduce the thermal resistance of the air side in the evaporator and, as a result, to increase the relative resistance of the refrigerant side. In other words, the overall heat transfer coefficient of the heat exchanger depends more on the refrigerant side if the air flow rate is higher. However, it should also be noted that for the evaporator evaluated herein, the refrigerant side of the copper tubing was enhanced, which reduced the thermal resistance of the refrigerant side, while the air side fins were flat, which increased the thermal resistance on the air side, thus, reducing the relative magnitude of refrigerant-side resistance. In summary, both the in-tube enhancement and flat air side fins offset the higher air side flow rate so that the relative magnitude of the thermal resistances are representative of many operating systems.

The remaining two independent parameters, namely the condenser water inlet temperature and the evaporator air inlet temperature, were varied to simulate a variety of operating conditions. Specifically, variations in the condenser water temperature simulate a range of environmental conditions and variations in the evaporator air temperature simulate a range of air conditioning applications. These two parameters are discussed in more detail as follows:

1. The three different condenser **water inlet temperatures** selected were 24 °C (75 F), 32 °C (90 F), and 40.5 °C (105 F).
2. The three different evaporator **air inlet temperatures** selected were 13 °C (55 F), 18.5 °C (65 F), and 24 °C (75 F).

3.2.2 System Control and Steady State

It takes from 1 to 2 hours to reach steady state before an operating point can be considered acceptable. As mentioned above, three out of six independent parameters, namely condenser water temperature, air inlet temperature, and refrigerant flow rate, must be adjusted simultaneously in order for the system to reach a steady condition..

Controlling the refrigerant flow rate by the needle valve also results in control of the amount of superheat at the compressor inlet. The amount of superheat is a strong function of water and air inlet temperatures, so any fluctuations in these temperatures lead to fluctuations in the amount of superheat. Thus, the needle valve is controlled by the computer (data acquisition system) to reduce the time required for the system to reach steady state.

The three temperature parameters, which are simultaneously adjusted, are monitored on the computer and when their fluctuations are within ± 0.1°C of the desired value then the operating point data are recorded. Since thermocouples can measure temperatures to ± 0.2°C, there are no valid reasons to set any finer limit on reaching steady state.

After the steady state operation has been reached, the data are taken over an approximately 5 minute period. Multiple readings of several key parameters are taken in order to reduce any precision errors in instrumentation readings. These multiple readings are

statistically processed to evaluate the fluctuations in instrument readings. The statistical analysis of an operating point is shown in Table 3.4 as the multiple readings of the key measured parameters are represented with mean values and the corresponding standard mean deviations. For example, the thermocouple at the compressor inlet has a standard mean deviation of 0.07 °C, which is significantly below the temperature uncertainty of ± 0.2 °C. The standard mean deviation of the evaporator exit pressure readings is only 0.17 kPa, which is considerably below the estimated pressure measurement uncertainty ±1.05 kPa. Fluctuations in the condenser water inlet temperatures, which are represented by the standard mean deviation of 0.11 °C in Table 3.4, are smaller than the temperature uncertainty of ± 0.2 °C.

Table 3.4. Data point steady state evaluation

Measured Quantity	Average Value of Multiple Readings †	Standard Mean Deviation of Multiple Readings †
Refrigerant Temperature @ Compressor Inlet [°C]	9.66	0.07
Refrigerant Pressure @ Evaporator Inlet [kPa]	429.15	0.91
Refrigerant Pressure @ Evaporator Outlet [kPa]	315.84	0.17
Refrigerant Pressure @ Condenser Inlet [kPa]	990.45	0.61
Refrigerant Flow Rate [kg/min]	3.727	0.003
Compressor Power Consumption [kW]	2.871	0.003
Condenser Water Inlet Temperature [°C]	32.43	0.11
Condenser Water Mass Flow Rate [kg/min]	79.06	0.09
Evaporator Air Inlet Temperature [°C]	18.35	0.04
Evaporator Air Velocity [m/s]	6.053	0.024

† Each of the measured parameters were read 20 times, and thus, the average value and the standard mean deviation represent statistical analysis of the multiple readings.

The refrigerant pressure in the condenser closely follows the condenser water temperature. Therefore, fluctuations in the condenser water temperature are proportional to fluctuations in the refrigerant pressure in the condenser. Since the condenser water temperature fluctuations are relatively high compared to the fluctuations of other reported temperature measurements, the fluctuations in the condenser refrigerant pressure are ±0.61 kPa. These condenser pressure fluctuations are higher than the fluctuations in the evaporator exit pressure of ±0.1 kPa, however, they are still well below the estimated pressure measurement uncertainty of ±1.05 kPa. The evaporator air inlet temperature fluctuations are small with the standard mean deviation being only about 0.04 °C.

The multiple instrument readings for each data point reduce the random precision errors in measurements. As reported in Table 3.4, the fluctuations in the instrument readings are well below the measurement uncertainties, assuring that an acceptable level of steadiness is achieved in the refrigeration system operation when data are recorded. Further analysis of the system steadiness and the data repeatability are given in the Appendix B, where the quality of the data used for comparison between the POE_1 and the mineral oil lubricants were assessed.

3.3 Lubricants

One mineral oil and three synthetic POE lubricants were used in this study. Because of proprietary concerns, lubricant properties and chemical composition which are not directly applicable to the scope of this project are not reported here. Since the objective of this study was to evaluate the influence of miscibility and viscosity on system performance, these are the only lubricant properties reported herein.

3.3.1 Lubricant Properties

The performance of an HFC-134a system with four lubricants, namely three polyol ester lubricants (designated as POE_1, POE_2, and POE_3) and an immiscible naphthenic mineral oil (designated as MO) were evaluated in the study. The POE_1 and the MO lubricants were selected by the lubricant manufacturer, for the purpose of analyzing of miscibility effects on system performance, and, as a result, the two lubricants had the same viscosity grade of ISO 32 (150 SSU) and similar viscosity dependence on the temperature. Applicable properties of these lubricants are provided in Table 3.5, and it can be inferred that the kinematic viscosity dependence on temperature is similar for the both the POE_1 and MO lubricants, and that trend is also plotted in Figure 3.3. The POE_1 lubricant was reportedly miscible with HFC-134a for all temperatures and refrigerant concentrations. The HFC-134a and mineral oil were assumed to have poor miscibility, based on information found in literature and presented in Section 2.8.

Table 3.5. Lubricant properties

	Mineral Oil	POE_1	POE_2	POE_3
Viscosity @ 40 °C [cSt]	29.99	33.8	25.6	26.41
Viscosity @ 100 °C [cSt]	4.38	5.6	5.2	5.38
Density @ 15.6 °C [g/cm^3]	0.9089	0.9917	1.0017	0.9889

The viscosity dependence on temperature is plotted in Figure 3.3 for all lubricants tested. It is based on two viscosity values reported in Table 3.5 and marked on the plot. The viscosity-temperature function which appears as a straight line in the semi-logarithmic plot was modeled by using standardized Equation 2.5 in Section 2.3.4.

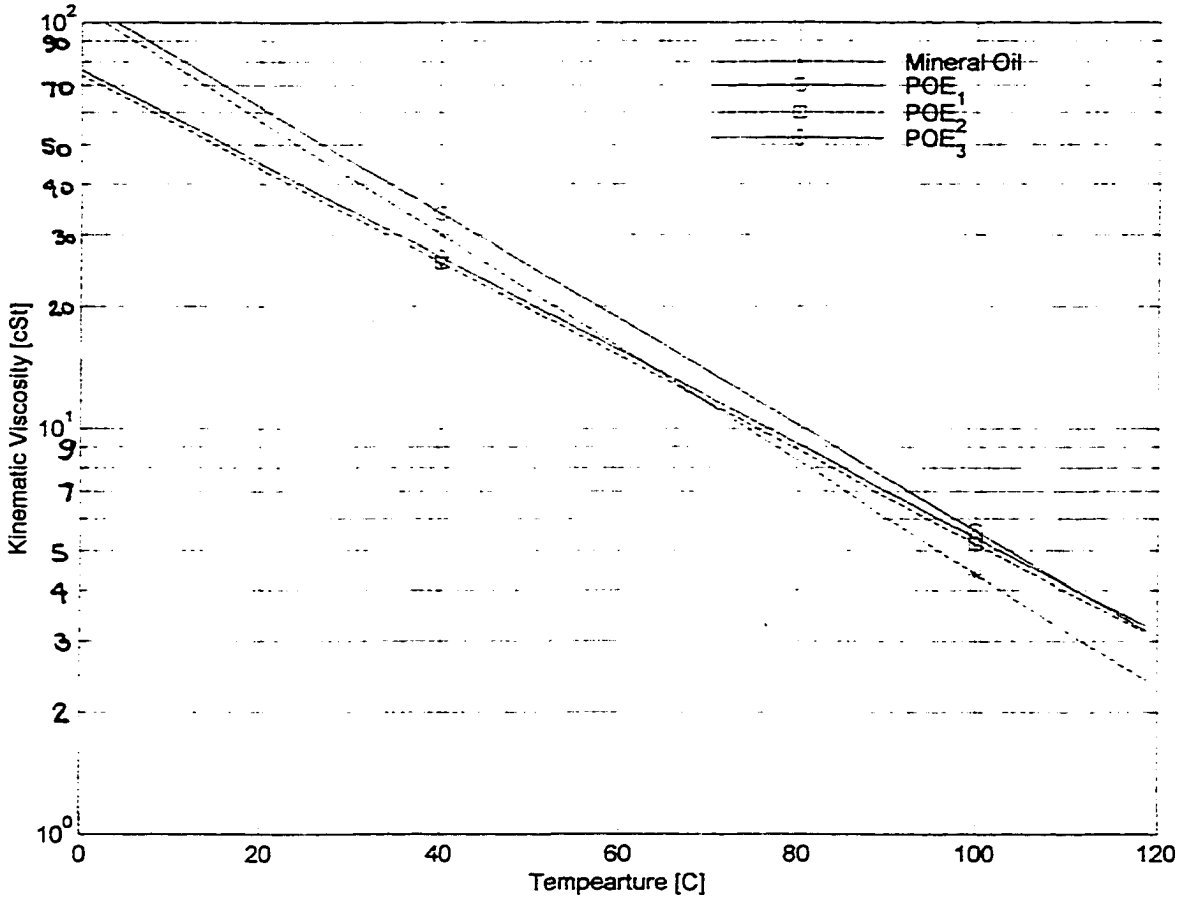

Figure 3.3. Kinematic Viscosity as a Function of Temperature for Utilized Lubricants

Preliminary information available to us suggested that the POE_2 lubricant might become immiscible at -5 °C. However, because specific critical solubility temperature data were not available for POE_2, it was necessary to conduct a miscibility test to determine the critical solubility temperature plot. This action was particularly important because if POE_2 is to be used in a study of the effects of partially miscible lubricant, then one must ensure that the critical solubility temperature is greater than the system temperature (i.e. refrigerant-side evaporator temperature).

The ISU Miscibility Test Facility, described in detail in Appendix B in this report, was utilized to determine the miscibility characteristics of the refrigerant/lubricant mixture (i.e. POE_2 and HFC-134a). Miniature pressure vessels (referred to as test cells) with glass

view ports on the sides and temperature-controlled baths are essential elements of the Miscibility Test Facility. After the test cells are charged with known amounts of refrigerant and lubricant, they are immersed in either a hot or a cold bath depending on the desired temperature range to be tested. As the desired temperature is reached in the bath, the miscibility of the lubricant/refrigerant mixture being tested is checked through the glass view ports.

The miscibility test results for the POE _2 lubricant with HFC-134a are presented in Table 3.6. The lower critical solubility temperature is -23 °C, and it occurred at 81 percent refrigerant concentration. It can also be observed in Table 3.6 that immiscible conditions occur at temperatures even lower than -23 °C over the refrigerant concentration range from 70 to 95 percent.

Table 3.6. Results of miscibility test of POE_2/HFC-134a mixture

Refrigeration Concentration by mass	Critical Solubility Temperature *
23%	< -40 C
71%	-30 C
81%	-23 C
85%	-24 C
90%	-25 C
95%	-33 C

* below this temperature the refrigerant/lubricant mixture is immiscible.

The miscibility test results in Table 3.6 are presented in the form of critical solubility temperatures plotted as a function of refrigerant concentration in Figure 3.4. It should be noted that this curve follows the classical dome-shaped curve with a peak near 80 percent refrigerant concentration, which is consistent with past reports of POE lubricant and HFC refrigerant miscibility studies. The upper miscibility dome was not investigated as the

required partial miscibility requirement was for evaporator temperatures only.

Since POE_2 was not partially miscible with HFC-134a at evaporator temperatures achievable in the test facility, it was considered to be a satisfactory lubricant to study lubricant viscosity effects on system performance but not necessarily in a partial miscibility study.

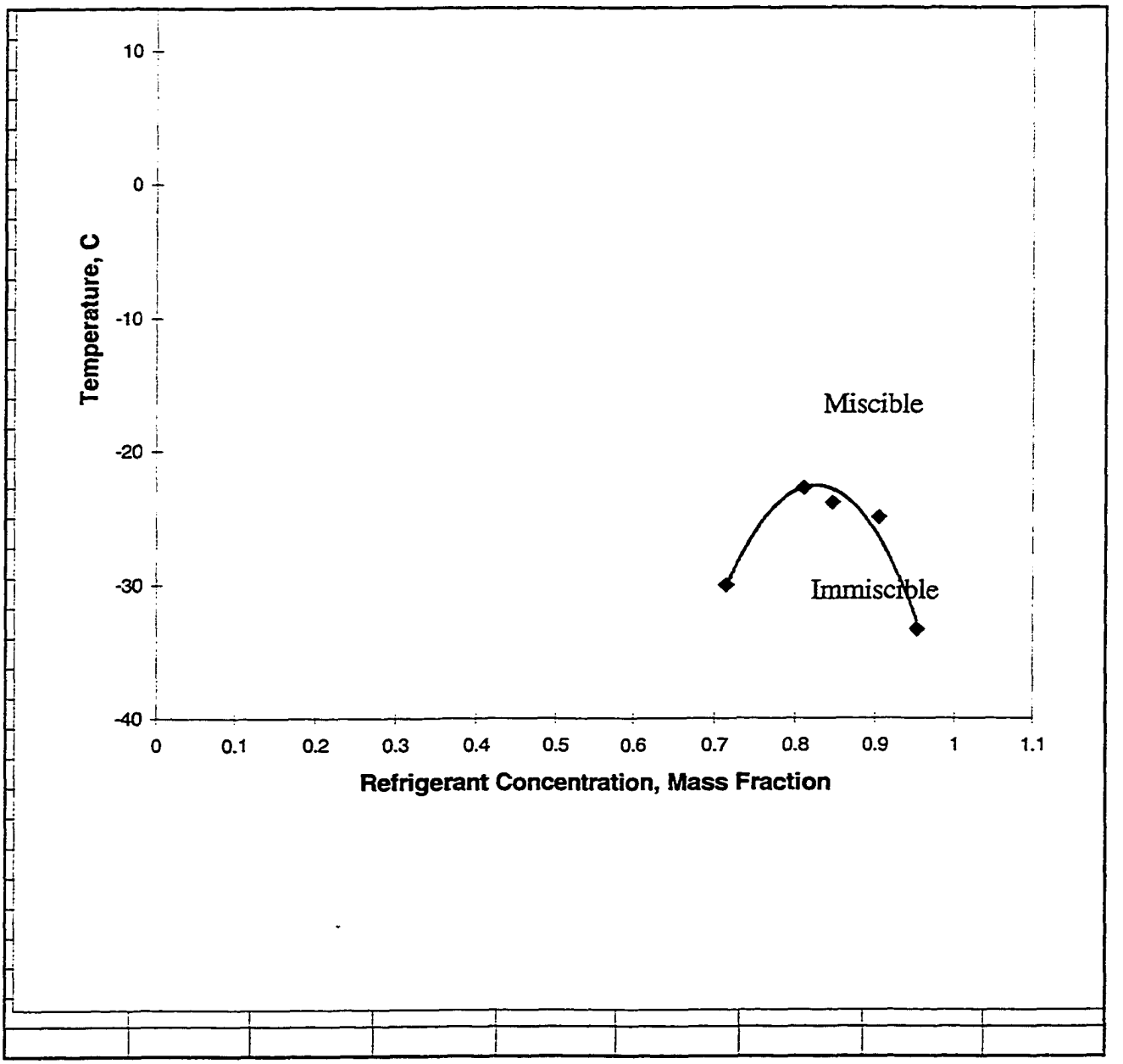

Figure 3.4. Critical Solubility Temperature Data for POE_2 with HFC-134a

It should be noted that POE_2 has a lower viscosity grade of ISO 22 (105 SSU) compared to the POE_1 lubricant, and, therefore, a comparison of these two synthetic lubricants was used to investigate lubricant viscosity effects on system performance. Properties of POE_2 are reported in Table 5.3, and the viscosity dependence is shown in Figure 3.3.

The last POE lubricant, namely POE_3, is partially miscible at evaporator temperatures, and therefore, this lubricant was used to further study miscibility effects on system performance. The lubricant was selected by screening (i.e., performing miscibility tests) a number of different POEs to find a truly partially miscible lubricant for the evaporator temperatures used in this study.

Available properties for POE_3 are given in Table 3.5 and plotted in Figure 3.3. The critical solution temperature of POE_3 and HFC-134a is around 10 °C, occurring at around 80 percent refrigerant concentration. The POE_3 critical solubility data shows the same dome-shape as was shown in Figure 3.4. The critical solubility data is obtained by using the ISU Miscibility Test Facility which is described in more detail in Appendix B.

3.3.2. Lubricant Circulation

The mass fraction of oil circulating in the refrigeration system (i.e. oil circulation rate) was measured by removing liquid samples from the high pressure line, located at the expansion valve inlet, while the system was operating. The refrigerant/lubricant liquid mixture sampling was performed in accordance with ANSI/ASHRAE Standard 41.4. The oil circulation rate was determined to be 0.3 percent of refrigerant mass. In addition, this value was almost constant as system operating conditions were varied, with the measured oil circulation rate varying less than ± 0.05 percent.

The oil circulation rate measurements were performed for all tested POE lubricants because they were miscible with HFC-134a in the high pressure line

3.3.3. Lubricant Change Procedure

Changing the lubricant in the compressor was performed in accordance with the triple-flush procedure outlined in Byrne et al. (1996). The triple-flush method is a procedure for the removal of mineral oil from a CFC-12 installation when it is retrofitted with HFC-134a. The method requires three lubricant changes to remove any traces of old oil residual. As a result of using this procedure, the residual can be reduced to less than 1 percent by volume. As specified by Byrne et al. (1996), the system was operated for 24 hours in between each oil change. The amount of lubricant added to the compressor, based on manufacturer recommendation, was around 1.4 kg (2.9 lb).

CHAPTER 4

COMPARISON AND ANALYSIS OF LUBRICANT EFFECTS ON SYSTEM PERFORMANCE

The results of the investigation of lubricant effects are presented by comparing the refrigeration system performance of different lubricants at the same operating conditions, i.e., having identical independent parameters except for the lubricant type. Specifically, comparisons of key performance parameters, such as coefficient of performance, capacity, power consumption, flow rate, and refrigerant properties are made to determine the extent to which different lubricants can affect the performance of a refrigeration system.

First, the effects of the refrigerant charge were investigated in order to eliminate this parameter from biasing the analysis. The refrigeration system was operated with a variety of charges, and the system performance was determined and compared.

Second, the effects of lubricant miscibility on system performance were analyzed by comparing the system performance of a miscible POE lubricant and an immiscible mineral oil in a system with a microfin-tube evaporator coil. In addition to presenting test results, the analysis includes reasons and explanations for the observed system behavior.

Third, the effects of lubricant viscosity for miscible lubricants were investigated by comparing the performance of the refrigeration system for two POE lubricants with different viscosity characteristics. Since both lubricants were miscible, the results emphasize the effects of lubricant viscosity.

Fourth, a partially miscible POE lubricant was tested in the refrigeration system and compared to the system performance of the other lubricants. The partial miscibility condition for the refrigerant/lubricant mixture occurred at the evaporator temperatures used in this study.

Last, a smooth-tube type evaporator coil was used to investigate the effects of lubricant miscibility. The study is similar to the miscibility study performed for the microfin-tube coil as detailed previously. Specifically, the testing of system performance was done with the same pair of lubricants, namely the miscible POE and the immiscible mineral oil.

4.1 Refrigeration Charge

The correct amount of refrigerant to be charged into the refrigeration system is the charge that gives the best system performance, hence it is referred to as the optimum charge. It was confirmed in this study that the refrigeration system operates most efficiently if it is charged close to the charge that results in a saturated liquid refrigerant leaving the condenser (a regime marked by the disappearance of two-phase flow at the condenser outlet). This charge is hereafter called the cut-off charge. As will be presented in this section, the difference between the optimum charge and the cut-off charge is less that 7 percent of the total charge. Nevertheless, it was essential for this study to determine and understand the effects of charge on system performance so that the system performance comparison of tested lubricants is independent of charge. Investigation of charge effects were conducted for both types of DX coils used in this study.

4.1.1 Significance of the Refrigerant Charge

The effects of charge on refrigeration system performance, as presented earlier in Section 2.5.1, are not substantial. However, the effects of extreme charges are evident on system performance. For instance, an insufficient charge produces a lower refrigeration effect (i.e. capacity) since there is not enough refrigerant for proper operation of the system. Otherwise, an excessive charge in the system increases the refrigerant capacity. However, this capacity increase results in an even larger increase in the power consumption, causing a

decrease in the system efficiency. In addition, an excessive charge causes high pressures at the compressor discharge. All of these issues are addressed in more detail in the next section.

A common practice in industry for systems installed in the field is to charge the system with refrigerant until subcooling is achieved at the condenser exit, which means that the refrigerant leaving the condenser is all liquid and that charge, as mentioned earlier, is called the cut-off charge. The refrigerant leaving the condenser in the liquid phase ensures that the condenser is utilized to its fullest potential. The larger the amount of subcooling, then the more energy can be transferred out of the condenser. Of particular importance for this study is that the refrigerant is in the liquid phase enabling accurate determination of the refrigerant properties. Conversely, if the refrigerant leaves the condenser in two-phase flow, it is difficult to determine the refrigerant properties. In addition, accurate readings of refrigerant flow rate are achieved only if the refrigerant is in the liquid phase, since the refrigerant flowmeter is installed in the high-pressure line at the condenser outlet.

Another reason to charge the refrigerant until subcooling is reached is that pressure drops through the high pressure lines at the condenser outlet during two-phase flow may be three or more times larger than those which occur for the liquid-only flow case. Excessive pressure drops in the high-pressure line during two-phase flow were shown to be a problem in this study, during the experimental facility building phase. In the current installation, the pressure drop in the high-pressure line for the case of liquid-flow might be as high as 10 percent of the total pressure produced by the compressor. If the refrigerant in the high-pressure line is two-phase, the pressure drops might be 30 to 40 percent of the compressor discharge pressure.

The optimum charge is the amount of refrigerant for which system indicates the best performance. In general, the optimum charge is in the vicinity of the cut-off charge, and it is a function of physical size of the system, refrigerant/lubricant solubility characteristics, and refrigeration application.

4.1.2 Amount of Subcooling

As mentioned in the previous section, the presence of liquid refrigerant in the high-pressure line is an indication that the system is charged with at least the cut-off charge. The amount of subcooling can indeed indicate how much above of the cut-off charge the system is charged. As shown in Figure 4.1, the amount of subcooling increases with an increase in refrigerant charge.

The data presented in Figure 4.1 was taken from the smooth-tube coil study and the results indicate that for the optimum charge there is about 4°C subcooling. The variation in charge can be presented as a charge percent difference relative to the optimum charge, which was 3.6 kg for the system with smooth tube coil.

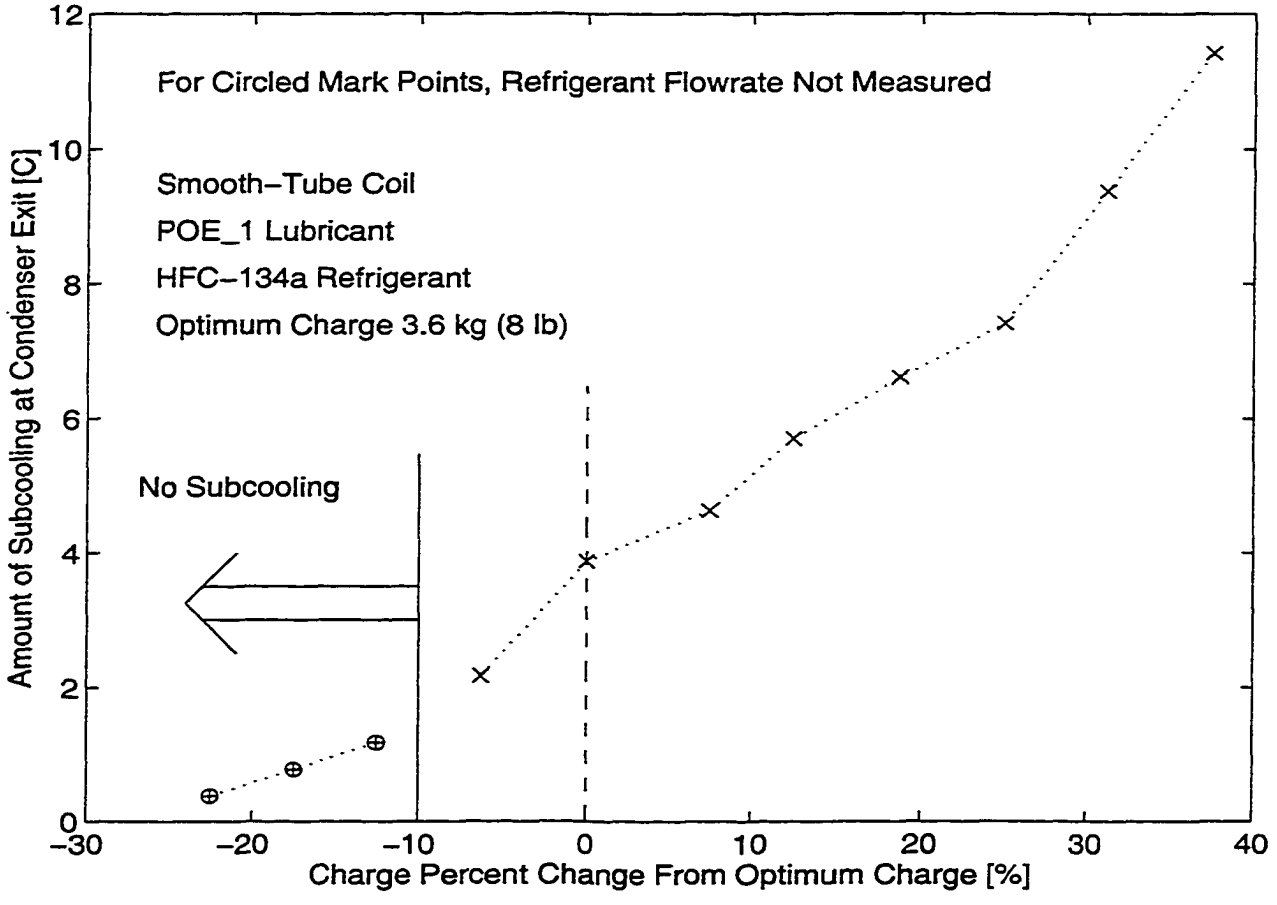

Figure 4.1. Amount of subcooling as function of refrigerant charge.

$$\text{Charge Percent Difference}[\%] = \frac{\text{Charge}[\text{kg}] - 3.6\text{kg}}{3.6\text{kg}} 100 \tag{4.1}$$

As shown in Figure 4.1, the amount of subcooling increases with an increase in refrigerant charge. For example, if the system is 40 percent overcharged then the amount of subcooilng is around 12 °C. Interestingly, for the system being undercharged by more than 10 percent, the small amount of subcooling existing at the condenser outlet was not sufficient to prevent refrigerant flashing in the high pressure line prior to the refrigerant flowmeter. It should be noted that this flashing prevented accurate flowrate measurements.

4.1.3 Charge Effects on System Performance with Microfin-Tube Coil

A detailed charge study (i.e. the charge of HFC-134a) was performed for POE_1 where the charge was varied from 3.2 kg (7 lb) to 5 kg (11 lb). Based on plotting the Coefficient Of Performance (COP) as a function of the refrigerant charge shown in Figure 4.2, the optimum charge for the system operating with POE_1 lubricant was found to be around 3.4 kg (7.5 lb). As mentioned earlier, the cut-off charge is close to the optimum charge, and it was found to be around 3.2 kg (7 lb).

There were no tests performed for charges below the cut-off charge, as can be observed in Figure 4.2, because the existence of two -phase flow in the refrigerant flowmeter prevented accurate flow measurements and also because the performance of the system decreased at charges below this value. It should be noted that the charge effect investigation presented in Figure 4.2 was conducted for an evaporator air temperature of 18.5 °C and a condenser water temperature of 32 °C. These conditions represent a medium set of conditions for all of the tests performed in this study.

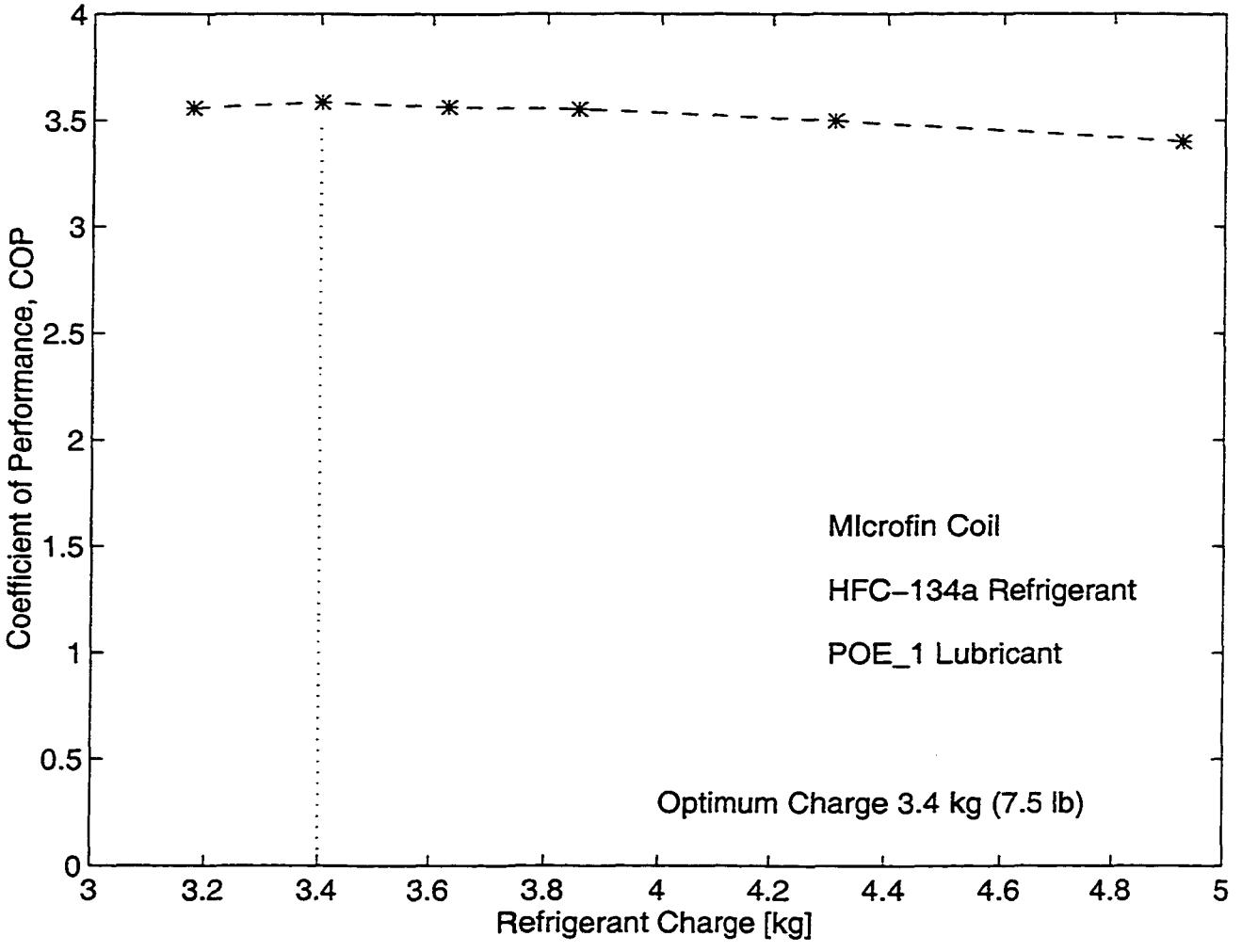

Figure 4.2. COP as a function of refrigerant charge

An additional observation regarding the HFC-134a charge can be made by further studying the trends plotted in Figure 4.2. For example, it can be observed that the COP is not a strong function of charge as evident by the COP decreasing only 0.7 percent if the charge is varied from the optimum to the cut-off charge, which as noted earlier is a 7 percent change in charge. In light of the charge not being a significant factor on system performance, the charge was optimized for the POE_1 lubricant and the same charge was used for tests with the other three lubricants. Based on experiences of working with different refrigeration systems and with different refrigerant/lubricant pairs, the optimum charge has been found to be primarily determined by the physical size of the refrigerant system, but not by the type of

refrigerant/lubricant pair. Also, as shown in this study the optimum charge is close to the cut-off charge.

The results presented in Figure 4.2 were conducted by varying the charge from 7 percent undercharged to a 45 percent overcharged condition. The changes in performance parameters are expressed in terms of percent differences or absolute differences.

Percent difference change in COP, refrigeration capacity and compressor power consumption are presented in Figure 4.3. As an example the percent difference in the COP is defined as

$$COP_{dif}[\%] = \frac{COP - COP_{optimum}}{COP_{optimum}} 100 \tag{4.2}$$

The percent differences for capacity and compressor power consumption are calculated in the same manner as COP percent difference in Equation 4.6. The variations in the refrigeration capacity due to charge are relatively small when compared to the variations in COP and compressor power consumption. The capacity variations are within ± 0.5 percent of the capacity determined for the referenced charge. It can be observed that the capacity is increasing with the addition of charge and then drops for the largest charge. Due to small changes in capacity variations, it can be inferred that changes in COP and compressor power consumption are proportional. Specifically, a decrease in system COP with a charge increase is almost exclusively caused by an increase in the compressor power consumption.

Varying the charge by ±10 percent of the optimum charge results in a COP percent difference change of only around 1 percent which is close to the magnitude of uncertainty in the COP difference of 1.1 percent as reported in Chapter 3. Hence, it can be concluded that the optimum COP corresponds to the reported optimum charge of 3.4 kg and that variations in charge (i.e. up to 10 percent) results in changes in COP less than the estimated uncertainty.

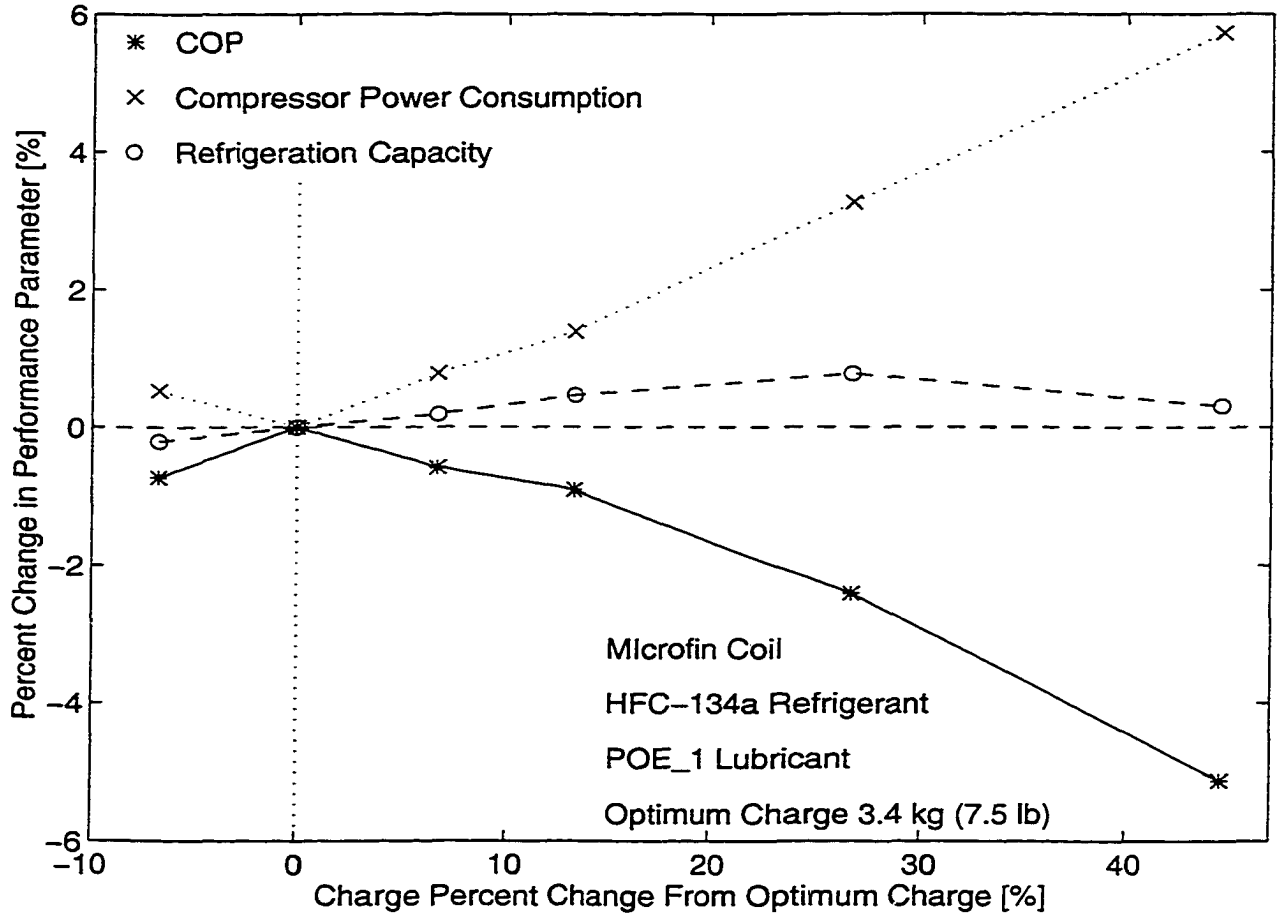

Figure 4.3. Percent change in performance parameters as a function of refrigerant charge in microfin-tube coil

Compressor efficiencies and refrigerant flow rate dependence are presented as a function of refrigerant charge. The charge variation is presented in terms of charge percent difference defined earlier in Equation 4.1 with the only change being that the optimum charge is 3.4 kg for the system with microfin-tube coil. Using the same approach as was done for the COP defined in Equation 4.3, the changes in refrigerant mass flow rate can be presented in terms of percent difference of the mass flow rate for the optimum charge operating point.

$$\dot{m}_{dif}[\%] = \frac{\dot{m} - \dot{m}_{charge=3.4kg}}{\dot{m}_{charge=3.4kg}} 100 \tag{4.3}$$

The differences in compressor efficiencies as a function of the percent variation from the optimum charge are also shown in Figure 4.4. These differences are presented as the difference between the actual efficiency and the efficiency recorded for the optimum charge

$$\eta_{dif}[\%] = \eta - \eta_{charge=3.4kg} \tag{4.4}$$

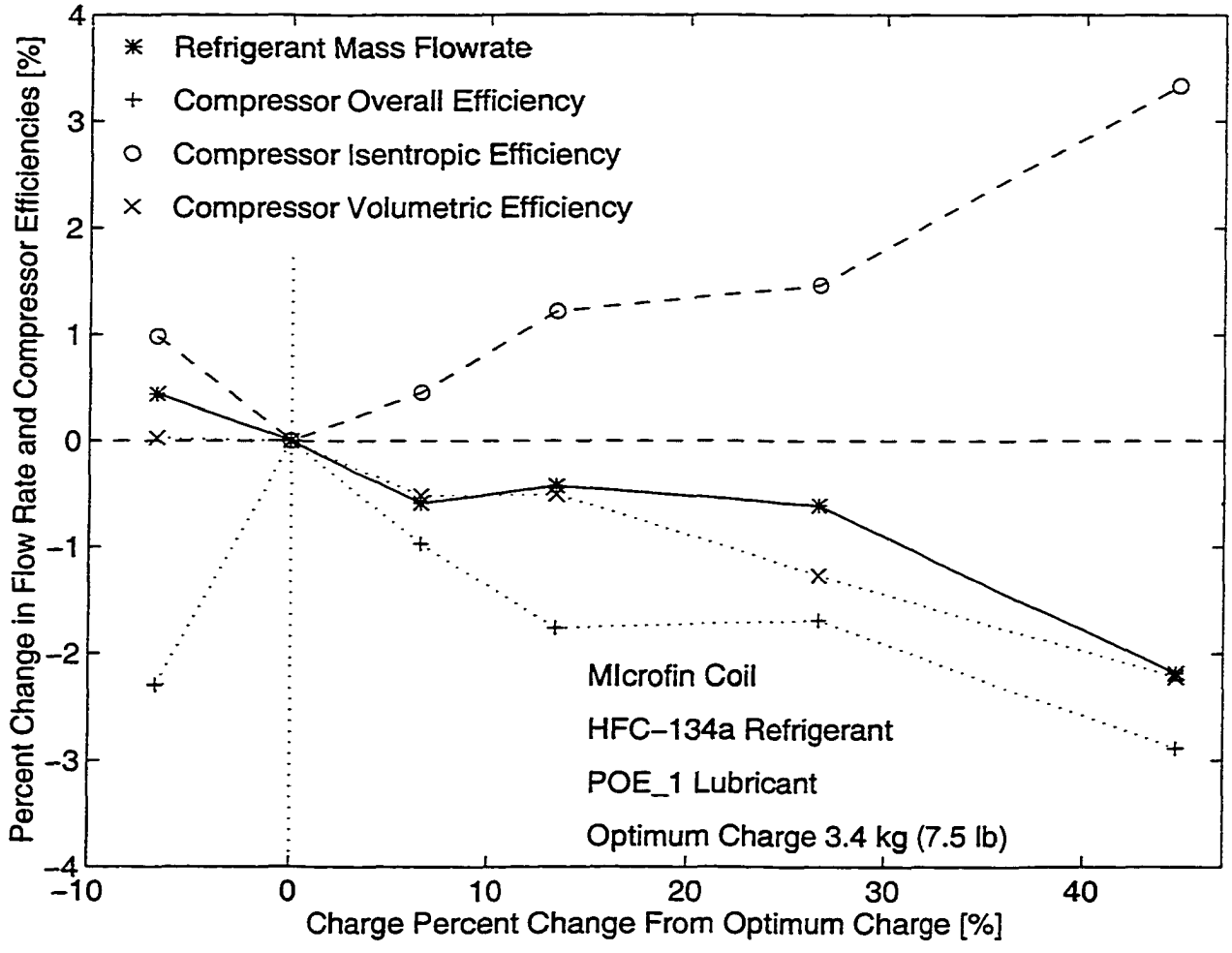

Figure 4.4. Percent change in flow rate and compressor efficiencies as a function of refrigerant charge in microfin-tube coil

Variations in the compressor volumetric efficiency and refrigerant mass flow rate with refrigerant charge are proportional since both parameters decrease with an increase in refrigerant charge. The same behavior is evident for compressor overall efficiency, with the only difference being that the peak efficiency coincides with the optimum charge. Isentropic efficiency behaves opposite to the other parameters presented in Figure 4.4 as the lowest efficiency coincides with the optimum charge. These variations in isentropic efficiency are caused by changes in refrigerant properties entering and leaving the compressor. The variations in suction and discharge compressor pressure are plotted in Figure 4.5 as differences between the measured pressure and the pressure for the optimum charge.

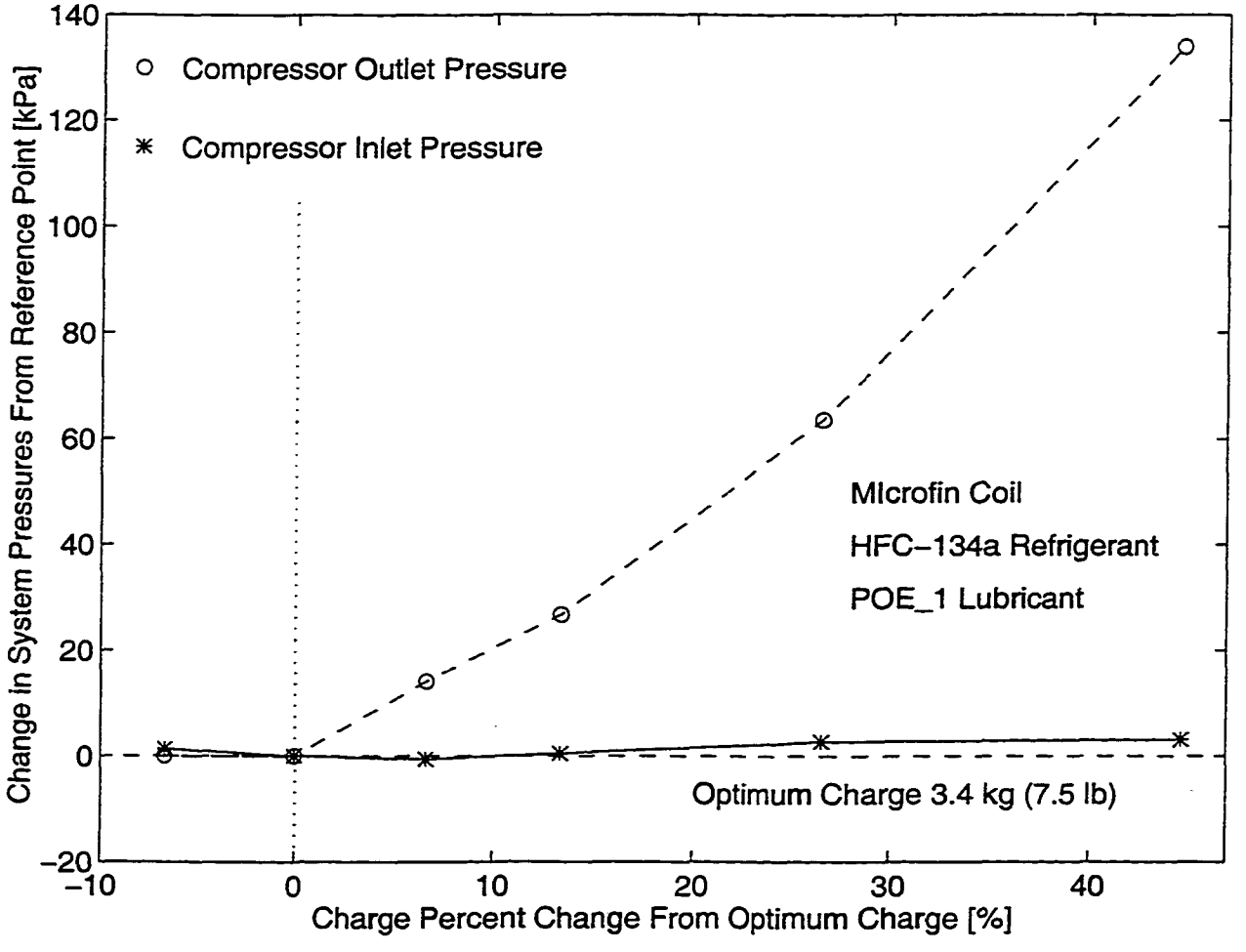

Figure 4.5. Change in pressure as a function of refrigerant charge in microfin-tube coil

It appears that the refrigerant charge has the largest effect on the compressor discharge pressure as presented in Figure 4.5. For example, for a 45 percent overcharged system the increase in discharge pressure is around 140 kPa (20 psi). On the other hand, the increase in the evaporator pressure with the charge increase is considerably smaller than that observed for discharge pressure e.g. for 45 percent overcharged condition, the evaporator pressure increases by about 4 kPa (0.6 psi) as shown in Figure 4.5.

A larger refrigerant mass (charge) in a constant volume system with relatively fixed temperatures results in larger pressures during system operation. This correlation between mass and pressure may be deduced from general trends in thermodynamic property relations. However, condenser pressure is considerably more sensitive to changes in refrigerant charge than evaporator pressure which is explained by the condenser having more degrees of freedom than the evaporator. Nevertheless, a question might be asked as to what actually happens with excess refrigerant in refrigeration system. Since the condenser has more degrees of freedom than the evaporator, the extra charge is stored in the condenser as subcooled liquid because liquid occupies the smallest volume. Thus, an increase in system charge results in larger liquid-refrigerant mass in the condenser and, consequently, a larger amount of subcooling. In order to accommodate more refrigerant in the condenser (i.e. an increase in the amount of subcooling) a smaller portion of condenser has to be occupied with two-phase flow which can only be accomplished by raising the condenser pressure and, therefore, reducing the refrigerant heat of evaporation. For instance, overcharging the system by 45 percent results in an increase in the amount of subcooling of 7 °C as shown in Figure 4.1.

The large increase in compressor discharge pressure due to overcharging leads to an increase in compressor power consumption as indicated in Figure 4.3. The compression work rate is proportional to the compression ratio, and since the discharge pressure increases for approximately constant evaporator pressure, the compression ratio increases, thus resulting in an increase of the compression work. Also, due to changes in the compressor discharge pressure, decreases also occur in volumetric efficiency and mass flow rate, as well as an increase in isentropic efficiency as reported in Figure 4.4.

In summary, of all the performance parameter, the compressor discharge pressure is the most sensitive to the refrigerant charge, and all other system performance changes are then the result of these pressure changes.

4.1.4 Charge Effects on System Performance with Smooth-Tube Coil

An investigation of charge effects on system performance was also performed for the test facility with the smooth-tube coil. The optimum charge was found to be 3.6 kg, which is larger than the optimum charge determined for the system with the microfin-tube coil. This difference in the optimum charge was expected since the physical size of the refrigeration system with smooth-tube coil is larger.

The main performance parameters, namely COP, capacity, and power consumption are plotted as functions of refrigerant charge in Figure 4.6

The percent difference in performance parameters are defined in Equation 4.2, and they are determined in reference to the magnitude for the optimum charge parameter. Similarly, the charge percent difference, which was defined earlier in Equation 4.1, was used to calculate the percent change from the optimum charge. The tests were conducted for an evaporator air temperature of 18.5 °C and a condenser water temperature of 32 °C.

The peak COP occurs at a charge of 3.6 kg of refrigerant. It is also evident that with charge variations of ±10 percent the COP changes less than 2 percent, which supports earlier results for the microfin-tube coil in that optimum charge is slightly larger than the cut-off charge. Further, the COP is not a strong function of charge as evident by the fact that the peak COP is relatively flat for variations of ±5 percent in the optimum charge.

It should be noted that three operating points were recorded with charges lower than the cut-off charge, as shown in Figure 4.6. For these points, there were no subcooling at the condenser exit, and therefore, the refrigerant flow rate was impossible to measure, resulting in refrigerant flow rate being calculated from the condenser energy balance.

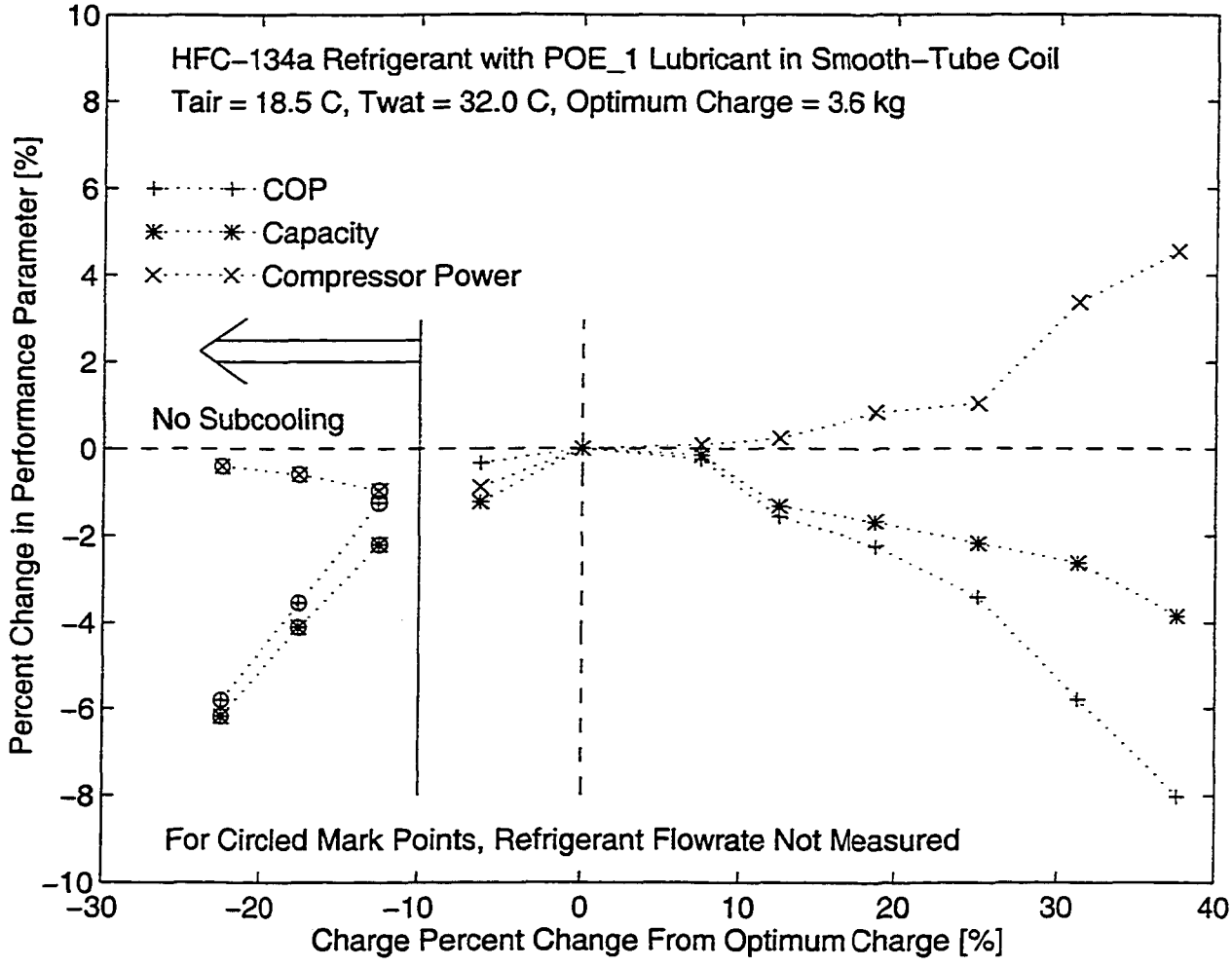

Figure 4.6: Percent change in performance parameters as a function of refrigerant charge in smooth-tube coil

Apparently for these undercharged conditions, there is a relatively large gradient in capacity leading to a drop in the COP.

As was found in the study with the microfin-tube coil, the compressor discharge pressure has the strongest dependence on refrigerant charge. This dependence can be observed in Figure 4.7 where the absolute difference in measured pressure and the pressure for the optimum charge, which was defined in Equation 4.9, are plotted as a function of the charge percent difference.

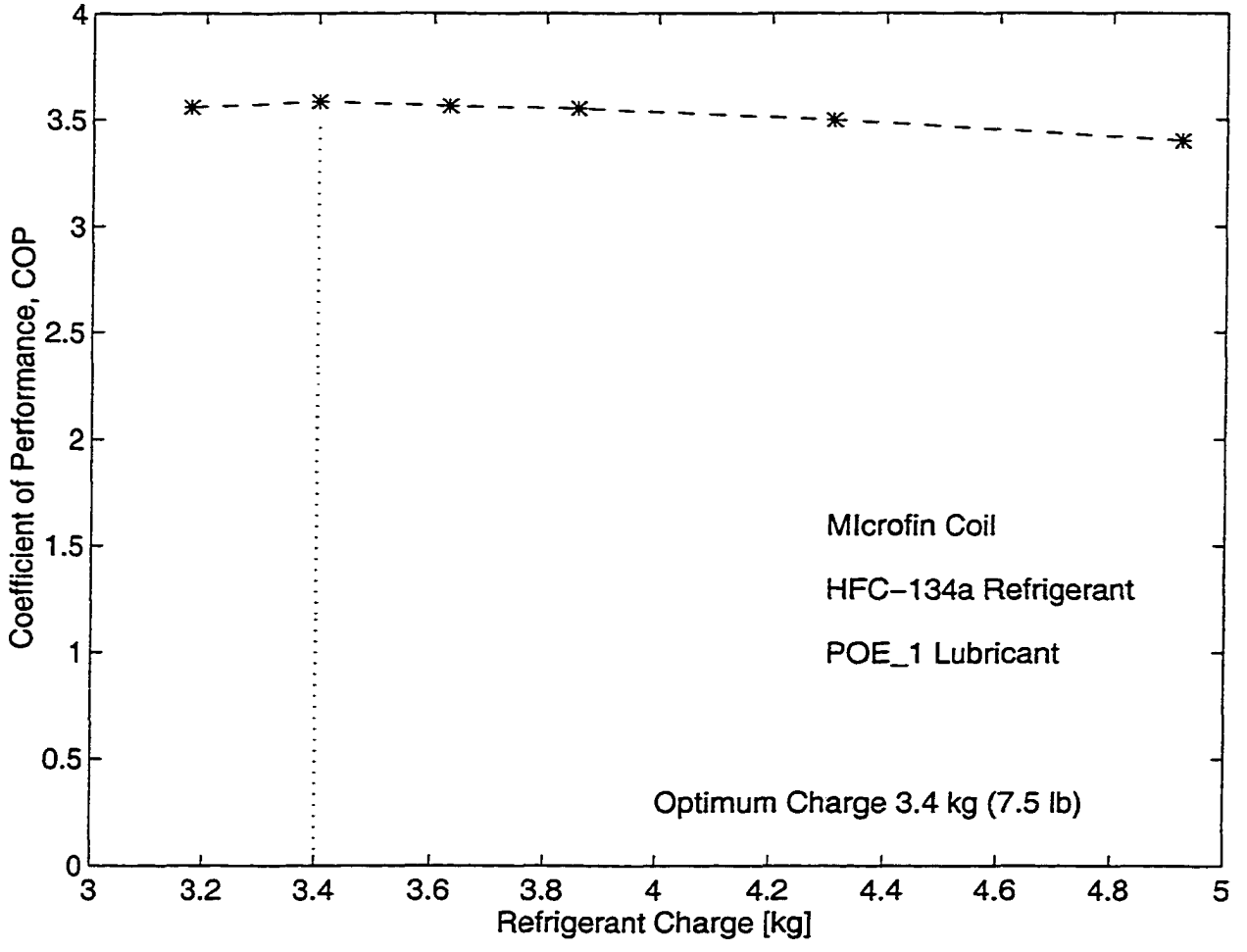

Figure 4.7. Change in pressure as a function of refrigerant charge in smooth-tube coil

The compressor discharge pressure increases with refrigerant charge. From the cut-off charge point to the 40 percent overcharged condition, the pressure difference is as high as 180 kPa (26 psi), representing a 20 percent increase over the pressure measured for the optimum charge. On the other hand, variations in the evaporator pressure are small being not larger than ±5 kPa (0.7 psi) for the entire range of charges used in study.

4.1.5 Effective Charge

The effective charge is the actual refrigerant charge reduced by the amount of refrigerant that is dissolved in the lubricant. As noted in Section 2.3.3, the HFC-134a refrigerant is highly soluble in POE lubricant, but poorly soluble in conventional mineral oils. Thus, for an equivalent actual charge, the system operating with POE lubricant would have a lower effective charge than the system operating with mineral oil. The difference in charges is equal to the amount of refrigerant dissolved in the POE assuming that no refrigerant dissolves in mineral oil.

An estimate of the amount of refrigerant dissolved in the lubricant can be obtained from the solubility data and information about the state of the oil/refrigerant mixture in the crankcase. The equilibrium solubility data is obtained from established experimental procedures as reported in Section 2.3.3. Since solubility data for HFC-134a and POE lubricant used in this study were not available it was decided to use Cavestri et al. (1993) solubility data provided in Tables 2.1 and 2.2. The selected POE lubricant has the same viscosity grade as the POE_1, and therefore, it was used to estimate amount of refrigerant dissolved in the lubricant.

When the air-conditioning system is not operating, its temperature is at a room temperature around 20 °C (70 °F) and at that temperature the refrigerant pressure in the system is at approximately 550 kPa (80 psi). At these conditions according to the solubility data, the amount of dissolved refrigerant is around 30 percent of oil mass. Since the oil mass in compressor is around 1.3 kg (2.8 lb), the amount of dissolved refrigerant is approximately 0.38 kg (0.84 lb) which corresponds to around 11 percent of total refrigerant charge.

When the system is operating, the compressor manufacturer reports the temperature of the lubricant in the crankcase to be between 45 °C (113°F) and 65 °C (149 °F) depending on compression ratio (Shimon, 1998). Shimon reported that the lubricant/refrigerant temperature was measured by the insertion of a thermocouple in the compressor oil sump and then measuring the temperature for a wide variety of operating conditions. The pressure in the compressor crankcase is the same as that of the evaporator with an average value for the data set of around 330 kPa. For these conditions in the compressor and by using Cavestri et

al. (1993) solubility data, the amount of dissolve refrigerant is around 8 percent of oil mass. This amount of refrigerant corresponds to approximately 4 percent of the refrigerant charge.

Estimates on the amount of dissolved refrigerant are based on solubility equilibrium data and since actual performance conditions in the compressor are not in equilibrium, it has been suggested by some authors, such as Short (1990), that estimates of refrigerant concentration in the lubricant might be inaccurate. Leung et al. (1998) measured absorption rates of several HFC refrigerants and a POE lubricant, and they reported for the conditions encountered in their study that it takes about one hour for POE lubricant to absorb all of the refrigerant HFC-134a that it can contain. The time needed to achieve a steady state operating point is around one hour, indicating that the actual amount of dissolved refrigerant could be adequately estimated with the equilibrium solubility data.

In can be concluded that the effective charge for the system with the mineral oil is larger than that for the POE lubricant. It can be inferred that amount of refrigerant dissolved in POE lubricant is between 11 and 4 percent of actual charge but most likely close to 4 percent.

This hypothesis of a difference existing for the effective charge is proven in the next section as the system performances with POE_1 and mineral oil are directly compared. A comparison of the compressor discharge pressure was utilized, and it was found that for the system operating with the mineral oil has a higher compressor discharge pressure, which was proportional to the differences in the effective charges between MO and POE_1.

4.1.6 Conclusions

The optimum charge is close to the cut-off charge, as was experimentally shown for two systems (i.e. with microfin-tube and smooth-tube coils). Due to the physical size of the system, the optimum charge is larger for system with the smooth-tube coil (3.6 kg) than for the system with the microfin-tube coil (3.4 kg). Charge effects on system performance were found identical for both systems.

The dependence of COP on refrigerant charge is not very strong as was indicated by the fact that variations in charge of ±10 percent of the optimum charge resulting in the COP reduction being not larger than the estimated uncertainty in COP of 1.1 percent. Therefore, the optimum charge determined for POE_1 lubricant was used to test other lubricants.

The system capacity peaks near the optimum charge and remains relatively constant for increases in refrigerant charge above the optimum charge (up to 40 percent). For undercharged conditions, as charge decreases capacity decreases while power consumption remains relatively constant resulting in a lower system performance.

On the other hand for overcharged conditions, an increase in power consumption for constant capacity causes a decrease in system performance. This increase in power consumption is due to an increase in the compressor discharge (condenser) pressure with excessive charge. The extra charge is stored in the condenser as liquid refrigerant. In order to accommodate such conditions, the condenser pressure has to increase and also as a result, the amount of subcooling increases, which can be directly observed in refrigeration system performance.

The refrigerant effective charge (i.e. the active charge during system operation) is different form the actual charge (i.e. the amount of refrigerant charged) by the amount of refrigerant dissolved in lubricant. For the same actual charge, it was estimated that the effective charge of the system operating with POE_1 lubricant would be 4 percent lower than the effective charge for the system operating with mineral oil. However, these small differences in the effective charges probably have an insignificant impact on system performance.

4.2 Effects of Lubricant/Refrigerant Miscibility

The performance of the POE_1 lubricant and the mineral oil (MO) with HFC-134a were examined for the system operating with microfin-tube coil. The comparison of system performance with these two lubricants is the basis for the investigation of the effects of lubricant miscibility. As mentioned earlier in the text, POE_1 is miscible while the mineral oil is immiscible with the HFC-134a refrigerant, however, both lubricants have the same viscosity grade and similar viscosity dependence on temperature as explained in Section 3.3.1. Therefore, testing lubricants with similar viscosity characteristics focuses the analysis to lubricant miscibility effects.

The results and analysis presented herein are performed by comparing the refrigeration system operating points corresponding to the same independent parameters (i.e. refrigerant charge; air and water inlet temperatures; air and water flow rates; and amount of superheat at the compressor inlet). Having all the independent parameters equal, enables one to determine lubricant effects on system performance.

4.2.1 COP

The COP is defined as the useful energy transfer (i.e. evaporator capacity) divided by the energy consumed (i.e., compressor power consumption), and it is plotted in Figure 4.8 for different operating conditions and for both lubricants. It is important to observe that the system operation is more efficient with the POE_1 lubricant than with the mineral oil. The results are consistent and since the COP is the most important indicator of refrigeration performance, it can be concluded that there is an energy saving potential related to the utilization of miscible over immiscible lubricant.

The differences in COPs for the two lubricants in Figure 4.8 appear to be of a smaller magnitude than the differences in COP due to variations in water and air temperatures. For instance the COP decreases for 25 percent if the water temperature is increased from 24 °C to

40° C, and it also decreases around 20 percent if the air temperature is reduced from 24 °C to 13 °C. The largest differences in COP due to lubricant type are around 5 percent.

An alternative presentation of the results given in Figure 4.8 is presented in Figure 4.9 where percent COP difference is plotted as function of operating temperatures. The percent COP difference, COP_{dif}, is defined as the difference between the COPs for the POE lubricant and the mineral oil divided by the COP for the mineral oil lubricant with the value expressed as a percentage.

$$COP_{dif}[\%] = \frac{COP_{POE_1} - COP_{MO}}{COP_{MO}} 100 \tag{4.5}$$

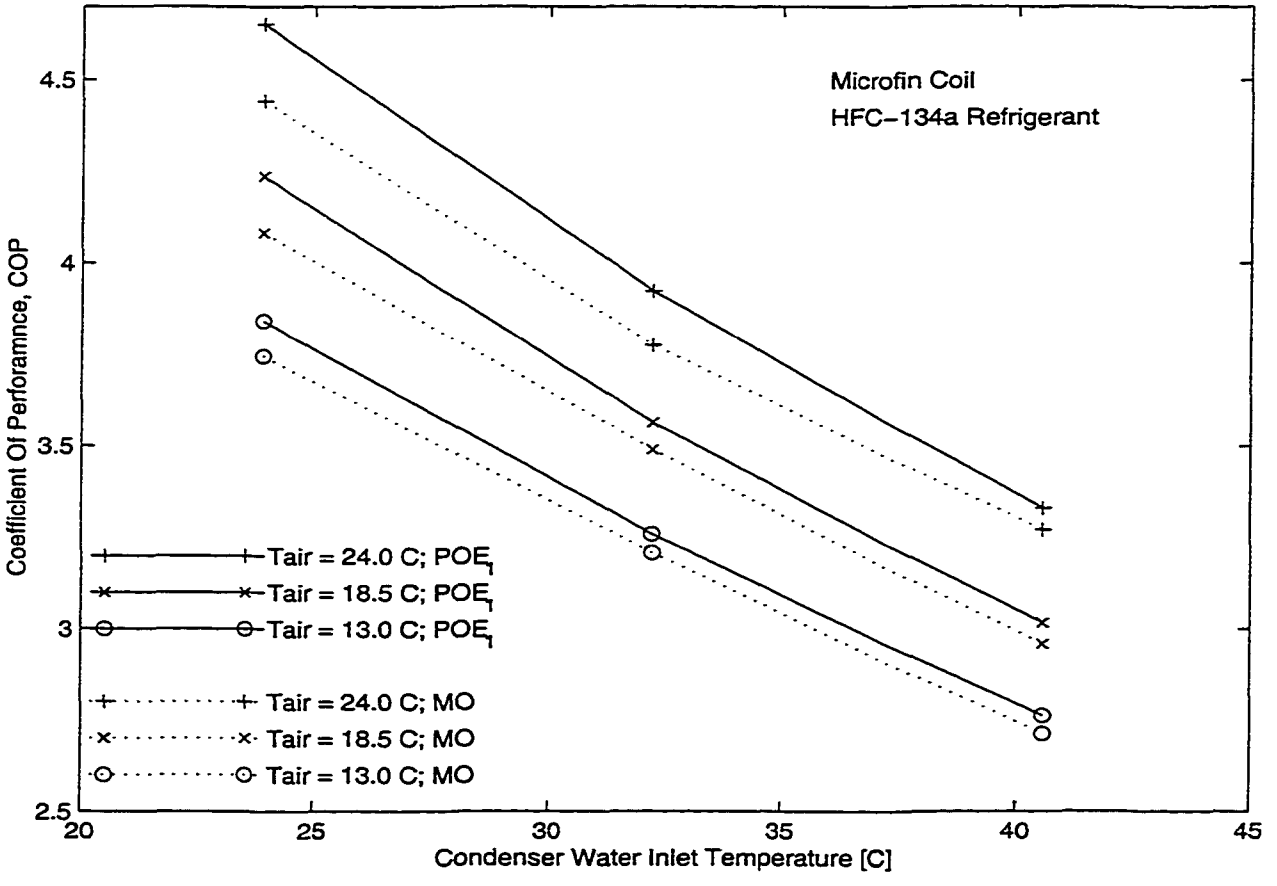

Figure 4.8. COP for POE_1 and MO with microfin-tube coil

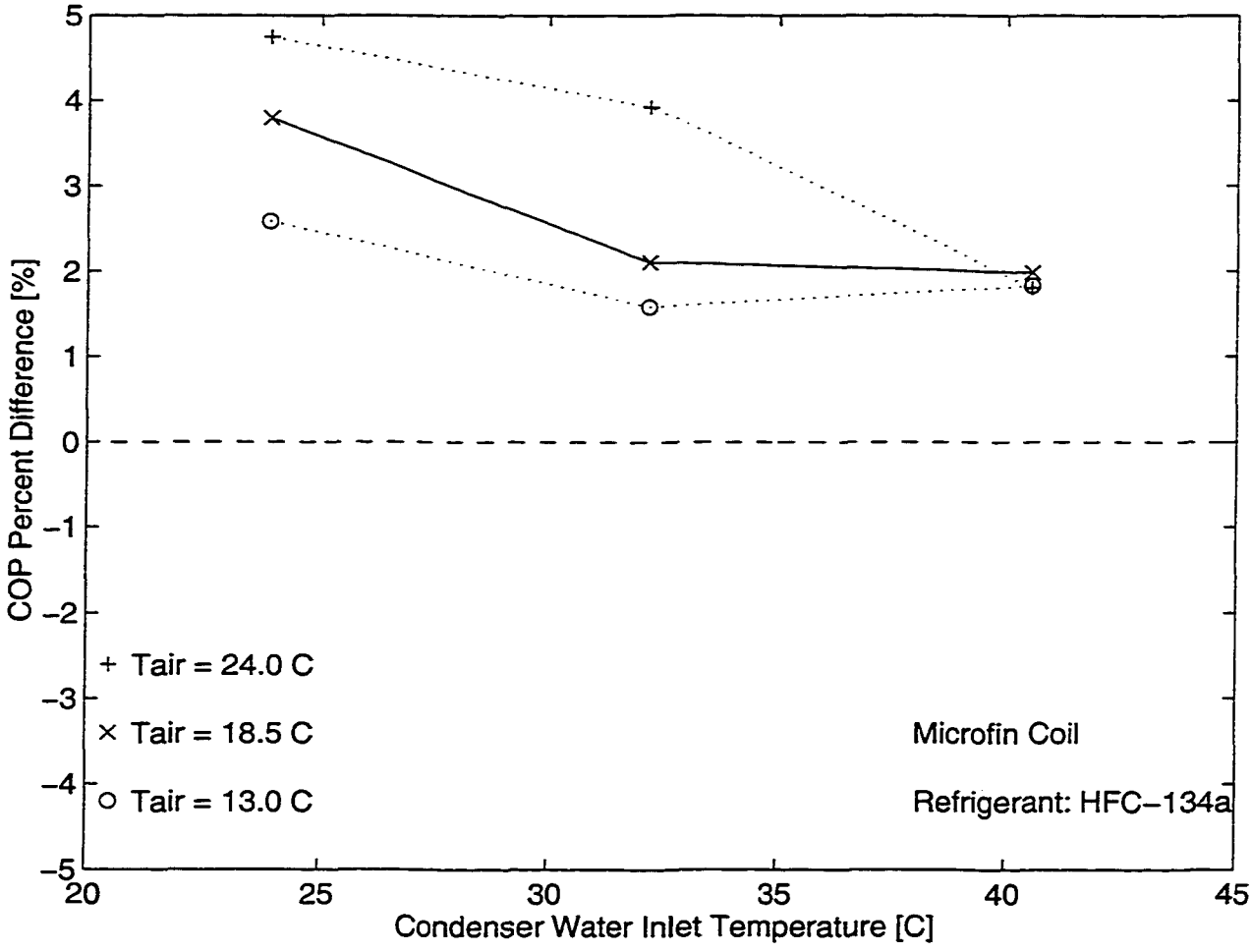

Figure 4.9. COP percent difference for POE_1 and MO with microfin-tube coil

Using this approach, the results clearly indicate that the system operating with the POE_1 lubricant has a larger COP than the system operating with the mineral oil. The COP percent differences are as high as 5 percent, and the largest percent differences correspond to the points with the highest evaporator temperature of 24 °C (75 F) and the lowest condenser water temperature of 24 °C (75 F). Also, it should be noted that the COP percent difference appears to decrease with an increase in water temperature and a decrease in air temperature. Only for the highest condenser water temperature of 40 °C (105 °F) do the differences among COP percent differences for different air temperatures disappear. The actual data presented in Figures 4.8 and 4.9, as well as data plotted in the remainder of the text, are provided in Appendix C.

Based on the measured parameters, the uncertainty in COP derived from the propagation-of-error method is around ± 0.03 or around ± 0.8 percent of the average COP in a data set, as was presented in Section 3.1.3 and reported in Table 3.3. Since all COP values for the POE_1 lubricant exceeded the COP values for MO by more than the estimated uncertainty, it can be concluded that observed differences in COP are large enough to be regarded as significant. In addition, the uncertainty for COP percent difference is around ± 1.1 percent which is a smaller value than any COP percent differences for the two lubricants which are between 1.5 and 5 percent.

The above results suggest that for an air conditioning application operating with air entering at 24 °C (75 F) for every $1000 spent on operating the refrigeration system there is the $50 potential saving in utilizing the POE_1 lubricant over the mineral oil in the compressor.

In order to further explore possible reasons for the better system performance with the miscible lubricant compared to the immiscible lubricant, further analyses of performance parameters are required. Capacity and compressor power consumption, as well as some other important parameters, are investigated below.

4.2.1 Evaporator Capacity

Evaporator capacity or cooling effect (i.e., the heat transfer rate from the air to the refrigerant in the evaporator) for the microfin-tube coil is shown as function of different operating conditions in Figure 4.10. The capacity for the mineral oil data is less than the capacity of the corresponding POE_1 lubricant data. However, these differences in capacity due to lubricant type (the largest is around 2 percent) are not as large as differences due to changing inlet air temperature and water inlet condenser water temperature. For instance, a change in the air temperature from 24 °C to 13 °C results in a 25 percent reduction in the capacity, while a change in water temperature from 24 °C to 40 °C results in a 15 percent reduction in the capacity.

In order to better illustrate differences in capacity due to lubricant type, the percent capacity differences between matching points are plotted against different operating conditions for the microfin-tube coil in Figure 4.11. The capacity percent difference is calculated in the same manner as the COP percent difference defined in Equation 4.5.

$$\text{Capacity}_{\text{dif}} = \frac{\text{Capacity}_{\text{POE}_1} - \text{Capacity}_{\text{MO}}}{\text{Capacity}_{\text{MO}}} 100 \tag{4.6}$$

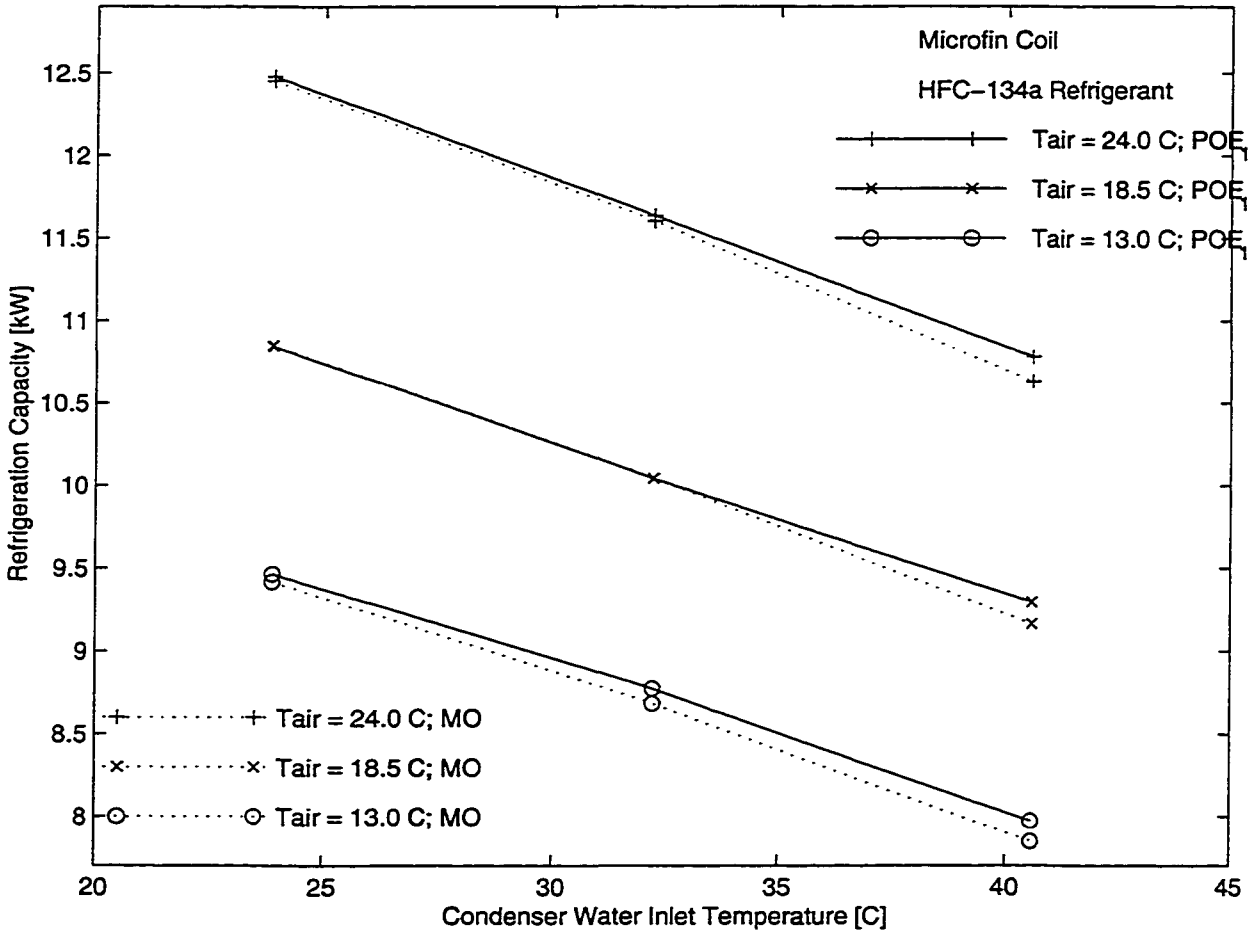

Figure 4.10. Capacity for POE_1 and MO with microfin-tube coil

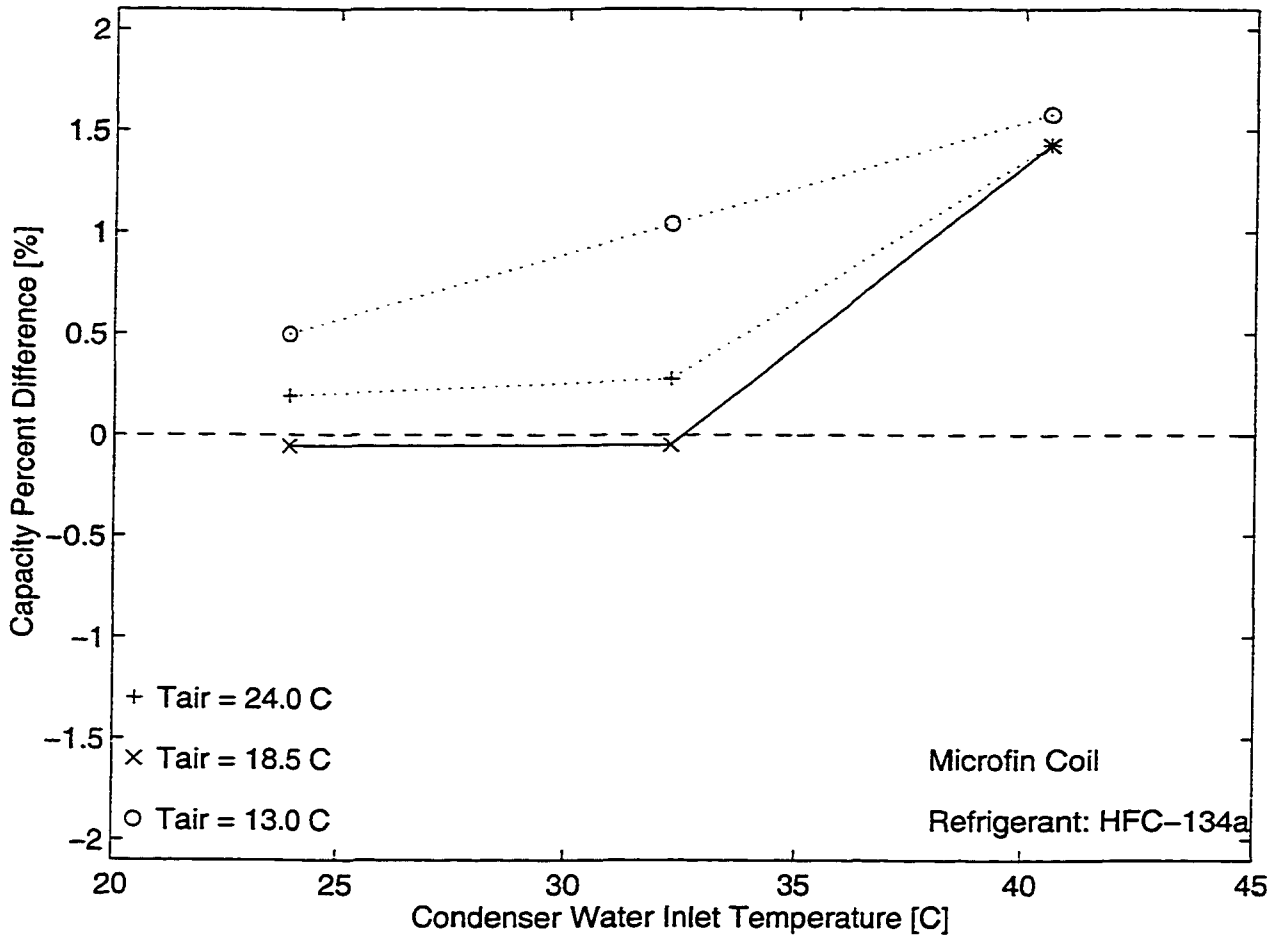

Figure 4.11. Capacity percent difference for POE_1 and MO with microfin-tube coil

The results presented in Figure 4.11 indicate that the POE_1 lubricant data show a higher capacity than the mineral oil data for a majority of points. The maximum difference is around 2 percent, which corresponds to the points at the highest condenser water temperature of 40 °C (105 F). As the water temperature decreases, the capacity percent differences decrease.

The uncertainty in capacity percent difference was reported to be around ± 0.4 percent in Section 3.1.3, and therefore, it can be concluded that observed differences in capacities between POE_1 and MO data in Figure 4.11 are less than the estimated uncertainty for some tested points. Nevertheless, many of the tests indicate a higher capacity for the POE_1 lubricant which could possibly be due to a larger evaporation heat transfer coefficient for the POE and HFC-134a mixture. As reported previously in Section 2.5.3,

miscible lubricants have been reported in the literature to result in larger refrigerant heat transfer coefficients during evaporation when compared to immiscisble lubricants.

Evaporator capacity for a given coil is proportional to the product of the overall heat transfer coefficient and the mean temperature difference between the refrigerant and air. An increase in the refrigerant-side heat transfer coefficient contributes to an increase in the overall heat transfer coefficient which, in turn, can result in the need for a smaller mean temperature difference between the refrigerant and air in order to achieve the same capacity. If the POE_1 has a higher refrigerant-side heat transfer coefficient with HFC-134a than the MO, then the temperature difference between refrigerant and air in the coil should be lower for POE_1 than for MO. In other words, since the air temperature is fixed (i.e. independent parameter), the observed refrigerant temperature should be higher for the POE_1 than for the MO.

A representative refrigerant temperature in the evaporator is the refrigerant saturation temperature with the reason being that 90 or more percent of the heat transfer occurs in a region where refrigerant is in the two-phase region. In addition, the refrigerant saturation temperature corresponds to a unique saturation pressure, so that a higher saturation temperature results in a higher saturation pressure. Therefore, in order to support the hypothesis of a higher heat transfer coefficient in the evaporator for POE_1, a higher pressure should have been recorded for POE_1 data.

These differences in pressure were indeed observed experimentally in that the evaporator pressure (which as discussed above is also a measure of refrigerant temperature based on saturated conditions) was consistently higher for the POE_1 than for the MO, being around 4 kPa or 1.5 percent higher for the POE case as shown in Figure 4.12. The pressure differences plotted in Figure 4.11 are obtained using the following equation

$$\mathrm{Pressure}_{dif} = \mathrm{Pressure}_{POE_1} - \mathrm{Pressure}_{MO} \tag{4.7}$$

The actual data is contained in Appendix C. It should also be noted that the higher evaporator pressure for the POE_1 compared to the MO leads to a lower refrigerant specific volume at the compressor inlet for POE_1, which in turn, results in a larger amount of

refrigerant being circulated through the system. The relationship between flow rate and specific volume is evident in Equation 4.8 by noting that the refrigerant mass flow rate, $\dot{m}$, is proportional to the ratio of the compressor volumetric efficiency, η_{vol}, and the refrigerant specific volume at the compressor inlet, v_{suc}, assuming that the piston displacement volume, RPD, and rotational speed, rpm, are constant.

$$\dot{m} = \frac{RPD\, rpm}{v_{suc}} \eta_{vol} \tag{4.8}$$

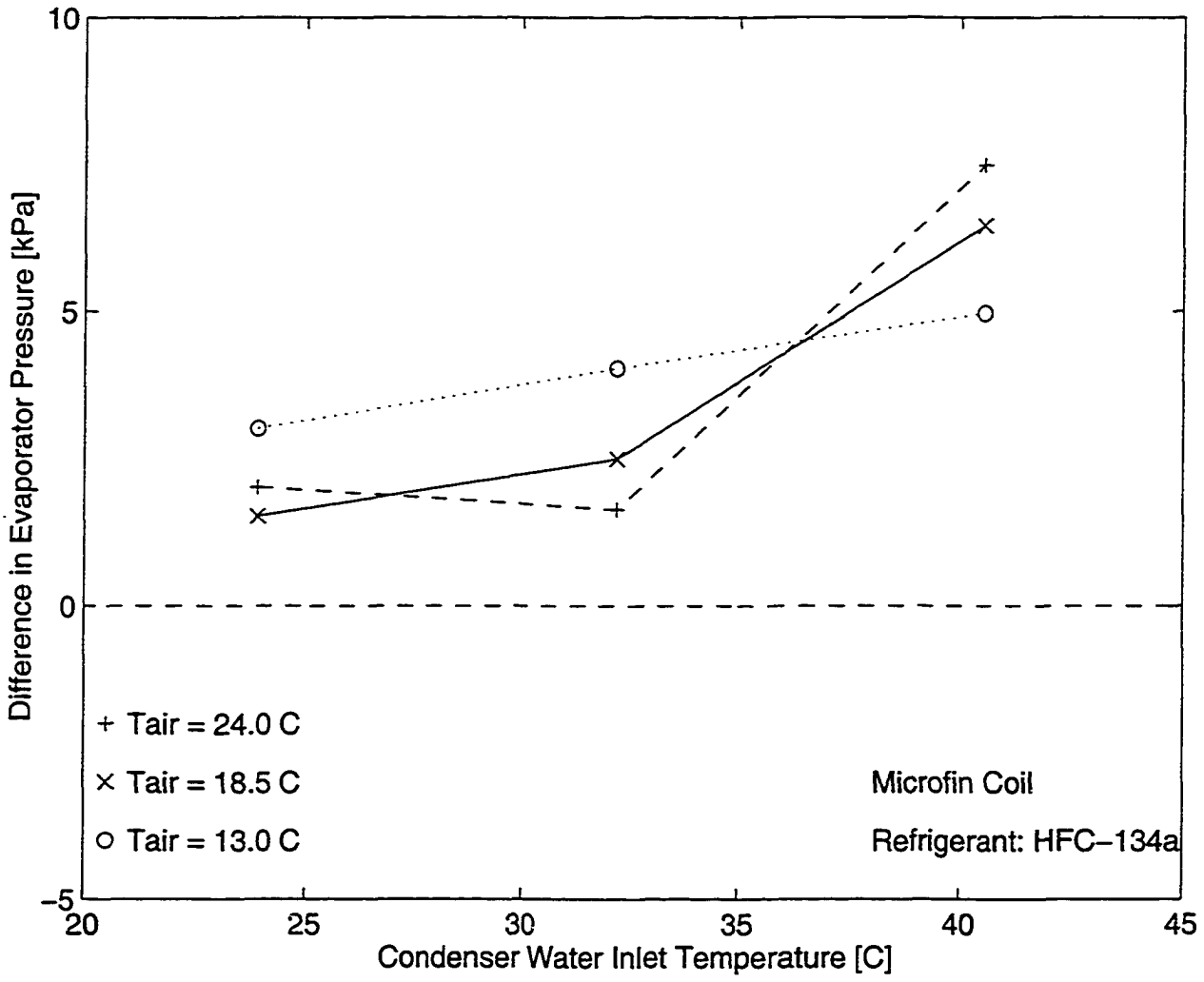

Figure 4.12. Difference in compressor suction pressure POE_1 and MO with microfin-tube coil

The differences in volumetric efficiencies due to the lubricant type were found to be negligible for these two lubricants, the largest being only around 0.2 percent, which is less than the estimated uncertainty of 0.34 percent for the volumetric efficiency, (reported earlier in Table 3.3). Thus, it can be inferred that differences in flow rates and, hence, capacities must be due to differences in suction specific volumes.

As shown in Figure 4.13 there are no significant differences in compressor volumetric efficiencies for the POE_1 and the MO, and therefore, all variations in refrigerant properties at the compressor inlet are accounted for by differences in the refrigerant mass flow rate.

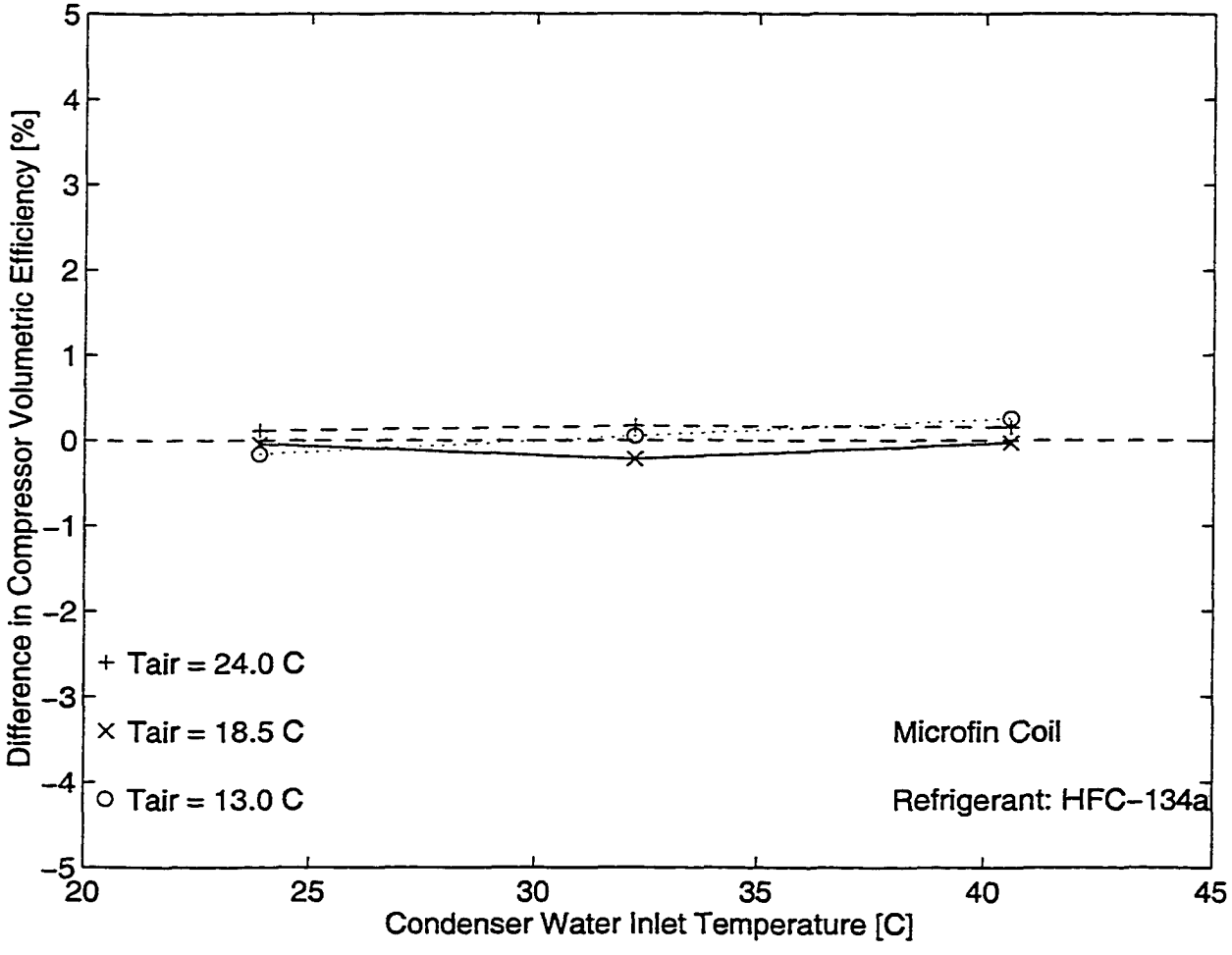

Figure 4.13. Difference in compressor volumetric efficiency for POE_1 and MO with microfin-tube coil

The refrigerant flow rate percent difference is determined similar to COP and capacity percent differences, and it is plotted as a function of operating conditions in Figure 4.14 below.

$$\dot{m}_{dif} = \frac{\dot{m}_{POE_1} - \dot{m}_{MO}}{\dot{m}_{MO}} 100 \tag{4.9}$$

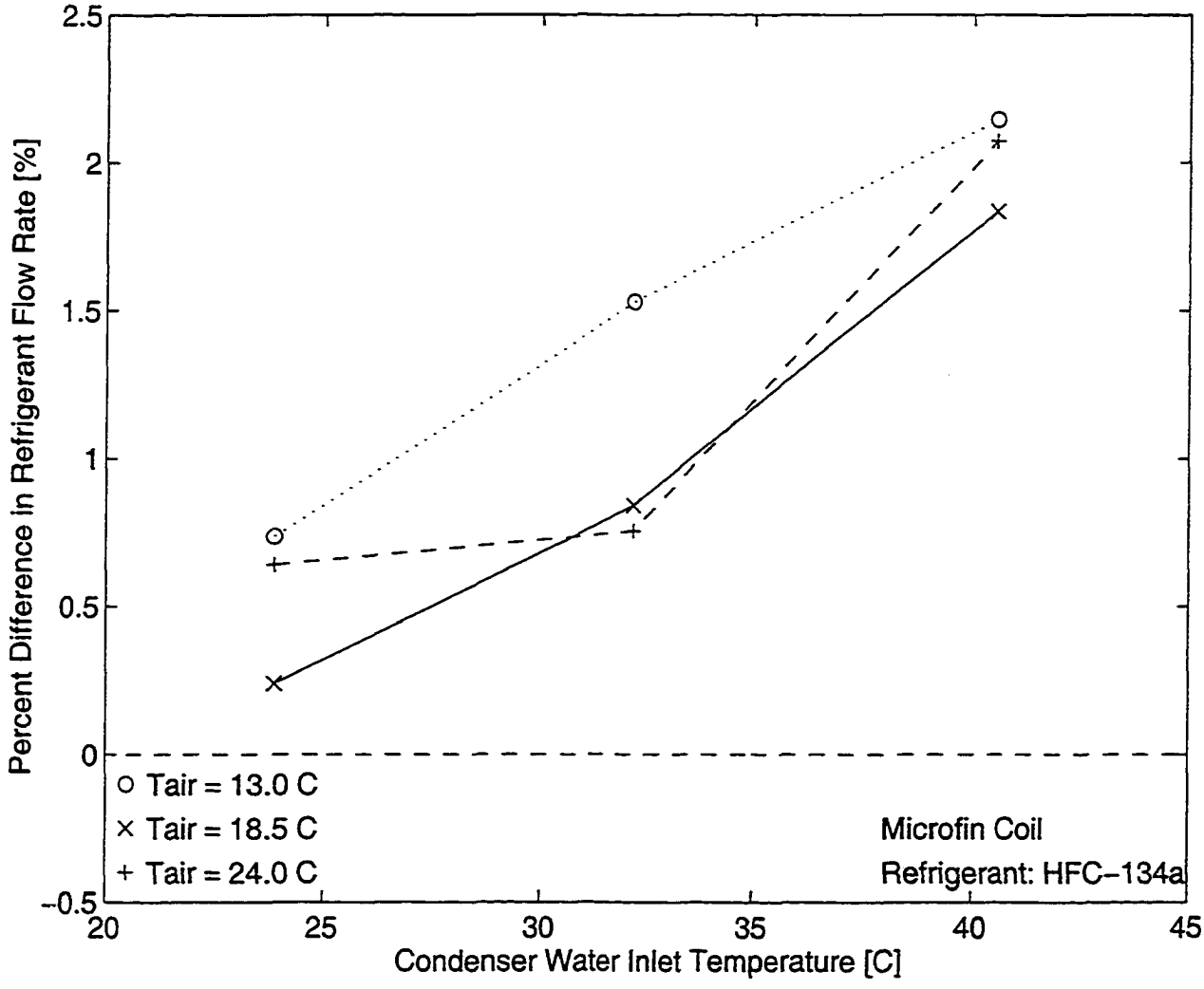

Figure 4.14. Percent difference in refrigerant flow rate for POE_1 and MO with microfin-tube coil

Specifically, the measured refrigerant flow rates for the POE case were about 0.5 to 2 percent higher than the MO flow rates. It is important to note that the uncertainty in the measured flow rate shown in Table 1 is about 0.2 percent. As stated earlier, the evaporator capacity differences are about 2 percent, which are similar to the differences found in flow rates.

Since the evaporator capacity is the product of the flow rate and the enthalpy change across the evaporator on the refrigerant side, the effect of enthalpy change should also be investigated. In this study, the differences in enthalpy change between POE and MO cases were small, with the enthalpy change being larger for the MO lubricant by about 0.5 percent compared to the POE lubricant. This difference in enthalpy of 0.5 percent is similar to the estimated uncertainty in the enthalpy change which is around 0.35 percent.

4.2.3 Compressor Power Consumption

The power consumption is larger for the compressor operating with the mineral oil than with the POE_1 lubricant as shown in Figure 4.15 for different operating conditions. The largest variations in the power consumption due to the lubricant type are around 5 percent.

Variations in the compressor power consumption due to lubricant type are smaller than variations due to changing air and water temperatures. For instance, an increase in the water temperature from 24 °C to 40 °C results in an increase in the power consumption of 16 percent while a decrease in air temperature from 24 °C to 13 °C results in a decrease in power consumption of 12 percent.

The power consumption data is also presented as the percent difference between POE_1 and mineral oil for different air and water inlet temperatures in Figure 4.16.

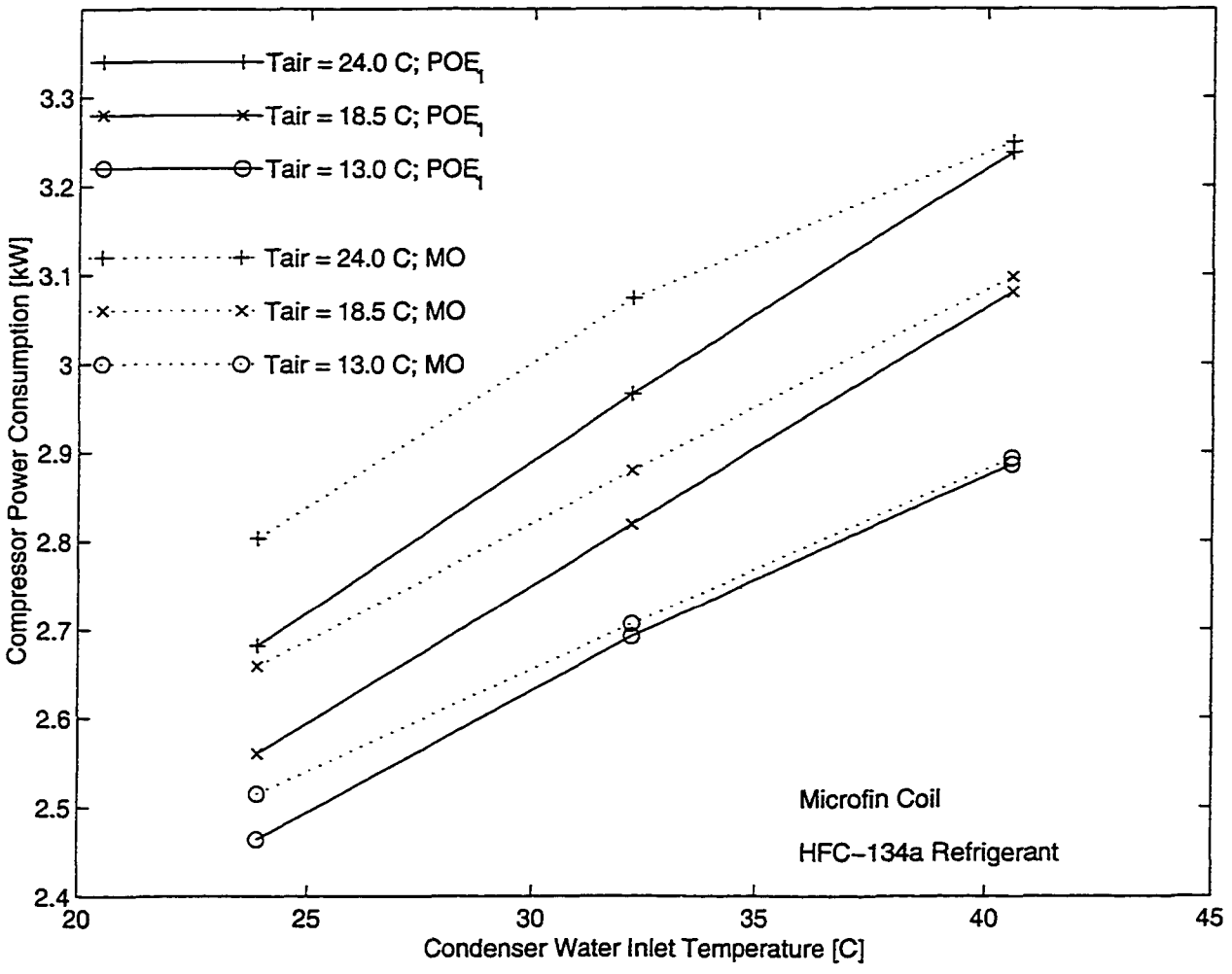

Figure 4.15. Compressor power consumption for POE_1 and MO with microfin-tube coil

The power percent difference is defined in the same manner as the COP and the capacity percent differences presented earlier in Equations 4.5 and 4.6.

$$\text{Power}_{dif} = \frac{\text{Power}_{POE_1} - \text{Power}_{MO}}{\text{Power}_{MO}} \tag{4.10}$$

The results in Figure 4.16 consistently show less power consumption for the compressor operating with the POE_1 lubricant than the compressor operating with the

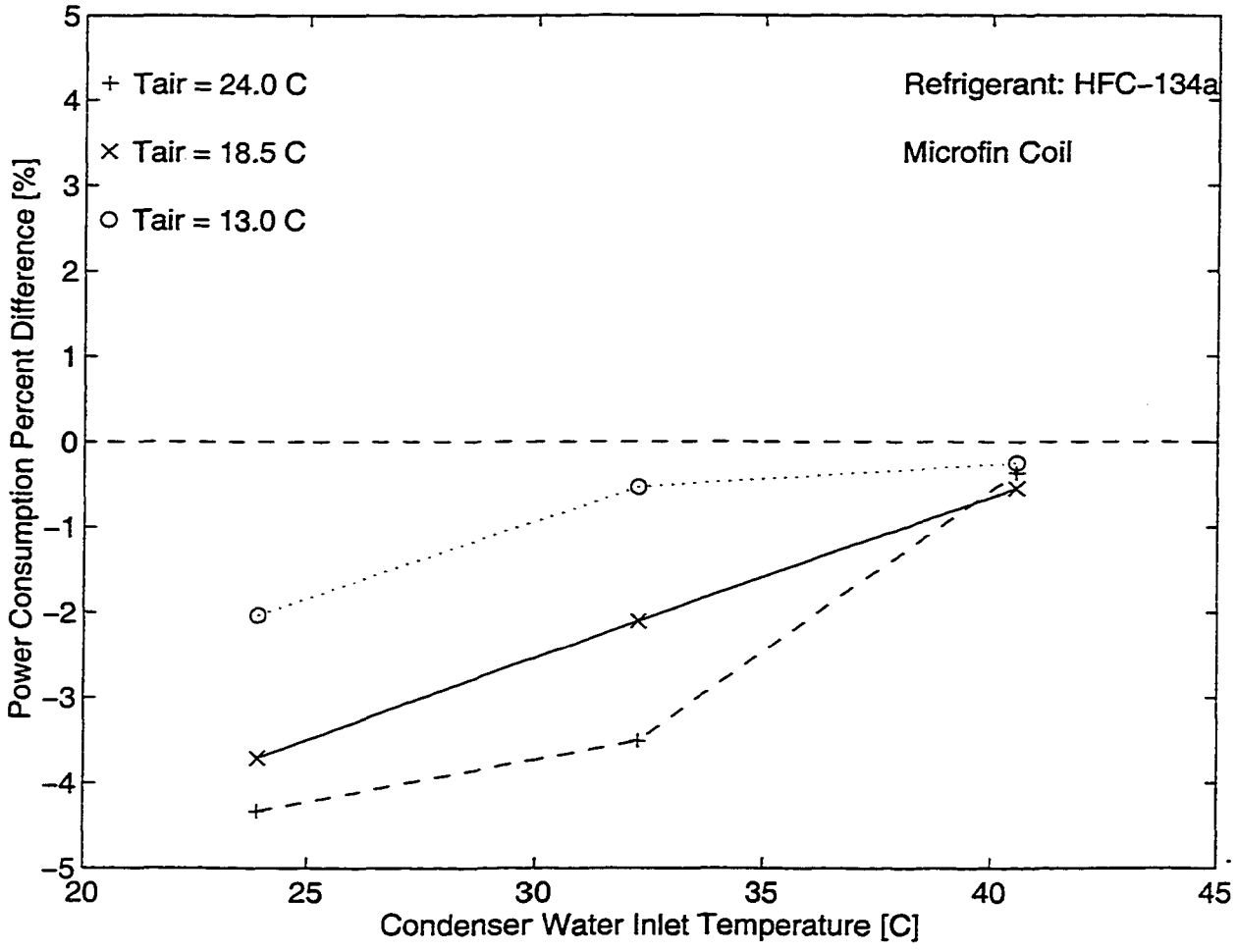

Figure 4.16. Percent difference in compressor power consumption for POE_1 and MO with microfin-tube coil

mineral oil. The largest difference is almost 5 percent, and it appears that the lower the water inlet temperature then the larger is the percent difference in power consumption.

The uncertainty calculated for the power percent difference is around 1 percent and observations of Figure 4.16 show that for most of the power consumption data for the MO exceeds that of the POE_1 by more than 1 percent. Only for the highest condenser water temperature is the difference in power consumption less than the estimated uncertainty.

Compressor power consumption is affected by refrigerant flow rate and system pressure, and, as noted earlier, these parameters can vary for the POE and the MO cases. Popovic and Shapiro (1995) showed that the compressor power consumption is proportional

to the work rate of polytropic compression, given below in Equation 4.11. According to the Popovic and Shapiro (1995) model, the polytropic exponent, n, is a strong function of refrigerant type and operating conditions and, thus, it is assumed to be the same for both the POE and MO lubricant cases.

$$\dot{W} = \dot{m}\left(\frac{n}{n-1} p_{suc} v_{suc}\left(\left(\frac{p_{dis}}{p_{suc}}\right)^{n-1/n} - 1\right)\right) \tag{4.11}$$

where:

$\dot{W}$ *compressor power consumption*

$\dot{m}$ *refrigerant mass flow rate*

p_{dis} *compressor discharge pressure*

p_{suc} *compressor suction pressure*

v_{suc} *compressor suction specific volume*

n *compression polytropic exponent*

Using this equation to calculate power for the POE_1 and MO case, it was found that the compressor employing MO results in a higher power consumption by about 0.4 to 2 percent compared to the POE_1. These calculated differences are less than the measured differences in the power consumption, which were as high as 5 percent, as presented earlier in Figure 4.16. It can be concluded that all differences in power consumption are not accounted for by the variations in the operating parameters in Equation 4.11. One possible explanation is the differences that exist in the miscibility characteristics of the refrigerant/lubricant mixtures. Since the POE_1 is miscible with HFC-134a inside the compressor, it has a lower effective viscosity than the MO during operation.

Assuming that HFC-134a is insoluble in MO, the difference in effective viscosity for POE_1 and MO can be approximately estimated using equilibrium solubility data. As described in Section 2.5.2, the temperature of lubricant/refrigerant mixture in compressor sump is proportional to compression ratio. For a given temperature and pressure (evaporator pressure) the equilibrium solubility data of Cavestri et al. (1993) can be used to predict that

about 8 percent of the refrigerant is dissolved in the POE_1 lubricant, which represents around 4 percent of the refrigerant charge.

A comparison of the compressor discharge pressure for the POE_1 and MO is presented in Figure 4.17 where the absolute difference between measured pressures for POE_1 and MO are plotted for different operating temperatures. The results support the hypothesis presented above that due to the different solubility characteristics of POE_1 and MO with HFC-134a, a difference in the effective charge exists, and consequently, the effective viscosity of the lubricants are different. As explained in section 4.1.4, the magnitude of the compressor discharge pressure is highly dependent on the amount of the excess charge. Referring to Figure 4.1.5, the difference in discharge pressure for a 4 percent overcharged conditions is around 10 kPa. This difference is comparable to the results presented in Figure 4.17 in which the discharge pressure for the MO data is higher than the pressure by POE_1 data for around 10 kPa.

Using the analytical equation developed for equilibrium solubility data, i.e. Equation 2.3, the actual viscosity of POE_1 is around 40 percent lower than the viscosity of pure POE_1 at the same temperature. Since the POE_1 and MO have a similar viscosity dependence on temperature, it can be concluded that the effective viscosity of MO is around 40 percent higher than the effective viscosity of POE_1 in the compressor sump for equilibrium conditions. Finally, it can be speculated that due to the higher effective viscosity of MO, and therefore, the higher friction, the compressor consumes more energy operating with MO than POE_1. This amount of energy consumption difference due to lubricant viscosity has been approximated earlier in this section using Equation 5.2.7 in which the effects of other performance parameters were estimated to be only between 0.5 and 2 percent.

A difference in compressor discharge pressure indicates a difference in refrigerant effective charge. The effective charge concept was introduced in Section 4.1.4, and it represents an active amount of refrigerant present during actual system operation. The differences in discharge pressure are related then to the solubility characteristics between the refrigerant and lubricant.

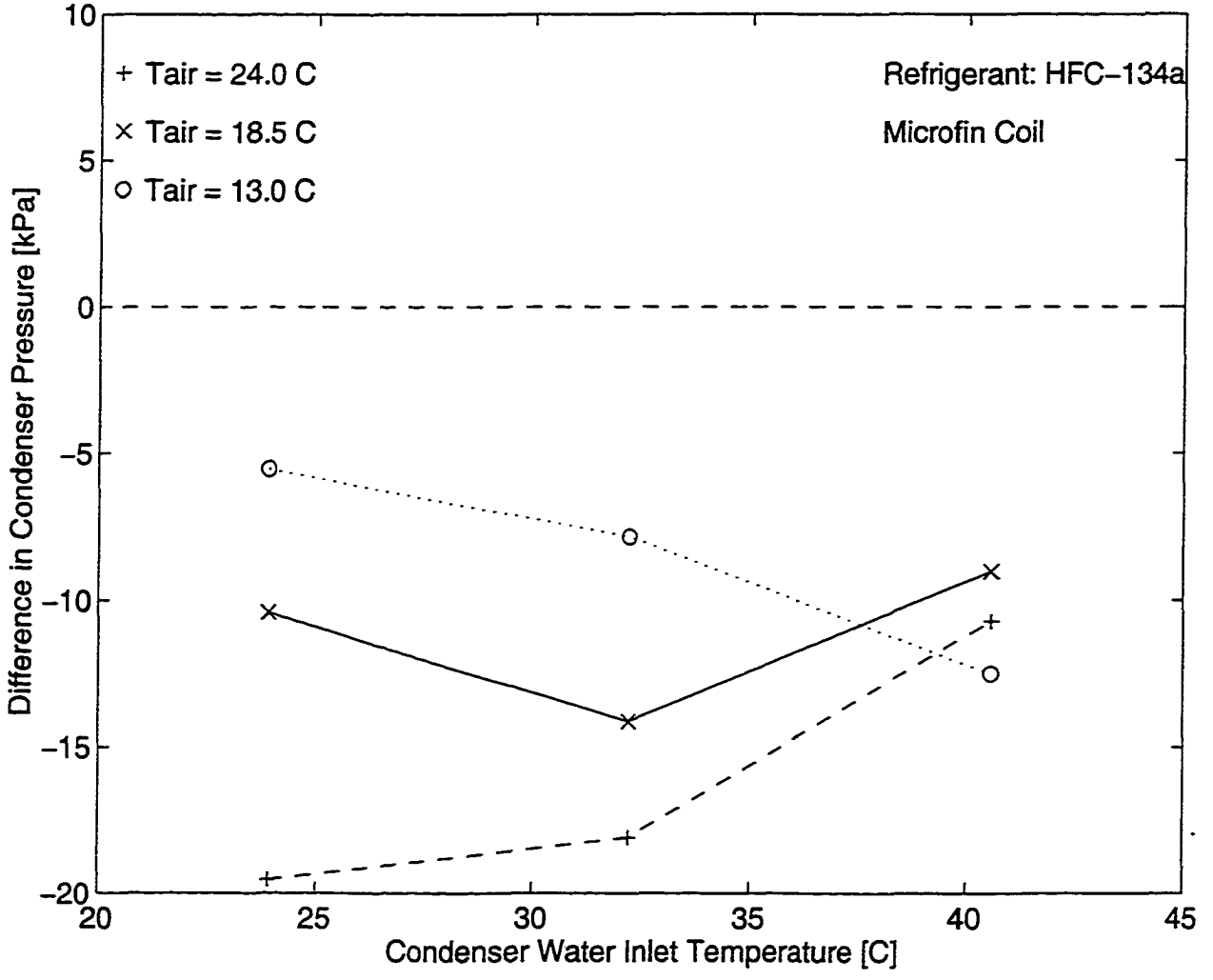

Figure 4.17. Difference in compressor discharge pressure POE_1 and MO with microfin-tube coil

Since the discharge pressure is consistently higher for the MO, this is an indication that the refrigerant effective charge for the MO is higher than for the POE_1. These results are in agreement with the assumption that HFC-134 is more soluble in the POE_1 than in MO.

4.2.4 Compressor Efficiencies

Differences between compressor isentropic efficiencies for POE_1 and MO are plotted in Figure 4.18 where the difference is

$$\eta_{I,diff} = \eta_{I,POE\_1} - \eta_{I,MO} \tag{4.12}$$

The differences in isentropic efficiency for most of the points are smaller than one percent, and with an uncertainty in the efficiency difference of around ±1 percent, it can be concluded that differences are insignificant.

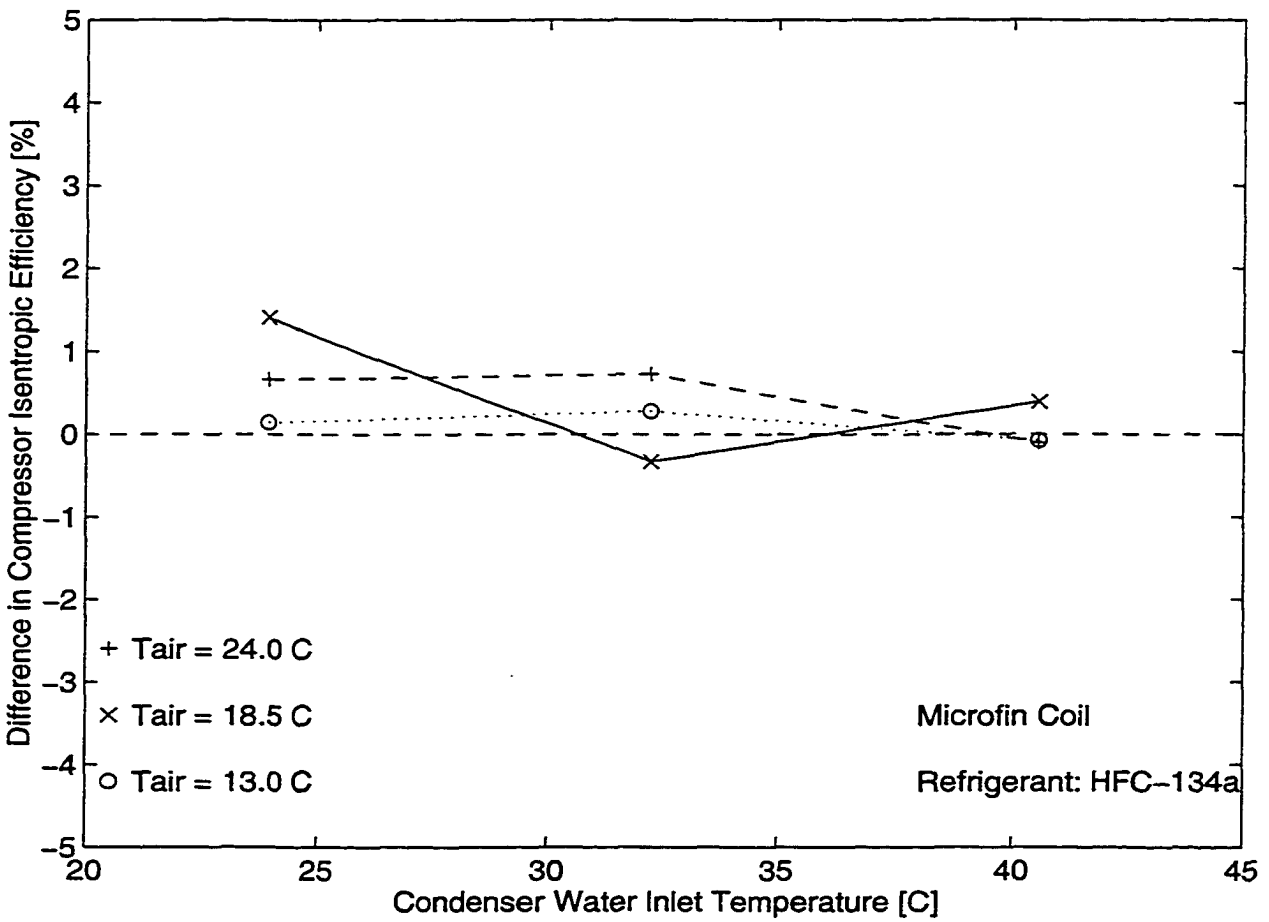

Figure 4.18. Difference in compressor isentropic efficiency for POE_1 and MO with microfin-tube coil

A comparison of volumetric efficiency for POE_1 and MO was presented earlier in Figure 4.13. The differences in volumetric efficiency were smaller than the estimated uncertainty for volumetric efficiency. Based on experimental data used to calculate volumetric and isentropic compressor efficiencies, it can be concluded that system performance differences due to the lubricant miscibility are affected more by the evaporator performance than the compressor performance.

4.3 Effects of Viscosity among Miscible Lubricants

Another miscible lubricant, namely POE_2, was selected for study with the goal of comparing difference in system performance among miscible lubricants with different viscosities. The POE_2 is miscible with HFC-134a refrigerant for all operating temperatures used in testing. The performance of the POE_2 lubricant was examined for the system operating with microfin-tube coil so that it can be directly compared to the performance results of POE_1. The comparison of system performance for these two lubricants, i.e. POE_1 and POE_2, was intended to provide understanding of the effects of lubricant viscosity for miscible lubricants. As mentioned earlier in the text, the POE_1 has a higher viscosity grade (ISO 32) than the POE_2 (ISO 22). Their viscosity dependence with temperature is different in that they have a similar viscosity at around 100 °C but as the temperature decreases then the differences in viscosity increase as explained in Section 3.3.1. Testing miscible lubricants with different viscosities focuses the effects of lubricant viscosity on system performance.

As stated earlier in Section 4.2, the results and analysis presented herein are performed by comparing the refrigeration system performance at the same values of the independent parameters (i.e. refrigerant charge; air and water inlet temperatures; air and water flow rates; and amount of superheat at the compressor inlet). Having all the independent parameters equal, results that system performance differences are due entirely to differences in the lubricants.

4.3.1 COP

The COP is plotted in Figure 4.19 as a function of condenser water inlet temperature and evaporator air inlet temperature for POE_1 and POE_2 lubricants. The COP is plotted on an expanded scale in order to better view the effects of the lubricant on system performance. It is apparent that the system performance for both POEs follows similar trends as the air inlet and water inlet temperatures vary. However, there are observable differences in COP values for the two POEs.

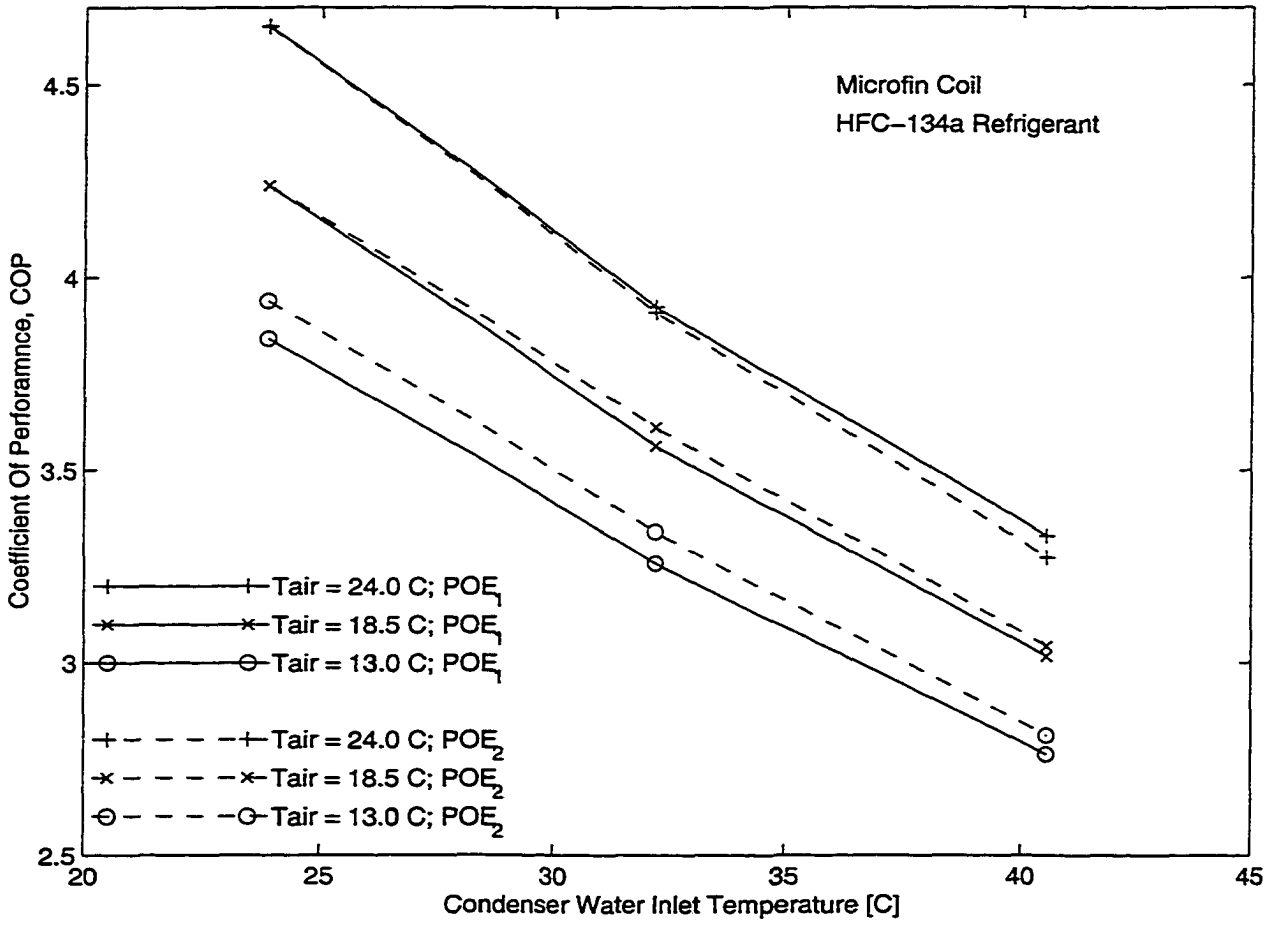

Figure 4.19. COP for POE_2 and POE_1 for the System with Microfin-Tube Coil

For the lowest air temperature of 13 °C, the POE_2 clearly indicates a larger COP than POE_1 with the differences being larger than the uncertainties in the COP, which are ± 0.03. The differences in the COP for an air temperature of 18.5 °C are similar in magnitude to the COP uncertainty with the COP being larger for POE_2. For the highest air temperature of 24 °C, it appears that POE_1 outperforms POE_2. A trend can be observed that as the evaporator air temperature decreases, the differences in COP between POE_2 and POE_1 increase.

An alternative presentation of the results given in Figure 4.19 is presented in Figure 4.20 where the COP percent difference is plotted as a function of operating temperatures.

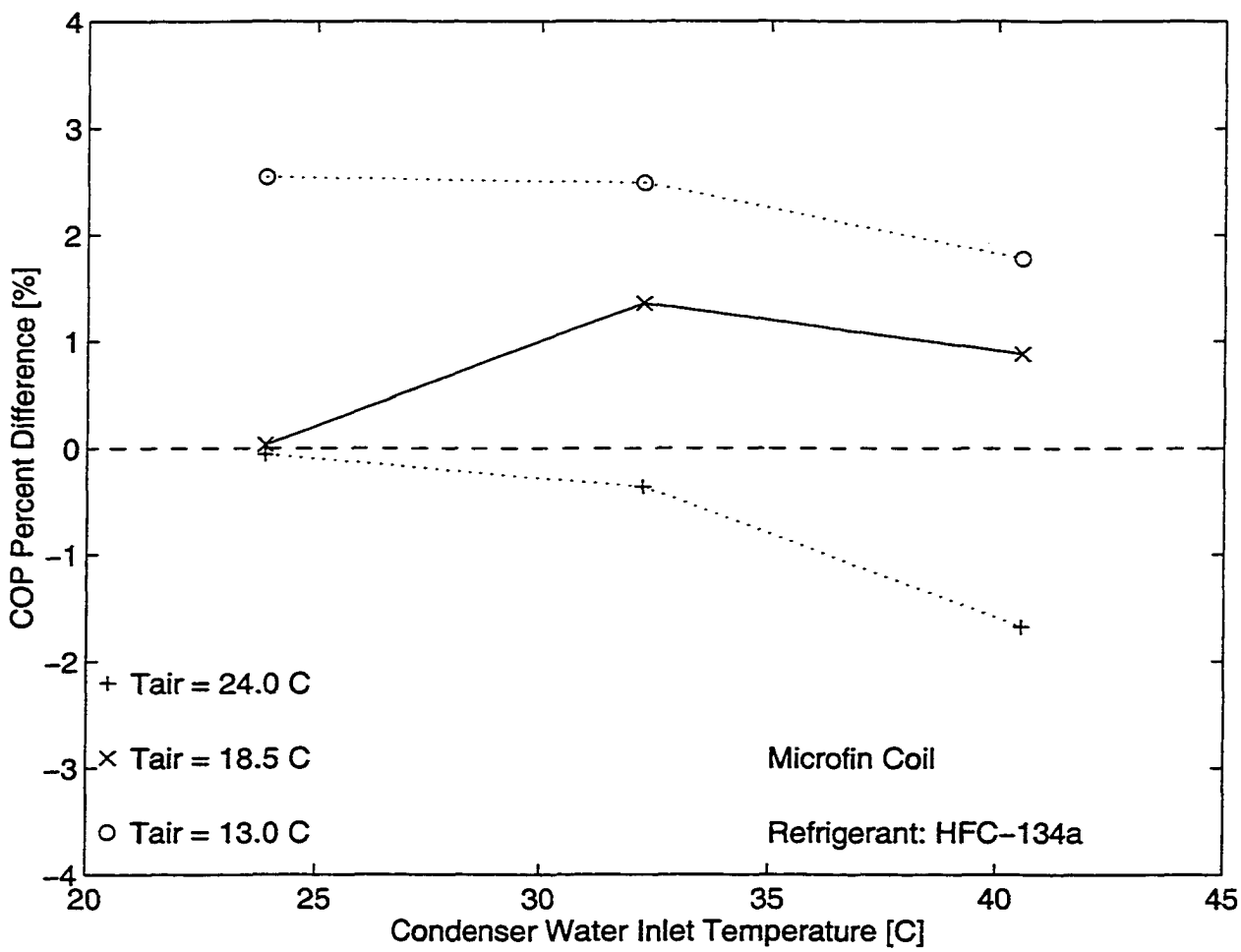

Figure 4.20. COP percent difference for POE_2 and POE_1 with microfin-tube coil

The COP percent difference, COP_{dif}, is defined as the difference between the COPs for the POE_2 and POE_1 oil divided by the COP for the POE_1, with the value expressed as a percentage.

$$COP_{dif}[\%] = \frac{COP_{POE_3} - COP_{POE_1}}{COP_{POE_1}} 100 \tag{4.13}$$

The COP percent difference between POE_2 and POE_1 is the largest for the lowest air temperature with the percent difference being larger than 2 percent. The uncertainty in the COP percent difference is around 1.1 percent as reported in Table 3.3, and therefore, it can be stated that the differences in the COP for the lowest tested air temperature of 13 °C are significant.

As the evaporator temperature increases the difference in COP between POE_2 and POE_1 diminishes, and the observed differences in COPs for air temperatures of 18.5 °C and 24 °C are not greater than the estimated uncertainty in the COP percent difference. The greater performance differences in the two lubricants at low temperatures might be due to larger differences in lubricant viscosities at lower temperatures.

In summary, the results suggest that the POE_2 lubricant outperforms the POE_1 lubricant for lower temperatures and that the COP can be improved by up to 2.5 percent. However, as the evaporator temperature increases, the superiority of POE_2 diminishes. For the highest evaporator air temperature of 24 °C the POE_1 indicates a higher COP than POE_2. It is also important to note that the performance of POE_2 is comparable or better than that of POE_1, and thus, it is definitely better than the performance with MO. A comparison of the POE_2 and the MO performance is also presented in Section 4.3.5. The actual data for the COP and other parameters presented herein can be found in Appendix C.

In order to explain the behavior of the test system with POE_2, other parameters need to be analyzed. The order in which performance parameters are compared is presented the same as was done in the previous Section 4.2, where lubricant miscibility effects were analyzed.

4.3.2 Evaporator Capacity

The first performance parameter to be investigated is the refrigeration capacity as this parameter indicates an overall performance of the evaporator coil. The capacity is plotted as a function of operating water and air temperatures by using an expanded scale in order for the data to be more easily compared and analyzed. It is apparent that the capacity for POE_2 is higher for all data points. All the differences in capacity between POE_2 and POE_1 are higher than the estimated uncertainty of ± 0.03 kW. The observed differences in capacity vary 0.16 to 0.3 kW with the largest difference occurring at the lowest air temperature of 13 °C. These results are significant, indicating that the utilization of the lower viscosity POE_2 lubricant significantly improves refrigeration capacity in comparison to the POE_1 lubricant.

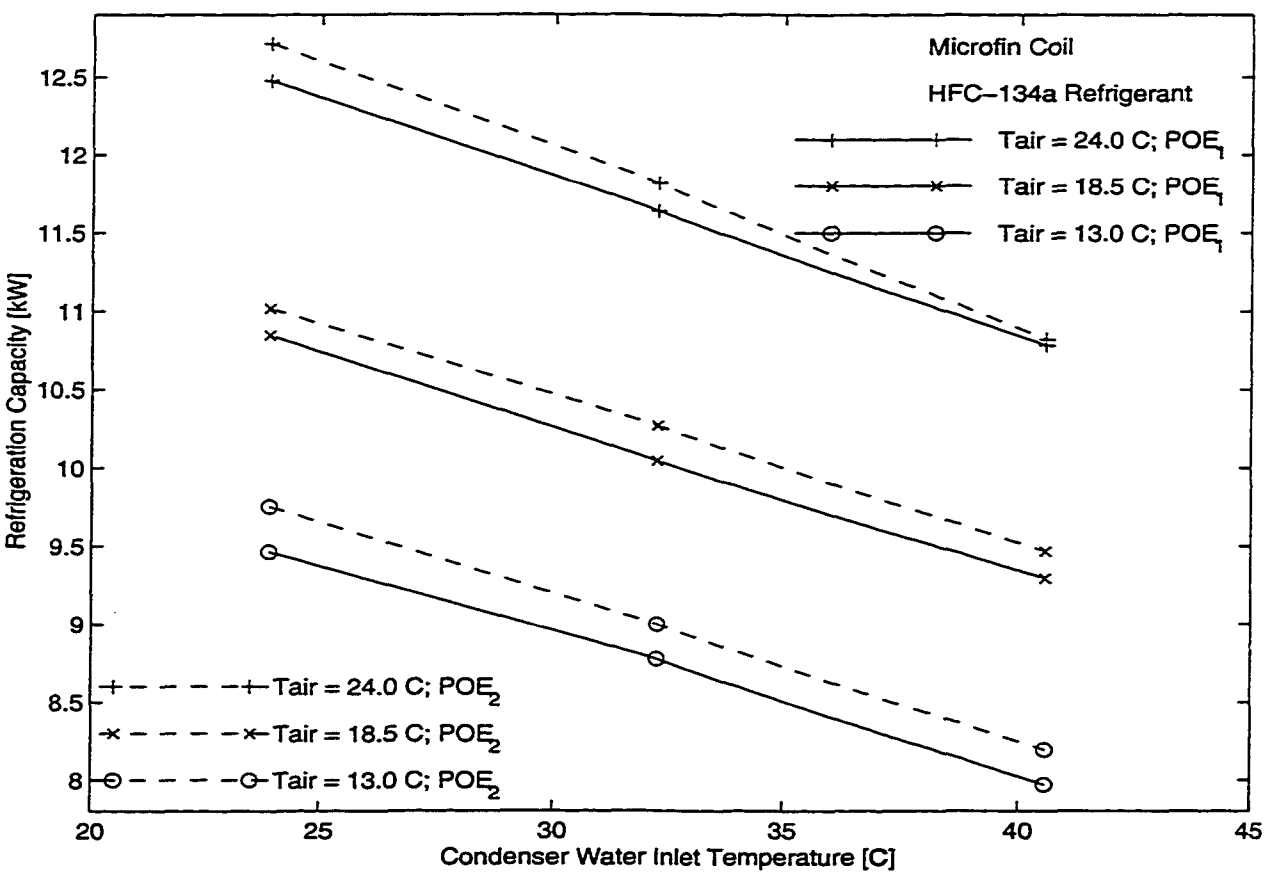

Figure 4.21. Capacity for POE_2 and POE_1 with microfin-tube coil

In order to better analyze the differences in capacity due to the lubricant type, the percent capacity differences between matching points are plotted as a function of different operating conditions for the microfin-tube coil in Figure 4.22. The capacity percent difference is calculated in the same manner as the COP percent difference defined earlier in Equation 4.13.

$$\text{Capacity}_{dif} = \frac{\text{Capacity}_{POE_2} - \text{Capacity}_{POE_1}}{\text{Capacity}_{POE_1}} 100 \tag{4.14}$$

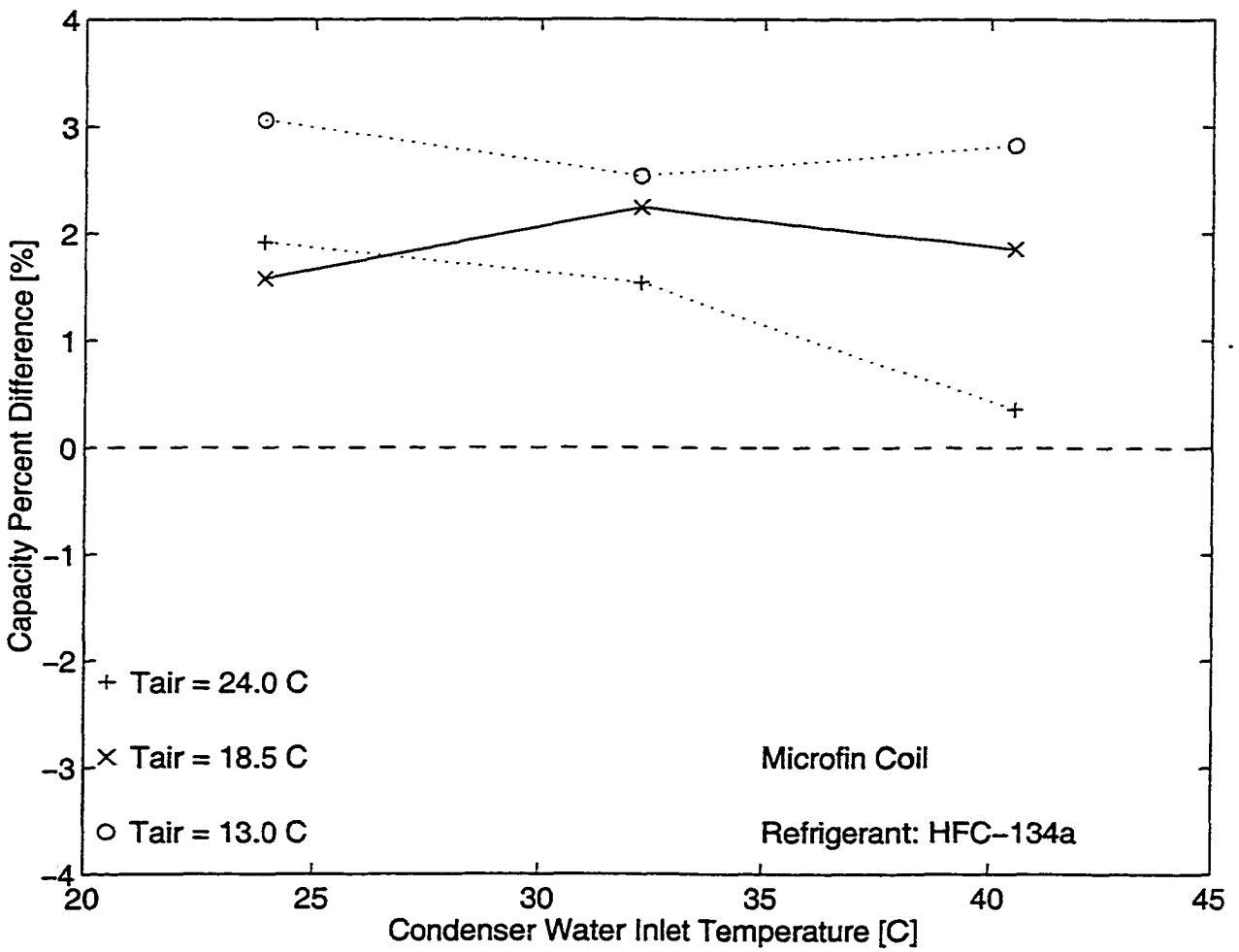

Figure 4.22. Capacity percent difference for POE_2 and POE_1 with microfin-tube coil

Except for the point corresponding to the highest evaporator air temperature and the highest condenser water temperature, all points indicate a capacity percent difference higher than 1.5 percent. Since the uncertainty in the capacity percent difference is 0.4 percent as reported in Table 3.3, the results indicate that differences in the capacity observed are significant and that the POE_2 lubricant improves the performance of the coil. In the previous section it was shown that if the POE_2 lubricant improves evaporation heat transfer in the coil, then the temperature difference between the refrigerant and the air will be lowered. The difference between the evaporator saturation pressures for POE_2 and POE_1 is plotted in Figure 4.23 and the pressure difference is defined as

$$\text{Pressure}_{dif} = \text{Pressure}_{POE_2} - \text{Pressure}_{POE_1} \tag{4.15}$$

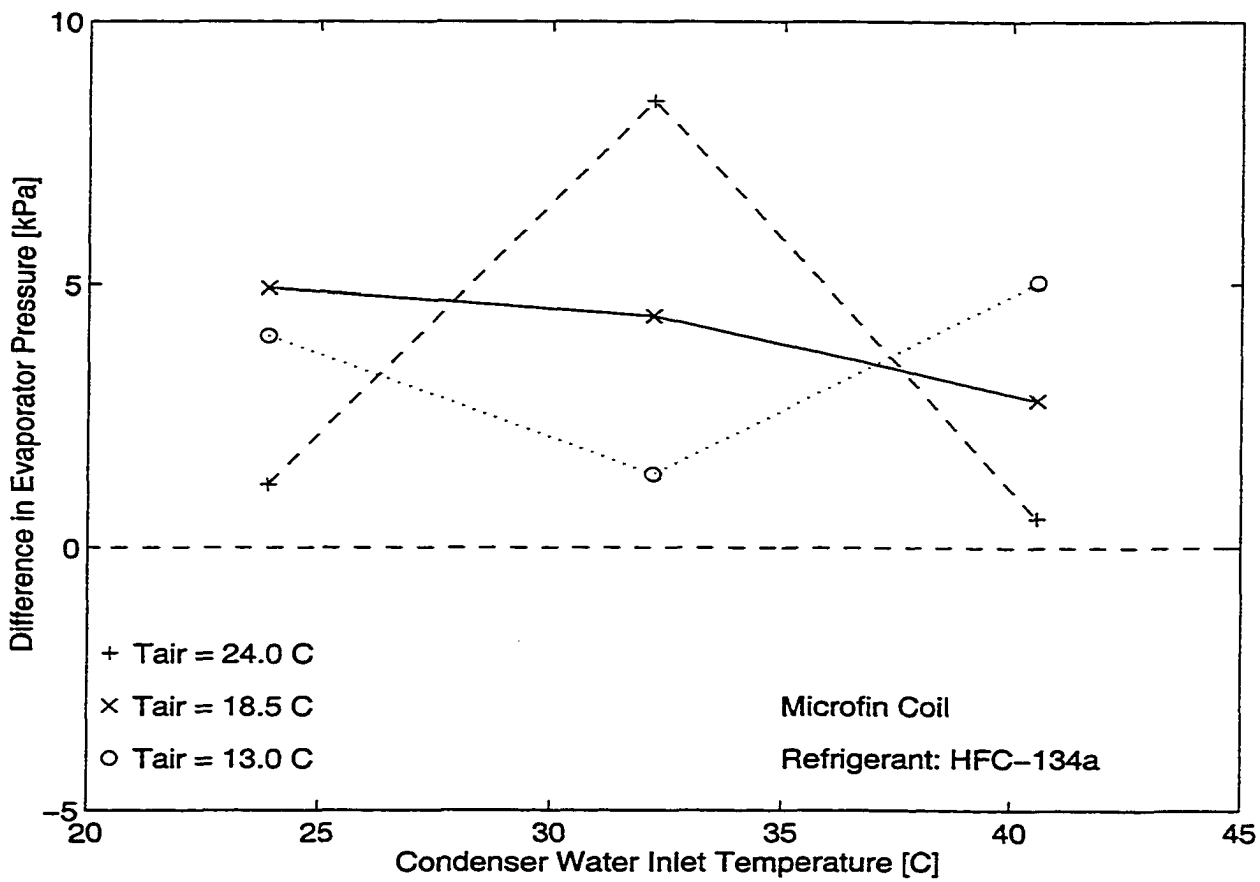

Figure 4.23. Difference in compressor suction pressure POE_2 and POE_1 with microfin-tube coil

The differences in suction pressure indicate that there is a higher evaporation heat transfer associated with the POE_2 lubricant, because the suction pressure is consistently higher for the POE_2 lubricant. The difference in suction pressure of about 4 kPa corresponds to a difference in saturation temperature of 1 °C for the HFC-134a refrigerant.

Due to a higher saturation pressure and temperature, the specific volume at the compressor inlet is smaller for the POE_2, and thus, the compressor is capable of pumping a larger amount of refrigerant through the system, which leads to a higher refrigerant flow rate. This behavior is shown in Figure 4.24 where the percent difference in mass flow rate is plotted for different operating temperatures.

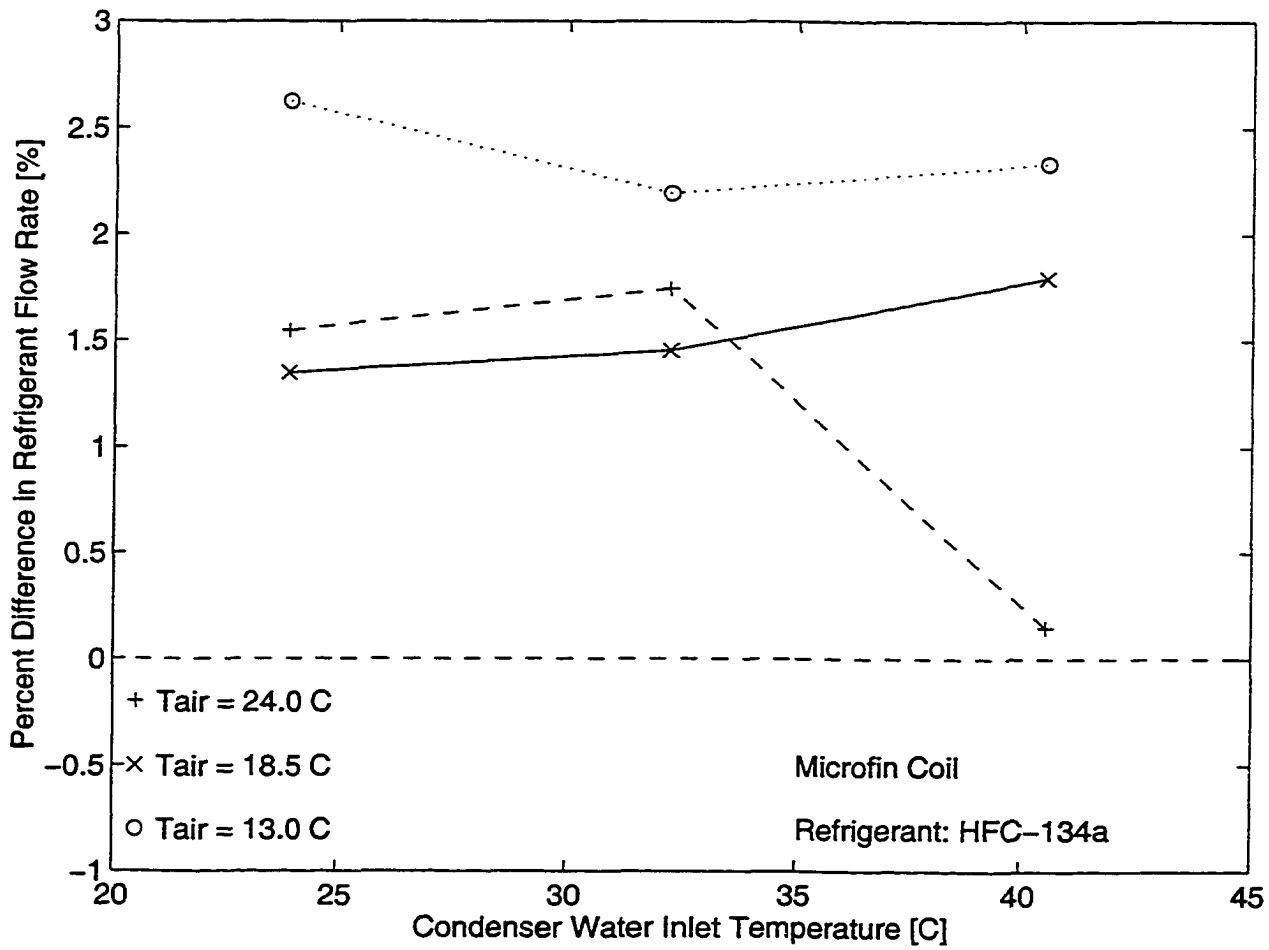

Figure 4.24. Percent difference in refrigerant flow rate for POE_2 and POE_1 with microfin-tube coil

The percent difference in the refrigerant flow rate is defined as the difference between the POE_2 and POE_1 flow rate divided by the flow rate for POE_1 expressed in percentile:

$$\dot{m}_{dif} = \frac{\dot{m}_{POE_1} - \dot{m}_{MO}}{\dot{m}_{MO}} 100 \tag{4.16}$$

The largest differences in refrigerant flow rate correspond to the lowest evaporator air temperature and these results are in agreement with the general trends observed for the POE_2 lubricant. As explained earlier in Section 4.2.2 and given in Equation 4.8, the flow rate is proportional to the volumetric efficiency and the refrigerant density entering the compressor. Differences in volumetric efficiency are presented in Figure 4.25.

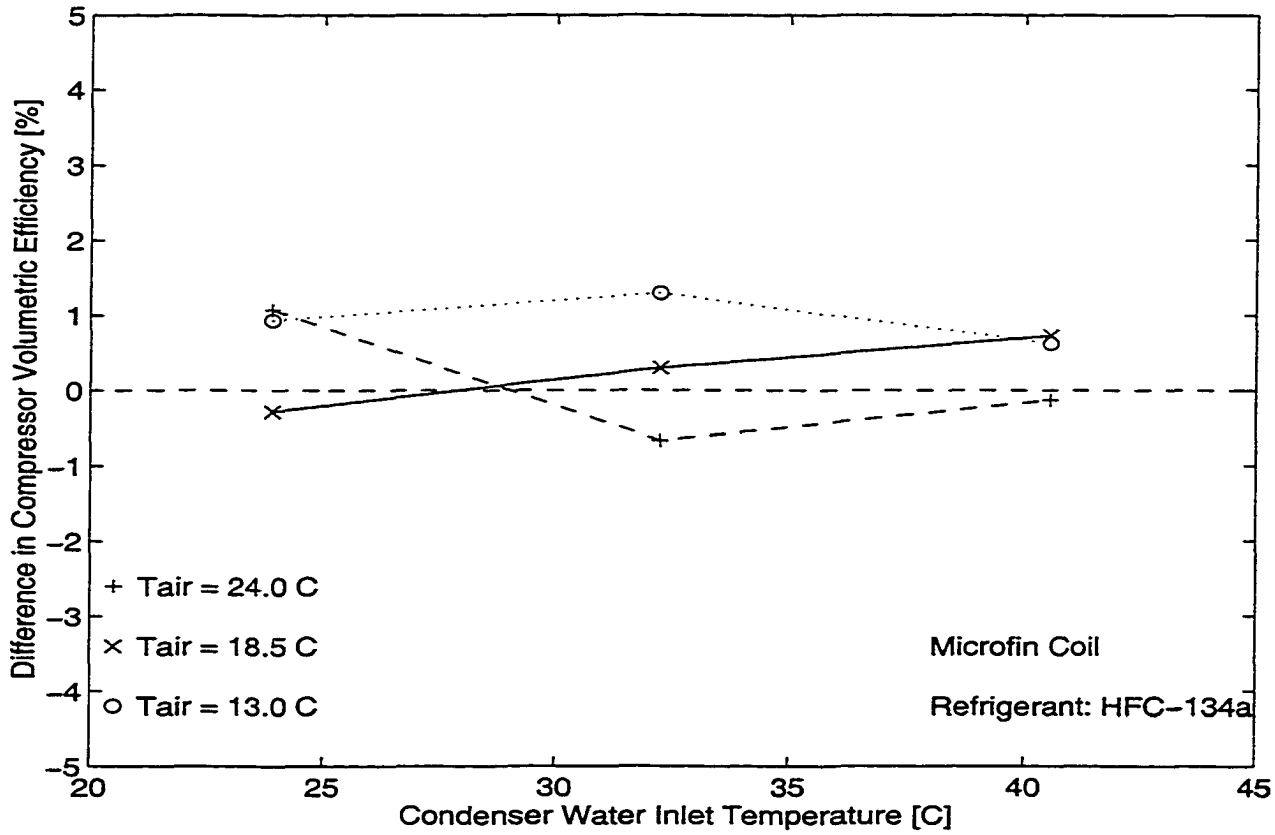

Figure 4.25. Difference in compressor volumetric efficiency for POE_2 and POE_1 with microfin-tube coil

Comparisons of volumetric efficiency are performed by plotting the absolute difference between volumetric efficiency magnitudes estimated for POE_2 and POE_1 data

$$\eta_{vol,diff} = \eta_{vol,POE\_2} - \eta_{vol,POE\_1} \tag{4.17}$$

The observed differences in volumetric efficiency for POE_1 and POE_2 are larger than those between POE_1 and MO lubricants presented earlier in Figure 4.14 in Section 4.2.2. The uncertainty in determining volumetric efficiency is around ±0.34 percent, while the uncertainty in the volumetric efficiency difference is around ±0.5. The differences for some points are as large as 1.0 percent, with the data appearing to be more consistent for the lowest air temperature of 13 °C. Thus, the volumetric efficiency for the lowest air temperature is significantly larger for the POE_2 lubricant compared to the POE_1 lubricant. These differences in volumetric efficiency combined with the lower refrigerant volume entering the compressor for POE-2 data compared to POE_1 data results in the refrigerant flow rate being larger for POE_2 data, from 2 percent to 2.5 percent larger, as presented in Figure 4.24.

In summary, due to the higher evaporation heat transfer rate for the HFC-134a/POE_2 mixture, the refrigerant temperature in the evaporator is higher, leading to a lower refrigerant volume entering the compressor and resulting in a higher flow rate through the compressor. Only for the lowest air temperature of 13 °C are the differences in volumetric efficiencies are significant to the point of contributing to the higher flow rate for POE_2. Since it appears that lubricant type has a major impact on the evaporation heat transfer, the performance of evaporator coil is studied in more detail in Chapter 5.

4.3.3 Compressor Power Consumption

The power consumption is larger for the compressor operating with POE_2 than with POE_1, as indicated in Figure 4.26. Except for the lowest air temperature of 13 °C, the power consumption is significantly higher for the POE_2 lubricant, being larger than the power consumption uncertainty of ±0.02 kW as was given in Table 3.2.

The differences in power consumption are not only due to different operating parameters (i.e. refrigerant properties and flow rates) but also due to different lubricant characteristics, which will be investigated in more detail in the remainder of this section.

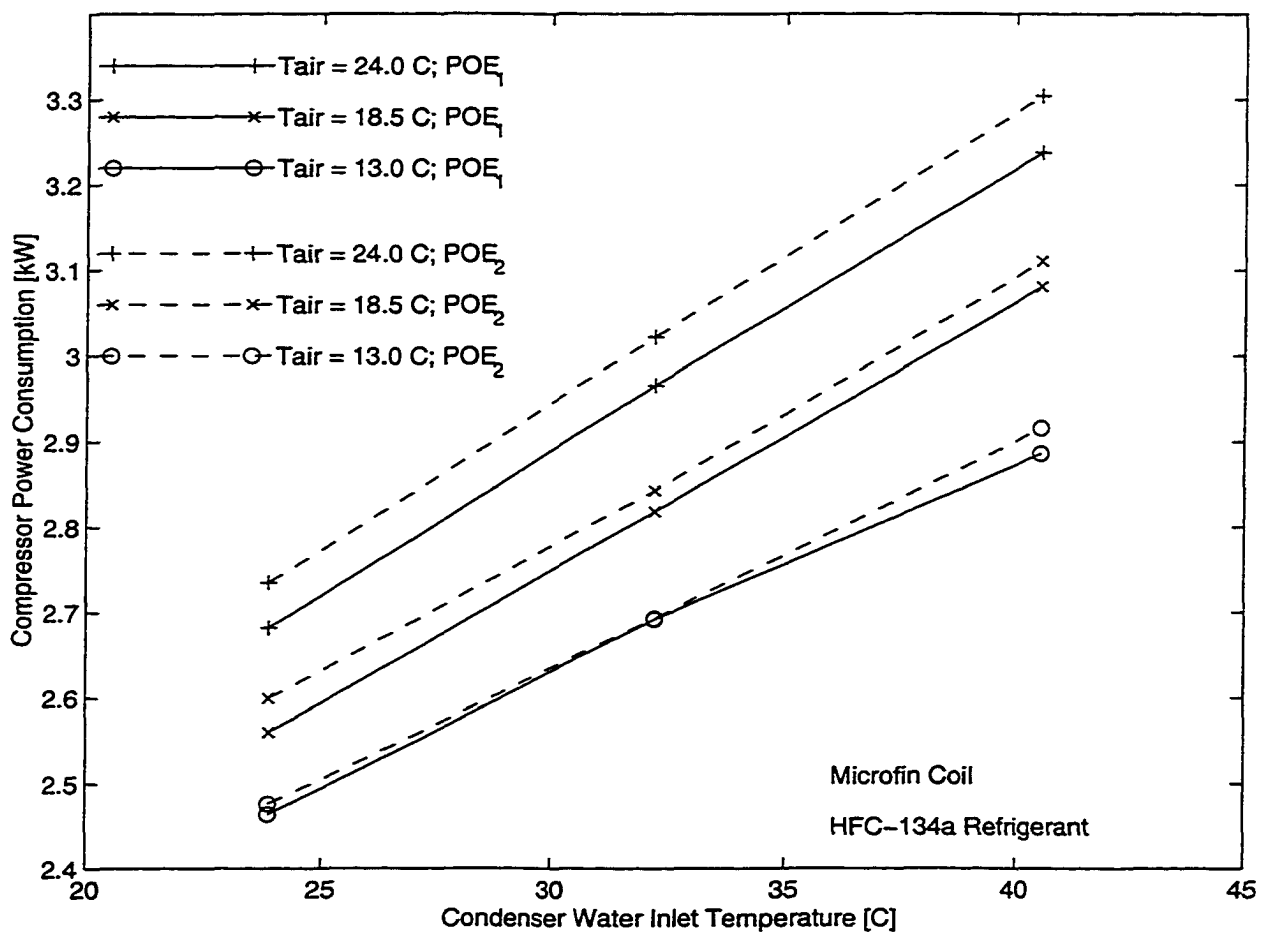

Figure 4.26. Compressor power consumption for POE_2 and POE_1 with microfin-tube coil

Alternatively, the power consumption is presented as the percent difference between power consumption of POE_2 and POE_1 in Figure 4.27:

$$\text{Power}_{dif} = \frac{\text{Power}_{POE_2} - \text{Power}_{POE_1}}{\text{Power}_{POE_1}} \tag{4.18}$$

The results confirm previous observations that for air temperatures of 18.5 °C and 24 °C the percent difference is larger than the estimated uncertainty of ±1 percent given in Table 3.3.

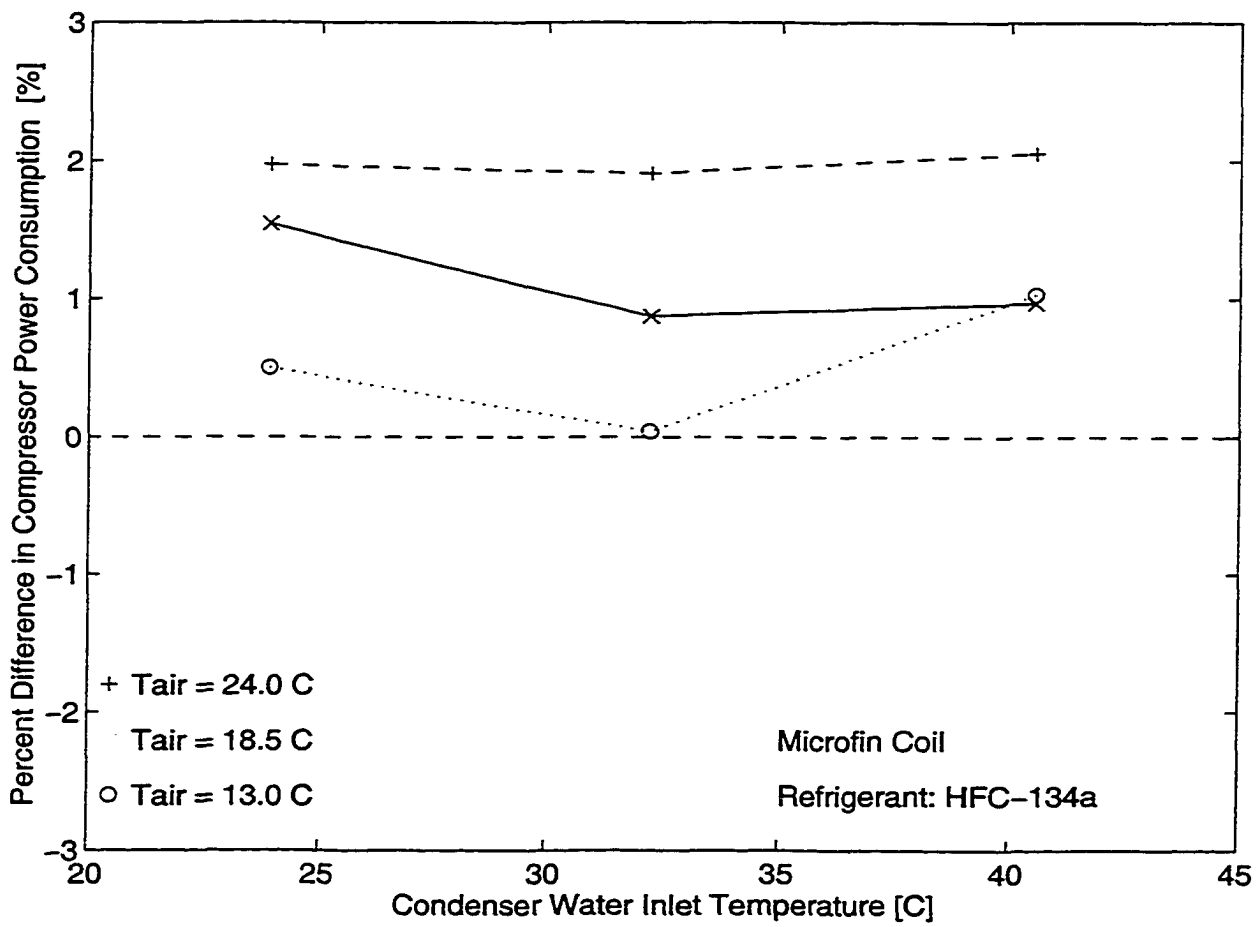

Figure 4.27. Percent difference in compressor power consumption for POE_2 and POE_1 with microfin-tube coil

In order to further analyze differences in power consumption between POE_2 and POE_1 due to different operating parameters (i.e. refrigerant flow rates and refrigerant properties), the expression for polytropic compression given earlier in Equation 4.11 in Section 4.2.3 was utilized. The differences in the power consumption calculated from operating parameters are greater than the measured differences in the power consumption. Similar to the explanation presented in the miscibility analysis, all of the differences in the power consumption may not be accounted for by the variations in operating parameters, and therefore, other factors also contribute to the differences in power consumption. One possible explanation is related to the different solubility characteristics of POE_1 and POE_2 when mixed with HFC-134a. These differences in solubility characteristics can result in different effective lubricant viscosities. In other words, since the compressor contains a miscible mixture with the refrigerant and lubricant fractions being determined by solubility, then the liquid mixture viscosity will be much different than that of the pure lubricant viscosity.

As defined earlier in Section 4.1, the solubility characteristics are related to the effective charge, and consequently, to the magnitude of the compressor discharge pressure. A lubricant which dissolves a larger amount of refrigerant at given operating conditions has a lower effective charge. Therefore, the system behaves as being overcharged, which is indicated by the magnitude of the compressor discharge pressure. The differences in the compressor discharge pressures for POE_2 and POE_1 data are plotted for different operating conditions in Figure 4.28

The pressure difference is defined as the absolute difference between the measured discharge pressure for POE_2 and POE_1 lubricants:

$$\text{Pressure}_{dif} = \text{Pressure}_{POE_2} - \text{Pressure}_{POE_1} \tag{4.19}$$

The compressor discharge pressure is consistently higher for the POE_2 lubricant, being 5 to 18 kPa higher, indicating that the effective charge of POE_2 is higher than that of POE_1, which also means that the system is slightly overcharged with the POE_2 lubricant.

Therefore, it can be concluded that over the range of compressor operating conditions, more refrigerant is dissolved in POE_2 than in POE_1. This trend is in agreement with some reports found in the literature and presented earlier in Section 2.3, namely that a lower viscosity lubricant dissolves more refrigerant.

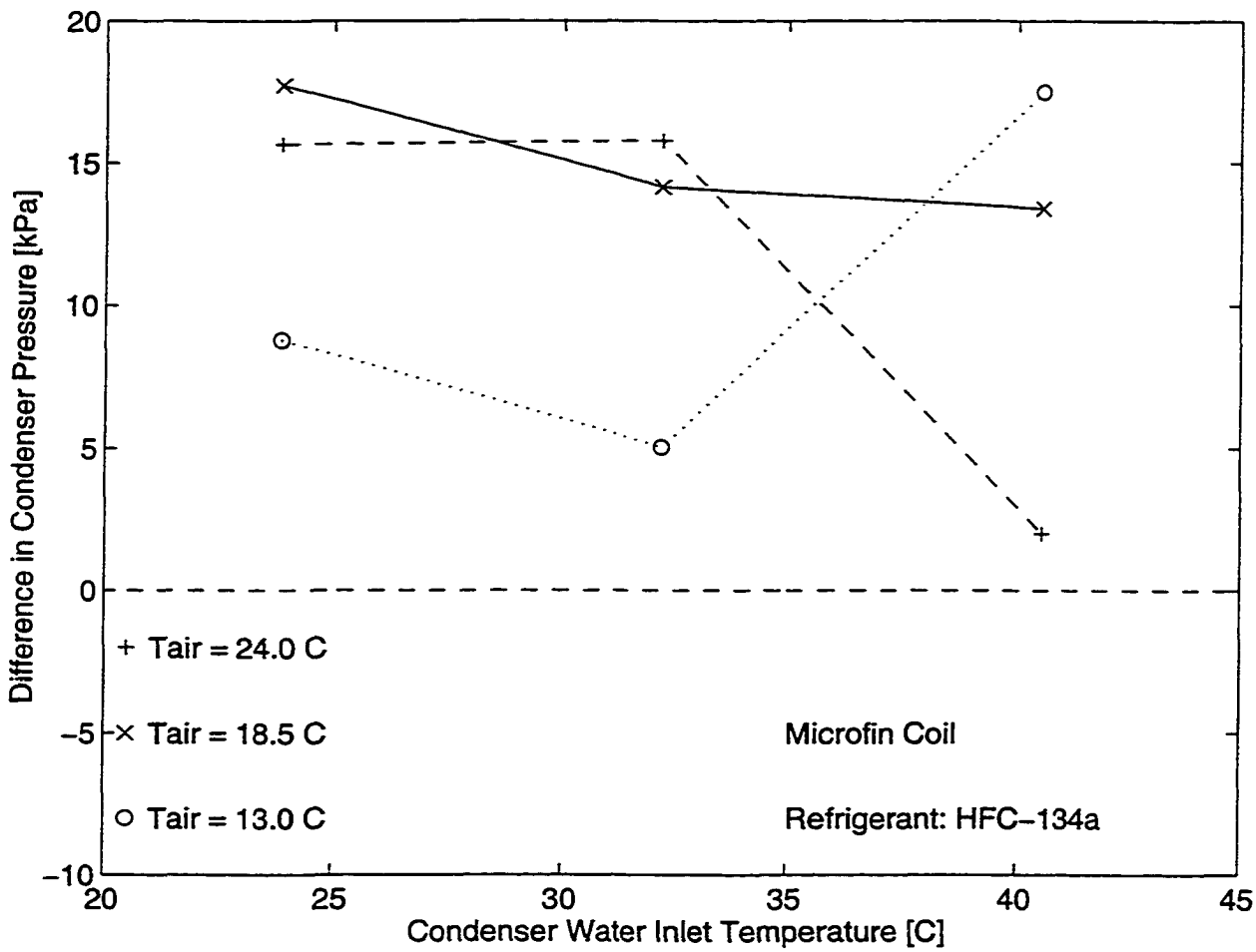

Figure 4.28. Difference in compressor discharge pressure POE_2 and POE_1 with microfin-tube coil

4.3.4 Compressor Efficiencies

The differences in compressor volumetric efficiency were presented earlier in Figure 4.25, and it was noted there that for some points the differences were larger than the estimated uncertainty. This trend is different from that which was observed for POE_1 and MO lubricants, in which all differences in compressor volumetric efficiencies were insignificant.

The comparison between compressor isentropic efficiencies for POE_2 and POE_1 is plotted in Figure 4.29 for a range of operating air and water temperatures.

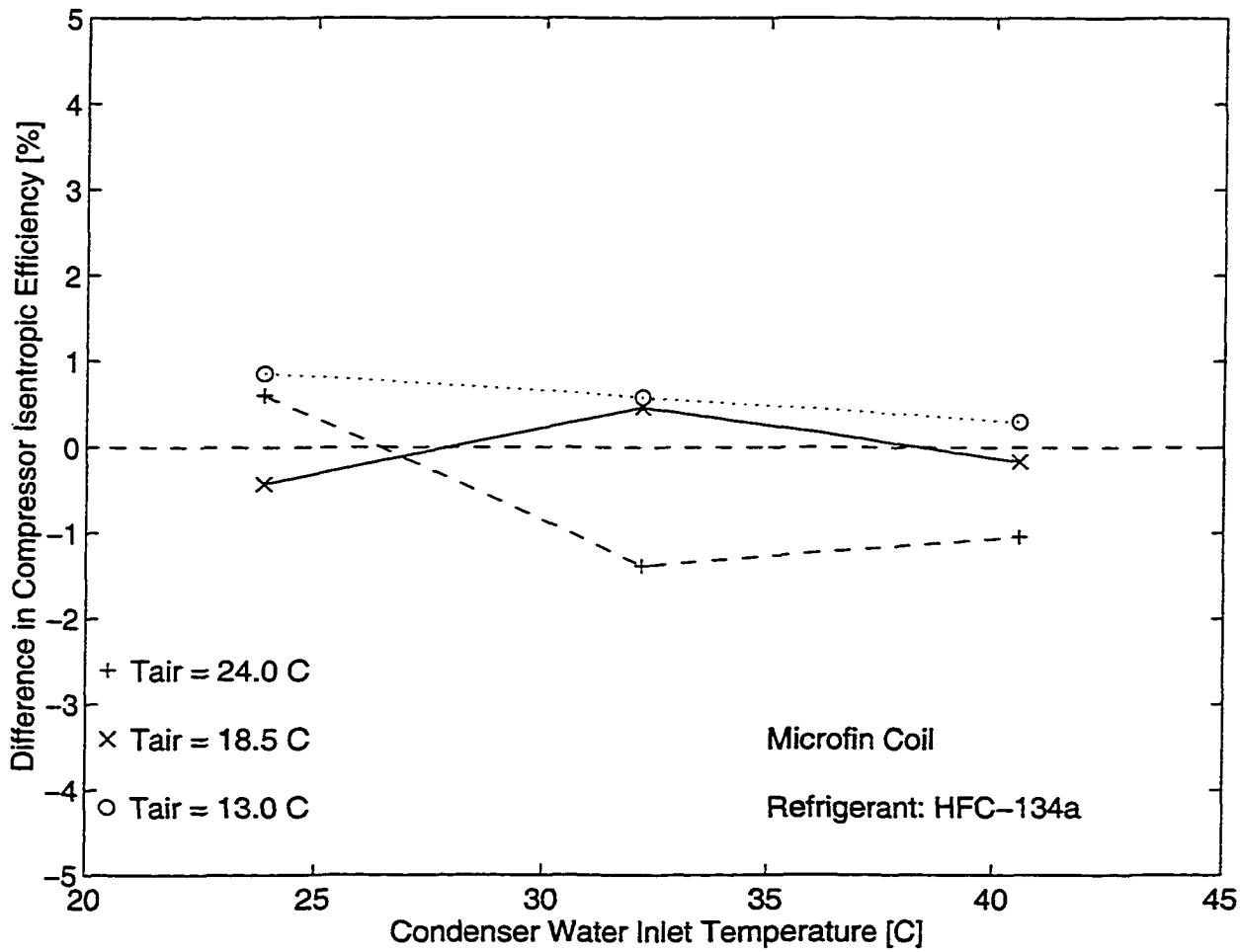

Figure 4.29. Difference in compressor isentropic efficiency for POE_2 and POE_1 with microfin-tube coil

The absolute difference in efficiency plotted in Figure 4.29 is defined in the same manner as was the difference in the volumetric efficiency given earlier in Equation 4.17. The uncertainty in the isentropic efficiency difference was estimated to be around 0.65 and for several points the difference in isentropic efficiency is larger than the uncertainty. However, no trends are apparent for the presented results, and therefore, the origin of these differences cannot be determined. One possible explanation is that the differences in the dependent operating parameters (i.e., refrigerant properties and refrigerant flow rate) are generating these differences.

It can be concluded that a lower viscosity lubricant, POE_2, has a significant effect on system performance in that it has a significantly larger capacity than that for POE_1. However, the power consumption is also consistently higher for POE_2 than it is for POE_1. The combination of capacity and power consumption for the lowest air temperature of 13 °C makes the overall COP significantly higher for POE_2 than for POE_1. The differences in capacity caused by a better evaporation heat transfer for POE_2. It should be also noted that the calculated differences in power consumption based on different refrigerant properties is higher than those actually measured on the system, which suggests that the compressor operation with POE_2 as a lower viscosity lubricant has some beneficial effects. Lastly, the data suggests that a smaller amount of refrigerant is dissolved in POE_2 than in POE_1.

4.4 Effects of Partial Miscibility

Partial miscibility of a refrigerant/lubricant liquid mixture represents a condition where two distinct liquid phases exist namely a refrigerant rich phase and a lubricant rich phase. As refrigerant flows through the coil and evaporates, the lubricant concentration increases, starting from above the measured 0.3 percent at the evaporator inlet to probably 60 percent or 70 percent flowing lubricant at the evaporator exit. The limiting concentration corresponds to the bubble point temperature of the refrigerant/lubricant mixture for which there is no further refrigerant phase change possible. In cases when partial miscibility can be achieved in the evaporator as the lubricant concentration shift, it was speculated that the

separation of the refrigerant/lubricant mixture into two phases might possibly provide additional evaporation of refrigerant resulting in an increased capacity.

A partially miscible lubricant, namely POE_3, was selected to investigate system performance for the case a partial miscibility condition being achieved in the evaporator. As reported earlier in Section 3.1.3, the POE_3 is partially miscible with HFC-134a refrigerant at the temperatures that exist in the evaporator during testing in this project. Also, it should be emphasized that POE_3 has the same viscosity characteristics as POE_2, i.e., the same viscosity grade and similar viscosity dependence on temperature. Since POE_2 has a lower viscosity than POE_1, it can be observed that the POE_3 is considered to have a lower viscosity than POE_1. Selection of such a lubricant enables one to study whether partial miscibility may have positive effects on system performance in addition to that of being a lower viscosity lubricant, the POE_2 lubricant presented earlier in Section 4.3.

The comparison of system performance for these two lubricants, i.e., POE_1 and POE_3, is the basis of the investigation of the effects of a partially miscibility lubricant/refrigerant in the evaporator. Some properties of both lubricants are given in Section 3.3.1. As stated earlier, the results and analysis presented herein are performed by comparing the refrigeration system performance at fixed values of the independent parameters, i.e., refrigerant charge; air and water inlet temperatures; air and water flow rates; and the amount of superheat at the compressor inlet. Having all independent parameters equal means that any differences in system performance are due to lubricant effects only.

4.4.1 COP

The presentation of results begins with the COP, which is plotted in Figure 4.30 as a function of the condenser water inlet temperature and the evaporator air inlet temperature. The COP is presented on an expanded scale in order to better view the effects of the lubricant on system performance. It is apparent, that the system performance for both POEs follows similar trends as the evaporator air inlet and condenser water inlet temperatures vary. The

COP values for the POE_1 lubricant are connected with the solid line so as to distinguish them from the POE_3 lubricant.

There are observable differences in the COP for the two POE lubricants. For the lowest air temperature of 13 °C and the lowest condenser water temperature of 24 °C, the POE_3 has a larger COP than the POE_1, with the difference being larger than the two uncertainties for COP. For the highest air temperature of 24 °C, the POE_1 consistently outperforms the POE_3 as the COPs are greater by more than the uncertainty in the COP, which is around ±0.03 as was given in Table 3.3.

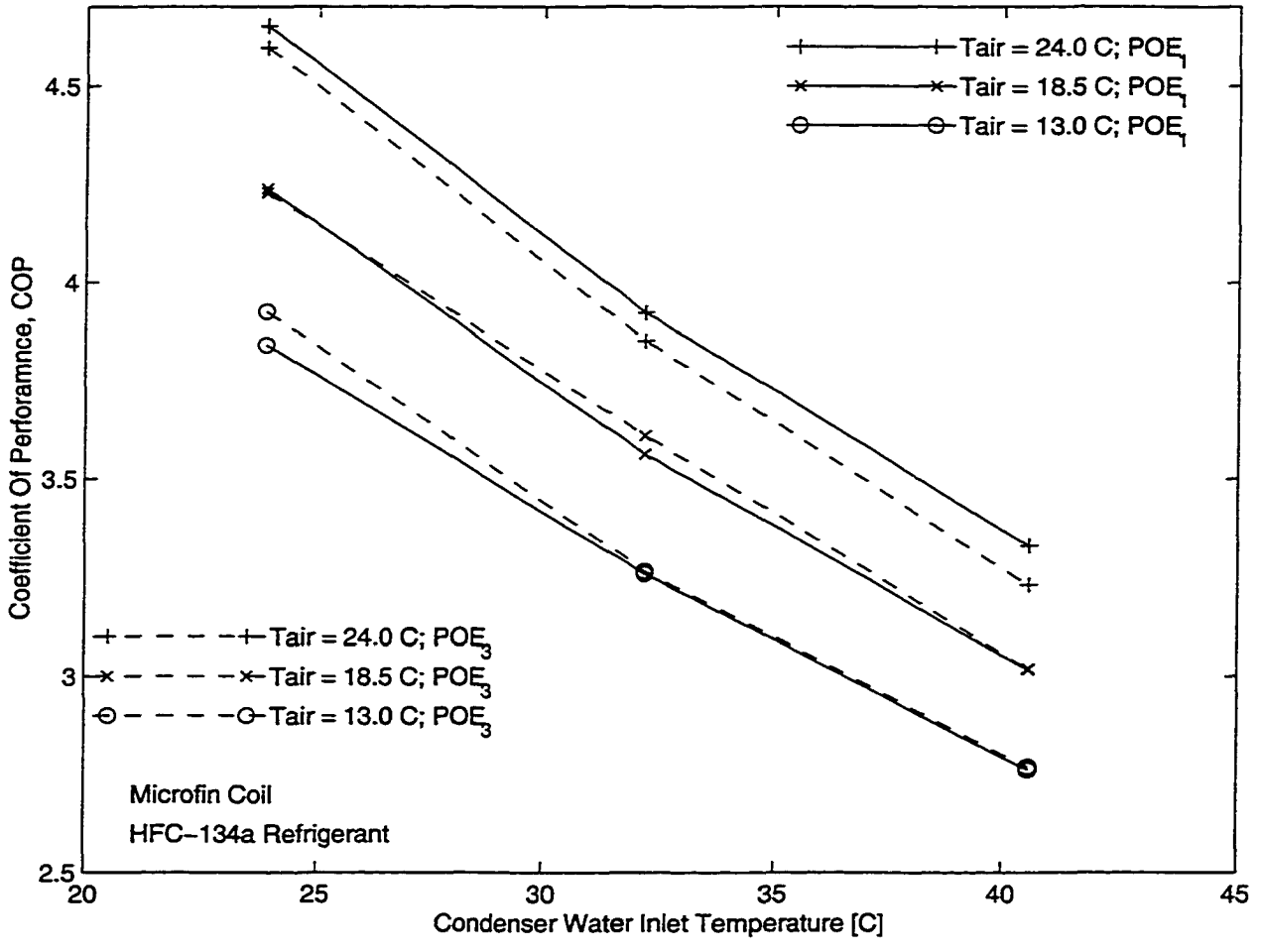

Figure 4.30. COP for POE_3 and POE_1 for the system with microfin-tube coil

An alternative presentation of the results given in Figure 4.30 is presented in Figure 4.31, where the COP percent difference is plotted as a function of operating temperatures. The COP percent difference, COP_{dif}, is defined as the difference between the COPs for the POE_2 and POE_1 lubricant divided by the COP for POE_1, with the value expressed as a percentage.

$$COP_{dif}[\%] = \frac{COP_{POE_3} - COP_{POE_1}}{COP_{POE_1}} 100 \tag{4.20}$$

Based on the uncertainty in COP percent difference of 1.1 percent, it can be inferred that significant differences in COP exist at the highest air temperature of 24 °C indicating that the POE_1 data have a higher COP than the POE_3 data. This is the similar behavior found in the performance of POE_2 lubricant shown in Figure 4.20. However, the differences in COP between POE_3 and POE_1 are larger than those observed for POE_1 and POE_2 lubricants. Overall for the highest evaporator temperature, the POE_1 significantly outperforms both lower viscosity lubricants with more significant differences observed for the partial miscibility lubricant POE_3.

For the other evaporator air temperatures, the COP differences are smaller than the uncertainty in COP percent difference with an exception of the point corresponding to the lowest air and water temperatures. For that point, the COP percent difference is larger than 2 percent, indicating a better system performance with the partially miscible POE_3 lubricant. Besides this point, the other results suggest that the difference in system performance between POE_1 and POE_3 are insignificant.

Since POE_3 has same viscosity characteristics as POE_2, the system performance with POE_3 should be similar to that of POE_2. As presented in Figure 4.20, the COP was significantly larger for lower air temperatures, namely 13 and 18.5 °C. Therefore, it appears that the partial miscibility may have had detrimental effects on system performance. However, it should be kept in mind that chemical composition of lubricants was not available, and therefore, it can not be stated that POE_3 and POE_2 lubricants have identical

properties. From the limited knowledge of lubricants' characteristics, i.e. lubricant miscibility and viscosity, it can only be inferred that partial miscibility in the evaporator has detrimental effects on system performance. The POE_3, as a lower viscosity lubricant should outperform POE_1 at lower air temperatures based on the results presented in the previous section for the POE_2 lubricant.

As was done in previous sections, the system performance is further investigated through comparisons of other performance parameters, starting with evaporator capacity.

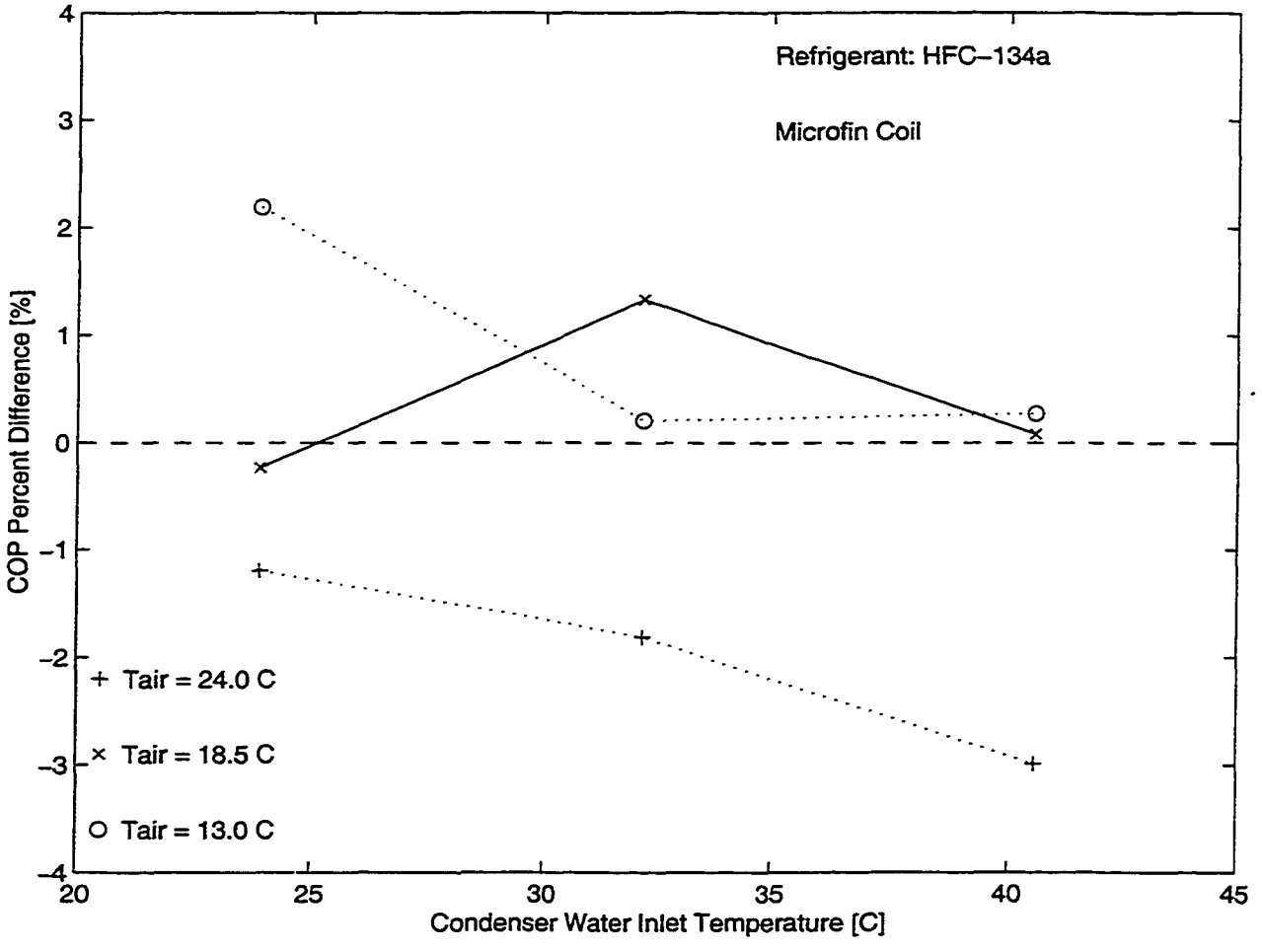

Figure 4.31. COP percent difference for POE_3 and POE_1 with microfin-tube coil

4.4.2 Evaporator Capacity

The capacity is plotted in Figure 4.31 as a function of operating water and air temperatures on an expanded scale in order for data to be more easily analyzed. It is apparent that there are no general trends in capacity differences due to the effects of these two lubricants. It appears that for the lower air temperature the capacity seems to be larger for POE_3 and for the highest air temperature the capacity appears to be higher for POE_1.

To better analyze the differences in capacity due to lubricant type, the capacity percent differences are plotted as a function of different operating conditions for the microfin-tube coil in Figure 4.33.

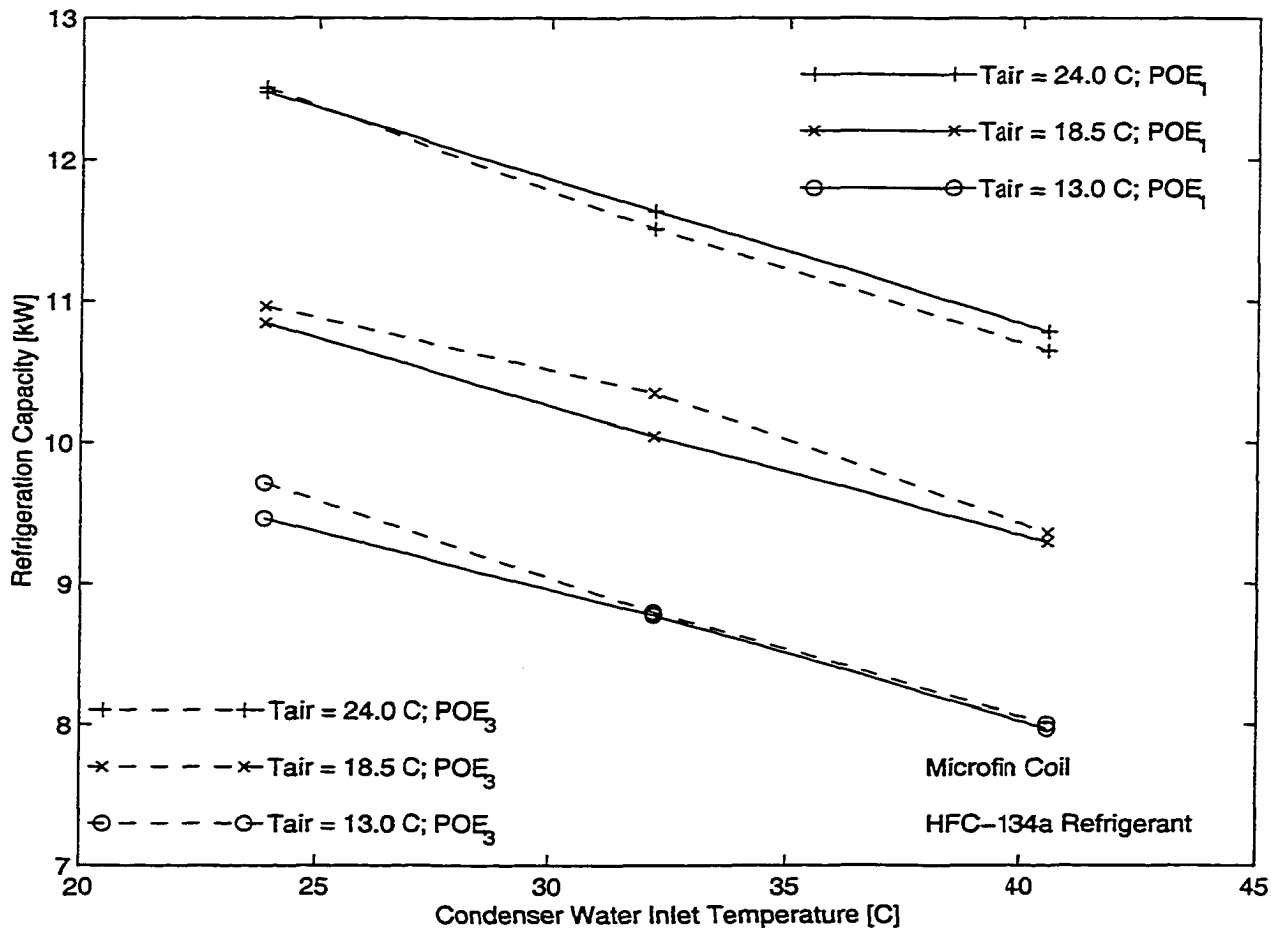

Figure 4.32. Capacity for POE_3 and POE_1 with microfin-tube coil

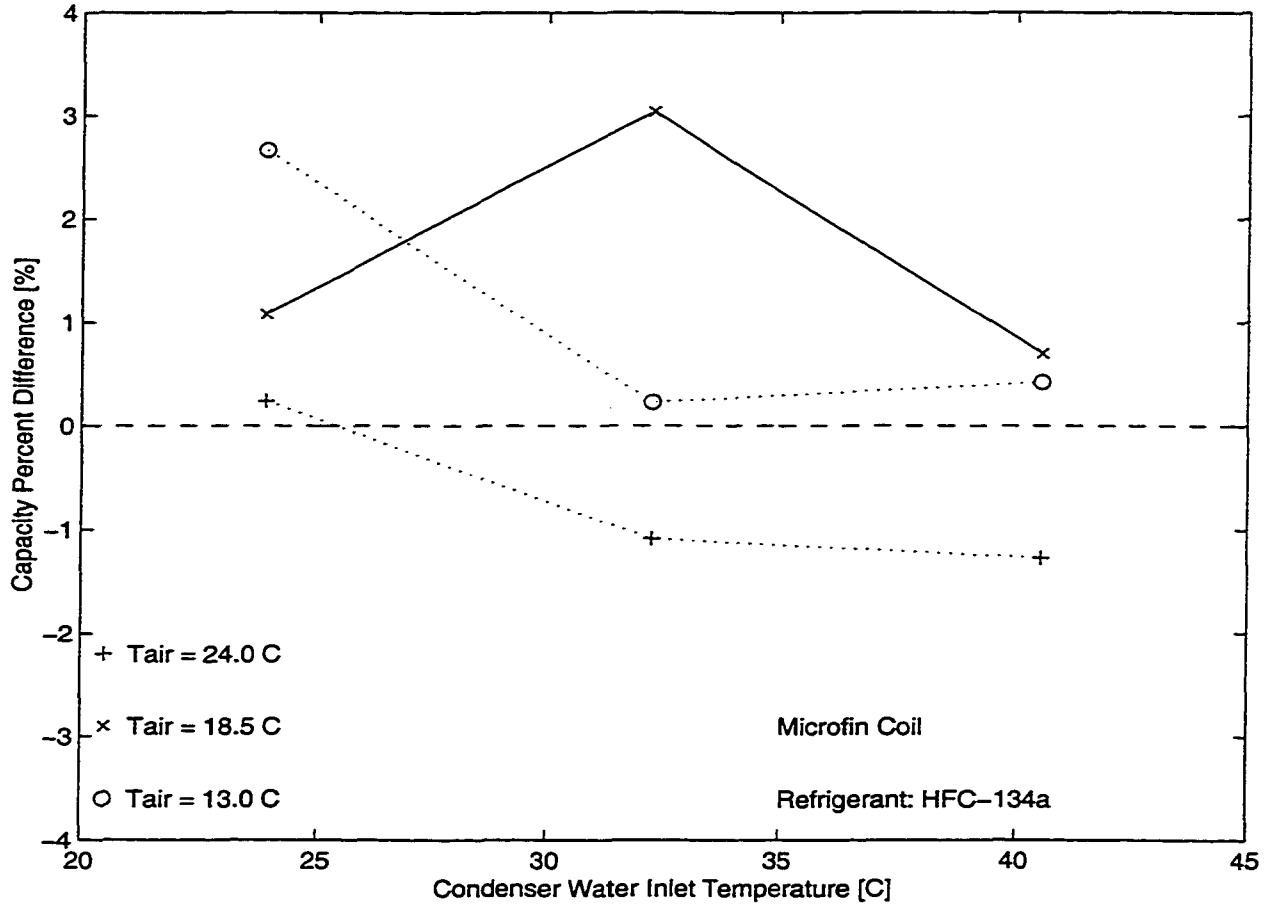

Figure 4.33. Capacity percent difference for POE_3 and POE_1 with microfin-tube coil

The capacity percent difference is calculated in the same manner as the COP percent difference defined in Equation 4.20.

$$\text{Capacity}_{dif} = \frac{\text{Capacity}_{POE_3} - \text{Capacity}_{POE_1}}{\text{Capacity}_{POE_1}} 100 \tag{4.21}$$

The evaporator pressure difference is plotted as a function of operating temperatures in Figure 4.34. Differences in measured evaporator pressure (i.e. compressor suction) for the POE_3 and POE_1 data follow trends observed for capacity.

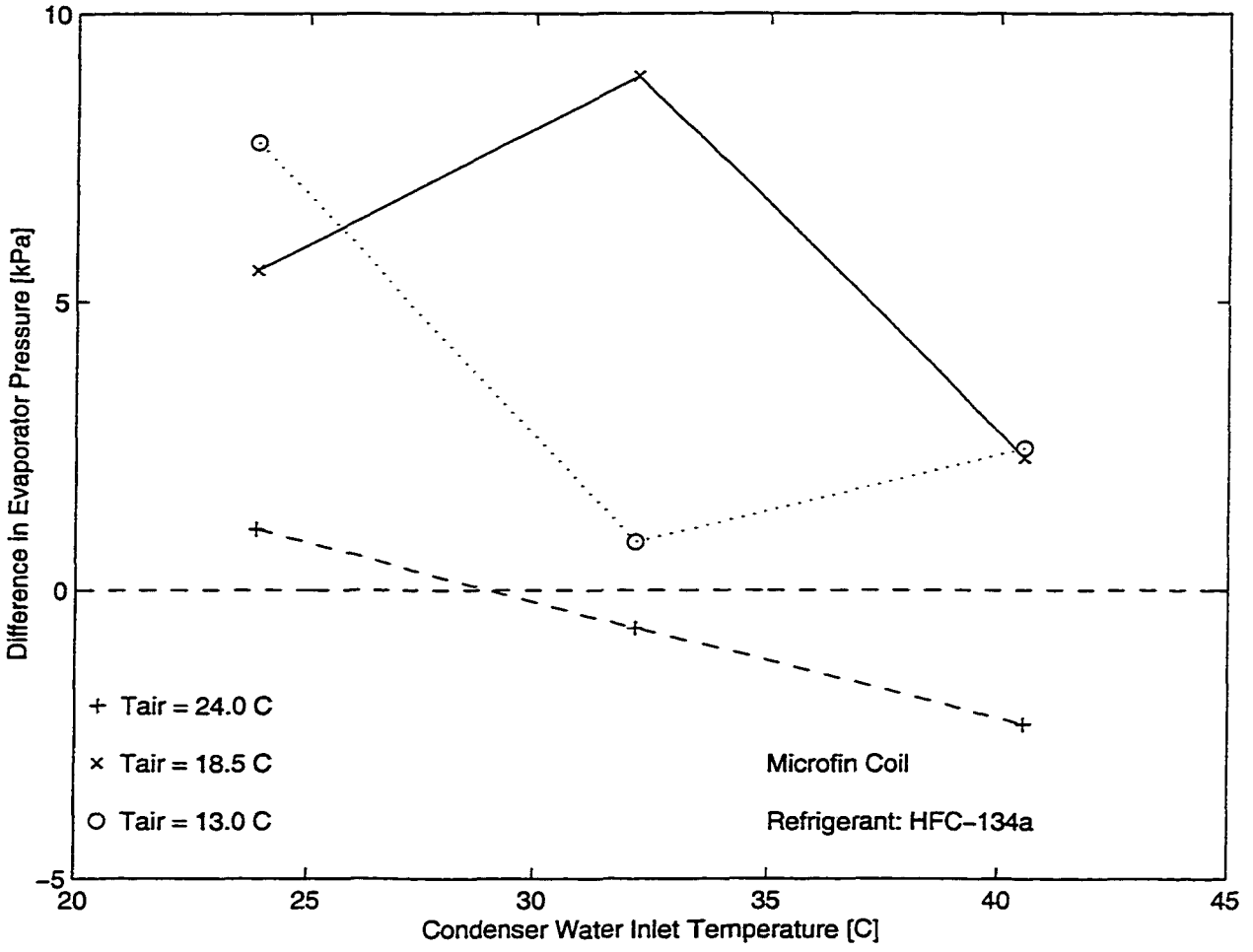

Figure 4.34. Difference in compressor suction pressure between POE_3 and POE_1 with microfin-tube coil

$$\text{Pressure}_{dif} = \text{Pressure}_{POE_3} - \text{Pressure}_{POE_1} \tag{4.22}$$

For lower air temperatures, the evaporator pressure for POE_3 is higher than that of POE_1. However, for the highest air temperature, differences in pressures are small. Recorded differences in volumetric efficiency were small, being less than 0.5 percent and thus less than the estimated uncertainty in the volumetric efficiency difference. Referring to Equation 4.8, the refrigerant flow rate is proportional to the compressor volumetric efficiency and density of refrigerant at the compressor inlet. Since differences in volumetric efficiency for POE_3 and POE_1 were insignificant, the differences observed in evaporator pressure

that were presented in Figure 4.34 directly affect refrigerant flow rate in Figure 4.35 plotted as functions of operating air and water temperatures. As evaporator pressure and consequently temperature increase, the refrigerant volume decreases (i.e. refrigerant density increases), and thus, the compressor is capable of pumping a larger quantity of refrigerant.

$$\dot{m}_{dif} = \frac{\dot{m}_{POE_1} - \dot{m}_{MO}}{\dot{m}_{MO}} 100 \tag{4.23}$$

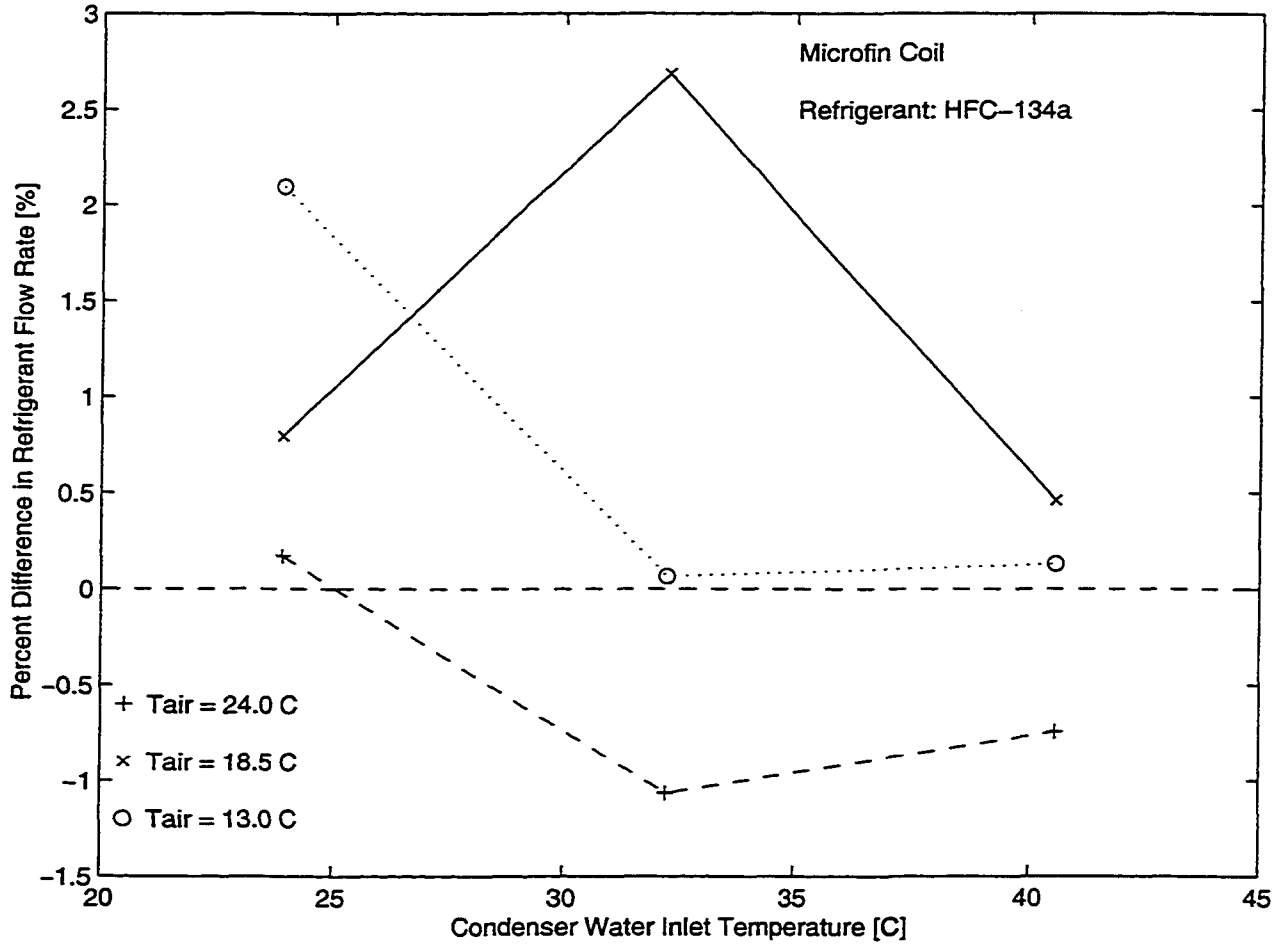

Figure 4.35. Percent difference in refrigerant flow rate for POE_3 and POE_1 with microfin-tube coil

The results presented for capacity, evaporator pressure, and mass flow rate do not suggest significant differences between POE_3 and POE_1. It appears that for lower air temperatures POE_3 has a higher evaporator pressure, however these results are somewhat scattered without specific trends. Even so, as mentioned earlier the higher evaporator pressure is associated with better evaporator performance. For the highest air temperature of 24 °C, the differences in measured pressures are small to the point of being insignificant.

Partial miscibility appears to have negative effects on the evaporator and, consequently, system performance. It was expected that POE_3, which has a lower viscosity than POE_1 and similar viscosity characteristics to POE_2, would perform similar to that of POE_2. This was particularly expected since significant differences were observed in refrigeration capacity between POE_2 and POE_1, which is not the case for POE_3 and POE_1 lubricants.

4.4.3 Compressor Power Consumption

The compressor power consumption is plotted as a function of operating conditions in Figure 4.36. For higher air temperatures of 18.5 and 24 °C, the power consumption is higher for the POE_3 lubricant compared to the POE_1 lubricant. For the lowest air temperature of 13 °C, the differences in power consumption are small and hardly distinguishable.

The uncertainty in the power consumption was reported to be ±0.02 kW and at the higher evaporator air temperatures of 18.5 and 24 °C the differences for measured power consumption are higher than the uncertainty value.

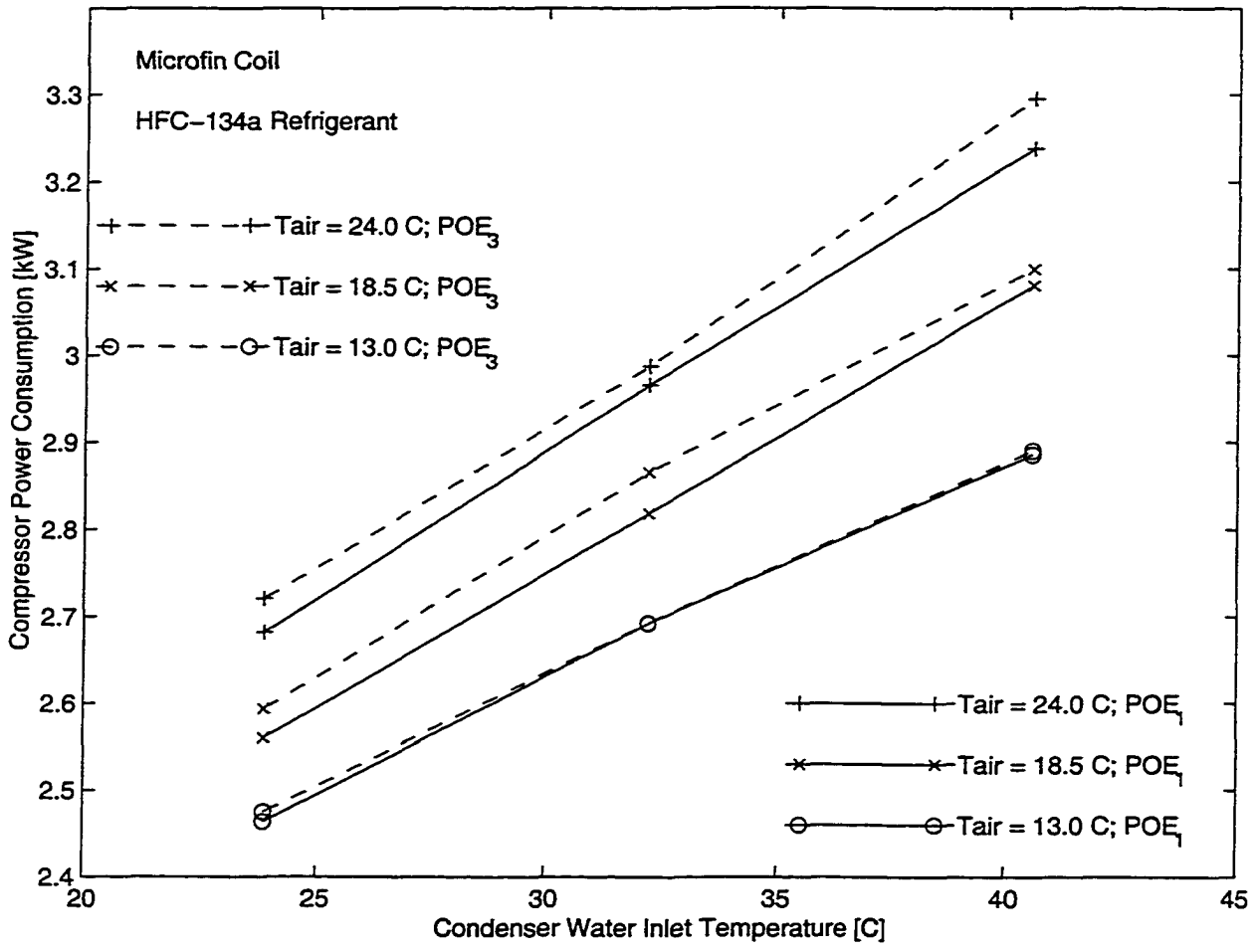

Figure 4.36. Compressor power consumption for POE_3 and POE_1 with microfin-tube coil

Alternatively, the power consumption is presented as a percent difference between power consumption of POE_3 and POE_1 lubricants in the same manner as for other lubricants. The results are presented in Figure 4.37 for a standard set of operating temperatures.

$$\text{Power}_{dif} = \frac{\text{Power}_{POE_3} - \text{Power}_{POE_1}}{\text{Power}_{POE_1}} 100 \tag{4.24}$$

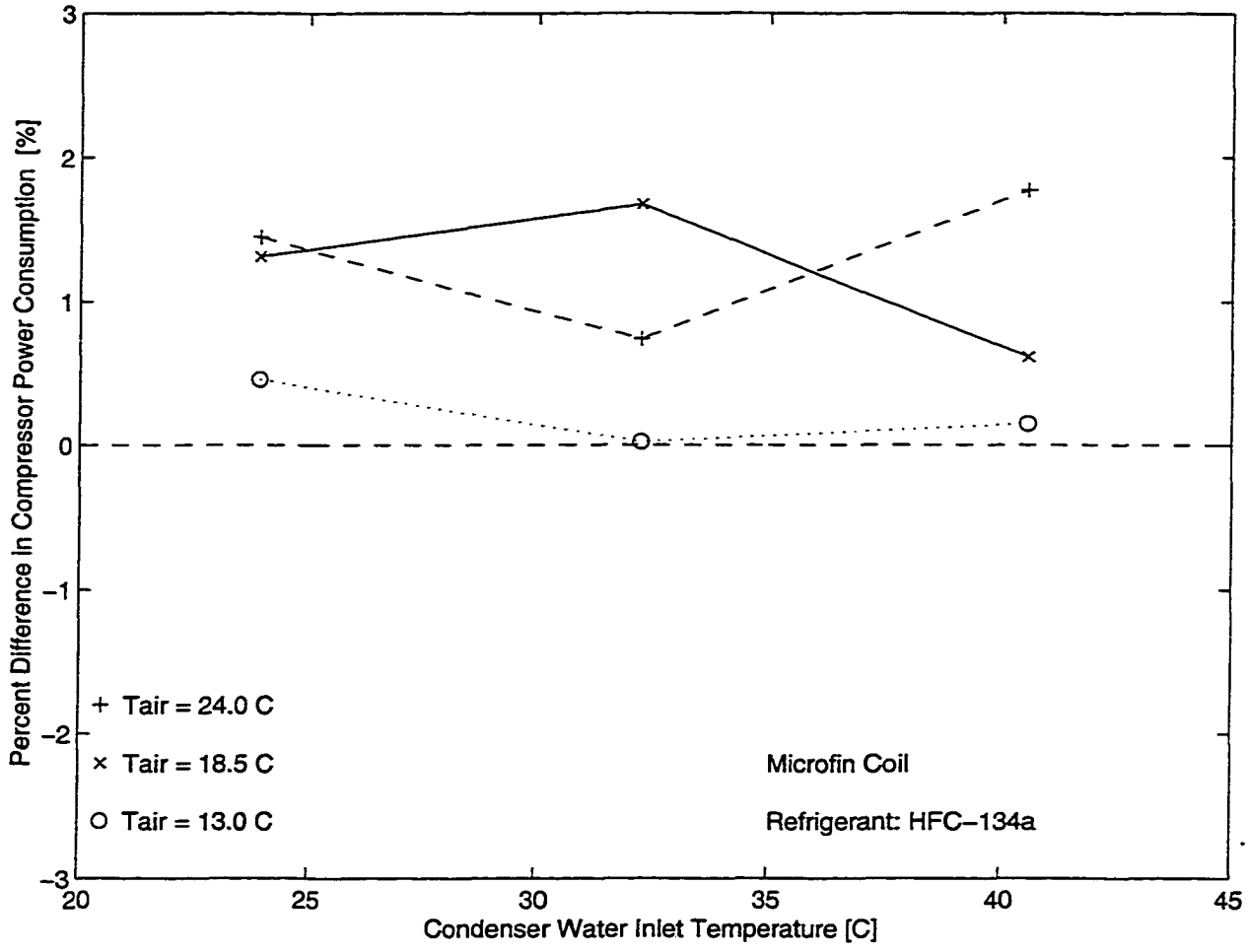

Figure 4.37. Percent difference in compressor power consumption for POE_3 and POE_1 with microfin-tube coil

As presented in Figure 4.36, the power consumption for the POE_3 lubricant was consistently higher. However, since the uncertainty in percent difference of power consumption is around ±1 percent, it can be concluded that power consumption differences between POE_3 and POE_1 are insignificant for the lowest air temperature of 13 °C. For air temperatures of 18.5 and 24 °C, the power consumption for POE_3 is higher than for POE_1, with the percent difference being greater than the compressor power consumption uncertainty.

The differences in power consumption are also correlated to the differences in operating parameters. This analysis is based on usung Equation 4.11 to determine the effects

of variations in the operating parameters, similar refrigerant flow rate and other refrigerant properties, on the observed variations in power consumption. It was found that the observed power consumption differences are proportional to the variations in refrigerant flow rate and other refrigerant properties, and apparently, the lubricant properties do not directly affect compressor performance.

Lastly, the differences in compressor discharge pressure are presented in Figure 4.38 where the absolute difference between POE_3 and POE_1 is plotted as functions of operating conditions.

$$\text{Pressure}_{dif} = \text{Pressure}_{POE_3} - \text{Pressure}_{POE_1} \tag{4.25}$$

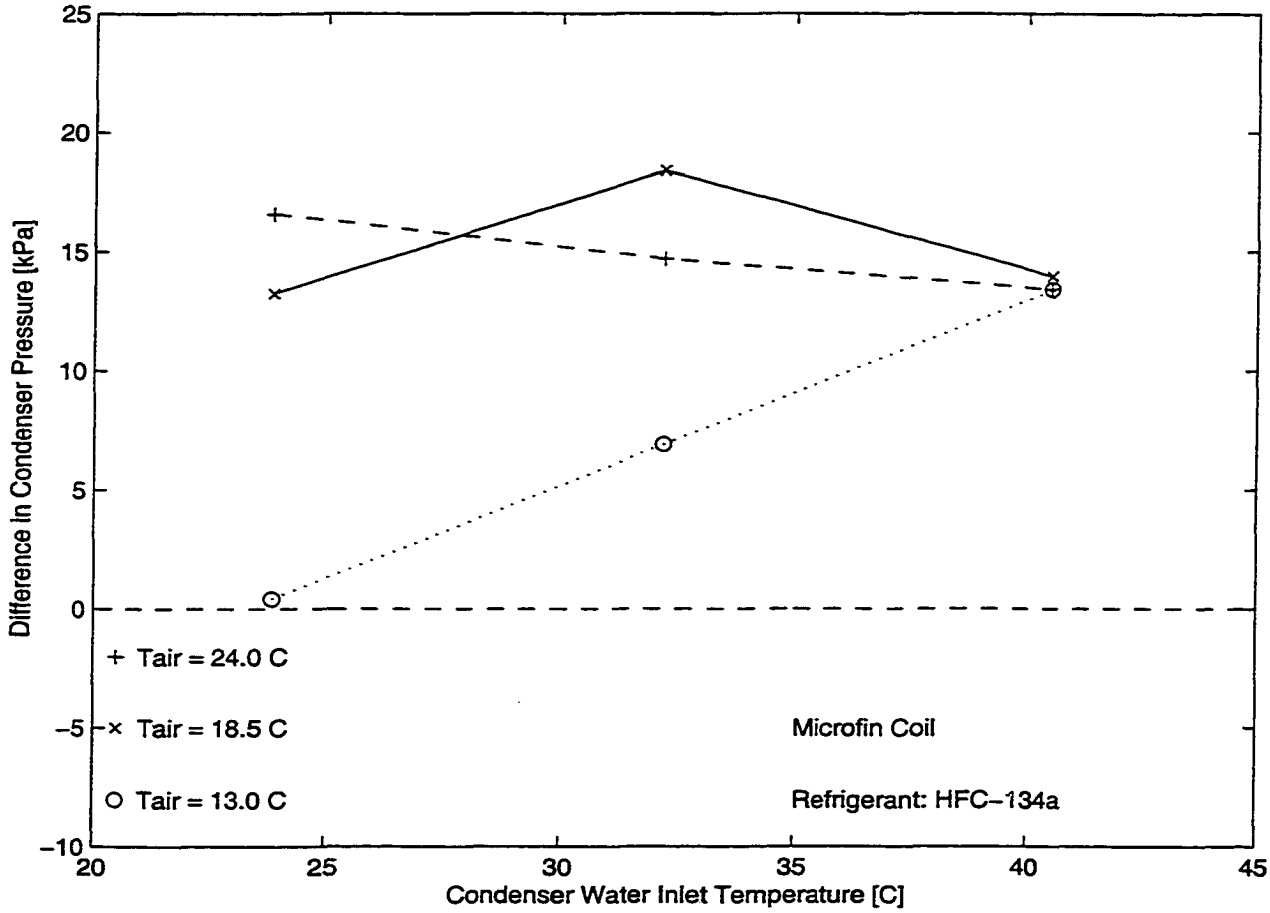

Figure 4.38. Difference in compressor discharge pressure POE_3 and POE_1 with microfin-tube coil

The measured compressor discharge pressure is consistently higher for POE_3 data when compared to the POE_1 data. The observed differences are as high as 20 kPa suggesting that the two POEs have different solubility characteristics with the HFC-134a refrigerant. As defined earlier in Section 4.1, the effective charge depends on the amount of refrigerant dissolved in the lubricant, and for the same actual charge, the system with a higher discharge pressure has a larger effective charge. As was the case for the other lubricants, the POE_1 data indicates the lowest discharge pressure suggesting that the POE_1 has the highest solubility with HFC-134a among tested lubricants.

4.5 Effects of Lubricant/Refrigerant Miscibility with a Different Coil

The results of the experimental study of the two lubricants for the smooth-tube coil, namely POE_1 and the mineral oil, are presented by plotting and analyzing the performance characteristics of the refrigeration system. These performance factors (e.g. COP, capacity, power consumption and efficiencies) are analyzed for a range of air and water temperatures in a similar manner as was done for the microfin-tube coil in Section 4.2. In addition to the standard set of nine operating points, the testing of this pair of lubricants was done for an additional condenser water temperature of 18.5 °C (65 °F).

The objective of the analysis of lubricant miscibility effects on the system performance with a different type of the coil is twofold: 1) to investigate the effects of heat transfer surface and 2) to analyze the effects of different refrigeration systems on lubricant comparisons. Therefore, the same miscible POE_1 and the immiscible MO were used in the system with the smooth-type of coil to allow for a direct comparison of the two coil types in reference to the lubricant miscibility effects.

4.5.1 Coefficient of performance (COP)

The COP is defined as the useful energy transfer (i.e. evaporator capacity) divided by the energy consumed (i.e., compressor power consumption), and it is plotted in Figure 4.39 for both lubricants at different operating conditions and. An important observation in Figure 4.39 is that the system operation is slightly more efficient with the POE lubricant than with the mineral oil. However, the maximum COP variation due to lubricant type is only around 2.5 percent, which is still significantly larger than the estimated uncertainty in the COP of 1.1 percent.

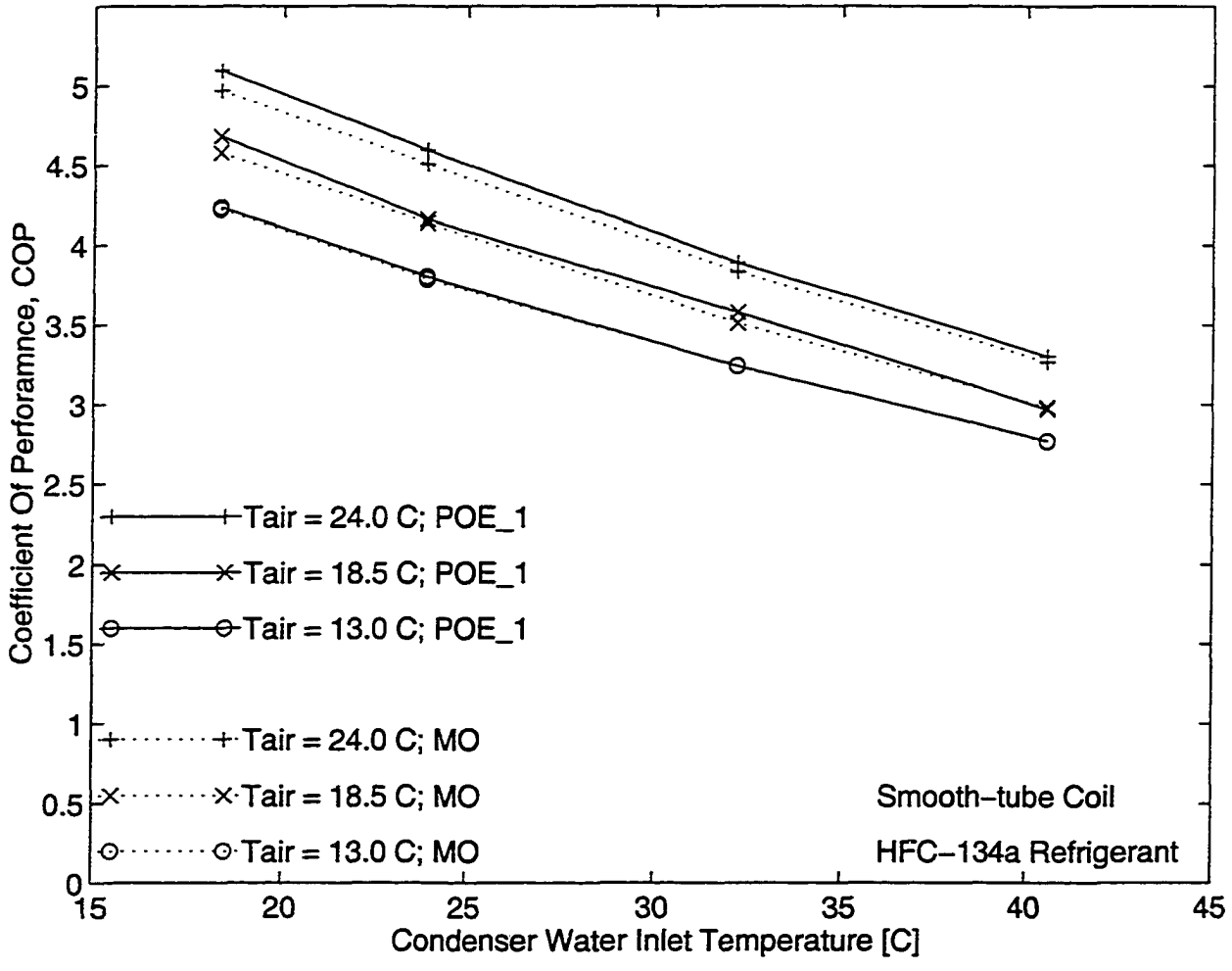

Figure 4.39. COP for POE_1 and MO for the system with smooth-tube coil

The COP, as the most important indicator of refrigeration performance, suggests that there are energy savings related to the POE utilization, which is a similar trend to that observed with the microfin-tube coil. However, the COP differences for the two lubricants are smaller for the system with the smooth-tube coil compared to the microfin-tube system.

Other observations in Figure 4.39 are that the differences in the COP between lubricant types are not as significant as the COP differences due to varying air and water temperatures. These differences can be illustrated by establishing a reference point corresponding to an air temperature of 13 °C and a water temperature of 18.5 °C. It can then be observed that an increase in the air temperature from the reference point of 13 °C to 24 °C, while keeping the same condenser water temperature, results in approximately a 25 percent COP increase. If the water temperature is increased from 18.5 °C to 40 °C then the COP decreases around 40 percent.

The results plotted in Figure 4.39 can also be presented as a percent difference as shown in Figure 4.40. The percent COP difference, COP_{dif}, is defined as the difference between the COPs for the POE lubricant and the mineral oil divided by the COP for the POE lubricant with the value expressed as a percentage:

$$COP_{dif}[\%] = \frac{COP_{POE_1} - COP_{MO}}{COP_{MO}} 100 \tag{4.26}$$

Using this approach, the results plotted in Figure 4.40 also show that the system operating with the POE lubricant has a larger COP than the system operating with the mineral oil. The percent differences are as high as 2.5 percent. The largest percent differences correspond to the points with the highest evaporator temperature of 24 °C (75 F) as for these points, the COP difference is significant being larger than the COP uncertainty of ±1.1 percent. Also, it should be noted that the COP percent difference diminishes to a fraction of a percent as the evaporator air temperature decreases.

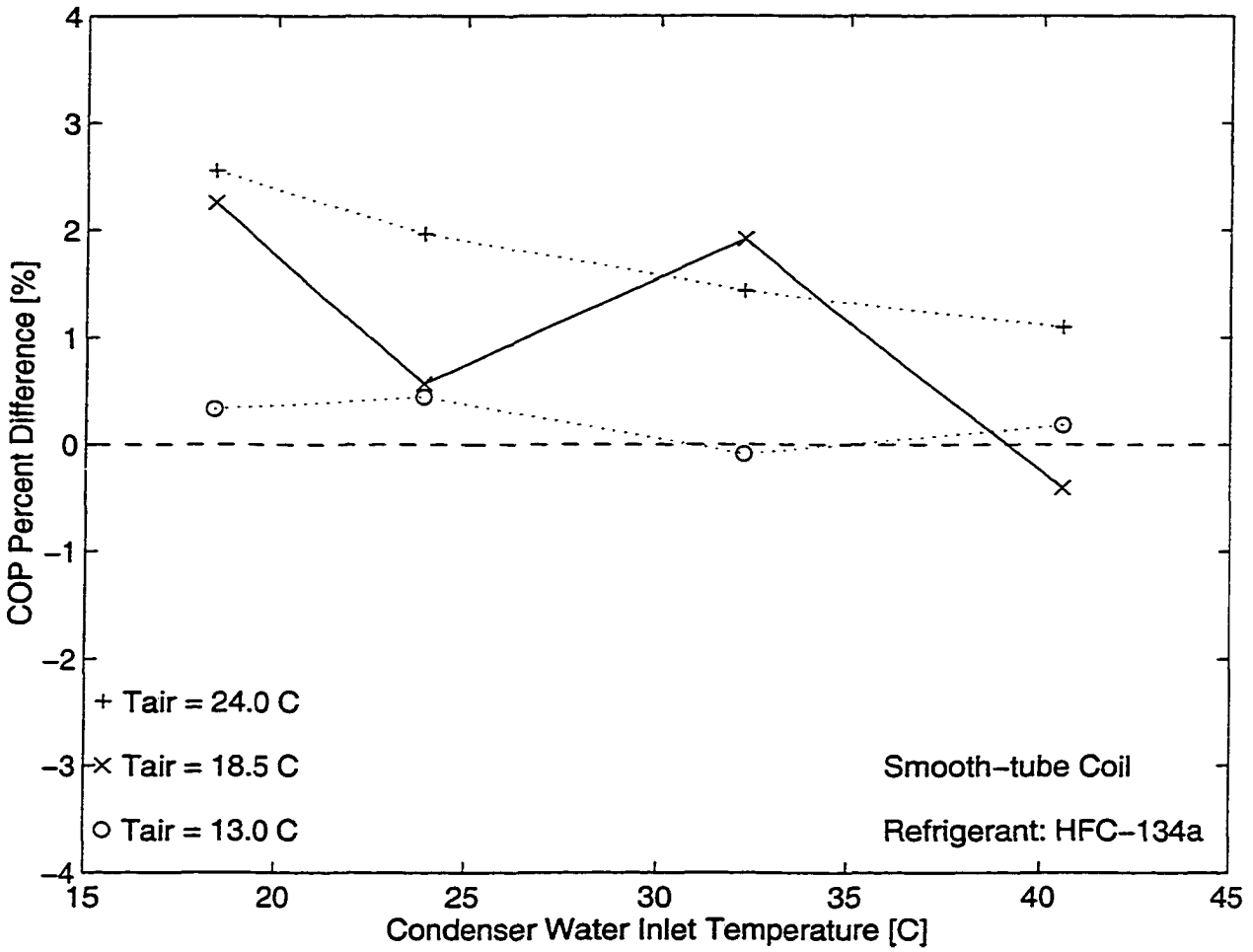

Figure 4.40 COP percent difference for POE_1 and MO with smooth-tube coil

For the lowest air temperature of 13 °C, even though POE_1 indicates a higher COP, the differences are smaller than the estimated uncertainty, and therefore, they are considered insignificant. The system behavior at air temperature of 18.5 °C appears to be lacking a definite trend.

These results suggest that for an air conditioning application, operating with air entering at 24 °C (75 °F) there is a $25 potential saving for every $1,000 spent on operating the refrigeration system with the POE lubricant instead of the mineral oil.

4.5.2 Evaporator Capacity

As done in the previous sections, further analysis of system performance is conducted by presenting lubricant effects on the evaporator capacity. The capacity or cooling effect (i.e., the heat transfer rate from the air to the refrigerant in the evaporator) is plotted versus different operating conditions in Figure 4.41. The capacity for the mineral oil data is larger than the capacity of the corresponding POE lubricant data, with the largest value being around 3 percent, which is significantly larger than the estimated uncertainty in capacity of around ±0.4 percent.

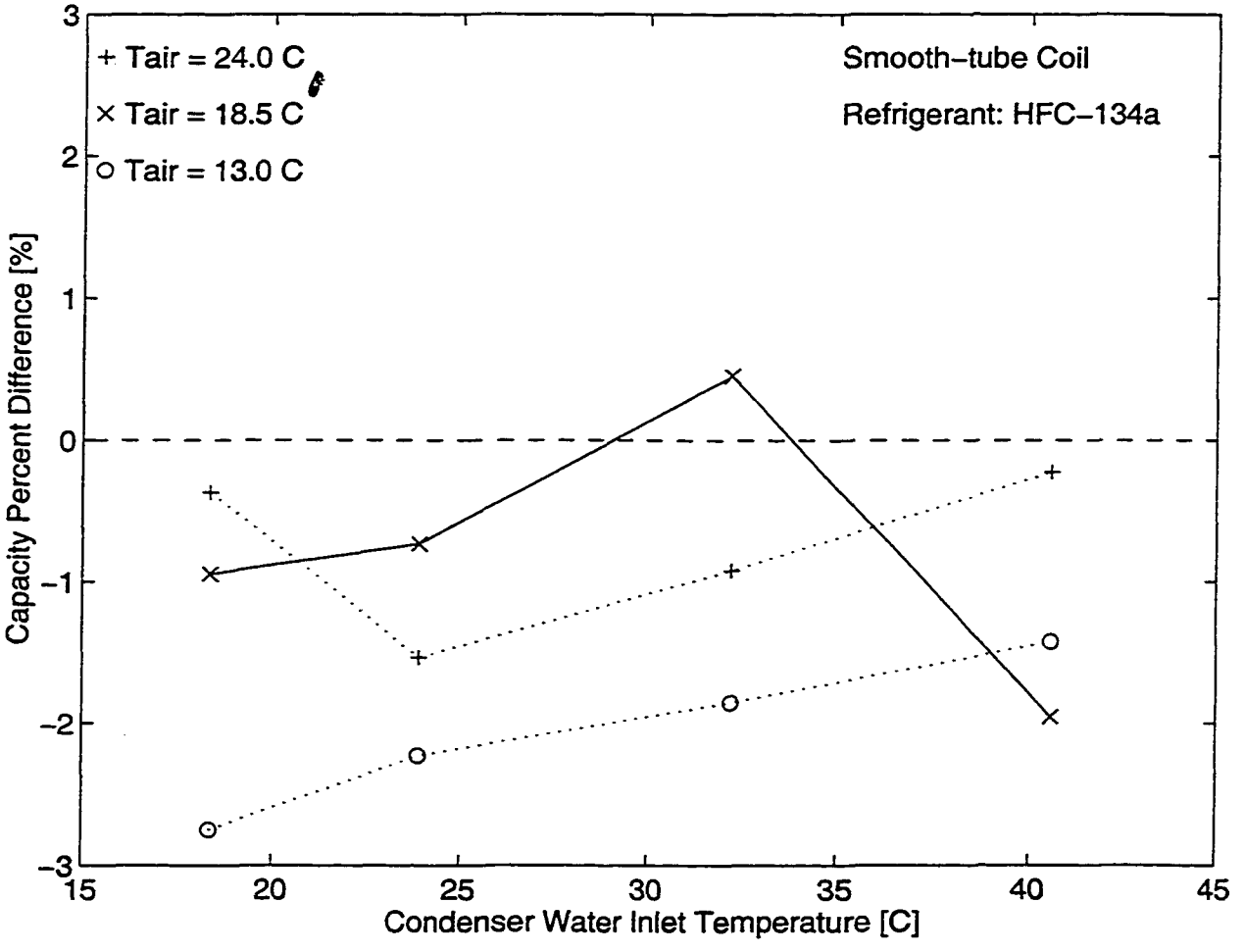

Figure 4.41 Capacity for POE_1 and MO with smooth-tube coil

In general, the capacity is a strong function of both the inlet air temperatures, with the maximum change being around 30 percent and the inlet condenser water temperatures, with the maximum change being around 25 percent. Nevertheless, differences in capacity due to lubricant miscibility effects are visible.

In contrast to the behavior observed for the system operating with the microfin-tube coil, the capacity appears to be larger for the immiscible lubricant suggesting that evaporator performance improves with the utilization of immiscible lubricant.

The percent capacity differences between matching points are plotted against different operating conditions in Figure 4.42. The capacity percent difference was calculated in the same manner as the COP percent difference defined in Equation 4.2.1:

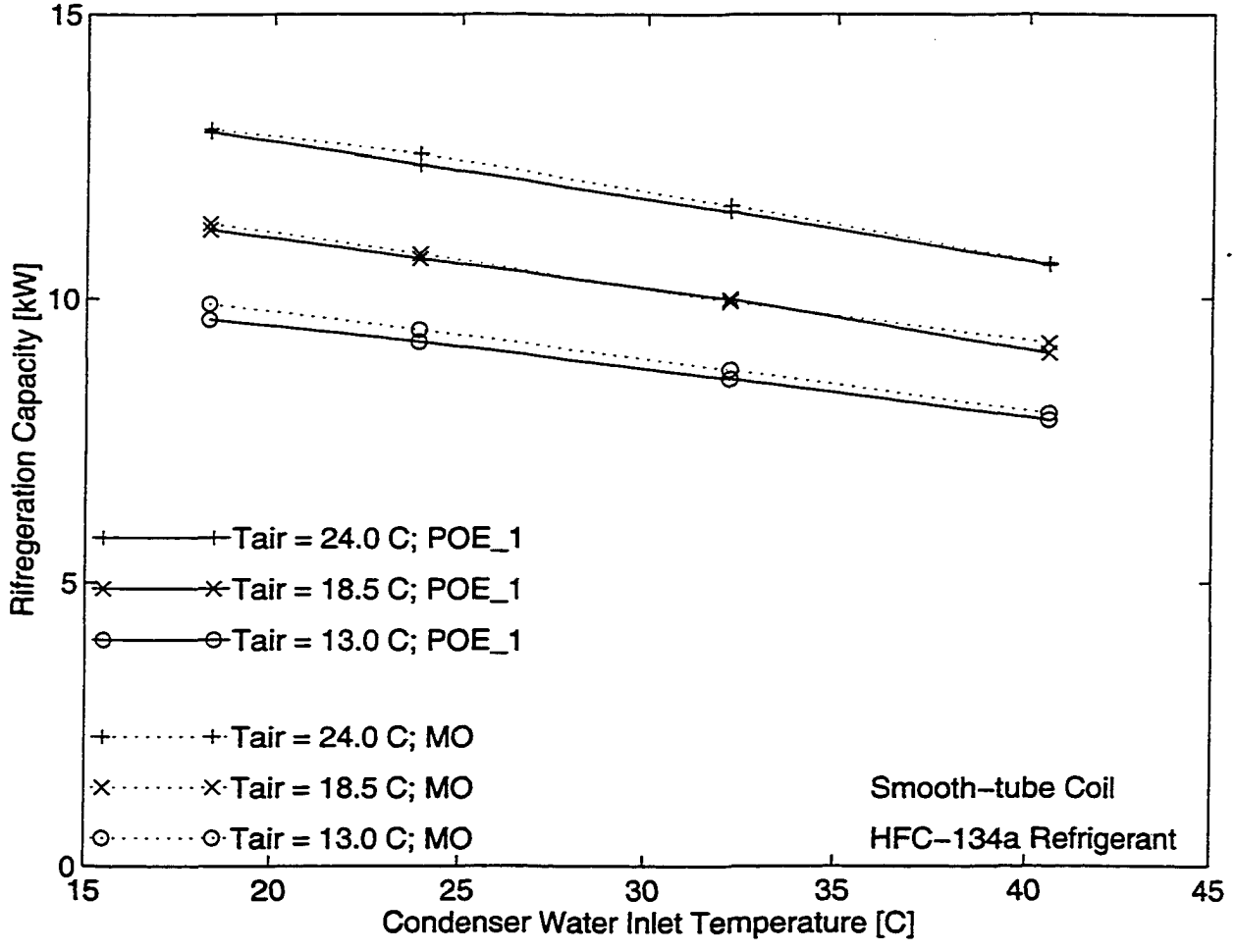

Figure 4.42. Capacity percent difference for POE_1 and MO with smooth-tube coil

$$\text{Capacity}_{dif} = \frac{\text{Capacity}_{POE_1} - \text{Capacity}_{MO}}{\text{Capacity}_{MO}} 100 \qquad (4.27)$$

Figure 4.42 shows that the mineral oil has a larger capacity compared to the POE_1, with the maximum difference being 3 percent at an air temperature of 13 °C (55 °F). The differences in capacity are especially evident at the lowest air temperature. Since the uncertainty in the capacity percent difference is around ±0.4 percent, it can be inferred that the capacity is significantly larger for the mineral oil data.

Based on the previous discussions about the effects of other tested lubricants, the differences in evaporator performance were correlated to the evaporation heat transfer. The argument is that if the evaporation heat transfer increases, then a smaller temperature difference is required in the evaporator assuming that other temperatures are fixed, the evaporator temperature must increase. The differences in evaporator temperatures are presented by utilizing measured evaporator pressures. Specifically, the absolute difference in pressure between POE_1 and MO are plotted as a function of operating conditions in Figure 4.43

The differences in the evaporator pressure, representing differences in evaporator pressure, are only consistent for the lowest air temperature of 13 °C, which shows the evaporator pressure as being higher for mineral oil, implying that the refrigerant side heat transfer might be higher for that lubricant. For the other two air temperatures, there are no apparent trends in the data. These results differ from those observed for the system with the microfin-tube coil in which the evaporator pressure was consistently higher for the POE_1 lubricant. Apparently, the type of heat transfer surface in refrigerant tubes is an important factor when analyzing lubricant effects on the system performance.

The differences in the measured refrigerant flow rate for POE_1 and MO follow the same trend observed for the evaporator pressure. The volumetric efficiency was higher for the MO data, but actual differences were rarely higher than the uncertainty in the volumetric efficiency difference of ±0.5 percent.

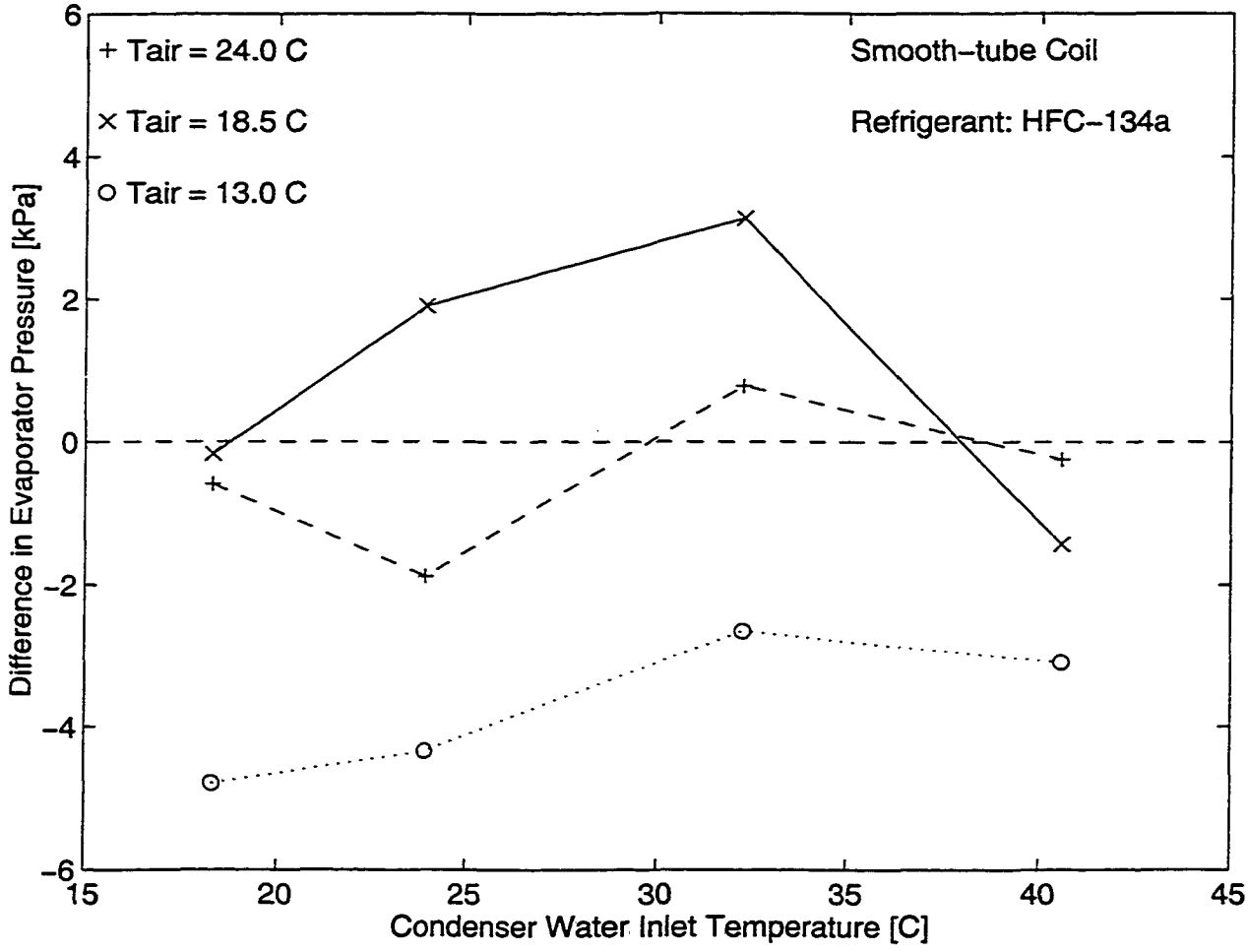

Figure 4.43. Difference in compressor suction pressure POE_1 and MO with smooth-tube coil

The percent difference in refrigerant flow rate is plotted as a function of operating temperatures shown in Figure 4.44.

$$\dot{m}_{dif} = \frac{\dot{m}_{POE_1} - \dot{m}_{MO}}{\dot{m}_{MO}} 100 \tag{4.28}$$

The presented data for evaporator pressure and refrigerant flow rate imply that the evaporator performance improves with using MO over POE_1. However, only significant differences were observed for the lowest air temperature of 13 °C.

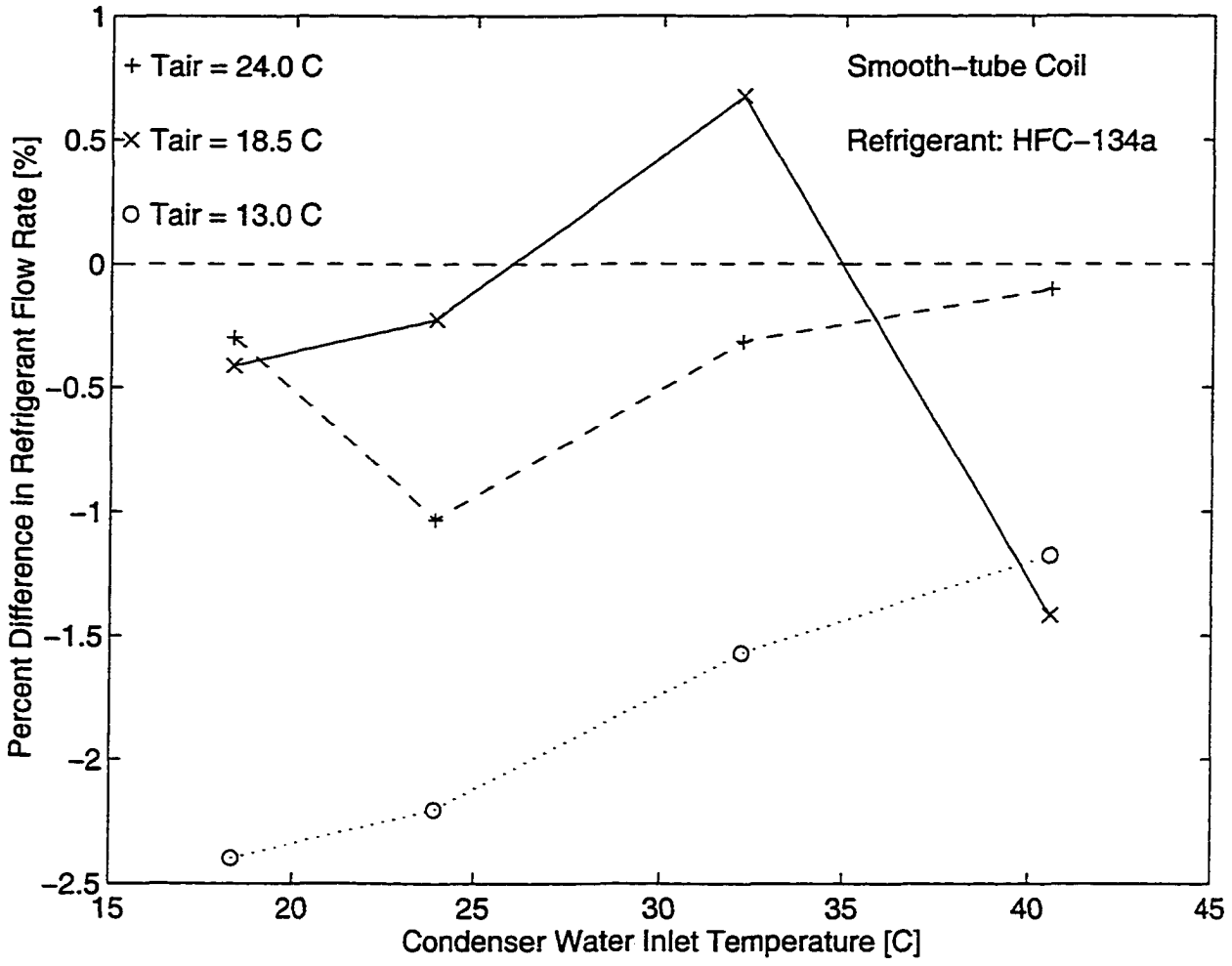

Figure 4.44. Percent difference in refrigerant flow rate for POE_1 and MO with smooth-tube coil

4.5.3 Compressor Power Consumption

The compressor power consumption is presented as a function of different operating conditions in Figure 4.45. The power consumption is slightly larger for the compressor operating with the mineral oil. In addition, the compressor power increases with increasing condenser water inlet temperature, as well as with increasing air inlet temperatures.

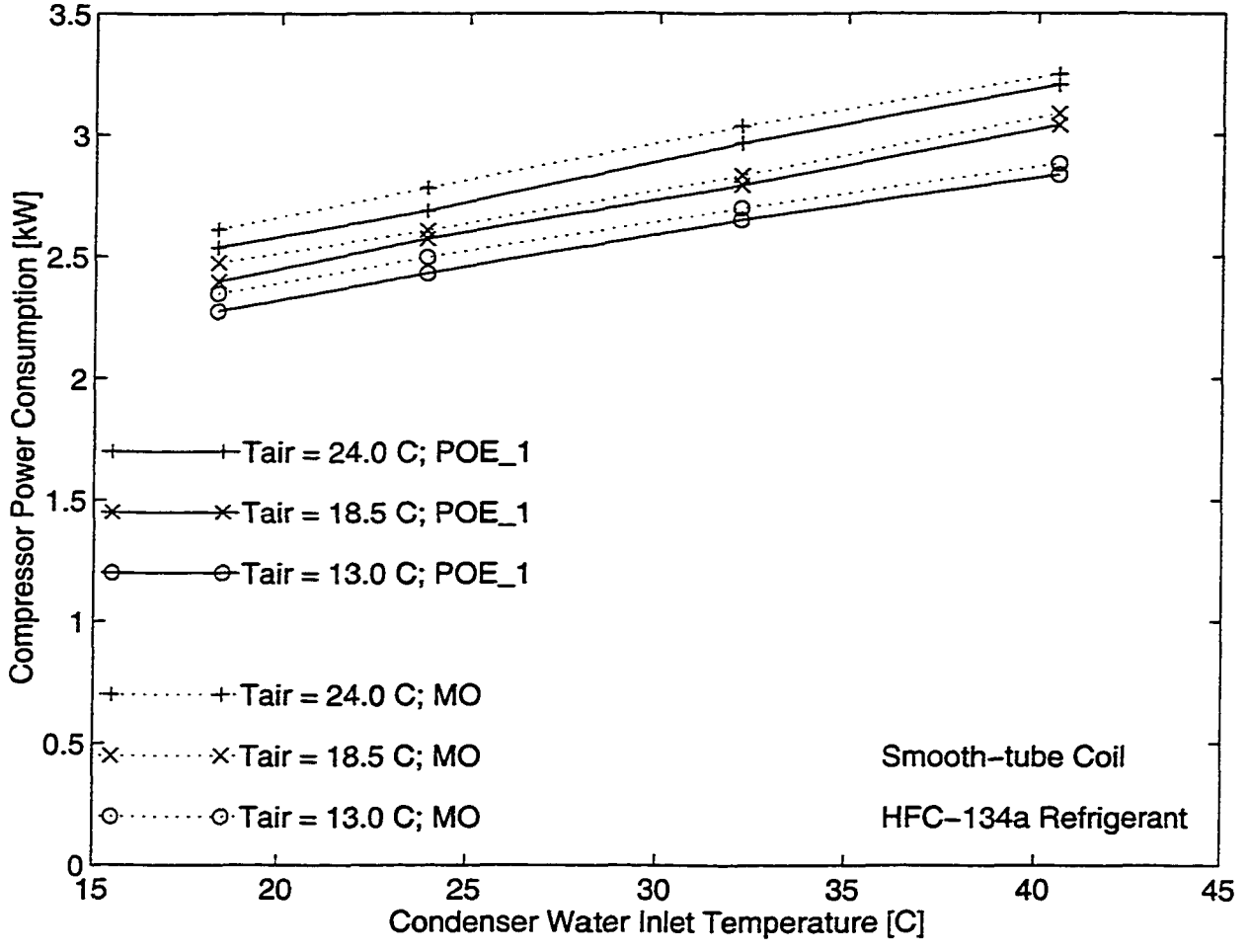

Figure 4.45. Compressor power consumption for POE_1 and MO with smooth-tube coil

Power consumption appears to be consistently larger for MO than for POE_1. The observed differences in power consumption are larger than the uncertainty in measuring the compressor power consumption, which is around ±0.02 kW. These results are comparable to the results observed for the system performance with the microfin-tube coil.

The power consumption as a percent difference between POE and mineral oil is plotted against the air and water inlet temperatures in Figure 4.46. The power percent difference is defined in the same manner as the COP percent difference as given in Equation 4.26. The largest difference is almost 4 percent, and, in addition, the differences for all other points are larger than the uncertainty in the percent difference in power consumption of ±1

percent, and thus, it can be inferred that the power consumption is significantly larger for MO than for POE_1.

The results in the compressor power consumption are similar to those observed for the system with the microfin-tube coil. The differences in power consumption are not only due to the differences in refrigerant flow rate and refrigerant properties but also to the actual characteristics of the lubricant. Following the argument presented in Section 4.2.3, one possible explanation is that due to the MO higher effective viscosity there is a higher compressor work, due to additional frictional work that the compressor has to overcome.

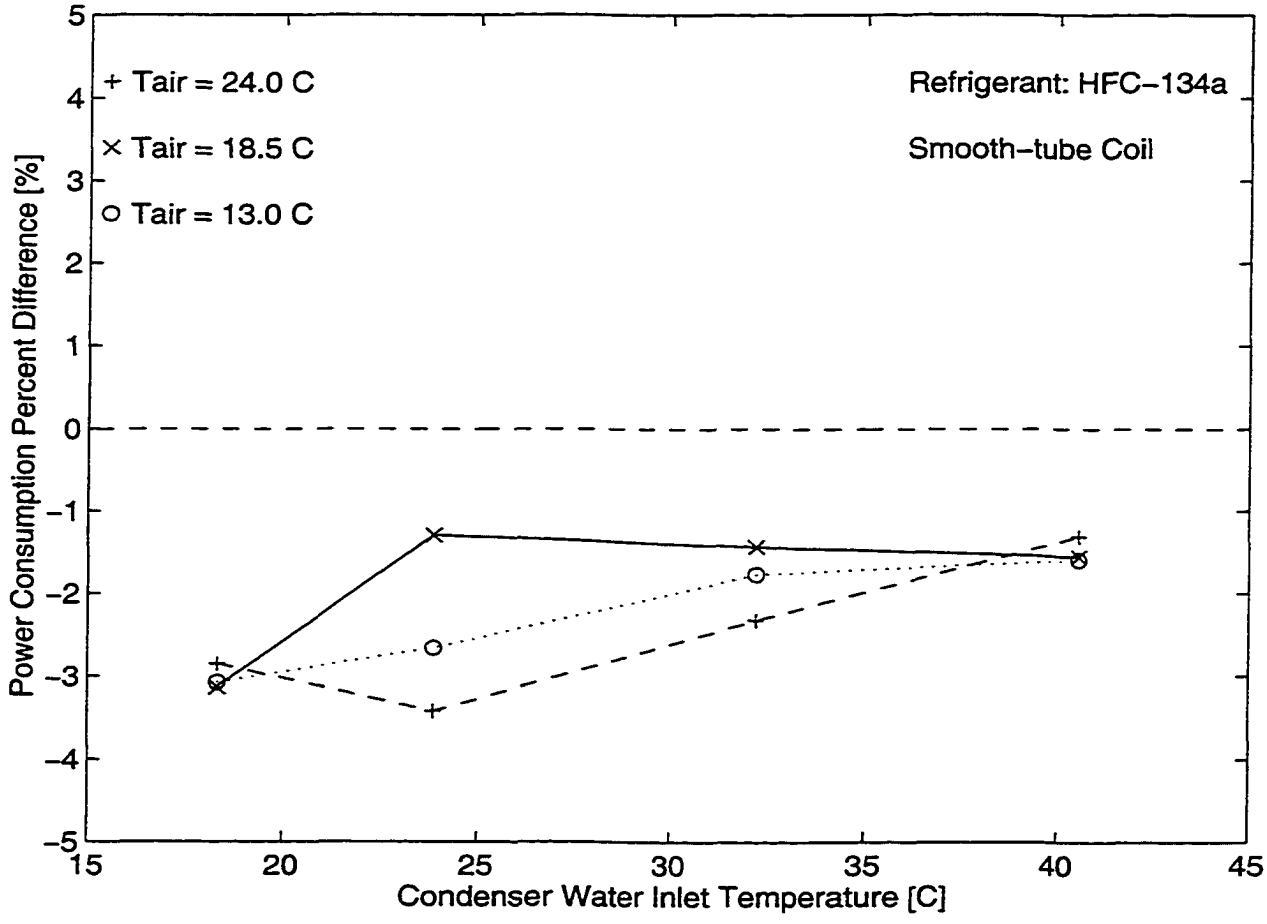

Figure 4.46. Percent difference in compressor power consumption for POE_1 and MO with smooth-tube coil

The system operating with MO has a higher effective charge, which further affects the magnitude of the compressor discharge pressure. The compressor discharge pressure for the MO is consistently higher than that of POE_1 with differences being similar in magnitude to those observed in the study with the microfin-tube coil. Again, it has been confirmed that due to the amount of dissolved refrigerant, the effective charge of the system with POE _1 is lower.

As reported in the previous sections, the lubricant effect on compressor efficiencies is not substantial. For both the isentropic and the volumetric efficiencies, the observed differences between POE_1 and MO were rarely larger than respective uncertainties.

4.6 Conclusions

The type of lubricant used can have a significant effect on a refrigeration system performance. For example, it was found that the coefficient of performance (COP) of the refrigeration system can vary as much as 5 percent between a miscible POE and an immiscible MO. Interestingly, the lubricant characteristics had a major impact on the evaporation heat transfer, which in turn, affected other performance parameters in the system. The effects of lubricant type on compressor performance are minimal, as evident by the fact that for most of the tested lubricants the compressor efficiencies were not significantly different. Therefore, it was decided to further analyze the evaporator performance, especially emphasizing the evaporation heat transfer. The chapter that follows is dedicated to quantitatively assessing differences in evaporation heat transfer for the different lubricants used.

It was found that refrigerant/lubricant miscibility has positive effects on system performance because all of the miscible lubricants tested indicated better performance than the immiscible lubricant. The superiority of miscible lubricants is more pronounced for the system operating with the microfin-tube coil as opposed to the smooth-tube coil.

For testing conducted with the microfin-tube coil, the COP results for all lubricants are presented in Figure 4.47. It is apparent that the COP for the mineral oil is lower than all

the other POE lubricants. The differences in COP are as high as 5.2 percent. For the most of the points, the differences in COP were larger than the uncertainty in COP percent difference of ±1.1 percent, and thus, these differences are significant.

Also, it is important to recognize that the observed differences in system performance between the three POE lubricants are not as large as the differences between miscible and immiscible lubricants. This fact supports the theory that miscibility is the most important characteristic of a lubricant in terms of affecting system efficiency.

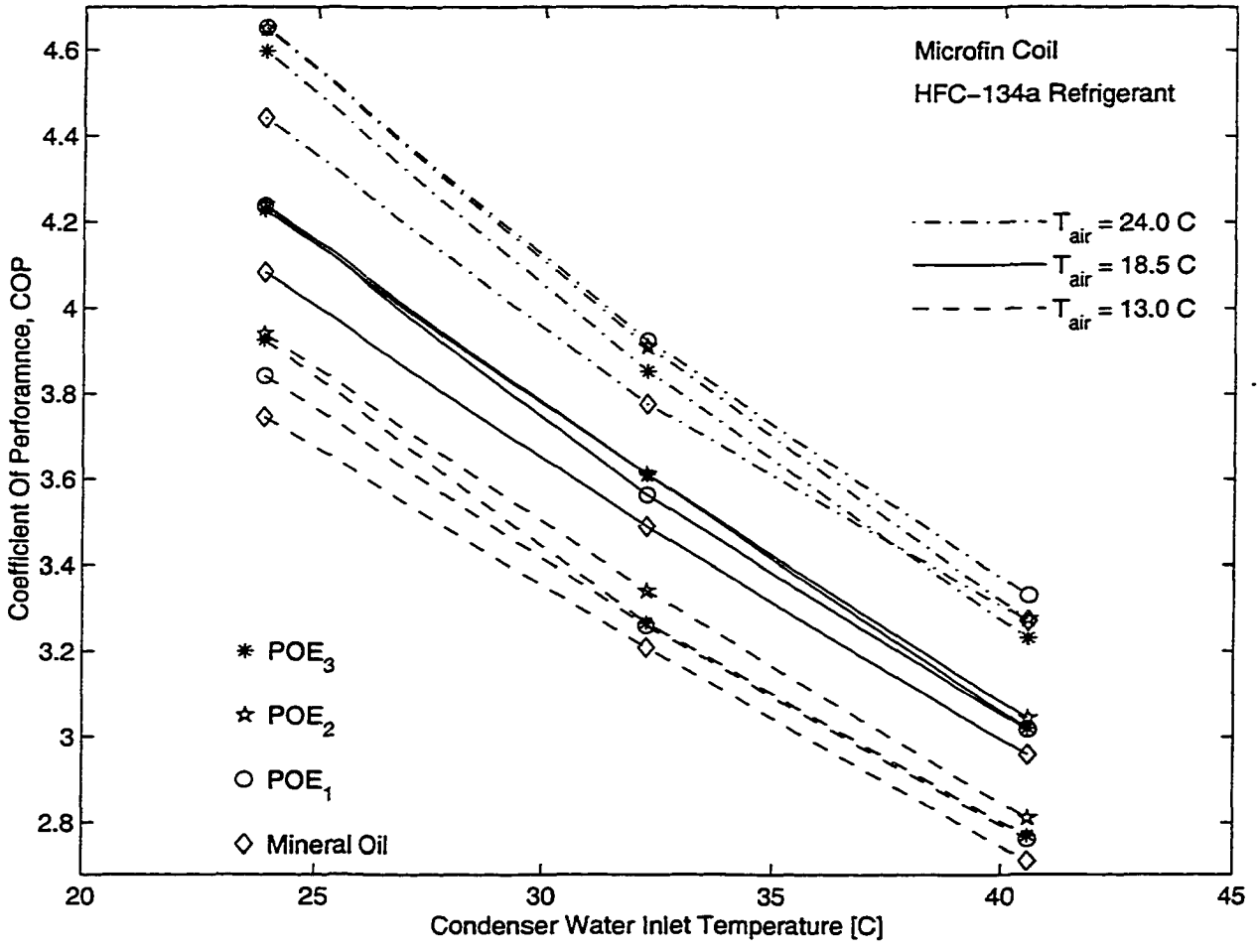

Figure 4.47. COP for lubricants tested with microfin-tube coil

Furthermore, as the condenser temperature increases, it appears that differences in COP between MO and POE lubricants decrease. For example, for the lowest air temperature of 13°C, the COP percent difference between POE_1 and MO is 2.6 percent at the lowest condenser water temperature of 24°C, while the difference is 1.8 percent at the highest water temperature of 40.5°C. For the highest air temperature, the COP percent difference changes from 4.7 to 1.8 percent for the same condenser water temperatures.

For the smooth tube coil, the differences in COP between miscible POE and immiscible MO were not as significant as differences in the COP observed for the microfin-tube coil. Only at the highest air temperature of 24°C was the COP for the POE_1 with the smooth-tube coil significantly higher than the COP for MO. The actual test results for all lubricants are presented in Appendix C. Interestingly, the heat transfer surface appears to be an important factor in studying the lubricant effects on system performance.

A major impact of lubricants on system performance is through the alteration of the evaporation heat transfer. If the evaporation heat transfer rate increases, the evaporator temperature increases, leading to improvement in the evaporator coil performance as well as the overall system performance. These findings are in agreement with several other studies, which indicate that a small amount of lubricant present in a refrigerant two-phase flow could induce an enormous change of the average evaporation heat transfer coefficient.

Among miscible lubricants, a lower viscosity lubricant, POE_2, appears to outperform both higher viscosity lubricant, POE_1, and partially miscible lubricant, POE_3, at evaporator air temperatures of 18.5°C and 24°C as refrigeration capacity is plotted in Figure 4.48 for different operating parameters.

These results are in agreement with the hypothesis that evaporation heat transfer can be improved with usage of a lower viscosity lubricant. Capacity differences between POE_2 and POE_1 are significant as they are consistently larger than the uncertainty in determining capacity difference of 0.4 percent.

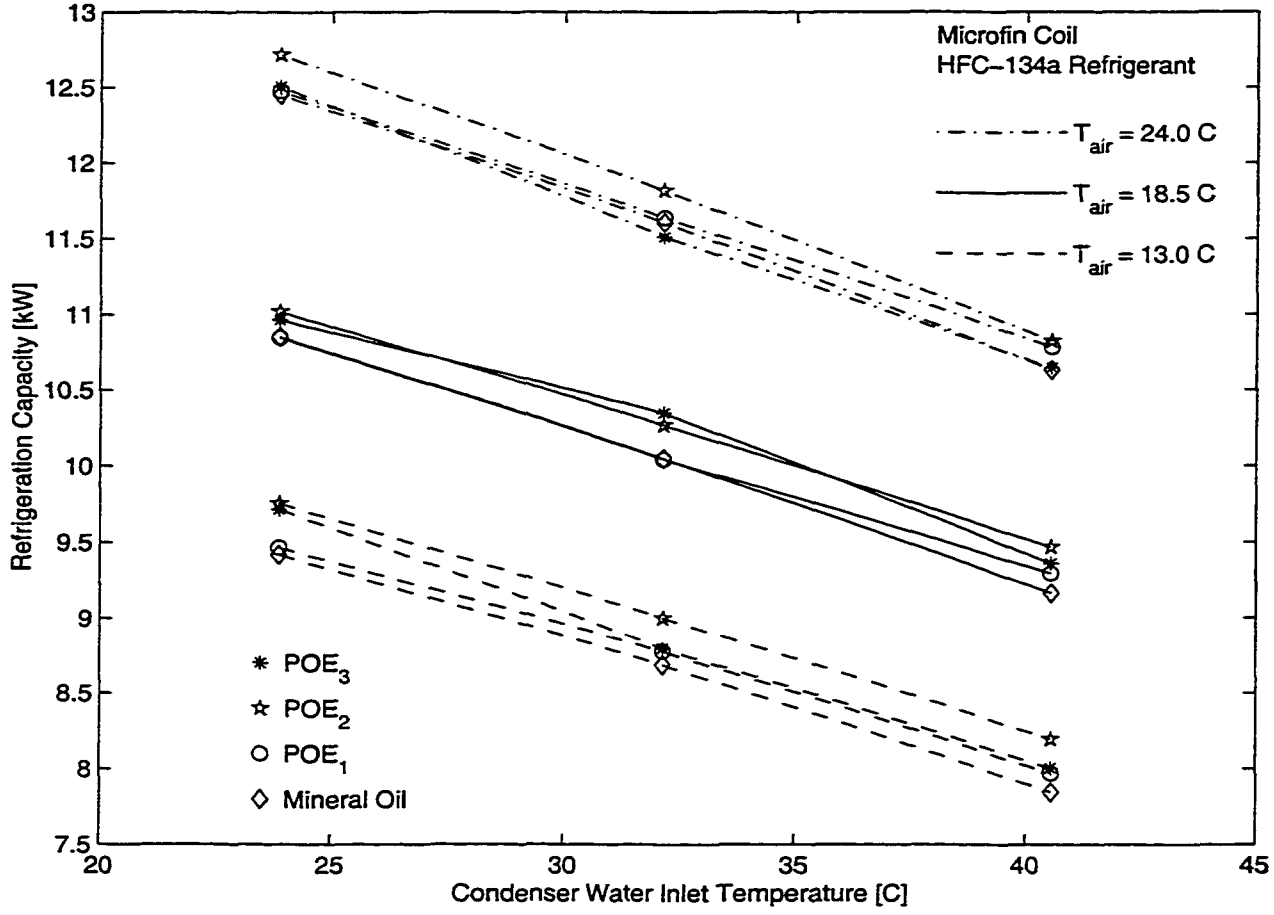

Figure 4.48. Capacity for lubricants tested with microfin-tube coil

Moreover, the capacity is significantly larger for POE lubricants when compared to MO, suggesting that the evaporation heat transfer of HFC-134a with miscible lubricants is better than with immiscible lubricant. On the other hand, results for the smooth-tube coil suggest that capacity improves when using an immiscible lubricant, again suggesting that refrigerant-side heat transfer surface plays an important role.

Compressor power consumption for the system with the microfin-tube coil is plotted in Figure 4.49. The compressor power consumption is higher for MO than for other POE lubricants for a majority of the test conditions. It should be noted that as condenser temperature increases the differences in power consumption between MO and other POE lubricants diminishes. Finally, for the highest condenser temperature of 40.5°C, the MO data

do not have the highest recorded power consumption. This trend coincides with the trend observed in the COP data, presented in Figure 4.47.

Also, it appears that as the evaporator air temperature increases then the differences in power consumption between immiscible and miscible lubricant increase. Based on the uncertainty in power consumption difference being around ±1 percent, the power consumption differences between MO and other POEs at the highest evaporator air temperature of 24°C and at lower condenser water temperatures of 24°C and 32°C were significant. However, for the lowest air temperature of 13 °C there were significant differences recorded between MO and POEs data only at the condenser water temperature of 24 °C.

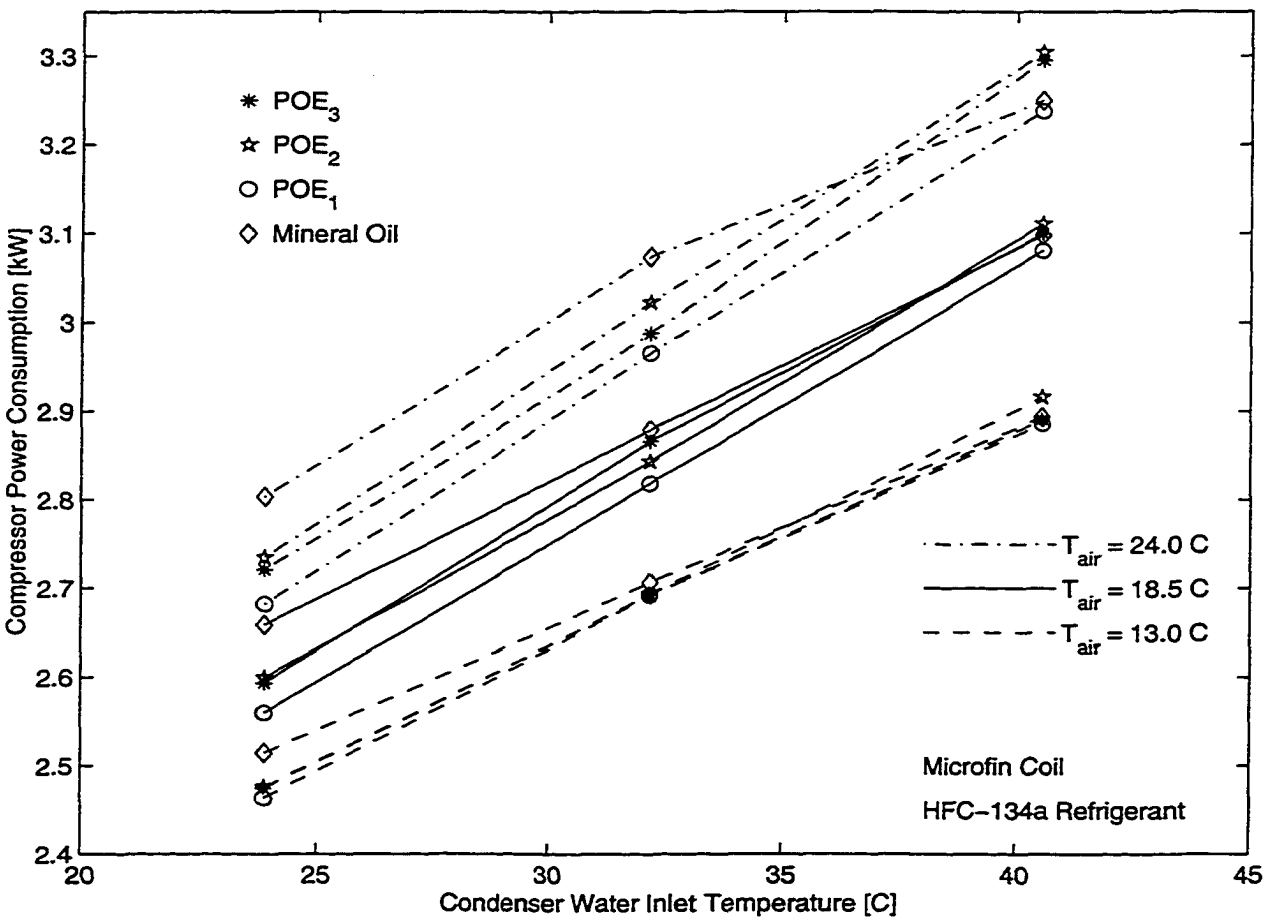

Figure 4.49. Compressor power consumption for lubricants tested with microfin-tube coil

The effects of refrigerant charge on system performance were studied to prevent this parameter from biasing the data. The dependence of COP on refrigerant charge was shown to be weak. For example, for variations in charge of ±10 percent of the optimum charge, the COP reduction is less than the estimated uncertainty in the COP. Therefore, the optimum charge determined for one lubricant was used to test all other lubricants.

It was estimated that for the same actual charge, there are differences in effective charges, due to the amount of refrigerant dissolved in the lubricant. For the immiscible mineral oil, the effective charge is 4 percent higher than for the miscible POE lubricant. The differences in the effective charge were shown to affect the magnitude of the condenser pressure. Using measured differences in the condenser pressure for different lubricants, it was possible to compare HFC-134a and lubricants mutual solubility characteristics.

CHAPTER 5

ANALYSIS OF EVAPORATOR PERFORMANCE

Lubricant effects on the performance of refrigeration system are mostly due to the effects of lubricants on the evaporator coil performance. Based on the results presented in the previous chapter, the lubricant that enters the refrigeration system induces substantial changes in evaporation heat transfer of HFC-134a refrigerant, thus resulting in a major impact on system performance. Therefore, a more detailed investigation of coil performance was conducted herein with the aim of determining quantitatively the extent to which lubricants alter two-phase heat transfer. The analyses were greatly aided by the results of study by Eckels (1993). This study presents pressure drops and an evaporation heat transfer model for HFC-134a and several POEs in a microfin-type tube. The microfin tube used in the Eckels (1993) study is identical to the tube used in the microfin-tube coil in this project.

In order to perform any viable analysis on the coil performance, the amount of lubricant in the evaporator must be determined. The circulation rate of lubricant through the operating system was measured for miscible POE lubricants on several occasions, and interestingly, it was found to be relatively uniform at around 0.3 percent of refrigerant mass. The results were consistent with variations in measured circulation rates being less than ± 0.05 percent. Thus, it may be speculated that a miscible oil circulation rate is only function of compressor type and system layout, but not a function of lubricant characteristics and operating conditions. It should be noted that the oil circulation rate is different than oil holdup which is the amount of lubricant contained in any component at any given instant of time.

As was described in Section 3.1.2, a direct expansion (DX) coil was utilized for testing in this project. The coil is a cross-flow heat exchanger with air flowing over a finned tube bundle. The refrigerant flows inside a copper tube bundle; it enters a feeder (distributor)

where refrigerant is branched in several independent streams which have multiple passes across the coil's flowing area. The main premise of the analysis presented in this chapter is that coil performance on the air-side is assumed to be the same for different lubricants, and that all observed differences in coil performance are due to changes in refrigerant-side heat transfer. Since were performed with air temperature and air flow rate being independent parameters, the above assumption about constant air-side heat transfer coefficient is validated.

In the next section, heat exchanger theory along with the evaporation heat transfer model is introduced as tools that are used in comparison of evaporation heat transfer for different lubricants.

5.1 Heat Exchanger Theory

The heat exchanger theory presented in this section describes an original procedure to deduce the magnitude of evaporation heat transfer from the performance of the entire coil by using an experimental model. Based on the observed performance of the coil, the overall heat transfer coefficient of the coil can be estimated, which, along with several reasonable assumptions, can eventually lead to information on the magnitude of the average evaporation heat transfer coefficient. All of the mentioned assumptions were validated by the experimental results.

5.1.1 Refrigerant Single-Phase Flow

The heat transfer rate required to evaporate refrigerant in the evaporator is around 95 percent of the total capacity for all conducted tests. The remaining 5 percent of the total capacity represents the heat transfer required to superheat the refrigerant vapor by 7.5 °C. The 7.5 °C superheat is an independent parameter, and it was hold constant for all tests.

In order to estimate the portion of the evaporator in which the single-phase refrigerant exists, the average heat transfer coefficient is determined from the Dittus-Boetler correlation (Incorpera and DeWitt, 1990):

$$Nu = 0.023\,\mathrm{Re}_D^{0.8}\,\mathrm{Pr}^{0.3} \tag{5.1}$$

After substituting dimensionless numbers with their definitions, the average heat transfer coefficient, h, is determined by the refrigerant mass flow rate, $\dot{m}$, and refrigerant properties

$$h = 0.023\frac{k}{D}\left(\frac{4\dot{m}}{\pi D\mu}\right)^{0.8}\left(\frac{c_p\,\mu}{k}\right)^{0.3} \tag{5.2}$$

The transport properties in Equation 5.2 were determined for the saturated refrigerant vapor at a pressure that was measured at the evaporator exit. Once the average heat transfer coefficient was estimated, the length of tubing required for heat transfer in the single-phase region, L_{sp}, can be calculated from Newton's Law of Cooling

$$L_{sp} = \frac{\dot{Q}_{one-phase}}{h\pi D\Delta T_{\mathrm{sup}}} \tag{5.3}$$

As mentioned earlier, the heat transfer rate for a single-phase refrigerant flow, $\dot{Q}_{one-phase}$, was estimated to be around 5 percent of the total evaporator capacity and that value was fairly constant for all data points. The amount of superheat at the compressor inlet, ΔT_{sup}, was kept constant for all tests at 7.5 °C. Since all parameters in Equation 5.3 can be determined, the tube length occupied with the refrigerant vapor was calculated to be around 10 percent of the total tube length, and thus, it can be inferred that only one-tenth of the coil volume was filled with superheated vapor.

At this point, it is reasonable to assume that any lubricant present with the refrigerant vapor in the coil has insignificant effects on the refrigerant heat transfer process in the single-phase flow region. Even if the lubricant affects the single-phase heat transfer, it would have a minimal impact on the magnitude of the coil capacity because only 5 percent of the capacity occurs in the refrigerant single-phase flow region.

5.1.2 Pressure Drop in Evaporator

The coil distributor (feeder) is a source of a considerable pressure drop, and since the pressure was not measured after the distributor, knowledge of its effect was essential in determining the state of refrigerant that was actually entering the evaporator tubes. In order to determine the amount of pressure drop in the evaporator tubes, and subsequently fix the state of refrigerant at the inlet to the evaporator tubing, an experimental correlation developed by Eckels (1993) was used. The correlation is based on extensive HFC-134a testing, performed on several types of refrigeration copper tubing, including the tube type that was built into the microfin-tube coil. In addition, the Eckels pressure drop model include several lubricants with varying concentrations. The model correlates experimental results to pressure drop estimates obtained from a separated flow model (Carey, 1992) for the particular flow conditions.

Separated Flow Model

The separated flow model is based on the assumptions of the constant vapor and liquid-phase velocities, and the existence of equilibrium between the two phases. The total pressure gradient is estimated to be the sum of the frictional and the momentum components:

$$-\frac{dp}{dz} = -\left(\frac{dp}{dz}F\right) + -\left(\frac{dp}{dz}A\right) \tag{5.4}$$

The frictional component of the pressure drop relation is proportional to the friction factor for the vapor phase, f_g, and the appropriate two-phase friction multiplier for the vapor phase, ϕ_g:

$$-\left(\frac{dp}{dz}F\right)=\left(\frac{2f_g G^2 x^2 v_f}{D}\right)\phi_g^2 \tag{5.5}$$

The friction multiplier adopted by Eckels (1993) was developed by Lockhart and Martinelli (1950) who approximated it as the function of their famous two-phase coefficient (X_{tt}):

$$\phi_g=\left(1+2.85X_{tt}^{0.523}\right),\quad where\ X_{tt}=\left(\frac{1-x}{x}\right)^{0.9}\left(\frac{\mu_g}{\mu_f}\right)^{0.1}\left(\frac{v_f}{v_g}\right)^{0.5} \tag{5.6}$$

Lockhart and Martinelli also defined the friction factor, f_g, as a function of the vapor phase Reynolds number, Re_g:

$$f_g=\frac{0.045}{\mathrm{Re}_g^{0.2}},\quad where\quad \mathrm{Re}_g=\frac{GxD}{\mu_g} \tag{5.7}$$

Assuming that the vapor compressibility is negligible, the following expression for the momentum component of the pressure gradient is derived:

$$-\left(\frac{dp}{dz}A\right)=G^2\frac{dx}{dz}\left[\left(\frac{2xv_g}{\alpha}-\frac{2(1-x)v_f}{(1-\alpha)}\right)+\frac{d\alpha}{dx}\left(\frac{(1-x)^2 v_f}{(1-\alpha)^2}-\frac{x^2 v_g}{\alpha^2}\right)\right] \tag{5.8}$$

where the void fraction, α, was determined from a generalized correlation developed by Butterworth (1975) in which the Thom (1964) correlation coefficients were utilized.

$$\alpha = \frac{1}{1+\left(\frac{1-x}{x}\right)\left(\frac{v_f}{v_g}\right)^{0.89}\left(\frac{\mu_f}{\mu_g}\right)^{0.18}} \tag{5.9}$$

The derivative of the quality in respect to the location along the tube length, $\frac{dx}{dz}$, in Equation 5.5 was assumed to be constant since that is a common practice when analyzing the two-phase flow.

Eckels (1993) Model

The pressure drop for the two-phase flow can be estimated by knowing the tube diameter, refrigerant flow characteristics, and refrigerant properties using the separated model, which was laid out in Equations 5.4 through 5.9. Eckels (1993) correlated his experimental measurements for HFC-134a with different lubricants and in different tubes with the separated flow model by using a concept of penalty factor, PF:

$$\Delta P = \Delta P_{corr}\, PF \tag{5.10}$$

Using the actual flow parameters in the separated flow model, the correlation pressure drop (ΔP_{corr}) is estimated, and then the penalty factor is introduced to account for the tubing type and the presence of a lubricant. Eckels curve-fitted penalty factors with the second-degree polynomial of the normalized refrigerant mass flux, $G = G_{act}/(250 kg/(m^2 s))$, and the nominal oil circulation rate, w.

The curve-fitted function for the smooth tubes is given in Equation 5.11 where the curve-fitting coefficients are provided in Table 5.1.

$$PF = a_0 + a_1 w + a_2 w G + a_3 w^2 G + a_4 w G^2 + a_5 w^2 G^2 + a_6 w^2 \qquad (5.11)$$

Table 5.1. Coefficients for Eckels penalty factor function for smooth tubes

	POE-m type 169 SUS D=9.52 mm	POE-m type 169 SUS D=12.7 mm	POE-m type 369 SUS D=9.52 mm	POE-b type 150 SUS D=9.52 mm
a_0	1.0	1.0	1.0	1.0
a_1	43.68	25.97	26.94	-11.33
a_2	24.01	-21.14	-17.23	9.998
a_3	0	0	0	768.0
a_4	0	0	0	0
a_5	143.6	159.5	81.67	-504.8
a_6	-341.8	-107.7	0	0

Eckels (1993) modeled the penalty factor function for the microfin tubes with a nine-member polynomial given in Equation 5.12 and the curve fitted coefficients are provided in Table 5.2.

$$PF = a_0 + a_1 w + a_2 G + a_3 wG + a_4 w^2 G + a_5 wG^2 + a_6 w^2 G^2 + a_7 w^2 + a_8 G^2 \qquad (5.12)$$

Table 5.2. Coefficients for penalty factor function for microfin tubes

	POE-m type 169 SUS D=9.52 mm	POE-m type 169 SUS D=12.7 mm	POE-m type 369 SUS D=9.52 mm	POE-b type 150 SUS D=9.52 mm
a_0	1.3118	0.6028	1.2795	0.4009
a_1	10.08	26.991	-4.073	7.397
a_2	-0.2146	1.5701	-0.1451	1.2048
a_3	0	-22.925	0	0
a_4	0	-2497	0	0
a_5	0	0	76.8	0
a_6	0	2147.6	-177.5	-36.01
a_7	0	462.1	239.7	0
a_8	0	-1.037	0	-0.5471

Using the penalty factor function for appropriate lubricant and tubing type, the pressure drop in the evaporator tubes was estimated. Assuming that the refrigerant enthalpy does not change in both the expansion processes through the metering device (i.e. the expansion valve) and in the distributor (i.e. the feeder), a refrigerant property (i.e. the enthalpy) at the inlet to the evaporator is known. From the known state of the refrigerant at the evaporator outlet and by utilizing the Eckels (1993) pressure drop correlation, the second refrigerant property at the evaporator tube inlet was determined.

The length of a tube occupied with the two-phase flow in the coil was divided into 50 equally spaced grid points. For each grid point, the pressure drop is calculated by Equation 5.11 using the refrigerant properties at the grid point pressure. These coupled equations were solved by an iterative procedure in which a pressure drop was guessed and then calculated by the outlined model. A new estimate on the pressure drop was then used as the next guess and the procedure was iterated until the convergence to a desired precision was achieved.

The obtained state of the refrigerant entering evaporator tubes is then used to analyze evaporator performance and, consequently, provides a method to compare the evaporation heat transfer with different lubricants.

5.1.3 Evaporator Performance

Evaporator cooling capacity is equal to the product of the overall heat transfer coefficient, UA, and the mean temperature difference for the counterflow heat exchanger. In addition, for different types of heat exchangers this product is adjusted with an empirical factor F, called the correction factor:

$$\dot{Q} = UA\ \Delta T_{lm}\ F \tag{5.13}$$

The correction factor, F, is unity for heat exchangers in which phase change occurs (Incorpera and DeWitt, 1990).

Equation 5.13 is derived for heat exchangers in which the fluids' temperatures are a continuous function of the position along the direction of the flow. In the evaporator coil used in this study, there is a discontinuity in temperature distribution, since a portion of the coil has a single-phase refrigerant flow. For example, the temperature distribution in the microfin-tube coil is presented in Figure 5.1 as a function of location along a refrigerant pass through the coil.

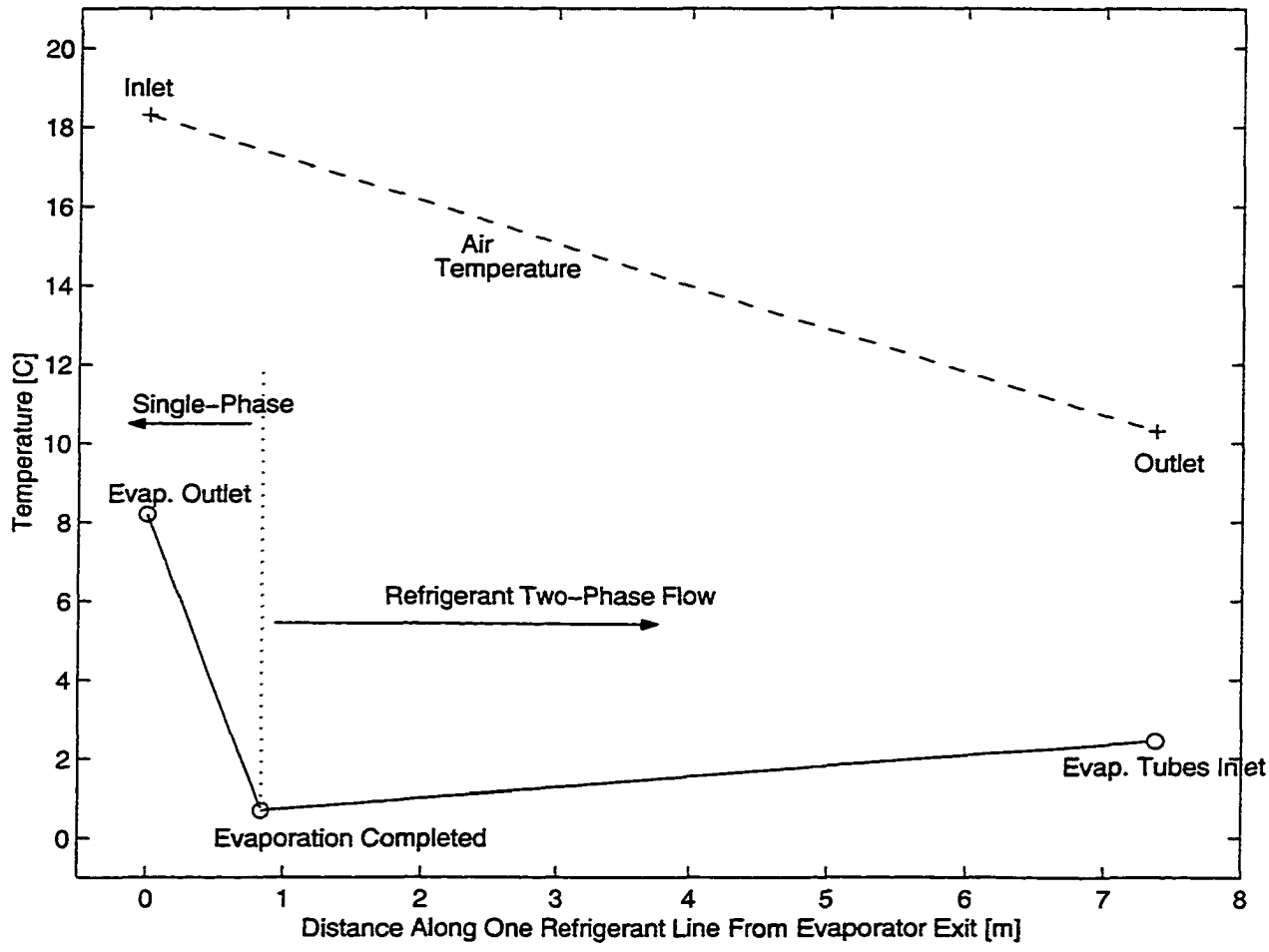

Figure 5.1. Temperature distribution in the evaporator for a sample data point

The length of tubing occupied with refrigerant vapor was estimated by the procedure explained earlier in Section 5.1.1. The location at which evaporation is completed represents the discontinuity in the refrigerant temperature profile. The temperature of the refrigerant

entering the evaporator tubes was estimated by using the pressure drop correlation as elaborated in Section 5.1.2. Temperature dependence with location along the tube is presented as linear for both the single and the two-phase refrigerant flow, even though that may not reflect an actual temperature distribution in the coil. Also, the air inlet and outlet temperatures are indicated in Figure 5.1 and connected with a dotted line that must not be mistaken for the actual air temperature distribution in the coil, which is probably exponential in nature. The actual air temperature distribution along the air flow of the coil was not measured, and in addition, it cannot be presented as a function of the coil dimension in the direction of the refrigerant flow.

In order to proceed with the analysis, the evaporator must be partitioned in the region occupied with the refrigerant vapor and the other region occupied with the two-phase refrigerant. For each part, the appropriate capacities, overall heat transfer coefficients, and temperature differences must be determined. Since evaporator performance is dominated by the characteristics of the two-phase refrigerant flow as it contributes to 95 percent of the capacity, and also, occupies about 90 percent of the evaporator volume, it was decided to simplify the analysis by eliminating the single-phase flow region from the analysis. Therefore, any effects of a lubricant on the evaporator performance will be only manifested in the magnitude of the two-phase heat transfer coefficient.

The logarithmic mean temperature, ΔT_{lm}, is a representative temperature difference in the coil. It is defined in terms of the air and refrigerant inlet and outlet temperatures in the reference to Figure 5.1 and with an assumption that the refrigerant outlet temperature corresponds to the temperature measured at the completion of the evaporation in the coil.

$$\Delta T_{lm} = \frac{\left(T_{air,out} - T_{ref,in}\right) - \left(T_{air,in} - T_{ref,out}\right)}{\ln\left(\frac{T_{air,out} - T_{ref,in}}{T_{air,in} - T_{ref,out}}\right)} \tag{5.14}$$

The reciprocal value of the overall heat transfer coefficient for the evaporator, $1/UA$, which represents the coil overall thermal resistance, is the sum of all thermal resistances:

$$\frac{1}{UA} = \frac{1}{h_{air}\, A_{air}} + \frac{1}{h_{ref}\, A_{ref}} \tag{5.15}$$

The thermal resistance due to the conduction through tube walls was neglected in Equation 5.15 since its magnitude is about 200 times smaller than the refrigerant thermal resistance. On the other hand, the refrigerant thermal resistance was comparable in magnitude to the air-side resistance, however being about tenfold smaller. In addition, it was assumed that there was no fouling on the evaporator surfaces since new evaporators were utilized in the controlled environment. With application of the above assumptions and expressed in terms of thermal resistances, the total coil thermal resistance is:

$$R_{tot} = R_{air} + R_{ref} \tag{5.16}$$

The overall heat transfer coefficient can be empirically determined from the collected data. Referring to Equation 5.13 from information on the evaporator capacity and measured or estimated fluids' temperatures, the UA value was calculated. Furthermore, the UA values can be compared for HFC-134a operating with different lubricants.

The refrigerant thermal resistance can be estimated for HFC-134a operating with the POE_1 lubricant, utilizing the model developed for the heat transfer coefficient by Eckels (1993), which will be presented in detail in Section 5.1.4. Once the refrigerant thermal resistance is determined, the air-side thermal resistance could be estimated from the total thermal resistance defined in Equation 5.16.

In order to compare heat transfer coefficients, the ratio of the overall heat transfer coefficient for the alternative HFC-134/lubricant mixture, U_{alt}, to the overall heat transfer coefficient for the conventional or the reference HFC-134/lubricant mixture can be expressed in terms of air and refrigerant thermal resistances:

$$\frac{UA_{alt}}{UA_{con}} = \frac{R_{ref,con} + R_{air}}{R_{ref,alt} + R_{air}} \tag{5.17}$$

For a given coil it is reasonable to assume that air-side thermal resistance is only a function of air properties and air flow characteristics. Thus, if the air properties and the air flow rate are constant, which is the case for the test conducted in this study, the air-side thermal resistance can be assumed to be constant, and, therefore, the air thermal resistance in Equation 5.17 is assumed to be equal for both conventional and alternative UA values.

If Equation 5.17 is divided by the conventional refrigerant thermal resistance $R_{ref,con}$, and if the ratio of thermal resistances is set to be equal to the ratio of the respective heat transfer coefficients $R_{ref,alt}/R_{ref,alt} = h_{alt}/h_{con}$, the following expression is obtained:

$$\frac{UA_{alt}}{UA_{con}} = \frac{1 + \left[\frac{R_{ref,con}}{R_{air}}\right]}{1 + \frac{h_{con}}{h_{alt}}\left[\frac{R_{ref,con}}{R_{air}}\right]} \tag{5.18}$$

From the above equation, the ratio of the average heat transfer coefficients for the refrigerant flow for the conventional (reference) and the alternative lubricant can be obtained:

$$\frac{h_{con}}{h_{alt}} = \frac{\frac{UA_{alt}}{UA_{con}}\left(1 + \left[\frac{R_{ref,con}}{R_{air}}\right]\right) - 1}{\left[\frac{R_{ref,con}}{R_{air}}\right]} \tag{5.19}$$

By estimating the ratio of the refrigerant heat transfer coefficients, the effects of a lubricant on evaporator performance were evaluated. As already discussed, the bulk of the refrigerant-side heat transfer is controlled by the heat transfer coefficient for the two-phase refrigerant flow. The refrigerant heat transfer ratio in Equation 5.19 will be also estimated by using the Eckels (1993) model, presented in the next section, because it is essential to estimate any effects on the heat transfer coefficient due to different refrigerant/lubricant properties and flow rates.

5.1.4 Evaporation Heat Transfer

In summary, the Eckels (1993) evaporation heat transfer model is an experimentally modified Kandlikar (1987) correlation. The average evaporation heat transfer coefficient in the Kandlikar correlation, h_{cor}, consists of convective and nucleate boiling terms, which are summed and then multiplied with the heat transfer coefficient, estimated for the saturated liquid at the given evaporation temperature:

$$h_{cor} = h_{fo}\left[C_1\, Co^{C_2}\left(25 F_{rl}\right)^{C_5} + C_3\, Bo^{C_4}\, F_{fl}\right], \tag{5.20}$$

where the heat transfer coefficient for liquid only, h_{fo}, is the coefficient determined for the saturated liquid at the same temperature. The correlation used is a slight variation to the Dittus-Boetler correlation given in Equation 5.1:

$$h_{fo} = 0.023\frac{k_f}{D}\left(\frac{4\dot{m}}{\pi D \mu_f}\right)^{0.8}\left(\frac{c_{pf}\,\mu_f}{k_f}\right)^{0.33} \tag{5.21}$$

Non-dimensional numbers that appear in the Kandlikar correlation, Equation 5.20, are

- Convection Number $Co = \left(\frac{1-x}{x}\right)^{0.8}\left(\frac{v_f}{v_g}\right)^{0.5}$
- Boiling Number $Bo = \frac{q''}{G i_{fg}}$
- Froude Number for liquid only $F_{rl} = \frac{G^2 v_f}{g D}$

Coefficients in the Kandlikar correlation are dependent on the mode of the phase change, and they are provided in Table 5.3. The coefficient, C_5, is zero for the vertical tubes, and for the horizontal tubes when the Froude number is greater than 0.04.

Table 5.3. Coefficients for Kandlikar correlation

	Co<0.65 Convective Boiling	Co>0.65 Nucleate Boiling
C_1	1.136	0.6683
C_2	-0.9	-0.2
C_3	667.2	1058
C_4	0.7	0.7
C_5	0.3	0.3

In the Eckels (1993) model, the average heat transfer coefficient from the Kandlikar correlation, h_{corr}, is quantitatively adjusted by the enhancement factor, EF, to take into account the differences between Kandlikar correlation estimates and the actual data:

$$h = h_{corr}\, EF \tag{5.22}$$

The heat transfer coefficient for the Kandlikar correlation was calculated by dividing the length of a refrigerant line in 50 equally-spaced grid points. The refrigerant properties at

each grid point are taken from the pressure distribution through the coil, which was presented in Section 5.1.2.

The enhancement factor, EF, is a curve-fitted second-degree polynomial function of the normalized refrigerant mass flux, $G = G_{act}/(250 kg/(m^2 s))$, and the nominal oil circulation rate, w. The function for the smooth type of tubing is provided in Equation 5.23, while the curve-fitted coefficients for several lubricants are given in Table 5.4

$$EF = a_0 + a_1 w + a_2 w G + a_3 w^2 G + a_4 w G^2 + a_5 w^2 G^2 + a_6 w^2 \quad (5.23)$$

Table 5.4. Coefficients for enhancement factor function for smooth tubes

	POE-m type 169 SUS D=9.52 mm	POE-m type 169 SUS D=12.7 mm	POE-m type 369 SUS D=9.52 mm	POE-b type 150 SUS D=9.52 mm
a_0	1.0	1.0	1.0	1.0
a_1	6.918	9.544	-7.05	3.963
a_2	0	0	0	0
a_3	-572.1	-283.0	-31.11	-411.0
a_4	0	0	0	0
a_5	304.9	0	0	202.1
a_6	0	-76.29	63.55	0

The enhancement factor of the curve-fitted function for the microfin tube is provided in Equation 5.24. Unlike Equation 5.23, the equation has nine coefficients, which are provided for tested lubricants in Table 5.5.

$$EF = a_0 + a_1 w + a_2 G + a_3 wG + a_4 w^2 G + a_5 wG^2 + a_6 w^2 G^2 + a_7 w^2 + a_8 G^2 \quad (5.24)$$

Table 5.5. Coefficients for penalty factor function for microfin tubes

	POE-m type 169 SUS D=9.52 mm	POE-m type 169 SUS D=12.7 mm	POE-m type 369 SUS D=9.52 mm	POE-b type 150 SUS D=9.52 mm
a_0	2.6858	3.1564	2.2933	2.452
a_1	17.27	20.984	-1.228	-25.95
a_2	-1.4266	-3.777	-0.9871	-1.01387
a_3	0	0	0.7632	14.87
a_4	0	870.7	0	0
a_5	3.732	-26.250	0	0
a_6	0	0	0	-50.28
a_7	-508.2	-820.7	0	194.7
a_8	0.3881	2.1115	0.2426	0.2426

5.1.5 Air-side Thermal Resistance

The air-side thermal resistance for a DX coil, which is the evaporator type used in this study, is relatively complex, especially due to the extended surface area for which the average heat transfer coefficient can be only experimentally determined. In general, the air thermal resistance is given as follows:

$$R_{air} = \frac{1}{\eta_o A_{air} h_{air}} \tag{5.25}$$

where the overall heat transfer surface efficiency for the air-side, η_o, is defined in terms of the fin efficiency, η_f, and the ratio of the finned area, A_{fin}, to the total air-side heat transfer area, A_{air}:

$$\eta_o = 1 - \frac{A_{fin}}{A_{air}}(1 - \eta_f) \tag{5.26}$$

The fin efficiency is commonly approximated with the expression for the straight fin, assuming an adiabatic tip and a uniform cross section (Incorpera and DeWitt, 1990).

$$\eta_f = \frac{\tanh(mL)}{mL}; where \quad m = \sqrt{\frac{2h_{air}}{k_{fin}\delta_{fin}}} \tag{5.27}$$

The length, L, that appears in Equation 5.27 is the half-length distance between the tubes. The characteristics of fin , m, is determined from the information on the fin thickness, δ_{fin}, the thermal conductivity of fin material, k_{fin}, and the average air heat transfer coefficient, h_{air}.

The average heat transfer coefficient for the air-side, h_{air}, must be determined experimentally because of the complexity of the surface. Kays and London (1984) developed a procedure in which the dimensionless heat transfer coefficient, Coburn -j factor, is expressed as a function of a Reynolds number for air flow. Kays and London (1984) reported the experimental results for a large variety of compact heat exchangers.

$$j = St\,\mathrm{Pr}^{2/3} = \phi(\mathrm{Re}) \tag{5.28}$$

The Coburn -j factor is a function of the Stanton and the Prandtl numbers, and when definitions of these non-dimensional numbers are substituted in Equation 5.28, the following expression for the average heat transfer coefficient is derived as

$$h_{air} = \frac{G_c c_p}{\sigma}\mathrm{Pr}^{-2/3}\,\phi(\mathrm{Re}), \tag{5.29}$$

where the Reynolds number is defined as function of the air mass flux, G, ratio of the free-to-the-frontal area, σ, the outside tube diameter, D, and the air viscosity

$$\mathrm{Re} = \frac{G\,D}{\sigma\,\mu_{air}} \tag{5.30}$$

In general, the function of Reynolds number, $\phi(\mathrm{Re})$, has to be determined experimentally for a specific coil. However, coil manufacturers consider such experimental relations confidential, therefore, there are a limited number of the correlations available. Gray and Webb (1986) derived a general correlation for a plate heat exchanger with plain fins as they combined data from several sources:

$$j = 0.14\,\mathrm{Re}^{-0.328}\left(\frac{S_t}{S_l}\right)^{-0.502}\left(\frac{s}{D}\right)^{0.0312}, \tag{5.31}$$

where S_t is the tube spacing normal to the air flow, S_l is the tube spacing in the air flow direction, and s is the spacing between the adjacent fins.

5.2 Performance Analysis of Microfin-Tube Coil

The microfin-tube coil is build of the same type of tubing that was used in the Eckels (1993) study from which the model for the two-phase flow pressure drop and the evaporation heat transfer was adopted for the analysis presented herein. The state of the refrigerant at the evaporator inlet was determined by the procedure outlined in Section 5.1.3 or more precisely by Equation 5.10. The penalty factor function, Equation 5.12, was selected for POE-m type, 169 SUS (ISO 32) viscosity grade with tubing diameter of 9.52 mm. The selected lubricant has the same viscosity grade and a similar chemical structure to the POE_1 lubricant. Hence, it was assumed that the heat transfer characteristics of HFC 134a/POE_1 mixture are known, and consequently they were used as the reference for comparison of the evaporation heat transfer coefficients of HFC-134a with other tested lubricants.

5.2.1 Overall Evaporator Performance

The evaporator overall performance is characterized by the overall heat transfer coefficient or the UA-value, which is determined from measured capacity and the fluids' temperatures as defined by Equation 5.13. It was assumed that the refrigerant in the evaporator only exists as two-phase flow as discussed in more detail in Section 5.1.3 with regards to the actual performance of the evaporator, the heat transfer rate of the two-phase refrigerant accounts for about 95 percent of the total capacity for all test points.

Estimated UA-values for the microfin-tube coil are plotted as a function of condenser water and evaporator air temperatures in Figure 5.2. It is clear that the POE_2 lubricant data indicates the largest overall heat transfer coefficients (UA -values) as they vary between 920 and 970 W/°C. Coil performance with POE_1 is better than with MO for all data points, and these results support the hypothesis postulated in Chapter 4 that differences in system performance detected for these lubricants are due to evaporator performance.

It can be inferred as a general trend that the UA-value decreases with an increase in condenser water temperature for all presented data. Interestingly, the UA-value for POE_2 lubricant is a weak function of evaporator air temperature. This is contrary to the behavior that was observed for POE_1 and mineral oil because for these two lubricants the UA-values are substantially decreased as evaporator temperature decreases. However, this trend is not apparent in POE_2 data as the differences in estimated UA-values are small, and, in addition, there are no apparent trends.

It should be emphasized that the uncertainty in estimating the UA value was estimated to be around ±9 W/K which represents around ±1.1 percent of the average UA value for the data set. All of the differences of estimated UA values are larger than the two uncertainties implying significance of the reported results.

In order to directly compare UA-values for the three lubricants, the UA-value estimated for POE_1 lubricant was then taken as the reference value and the UA values of the other two lubricants were compared to the reference UA-value. The UA-value for mineral oil is consistently lower compared to the UA-value for POE_1 lubricant as shown in

Figure 5.3 where the ratio of UA-value for mineral oil to the UA-value for POE_1 lubricant, $\frac{UA_{M\_Oil}}{UA_{POE\_1}}$, is plotted as a function of condenser water and evaporator air temperatures.

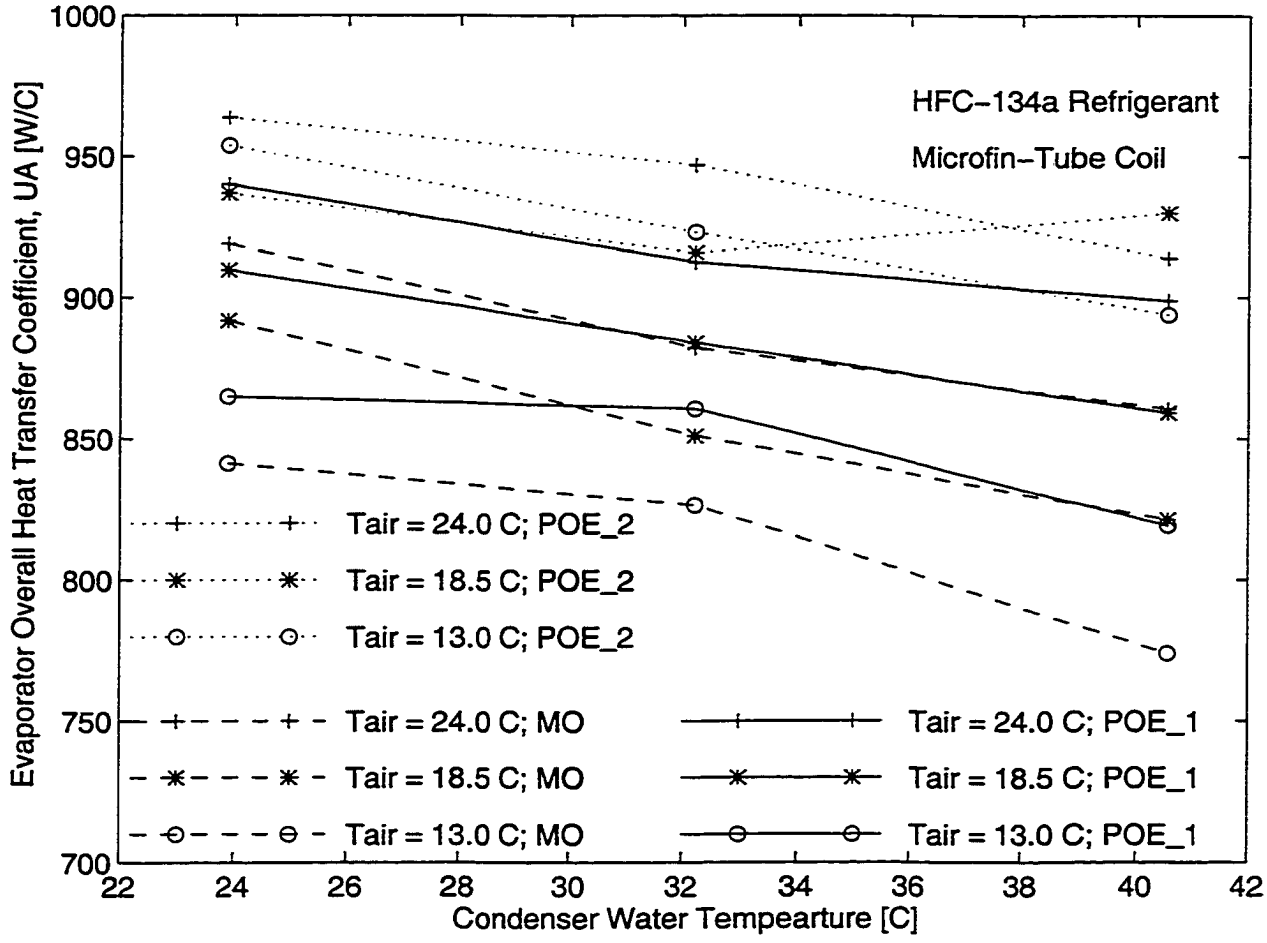

Figure 5.2. Microfin-tube coil UA-values for three lubricants

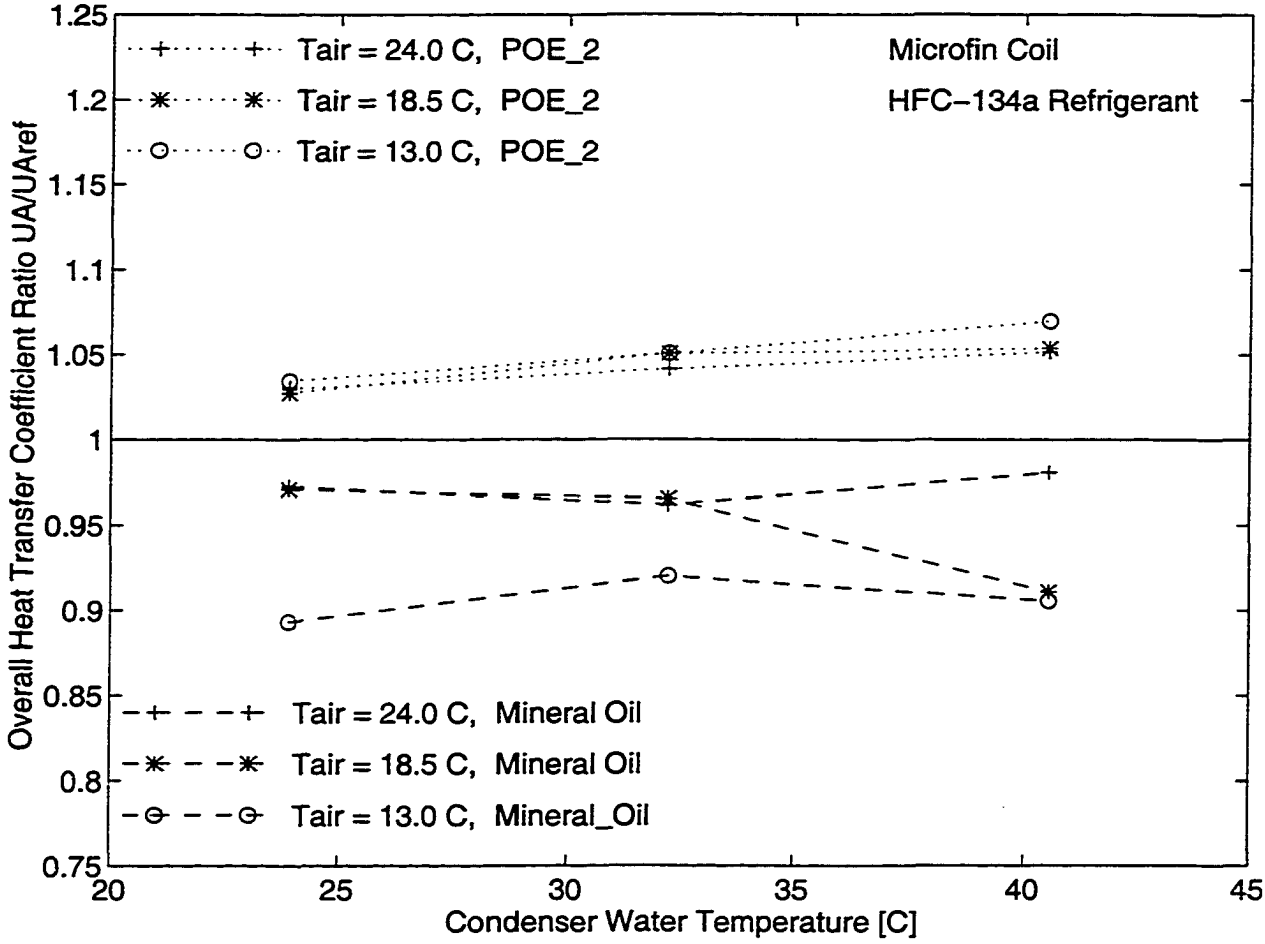

Figure 5.3. Ratio of UA-value to UA-value for reference POE_1 lubricant

The UA-value ratio indicates that the UA-value for the mineral oil is up to 10 percent lower compared to the UA-value for POE_1 lubricant. The largest differences were observed for the lowest air temperature of 13 °C. These differences in UA-values must be caused by differences in the refrigerant/lubricant heat transfer coefficient because the properties and flow characteristics on the air-side were kept constant. Therefore, it can be inferred that the two-phase heat transfer coefficient for HFC-134a with POE_1 is greater than that of HFC-134a and mineral oil. The differences in these heat transfer coefficients are further studied Section 5.2.3.

The ratio of UA-value for the POE_2 lubricant to the UA-value for the POE_1 lubricant, $\frac{UA_{POE\_2}}{UA_{POE\_1}}$, is also shown as a function of condenser water and evaporator air temperatures in Figure 5.3. The UA-values for the POE_2 lubricant are consistently higher than those of POE-1 for up to 5 percent. A general trend can be observed that differences in UA values increase with an increase in condenser water temperature. It can be concluded that the POE_2 lubricant enhances two-phase heat transfer of HFC-134a refrigerant more than the POE_1 lubricant. In addition, it should be emphasized that the oil concentration was 0.3 percent for both lubricants, and, therefore, the amount of lubricant circulating through the evaporator did not cause the observed differences in UA-values.

The uncertainty associated with calculating the UA-value was around ±1.1 percent of the average UA-value in the data set as given in Table 3.3. The observed differences in UA values can be labeled as significant as they are larger than the estimated uncertainty. In conclusion, the POE_2 lubricant enhances HFC-134a evaporation heat transfer coefficient more than the POE_1 lubricant. The immiscible mineral oil has negative effects on coil performance since the lowest evaporation heat transfer rates were recorded. Further analysis on coil performance is presented in the next section.

5.2.2 Evaporation Heat Transfer Coefficient

As mentioned in the introduction to this section, the tube utilized to build the microfin-tube coil has the same nominal diameter of 9.52 mm (3/8 in.), and the same type of surface enhancement as the tube used in the Eckels (1993) study. In addition, the POE_1 lubricant has similar characteristics to the POE-m type lubricant used by Eckels, including the viscosity grade of 169 SUS. Therefore, it is reasonable to assume that the Eckels model for the POE-m type lubricant can be used to estimate the average evaporation heat transfer coefficient for coil operation with HFC-134a/POE_1 mixture. Hence, the HFC-134a/POE_1 data set was used as the reference to which other lubricant data were compared and,

consequently, the characteristics of the evaporation heat transfer process were analyzed in detail.

The average evaporation heat transfer coefficient for HFC-134a/POE_1 was determined from the procedure outlined in Section 5.1.4. Specifically, the average evaporation heat transfer coefficient is calculated from Equation 5.22 in which Eckels (1991) heat transfer enhancement factor is determined by Equation 5.24, where the curve-fitting coefficients are given in the first column of Table 5.5. The entire length of one evaporator refrigerant line was divided into 50 nodal points with known inlet and outlet states. The evaporator inlet state is determined from estimate of a pressure drop through the refrigerant line length. The temperature drop across the evaporator was on average 1.8 °C (3.2 °F) which is equivalent to the pressure drop of around 20 kPa (3 psi). Furthermore, it was assumed that the temperature has a linear distribution through the refrigerant line length since the same distribution was assumed for pressure. The inlet quality was estimated to be between 15 and 25 percent depending on operating conditions. Applying the Eckels' model with the appropriate entering measured oil circulation rate, it was calculated that the average evaporation heat transfer coefficient is between 7 and 8.5 kW/(m^2 K) (1230 to 1500 Btu/(hr. ft^2 °F)).

Furthermore, the average heat transfer coefficient was used to determine the refrigerant thermal resistance, which is defined as the reciprocal of the product of the average heat transfer coefficient and an appropriate heat transfer area. The remainder of the total thermal resistance is attributed to the air-side heat transfer as defined in Equations 5.15 and 5.16. However, it should be emphasized that thermal resistance due to tube wall conduction, fin-to-tube contact resistance, and fouling were neglected, and if they are of significant magnitude, then they can be considered to be included in the air-side thermal resistance. The refrigerant and the air thermal resistances are plotted as functions of condenser water and evaporator air temperatures in Figure 5.4.

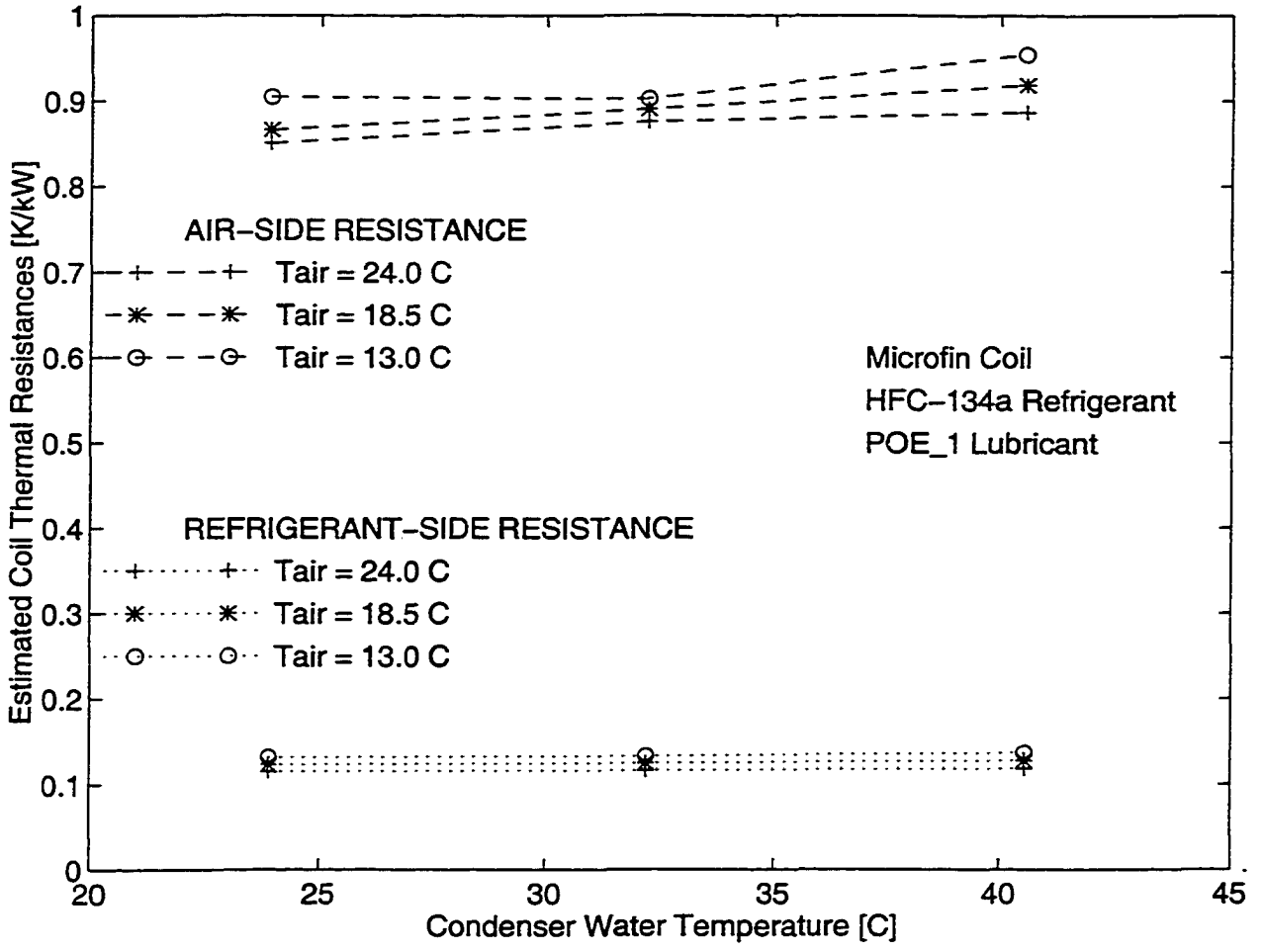

Figure 5.4. Estimated microfin-tube coil thermal resistances for POE_1 data

The air-side thermal resistance is about nine fold larger than the refrigerant-side resistance, which is a reasonable estimate because the air-side thermal resistance represents the bulk of the total coil resistance (Incorpera and DeWitt, 1990). It appears that the air-side thermal resistance increases with an increase in condenser water temperature and a decrease in evaporator air temperature. Therefore, the larger the difference in fluid temperatures in the coil, then the larger are the variations in the air-side thermal resistance. On the other hand, the estimated refrigerant thermal resistance is constant for variations in evaporator and condenser parameters as shown in Figure 5.4.

The estimated air thermal resistance is assumed to be a constant for other lubricant data sets, i.e., mineral oil and POE_2 lubricant, since the air flow properties were kept

identical. If the air thermal resistance is assumed constant, the ratio of evaporation heat transfer coefficients for mineral oil and POE_1 data, $\frac{h_{POE\_1}}{h_{M\_Oil}}$, can be estimated following the procedure described in Section 5.1.3. Specifically, the evaporation heat transfer ratio can be determined from Equation 5.19 which is rearranged for the comparison of POE_1 lubricant and mineral oil data

$$\frac{h_{POE\_1}}{h_{M\_Oil}} = \frac{\frac{UA_{M\_Oil}}{UA_{POE\_1}}\left(1+\left[\frac{R_{ref}}{R_{air}}\right]_{POE\_1}\right)-1}{\left[\frac{R_{ref}}{R_{air}}\right]_{POE\_1}} \tag{5.32}$$

The ratio of UA-values, $\frac{UA_{M\_Oil}}{UA_{POE\_1}}$, is determined from experimental values as presented earlier in Section 5.2.1 in Figure 5.3. The ratio of refrigerant-to-air thermal resistance for the reference POE_1 lubricant, which appears in Equation 5.32, $\left[\frac{R_{ref}}{R_{air}}\right]_{POE\_1}$ is estimated from the Eckels (1991) model as explained earlier and quantitatively shown in Figure 5.4. The refrigerant-to-air thermal resistance ratio is on average around 13 percent for POE_1 data.

The evaporation heat transfer ratio estimated from Equation 5.32. is plotted as a function of air and water temperatures in Figure 5.5. The evaporation heat transfer coefficient for POE_1 is consistently larger than that of mineral oil by about 20 and 60 percent. Also, it appears that the evaporation heat transfer coefficient ratio increases with an increase in condenser water temperature.

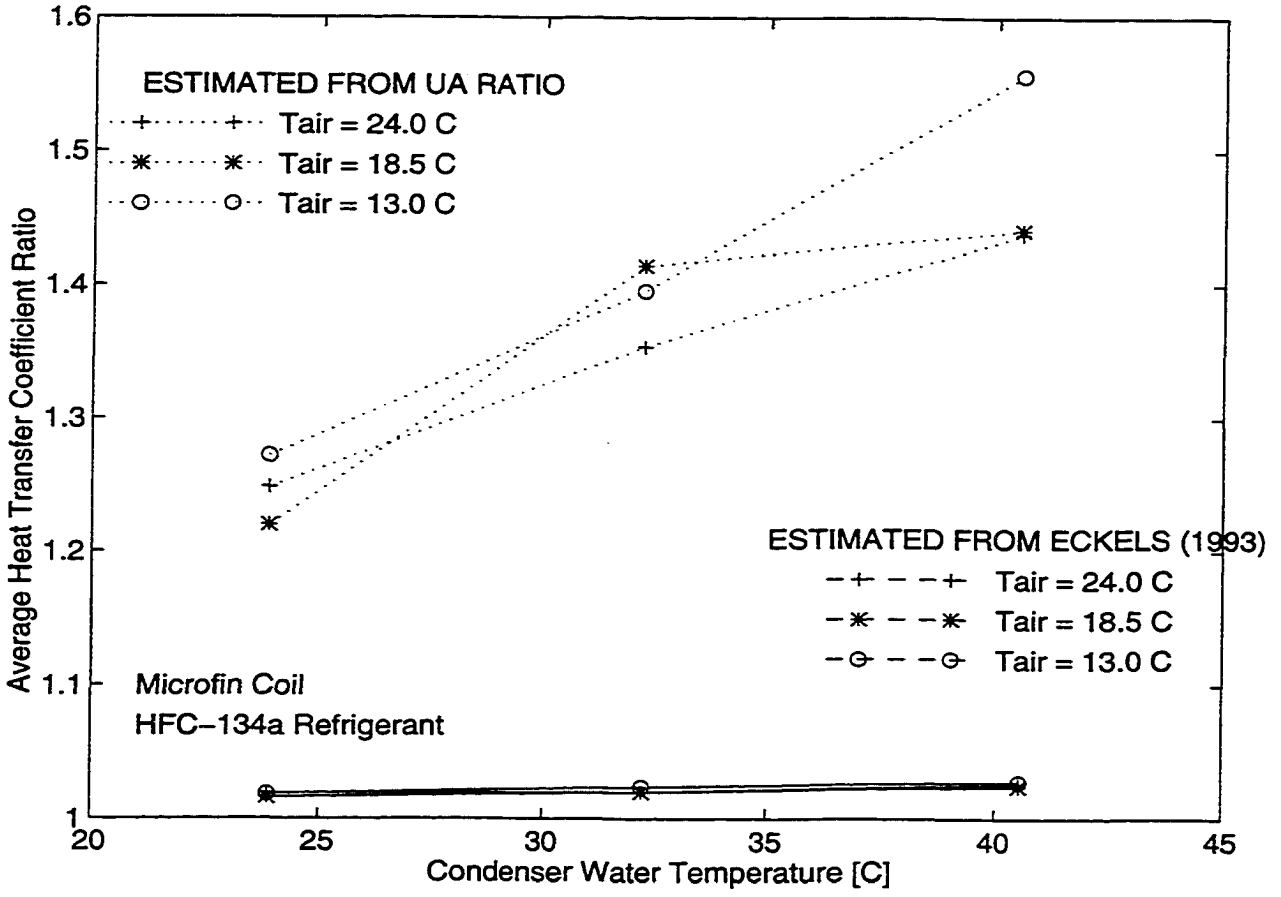

Figure 5.5. Ratio of HFC-134a/POE_1 to HFC-134a/Mineral Oil evaporation heat transfer coefficients

Also, the ratio of heat transfer coefficients was estimated from the Eckels (1993) model in order to account for any differences that may exist in oil circulation, refrigerant mass flux, and refrigerant temperature. The mineral oil data was analyzed in the Eckels model with assumption of having no lubricant present (i.e., pure refrigerant). The heat transfer ratio estimated from the Eckels model is fairly constant and is significantly smaller than the heat transfer coefficient ratio estimated from the UA-value ratio, Equation 5.32, only around 2 percent.

The evaporation heat transfer coefficient for HFC-134a/POE_1 is larger than that of the pure refrigerant due to the presence of lubricant as shown by the Eckels (1993) enhancement factor functions used for these estimates, in other words the heat transfer is enhanced with the presence of lubricant as shown in Figure 5.6.

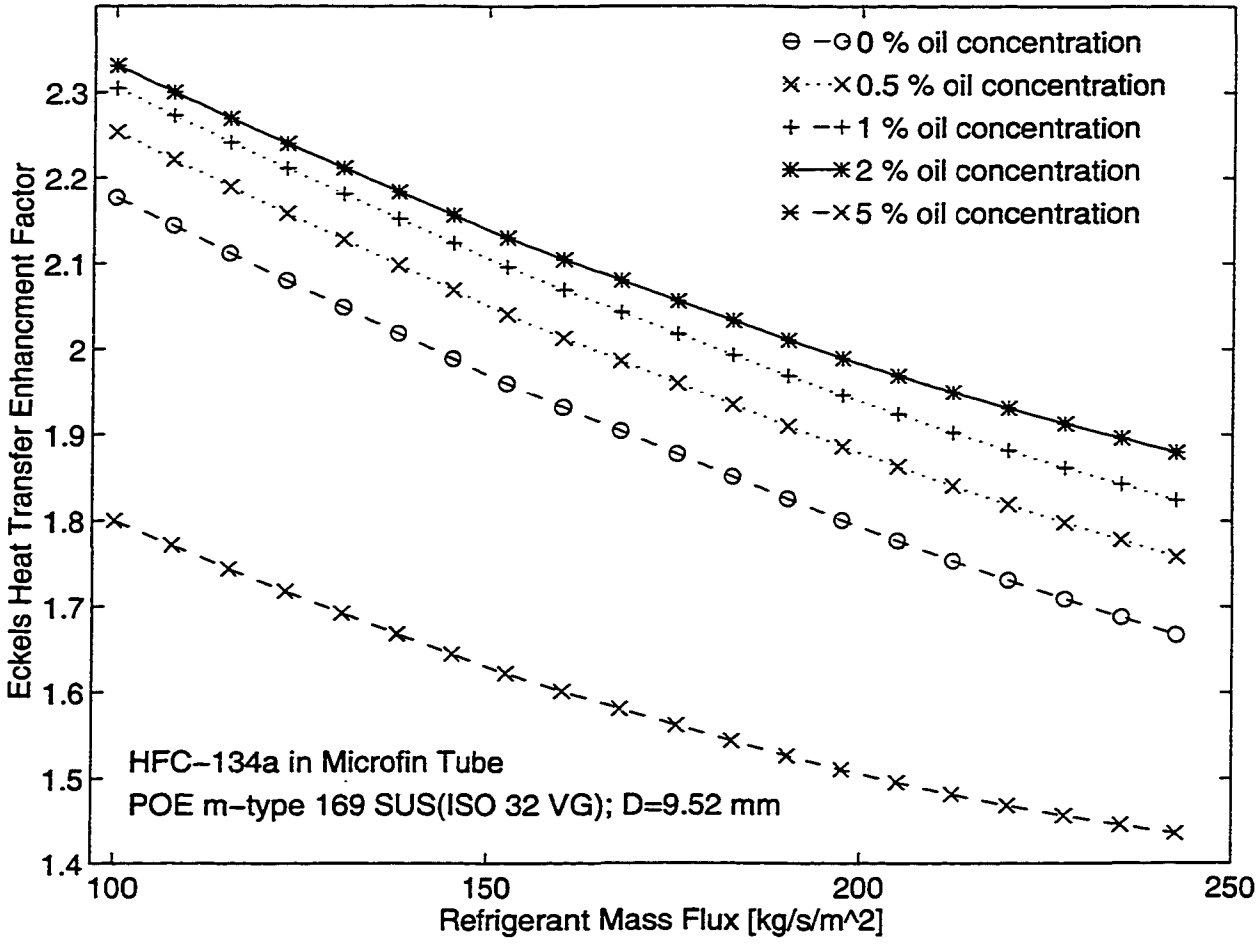

Figure 5.6. Eckels enhancement factor function used for microfin-tube coil

The enhancement factor function used to estimate the refrigerant heat transfer coefficient indicates that for oil concentrations of up to 2 percent, the heat transfer coefficient increases. For larger oil concentration rates, the heat transfer coefficient deteriorates as shown in Figure 5.6. Since the measured oil circulation rate was 0.3 percent of the refrigerant mass for POE_1, the heat transfer coefficient would be greater than the heat transfer coefficient of the pure refrigerant, which was used to simulate the mineral oil data.

So the refrigerant evaporation heat transfer rate is superior for the HFC-134a/POE-1 mixture than for the immiscible HFC-134a/mineral oil mixture. However, the differences in the evaporation heat transfer coefficient estimated from the experimental results are greater than the differences which would exist between pure refrigerant and refrigerant lubricant

mixture with 0.3 percent circulation. Therefore, the immiscible lubricant decreases the evaporation heat transfer of pure refrigerant. One possible explanation could be that the immiscible lubricant coats the interior of tubes and reduces the heat transfer rate by increasing the thermal resistance.

A comparison of evaporation heat transfer coefficients for POE_2 and POE_1 was also conducted, following the same procedure as was used for comparisons of POE_1 and MO presented in Figure 5.5. The POE_1 data was used as the reference because the heat transfer characteristics of POE_1 were assumed known from the Eckels (1993) model.

The ratio of average heat transfer coefficients for POE_2 and POE_1, similar to that defined earlier in Equation 5.32 and given in Equation 5.33, was calculated from known UA values and the ratio of refrigerant and air thermal resistances for POE_1

$$\frac{h_{POE\_2}}{h_{POE\_1}} = \frac{\left[\frac{R_{ref}}{R_{air}}\right]_{POE\_1}}{\frac{UA_{POE\_1}}{UA_{POE\_2}}\left(1+\left[\frac{R_{ref}}{R_{air}}\right]_{POE\_1}\right)-1} \tag{5.33}$$

The estimated evaporation heat transfer for the POE_2 lubricant is between 20 percent and 80 percent higher than that for the POE_1 lubricant. Apparently, as the evaporator temperature decreases, the evaporation heat transfer enhancement for POE_2 over POE_1 increases. It is paramount to recognize that lubricant properties have an impact on the evaporation heat transfer and, as such, affect the overall system performance.

Also as shown in Figure 5.7, the ratio of heat transfer coefficients based on differences in coil operating conditions (i.e., refrigerant properties) between POE_2 and POE_1 estimated using the Eckels (1993) evaporation heat transfer model were only around two percent higher for POE_2. Thus, the estimated differences in evaporation heat transfer deduced from the experimental data were definitely not caused by different operating conditions.

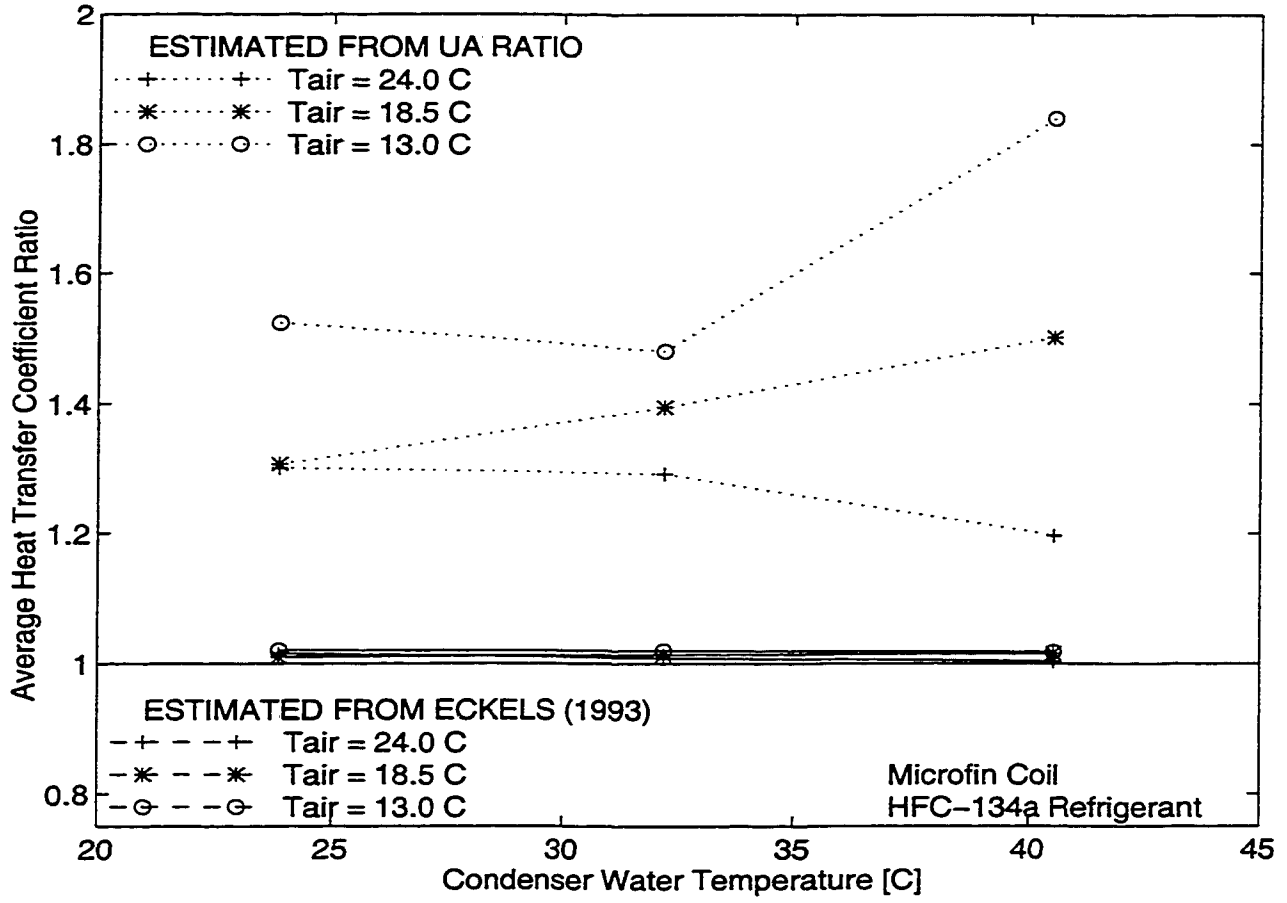

Figure 5.7. Ratio of HFC_134a/POE_2 to HFC-134a/POE_1 evaporation heat transfer coefficients

As stated earlier in Section 4.3, the POE_2 lubricant was selected for study in order to compare the system performance of miscible lubricants with different viscosities, and indeed, the lubricant viscosity appears to have an impact on magnitude of evaporation heat transfer.

These findings support experimental results reported by Eckels (1991), who found that the HFC-134a evaporation heat transfer coefficient is higher with the addition of a lower viscosity miscible lubricant than with a lubricant of similar composition but a higher viscosity. Eckels (1991) experimentally compared heat transfer coefficients in the microfin tube with two lubricants of different viscosity grades. These results are shown in Figure 5.8 in which the heat transfer enhancement factor is plotted as a function of the mass flux for an oil circulation rate of 0.5 percent.

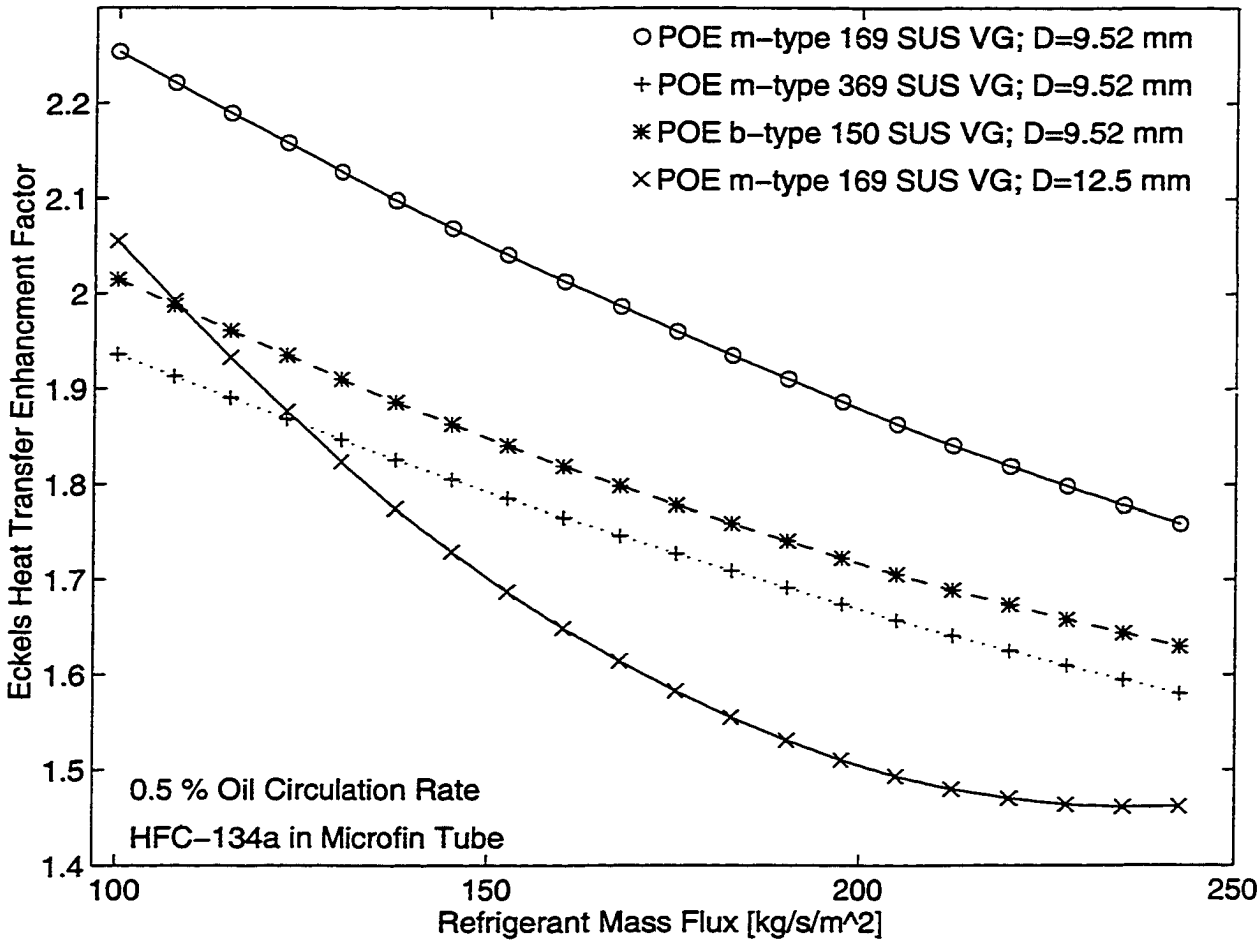

Figure 5.8. Eckels enhancement factor function for oil circulation rate of 0.5 percent

For similar POE m-type lubricants, the lubricant with the lower viscosity grade (i.e. 169 SUS) indicates a higher evaporation heat transfer compared to the lubricant with a higher viscosity grade (369 SUS). These results are presented in terms of enhancement factors to the Kandlikar correlation introduced in Section 5.1.4.

The trends observed in this study are in agreement with Eckels findings. The HFC-134a evaporation heat transfer is more enhanced with a lower viscosity POE_2 than with a higher viscosity POE_1. Furthermore, the evaporation heat transfer differences increase with a decrease in evaporator temperature, which coincides with larger differences in viscosities among the two lubricants. Looking back on Figure 3.4, as the temperature decreases the differences in viscosity between POE_1 and POE_2 increases. Hence, the trend observed in

Figure 5.7 in which the evaporation heat transfer ratio increases with a decrease in evaporator temperature are probably caused by larger differences in lubricant visosisties.

5.3 Performance Analysis of Smooth-Tube Coil

UA values for the smooth-tube coil are plotted in Figure 5.9 for different operating conditions. The coil UA-value is determined from the experimental results using Equation 5.13 and by neglecting the small portion of the coil, less than 5 percent of the heat transfer that has refrigerant in the vapor phase. The procedure used to deduce the UA-value for the smooth-tube coil is the same as that used for the microfin-tube coil presented in Section 5.1.3.

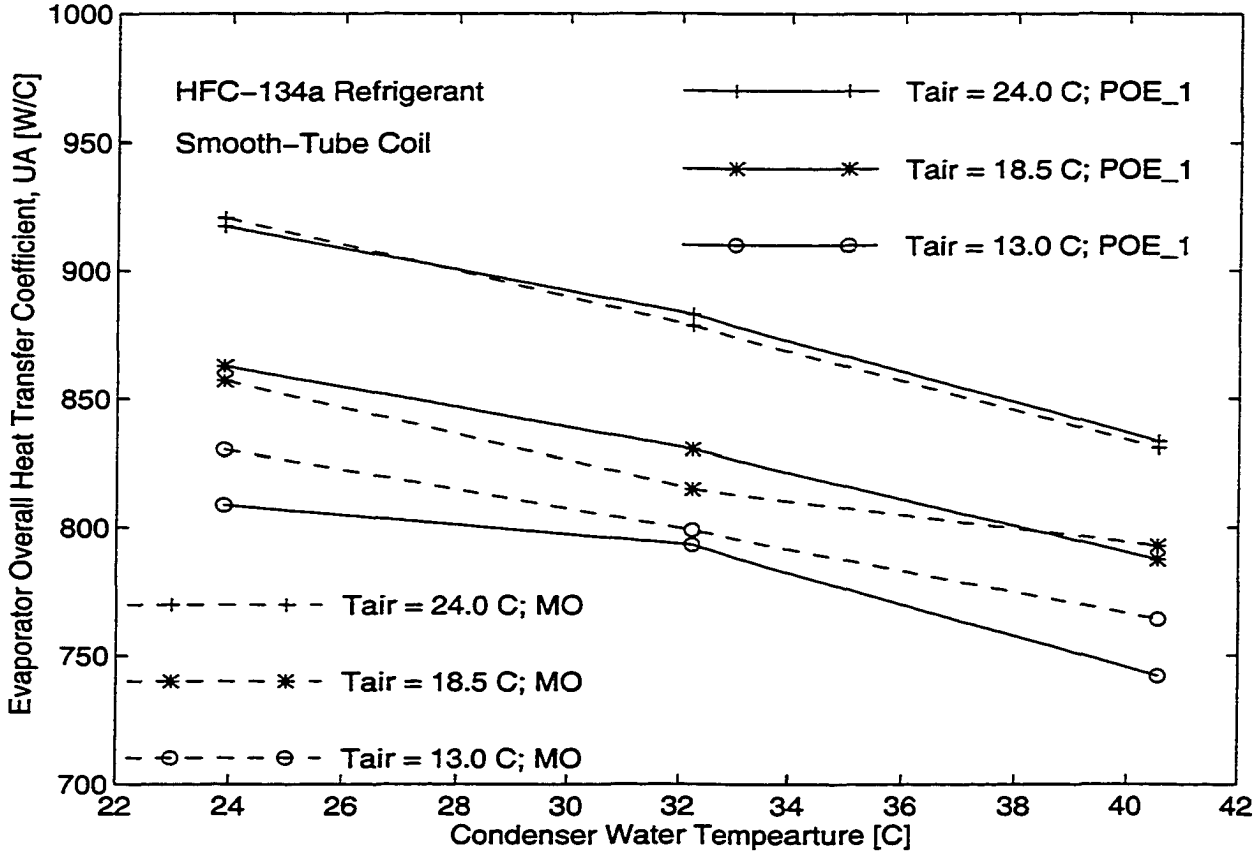

Figure 5.9. Smooth-tube coil UA-values for POE_1 and MO lubricants

Unlike the result observed for the microfin-tube coil, the differences in estimated UA-values for the smooth-tube coil are small being less than the uncertainty in the UA value, which was reported to be around ±9 W/K. Therefore, the differences in UA-values are insignificant and apparently the lubricant type does not affect the performance of the smooth tube coil. The ratio of UA-values, UA_{MO}/UA_{POE_1}, is plotted as a function of operating conditions in Figure 5.10.

In summary, the differences in UA values for the smooth-tube coil are small and when compared to the uncertainty of the UA value of ±1.1 percent, these differences are insignificant. Lubricant does not affect coil performance in smooth tubes.

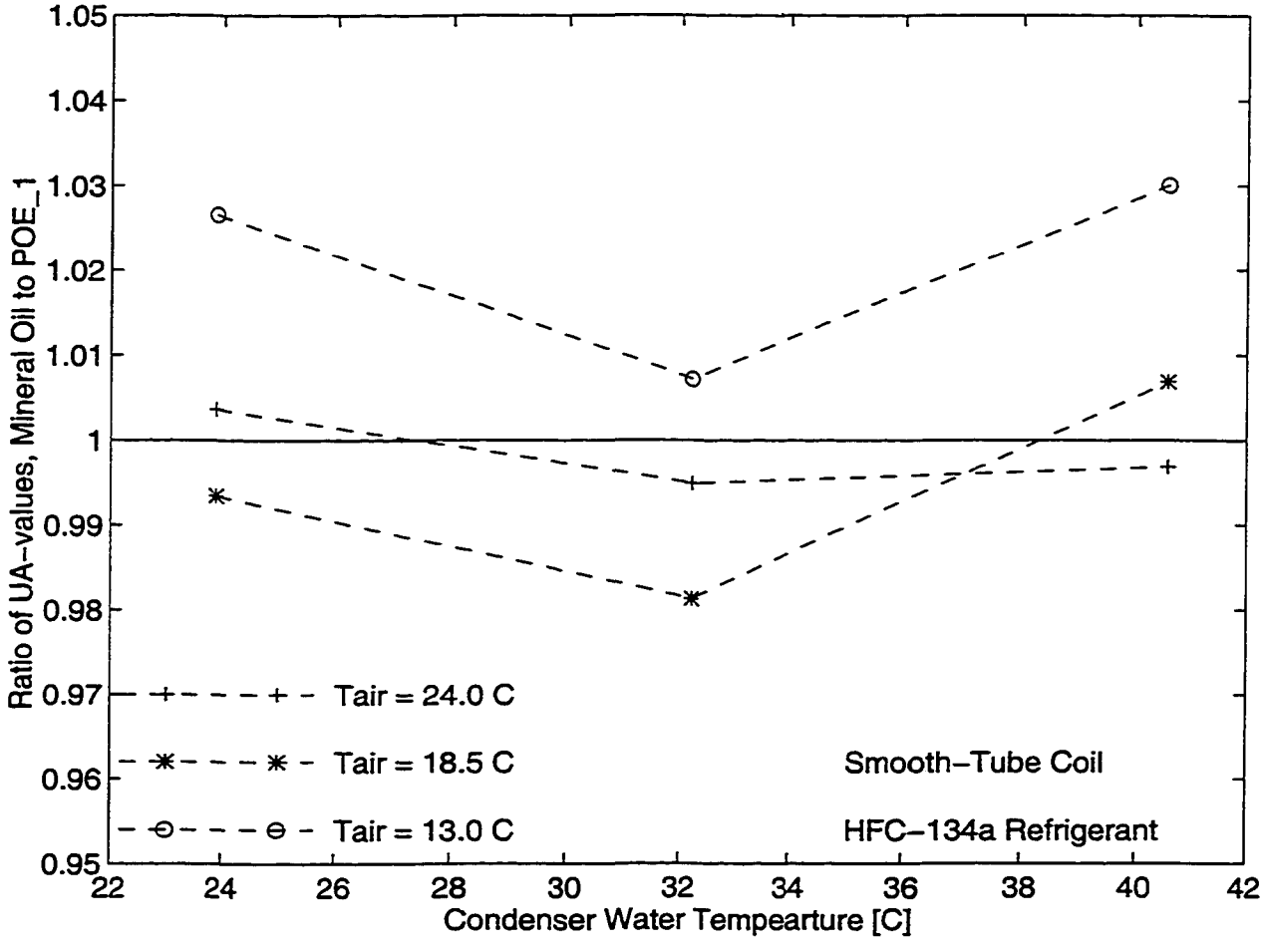

Figure 5.10. Ratio of MO UA-value to POE_1 UA-value in smooth-tube coil

5.4 Conclusions

The coil performance can be greatly affected by the presence of the lubricant since the lubricant alters the evaporation heat transfer as shown for the microfin tube coil. The average evaporation heat transfer ratio was derived from experimental results utilizing an existing model for evaporation heat transfer and pressure drop of HFC-134a with a POE lubricant. This model used a lubricant and tubing which is similar to the POE_1 lubricant and the microfin tubing.

The UA values for the POE_1 lubricant are up to 10 percent higher than that for MO in the microfin tube coil, indicating that evaporation heat transfer is higher with miscible POE_1 than with immiscible MO. Further it was shown that, the estimated evaporation heat transfer coefficient is 20 to 60 percent higher with the POE_1 than with the MO with differences in heat transfer increasing with an increase in condenser water temperature. These results are in agreement with the findings of other authors who found that the evaporation heat transfer improves with the utilization of miscible over immiscible lubricant as was described in Section 2.5.3.

A lower viscosity miscible lubricant POE_2 has around a 5 percent higher UA value than POE_1, which corresponds to a 20 percent to 80 percent higher evaporation heat transfer coefficient compared to the MO. These results support earlier experimental findings regarding miscible lubricants of similar chemical composition, namely that the evaporation heat transfer is higher with a lower viscosity lubricant. In addition, the differences in evaporation heat transfer between POE_2 and POE _1 increase with a decrease in evaporator temperature, which coincides with differences in the lubricant viscosities.

For the smooth tube coil there were no significant differences in the UA-values, and, consequently, lubricant properties appear not to affect coil performance for smooth tubes. Most of the observed differences in the UA-values between POE_1 and MO were small being even less than the estimated uncertainty in determining the UA value of ±9 W/°C.

Finally, a comparison of the performance of two coils with two lubricants, POE_1 and MO, is presented in Figure 5.11. The UA enhancement factor, $UA_{microfin}/UA_{smooth}$, is plotted as a function of the operating temperatures. It is clearly visible that the microfin tube

coil outperforms the smooth-tube coil by up to 10 percent in overall heat transfer coefficient and that the enhancement is more pronounced for the POE_1 miscible lubricant.

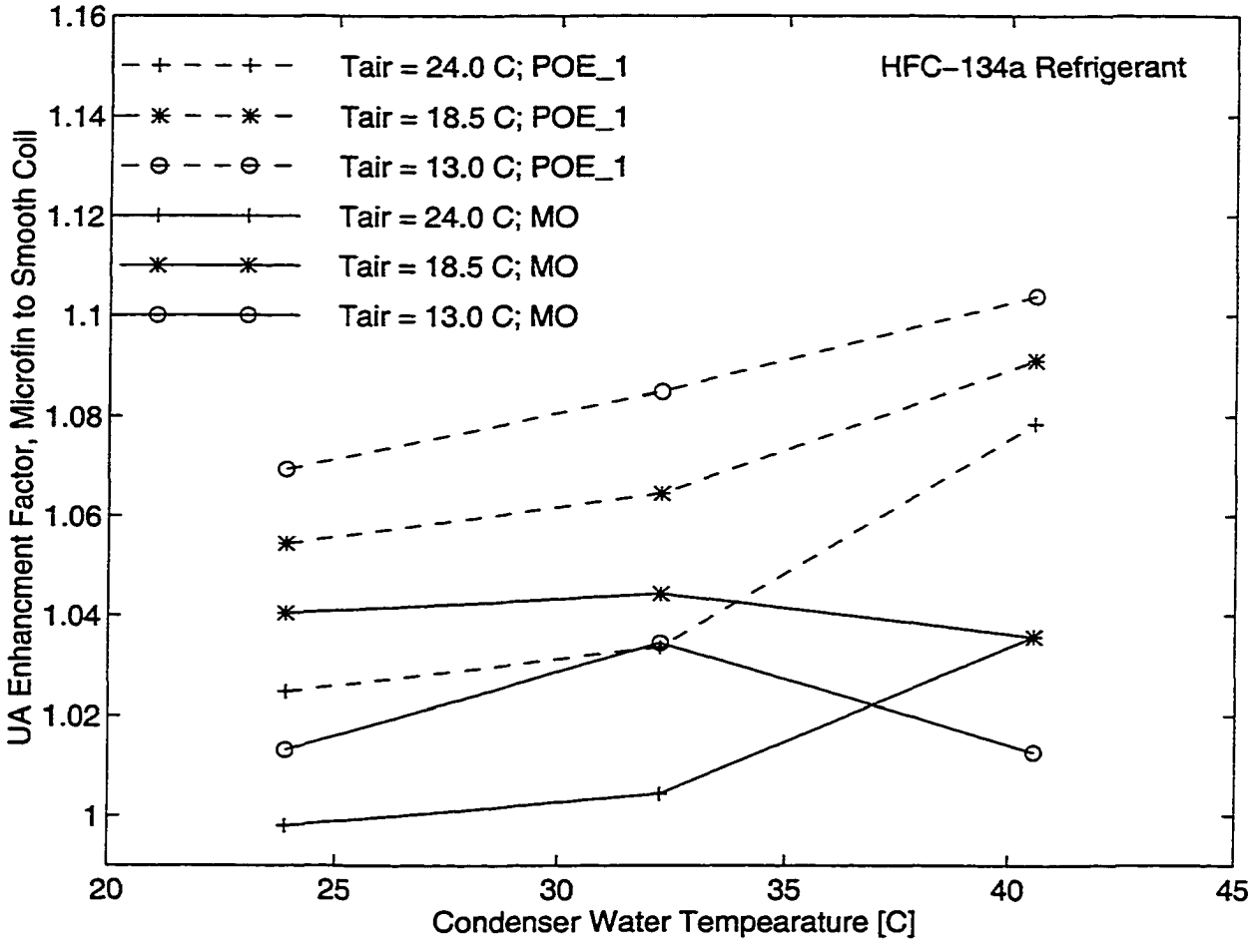

Figure 5.11. UA Enhancement Factor for Microfin-Tube Coil to Smooth-Tube Coil

CHAPTER 6

CONCLUSIONS

Lubricant effects on system performance are measurable, as evident by the differences in system efficiencies due to the lubricant type being larger than the estimated uncertainty. For example, the coefficient of performance could be improved by as much as 5 percent by selecting a miscible over an immiscible lubricant. Therefore, there are potential energy savings associated with the lubricant selection for a particular refrigeration application.

All miscible and partially miscible POE lubricants outperformed an immiscible mineral oil in a system with HFC-134a refrigerant. For all POE lubricants, the COP was higher, implying that refrigerant/lubricant miscibility has positive effects on the system performance. The superiority of the POE lubricant over the mineral oil was especially pronounced for the system with the microfin-tube coil. For all miscible lubricants, the lubricant circulation rate was fairly uniform, around 0.3 percent of the refrigerant mass.

This study found that the major impact of a lubricant on system performance is reflected through the magnitude of evaporation heat transfer rate. The small amount of circulating lubricant can significantly alter the evaporation heat transfer, which leads to changes in the evaporator temperature. For example, if evaporation heat transfer increases, a smaller temperature difference is needed in the evaporator, which for the fixed air temperature leads to a higher evaporator temperature. Additionally, the higher temperature in the evaporator results in a decrease in refrigerant volume, which in turn, allows a larger amount of refrigerant to be circulated through the system, resulting in a higher refrigerant flow rate.

Since the evaporator performance plays such an important role in an analysis of lubricant effects on system performance, the evaporator performance was studied in more detail by utilizing an existing heat transfer model. The evaporation heat transfer coefficient

was shown to be 20 percent to 60 percent higher with the miscible POE lubricant than with the immiscible mineral oil. These results are in agreement with findings of some other authors who have reported that the evaporation heat transfer rate improves with the use of miscible over immiscible lubricants.

For the case of miscible POE lubricants, the lubricant viscosity affects evaporation heat transfer, specifically, the lower viscosity lubricant outperformed a higher viscosity lubricant resulting in an improved system capacity. In addition, the evaporation heat transfer coefficient for the lower viscosity lubricant were 20 percent to 80 percent higher. These results support earlier experimental findings regarding miscible lubricants of similar chemical composition in which the evaporation heat transfer coefficient is higher with a lower viscosity lubricant. In addition, the differences in evaporation heat transfer between the two different POE lubricants increased with a decrease in evaporator temperature, which coincides with differences in lubricant viscosities.

Lubricant partial miscibility in an evaporator resulted in a reduced performance compared to a fully miscible lubricant. For example, even though the partially miscible lubricant was considered to be a lower viscosity lubricant, its performance was only comparable to the higher viscosity lubricant.

In contrast to the evaporator performance, the effects of lubricant type on compressor efficiencies were not substantial, as evident by the observed differences in both the isentropic and the volumetric efficiencies between tested lubricants being rarely larger than the respective uncertainties.

The majority of observed differences in compressor power consumption were accounted for by variations in refrigerant properties and flow rates. Specifically, variations in power consumption were most likely due to the differences in lubricant effective viscosities. Even though miscible and immiscible lubricants have the same viscosity grades, the miscible lubricant was capable of diluting a larger amount of refrigerant, which, in turn, resulted in a lower effective viscosity. The lower effective viscosity is associated with lower power consumption, which is further explained by a lower compressor frictional work. The same behavior was found when comparing two miscible lubricants with different viscosities in that the lower viscosity lubricant needed less compression work to overcome friction.

The effect of refrigerant charge on system performance was studied to ensure that this parameter did not bias the performance data. It was found that the dependence of COP on refrigerant charge is weak in that variation in charge of ±10 percent of the optimum charge resulted in COP reductions which were less than the estimated uncertainty in the COP. Therefore, the optimum charge that was determined for one lubricant was used to test all other lubricants.

It was estimated that for the same actual charge, there are differences in the effective charges, due to the amount of refrigerant dissolved in the lubricant. For the immiscible mineral oil, the effective charge is 4 percent higher than for the miscible POE lubricant. The differences in the effective charge were shown through the magnitude of the condenser pressure. Using this approach, it was possible to compare refrigerant/lubricant mutual solubility characteristics.

The effects of lubricant type on different types of coils, namely the smooth-tube and microfin-tube coils, were also evaluated. It was observed that the effect of lubricant type on performance was more pronounced for the microfin-tube coil. For example, the differences in the overall heat transfer coefficient between miscible and immiscible lubricants for the smooth-tube coil type were smaller than the estimated uncertainty. The microfin-tube coil outperformed the smooth-tube coil by up to 10 percent in terms of the overall heat transfer coefficient. In addition, the performance enhancement (i.e. the heat transfer enhancement for the microfin tube coil compared to the smooth tube coil) is more pronounced for the miscible POE lubricant.

In summary, lubricant selection should not only to be based on system reliability, but also, on the system performance and efficiency as evident by the fact that the use of miscible lubricants and a lower viscosity lubricant resulted in improved performance.

APPENDIX A

UNCERTAINTY ANALYSIS

The uncertainty analysis was performed using propagation-of-error theory. The propagation error is based on the idea that the uncertainty of a dependent variable is proportional to the sum of uncertainty contributions of each independent parameter that constitute the magnitude of the analyzed dependent variable. Thus applied to this study, all derived uncertainties were directly estimated from measured parameters.

To illustrate the procedure of determining uncertainties that were reported in Chapter 3 in Table 3.3, two examples are provided in estimating uncertainty in refrigeration capacity and capacity percent difference.

Evaporator Capacity

Evaporator capacity is defined as the product of refrigerant mass flow rate and enthalpy change in the evaporator

$$\dot{Q}_{evap} = \dot{m}_{ref}\left(h_{in} - h_{out}\right) \tag{A.1}$$

The uncertainty in evaporator capacity, Equation A.2, is proportional to the root mean square sum of the uncertainty contributions of each independent parameter that defines capacity in Equation A.1

$$\Delta \dot{Q}_{evap} = \sqrt{\left(\frac{\partial \dot{Q}_{evap}}{\partial \dot{m}_{ref}}\right)^2 \left(\Delta \dot{m}_{ref}\right)^2 + \left(\frac{\partial \dot{Q}_{evap}}{\partial h_{in}}\right)^2 \left(\Delta h_{in}\right)^2 + \left(\frac{\partial \dot{Q}_{evap}}{\partial h_{out}}\right)^2 \left(\Delta h_{out}\right)^2} \tag{A.2}$$

Each independent parameter in equation A.1 has uncertainly associated with it, which is marked with Δ. The uncertainty is multiplied with the partial derivative of capacity with respect to the independent parameter in question. When partial derivatives are determined the uncertainty in evaporator capacity expression is given in the following format

$$\Delta \dot{Q}_{evap} = \sqrt{\left(\overline{h}_{in} - \overline{h}_{out}\right)^2 \left(\Delta \dot{m}_{ref}\right)^2 + \left(\dot{m}_{ref}\right)^2 \left(\Delta h_{in}{}^2 + \Delta h_{out}{}^2\right)} \qquad \text{(A.3)}$$

The actual values for parameters in Equation A.3, such as enthalpy and flow rate, are taken as the average values in a data set. Therefore, these parameters have bars above the symbols in Equation A.3. The average values for some operating parameters are provided in Table A.1. In addition the associated uncertainties of these parameters are included.

Table A.1. Average values and uncertainties in some operating parameters

Parameter Name	Symbol	Average Value	Uncertainty
Refrigerant Mass Flow Rate	$\dot{m}_{ref}$	3.7864 kg/min	0.007 kg/min
Enthalpy at Evaporator Inlet	h_{in}	92.98 kJ/kg	0.307 kJ/kg
Temperature at Evaporator Inlet	T_{in}	29.83 °C	0.21 °C
Pressure at Evaporator Inlet	p_{in}	825.22 kPa	1.05 kPa
Enthalpy at Evaporator Outlet	h_{out}	257.89 kJ/kg	0.191 kJ/kg
Temperature at Evaporator Outlet	T_{out}	9.44 °C	0.21 °C
Pressure at Evaporator Outlet	p_{out}	315.35 kPa	1.05 kPa
Evaporator Capacity	$\dot{Q}_{evap}$	10.43 kW	
Coefficient of Performance	COP	3.817	
Compressor Power Consumption	$\dot{W}_{comp}$	2.7586 kW	

The refrigerant flow rate is a directly measured value, as the uncertainty in flow rate is directly related to the flow meter as explained in Chapter 3. On the other hand, the uncertainties in the inlet and outlet refrigerant enthalpies were derived from directly mesured pressures and temperatures.

Since the enthalpy is a function of measured temperature and pressure, its uncertinty can be determined by using the propagation-of-error method. An example is given for the inlet enthalpy, as its uncertainty is proportional to sum of uncertainties in measured inlet pressure and temperature.

$$\Delta h_{in} = \sqrt{\left(\frac{\partial h_{in}}{\partial p_{in}}\right)^2 (\Delta p_{in})^2 + \left(\frac{\partial h_{in}}{\partial T_{in}}\right)^2 (\Delta T_{in})^2} \tag{A.4}$$

For example, the partial derivative of enthalpy with respect to temperature is determined numerically with the change in enthalpy for a 1 °C in temperature is change at the constant average inlet pressure.

$$\frac{\partial h_{in}}{\partial T_{in}} \approx \frac{\bar{h}_{in} - h_1}{T_{in} - T_1} = \frac{92.98 - 94.28}{29.83 - 30.83} = 1.448 \frac{kJ / kg}{C} \tag{A.5}$$

Similarly, the partial derivative of inlet enthalpy with respect to the inlet pressure is determined. Both partial derivatives along with known uncertainties for measured pressure and temperature are substituted in Equation A.5 and the uncertainty in inlet enthalpy was determined to be 0.307 kJ/kg. An identical procedure is performed to determine the uncertainty of the outlet enthalpy, which was found to be 0.191 kJ/kg.

Since all parameters required in Equation A.3 have been defined, the actual values are substituted in Equation A.3 utilizing information from Table A.1.

$$= \sqrt{\left((92.98 - 257.9)\frac{kJ}{kg}\right)^2 \left(1.17x10^{-4}\frac{kg}{s}\right)^2 + \left(0.0631\frac{kg}{s}\right)^2 \left(0.307^2 - 0.191^2\right)\frac{kJ^2}{kg^2}}$$

Furthermore, contribution of uncertainty of each parameter is given in equation A.6 from which it can be inferred that uncertainties in the refrigerant flow rate and the inlet enthalpy have substantially larger contribution to the uncertainty in evaporator capacity than the uncertainty in the outlet enthalpy.

$$\Delta \dot{Q}_{evap} = \sqrt{3.702x10^{-4} + 3.756x10^{-4} + 1.449x10^{-4}}\ kW \qquad (A.6)$$

Summing all terms it was estimated that uncertainty in evaporator capacity is 0.03 kW

$$\Delta \dot{Q}_{evap} = 2.984x10^{-2}\ kW \approx 0.03\,kW$$

which when calculated as percentage of the average capacity in data set is around 0.3 percent

$$\frac{\Delta \dot{Q}_{evap}}{\dot{Q}_{evap}} = \frac{0.03}{10.43} \approx 0.3\%$$

APPENDIX B

MISCIBILITY TEST FACILITY

The test facility is designed to measure miscibility for any lubricant/refrigerant mixture over the following operating range.

- Concentration range of 0 % to 100 % refrigerant mass fraction
- Temperature from -40° C to 90° C
- Pressures up to 500 psia

The miscibility tests reported in this study were conducted and reported by Ms. Mee-Hyeen Kang, a research assistant in the Refrigeration Laboratory in the Department of Mechanical Engineering at Iowa State University (ISU). A detailed description of the test facility is presented below.

The ISU Miscibility Test Facility consists of instrumented test cells for charging with known refrigerant/lubricant mixtures, hot and cold temperature baths, and, finally, a high and low temperature control system for controlling the temperature of the bath fluids. The test cells are miniature pressure vessels with glass view ports on the sides. The cells contain known amounts of refrigerant and lubricant. The bath system consists of hot and cold baths, along with a test cell mounting system, which attached to a vibrating agitator for mixing the cell contents. The high and low temperature control system consists of two separate flow loops with a high temperature flow loop connected to the hot bath and a low temperature flow loop connected to the cold bath. The high temperature flow loop contains heaters, pumps, and controllers while the low-temperature flow loop has as its primary component a low-temperature refrigeration system. The Test Facility is designed to measure miscibility for any lubricant/refrigerant mixture over the following operating range.

1. Concentration range of 0 % to 100 % refrigerant mass fraction
2. Temperature from -40° C to 90° C
3. Pressure up to 500 psia

Miscibility tests require a temperature measurement, a concentration measurement, and knowledge of the miscibility condition obtained from viewing the test cell contents through the glass ports.

Description of Test Cell and Bath Assembly

The major components of the Miscibility Test Facility are the test cells containing the lubricant/refrigerant mixture, the high and low temperature bath assemblies, and the temperature/pressure instrumentation. These major components are described below. The description of the high and low temperature control system, which is connected to the hot bath and the cold bath respectively, is presented separately in another section.

Test Cells

The test cells are of a double-port seal-cap type liquid indicator, which consists of a 31.75 mm (1.25 inch) pipe cross with sight windows screwed into opposing ports. A valve for charging the refrigerant into the cell is screwed into one of the two remaining ports. A 3 1/2 inch copper tube is screwed into the other port, and attached to a pressure transducer for measuring pressure inside of the cell during testing.

The overall volume of each test cell may vary slightly, and, as such, they are calibrated. However, the cells are expected to have volumes around 56.5 ml. When charging test cells, each cell is filled with a mixture of refrigerant/lubricant so that the vapor space is less than 15 % of the total volume. In addition, since temperature and pressure data are available, changes in the liquid concentration due to the vapor space can be calculated in order to determine the effect of the vapor space.

Hot and Cold Bath Assembly

Two constant temperature baths are used for maintaining the test cells and contents at a uniform temperature during testing. The hot bath is used to maintain temperatures from 20° C to 90° C, while the cold bath is used to maintain temperatures in the range of - 40° C to 20°C. The test cells mounted in a holder are submersed in one of the two 20 x 12 x 12 inch

glass baths (which hold 10 gallon fluid). In the case of cells instrumented for pressure, and hence solubility, the pressure transducer extend above the bath fluid level. The glass allows for visibility of the test cells so that one can observe miscibility occurring due to temperature changes during the tests.

The cold bath is filled with a fluid which is composed of 65 % pure ethylene glycol and 35 % water. Pure ethylene glycol is used as the bath fluid since it is transparent, and it does not freeze at lower temperatures. The cold bath is a 10 gallon glass container and it is insulated on all sides to maintain a uniform steady temperature. The insulation on the cold bath consists of a double-pane plexiglas window mounted on the front of the glass container and 2 inches of styrofoam on the other sides. A nitrogen purge through plastic tubing is connected to the space between the windows to prevent frosting.

The hot bath is filled with a fluid which is composed of water and a liquid rust protector. The minimum temperature in the hot bath depends on the lowest temperature in the building water supply. The hot bath, which is a glass container just like the cold bath, will also be insulated on all sides. Specifically, a single-pane plexiglas window is mounted with a half-inch air space in front, and 2 inches of styrofoam is mounted on the remaining sides.

A plexiglas mounting system which holds the test cells in place will be constructed. As mentioned earlier an eight cell mounting system for the miscibility tests. Also, each bath has a vibration/agitator system consisting of a cam, belt, gear, and a variable speed motor for the purpose of keeping the contents of the cells mixed.

Sensors and Instrumentation

Two resistance temperature detectors (RTD) measure the precise temperature of each bath. These RTDs are made of platinum and they are connected to a current transmitter, a signal conditioner, and power supply. The current transmitters (signal conditioners) are used with the RTDs to linearize the response, providing a 4 mA to 20 mA signal that is linear over the temperature range - 51°C to 149°C. This signal produces 1 to 5 volts output when measured across a 250 ohm load resister. The data acquisition equipment then monitors this voltage output. The calibration of output voltage vs. temperature shows that all RTDs should have a linear response. These temperature measurements have an uncertainty of ±0.1°C.

For miscibility testing, the required data is refrigerant/lubricant concentrations, temperatures, and an observation of phase separation (taken visually through glass ports on the sides of the test cells). The measurements of refrigerant and lubricant concentration are made when the test cells are charged. The glass ports for observing phase separation and, hence, miscibility conditions were described previously.

Measuring the temperature of the cells requires some additional explanations. Specifically, the temperatures of the test cells are measured by the use of a reference cell in each bath. The reference cell is filled with 100 % pure lubricant to provide a " worst case " heat transfer scenario, and it is assembled with an internal thermocouple to determine equilibrium (steady state) temperature conditions. The temperature difference between this internal RTD and another RTD mounted in the bath fluid indicates when thermal equilibrium between the inside of cell and the bath has been obtained. Depending on the magnitude of the temperature change, thermal equilibrium conditions can usually be obtained in about one-half hour.

A computerized data acquisition system, which consists of a personal computer, a switching unit, and a voltmeter constantly monitor the temperature and pressure. This data acquisition system provides a sufficient number of channels to monitor and record all signals generated by the installed sensors. The sensors to be read include the pressure transducers and the platinum RTDs with signal conditioners. All of these sensors can be monitored using the data acquisition equipment found in a typical laboratory.

Description of the Temperature Control System

A diagram of the low temperature control system connected to the cold bath is shown in Figure A.1. The bath fluid is cooled by a heat exchanger connected to a low temperature refrigeration system. Appropriate settings of the temperature controller, the bypass valve, and the compressor controls are used to obtain a specific temperature for the bath. Since the bath temperature is dependent upon the amount of fluid flow through the heat exchanger, the fluid flow is controlled by using a flowmeter and a bypass valve. To obtain desired

temperatures, both the amount of flow through the heat exchanger and the compressor are controlled. After maintaining a steady bath temperature, a final adjustment is made by the temperature controller which regulates a 1,000 watt heater

A diagram of the high temperature control system connected to the hot bath is shown in Figure A.2. The bath water is heated by using a 1,000 and a 2,000 watt heaters along with temperature controller. The high temperature of 90° C requires the use of both heaters. Once approach for testing is that, water is first heated and then a heat exchanger is used to reduce the temperature of the hot-bath water as needed. The flow through the heat exchanger is controlled by using two adjusting valves.

Experimental Procedures

Experimental procedures were developed for accurate and convenient measurement of the miscibility of a lubricant/refrigerant mixture. A typical operating procedure for taking data over a range of compositions involves the cleaning and assembly of the test cells, evacuating the test cells, injecting known amounts of refrigerant and lubricant, setting the desired temperature of the bath, obtaining steady-state and equilibrium conditions, and taking data.

An overview of the major steps required to perform miscibility tests are follows:

- Prior to each test, the test cells are rinsed thoroughly using a solvent which removes any lubricant from prior tests remaining in the cells and pressure transducers
- The front and back windows of the cell along with the seals are cleaned and replaced if necessary
- After cleaning, the back window and the pressure transducer are tightly assembled
- A predetermined amount of lubricant is injected using a glass syringe through the front window space
- After replacing and tightening the front window, the assembled test cells are placed upside-down on a stand for evacuation

- A vacuum pump is hooked up to the valve and a vacuum removes any dissolved moisture or air from the lubricant inside the cell
- If the cells do not hold a vacuum or set pressure, fittings are tightened
- Refrigerant is injected into each cell from a refrigerant canister using a manifold which allows for evacuation of the connecting lines
- Before and after injection of the lubricant and the refrigerant, each cell is weighed on a electronic balance to calculate the concentration of the liquid inside of the cell
- The test cells are mounted in the plexiglas holder and then the holder is placed in one of the two baths to be heated or cooled to a desired temperature
- The bath temperature are brought to steady state and thermal equilibrium conditions
- When the following three conditions are met, steady state and thermal equilibrium conditions are assumed to be obtained:

1. **The bath temperature is within the ± 2.0°C of the set point temperature**
2. The temperature difference between the dead cell and the bath is within ± 0.8°C

- The miscibility data is taken and recorded for the refrigerant/lubricant mixture in each cell by careful visual inspection.

APPENDIX C

PERFORMANCE PARAMETERS DATA

The performance data is presented in the following tables.

Table C1. Coefficient of Performance COP Data

Evaporator Air Temperat. [°C]	Condenser Water Temperat. [°C]	Microfin-Tube Coil				Smooth-tube Coil	
		MO	POE_1	POE_2	POE_3	MO	POE_1
	24.0	3.74	3.84	3.84	3.82	3.79	3.80
13.0	32.3	3.21	3.26	3.34	3.27	3.24	3.24
	40.6	2.71	2.76	2.81	2.77	2.77	2.77
18.5	24.0	4.08	4.24	4.24	4.22	4.14	4.16
	32.3	3.49	3.56	3.61	3.61	3.51	3.58
	40.6	2.96	3.02	3.04	3.02	2.98	2.97
24.0	24.0	4.44	4.65	4.65	4.60	4.51	4.60
	32.3	3.78	3.92	3.91	3.85	3.83	3.89
	40.6	3.27	3.33	3.27	3.23	3.27	3.30

Table C.2. COP Percent Difference Data

Evaporator Air Temperat. [°C]	Condenser Water Temperat. [°C]	Microfin-tube Coil †				Smooth-tube Coil ‡	
		MO	POE_1	POE_2	POE_3	MO	POE_1
	24.0	0	2.58	5.19	4.83	0	0.44
13.0	32.3	0	1.58	4.11	1.79	0	-0.09
	40.6	0	1.83	3.64	2.11	0	0.18
18.5	24.0	0	3.79	3.83	3.43	0	0.57
	32.3	0	2.10	3.49	3.38	0	1.91
	40.6	0	1.98	2.88	1.98	0	-0.41
24.0	24.0	0	4.74	4.68	3.49	0	1.96
	32.3	0	3.93	3.55	2.04	0	1.44
	40.6	0	1.80	0.09	-1.24	0	1.10

† Percent difference calculation used Microfin-tube coil data
‡ Percent difference calculation used Smooth-tube coil data

$$COP_{dif} = \frac{COP_{POE} - COP_{MO}}{COP_{MO}} 100$$

Table C.3. Refrigeration Capacity data in kW

Evaporator Air Temperat. [°C]	Condenser Water Temperat. [°C]	Microfin-Tube Coil				Smooth-tube Coil	
		MO	POE_1	POE_2	POE_3	MO	POE_1
13.0	24.0	9.42	9.46	9.75	9.72	9.45	9.24
	32.3	8.68	8.77	9.00	8.79	8.75	8.59
	40.6	7.85	7.97	8.20	8.00	7.97	7.86
18.5	24.0	10.85	10.85	11.02	10.96	10.78	10.70
	32.3	10.05	10.04	10.27	10.35	9.95	9.99
	40.6	9.16	9.29	9.47	9.36	9.21	9.03
24.0	24.0	12.45	12.48	12.72	12.51	12.54	12.35
	32.3	11.60	11.64	11.82	11.51	11.64	11.53
	40.6	10.63	10.78	10.82	10.65	10.61	10.59

Table C.4. Capacity Percent Difference Data

Evaporator Air Temperat. [°C]	Condenser Water Temperat. [°C]	Microfin-tube Coil †				Smooth-tube Coil ‡	
		MO	POE_1	POE_2	POE_3	MO	POE_1
13.0	24.0	0	0.50	3.57	3.17	0	2.28
	32.3	0	1.04	3.60	1.27	0	-1.89
	40.6	0	1.58	4.45	2.01	0	-1.44
18.5	24.0	0	-0.06	1.52	1.01	0	-0.74
	32.3	0	-0.05	2.19	2.99	0	0.45
	40.6	0	1.43	3.31	2.18	0	-1.99
24.0	24.0	0	0.19	2.11	0.43	0	-1.55
	32.3	0	0.28	1.82	-0.81	0	-0.93
	40.6	0	1.43	1.79	0.14	0	-0.23

† Percent difference calculation used Microfin-tube coil data
‡ Percent difference calculation used Smooth-tube coil data

$$Capacity_{dif} = \frac{Capacity_{POE} - Capacity_{MO}}{Capacity_{MO}} 100$$

Table C.5. Compressor Power Consumption Data in kW

Evaporator Air Temperat. [°C]	Condenser Water Temperat. [°C]	Microfin-Tube Coil				Smooth-tube Coil	
		MO	POE_1	POE_2	POE_3	MO	POE_1
13.0	24.0	2.51	2.46	2.48	2.48	2.50	2.43
	32.3	2.71	2.69	2.69	2.69	2.70	2.65
	40.6	2.89	2.89	2.92	2.89	2.88	2.84
18.5	24.0	2.66	2.56	2.60	2.59	2.61	2.57
	32.3	2.88	2.82	2.84	2.87	2.83	2.79
	40.6	3.10	3.08	3.11	3.10	3.09	3.04
24.0	24.0	2.80	2.68	2.73	2.72	2.78	2.69
	32.3	3.07	2.97	3.02	2.99	3.04	2.97
	40.6	3.25	3.24	3.30	3.30	3.25	3.21

Table C.6. Power Consumption Percent Difference Data

Evaporator Air Temperat. [°C]	Condenser Water Temperat. [°C]	Microfin-Tube Coil				Smooth-tube Coil	
		MO	POE_1	POE_2	POE_3	MO	POE_1
13.0	24.0	0	-2.03	-1.54	-1.58	0	-2.66
	32.3	0	-0.53	-0.49	-0.51	0	-1.77
	40.6	0	-0.25	0.78	-0.10	0	-1.60
18.5	24.0	0	-3.71	-2.23	-2.63	0	-1.29
	32.3	0	-2.10	-1.25	-0.03	0	-1.43
	40.6	0	-0.55	0.42	0	0	-1.56
24.0	24.0	0	-4.33	-2.45	-2.95	0	-3.42
	32.3	0	-3.51	-1.67	-2.79	0	-2.32
	40.6	0	-0.37	1.68	1.40	0	-1.31

† Percent difference calculation used Microfin-tube coil data
‡ Percent difference calculation used Smooth-tube coil data

$$\text{Power}_{dif} = \frac{\text{Power}_{POE} - \text{Power}_{MO}}{\text{Power}_{MO}} 100$$

Table C.7. Refrigerant Mass Flow Rate Data in kg/min

Evaporator Air Temperat. [°C]	Condenser Water Temperat. [°C]	Microfin-Tube Coil				Smooth-tube Coil	
		MO	POE_1	POE_2	POE_3	MO	POE_1
13.0	24.0	3.31	3.34	3.42	3.41	3.34	3.27
	32.3	3.26	3.31	3.39	3.31	3.31	3.26
	40.6	3.16	3.23	3.31	3.24	3.24	3.20
18.5	24.0	3.78	3.79	3.84	3.82	3.77	3.76
	32.3	3.72	3.75	3.81	3.85	3.72	3.74
	40.6	3.66	3.72	3.79	3.74	3.71	3.65
24.0	24.0	4.28	4.31	4.38	4.32	4.35	4.30
	32.3	4.27	4.30	4.38	4.25	4.30	4.29
	40.6	4.20	4.29	4.29	4.25	4.23	4.22

Table C.8. Refrigerant Flow Rate Percent Difference Data

Evaporator Air Temperat. [°C]	Condenser Water Temperat. [°C]	Microfin-Tube Coil				Smooth-tube Coil	
		MO	POE_1	POE_2	POE_3	MO	POE_1
13.0	24.0	0	0.74	3.38	2.85	0	2.20
	32.3	0	1.53	3.75	1.60	0	-1.57
	40.6	0	2.15	4.53	2.28	0	-1.18
18.5	24.0	0	0.24	1.59	1.05	0	-0.23
	32.3	0	0.84	2.31	3.70	0	0.67
	40.6	0	1.84	3.66	2.19	0	-1.42
24.0	24.0	0	0.64	2.20	0.81	0	-1.03
	32.3	0	0.75	2.51	-0.32	0	-0.32
	40.6	0	2.07	2.22	1.31	0	-0.10

† Percent difference calculation used Microfin-tube coil data
‡ Percent difference calculation used Smooth-tube coil data

$$\dot{m}_{dif} = \frac{\dot{m}_{POE} - \dot{m}_{MO}}{\dot{m}_{MO}} 100$$

Table C.9. Compressor Suction Pressure Data in kPa

Evaporator Air Temperat. [°C]	Condenser Water Temperat. [°C]	Microfin-Tube Coil				Smooth-tube Coil	
		MO	POE_1	POE_2	POE_3	MO	POE_1
13.0	24.0	272.8	276.8	280.8	284.6	274.1	269.8
	32.3	282.7	286.7	288.1	287.5	283.1	280.4
	40.6	289.5	294.5	299.5	297.0	291.6	288.5
18.5	24.0	308.7	310.2	315.1	312.7	305.9	307.8
	32.3	317.2	319.7	324.1	328.7	313.7	316.8
	40.6	326.2	332.6	335.4	330.9	326.6	325.1
24.0	24.0	348.0	350.0	351.2	351.0	349.8	347.9
	32.3	358.0	359.6	368.1	359.0	357.4	358.2
	40.6	368.4	375.9	376.4	373.6	366.5	366.2

Table C.10. Compressor Discharge Pressure Data in kPa

Evaporator Air Temperat. [°C]	Condenser Water Temperat. [°C]	Microfin-Tube Coil				Smooth-tube Coil	
		MO	POE_1	POE_2	POE_3	MO	POE_1
13.0	24.0	774.6	769.1	777.0	769.5	758.7	749.3
	32.3	966.8	959.0	964.0	965.9	950.7	943.9
	40.6	1193	1180	1198	1194	1164	1152
18.5	24.0	789.2	778.8	796.6	789.7	770.2	776.8
	32.3	983.8	969.7	983.8	993.8	960.2	954.7
	40.6	1207	1198	1212	1216	1189	1186
24.0	24.0	813.2	793.6	809.3	810.2	800.1	794.6
	32.3	1010	991.8	1008	1006	987.0	984.9
	40.6	1239	1228	1230	1241	1205	1188

Table C.11. Compressor Volumetric Efficiency Data

Evaporator Air Temperat. [°C]	Condenser Water Temperat. [°C]	Microfin-Tube Coil				Smooth-tube Coil	
		MO	POE_1	POE_2	POE_3	MO	POE_1
13.0	24.0	80.6	80.4	81.4	80.1	81.2	80.8
	32.3	77.1	77.1	78.4	77.0	78.1	77.6
	40.6	73.2	73.4	74.1	72.9	74.3	74.2
18.5	24.0	81.9	81.9	81.6	81.3	82.6	81.9
	32.3	78.9	78.7	79.0	78.8	79.6	79.3
	40.6	75.3	75.3	76.0	75.2	76.3	75.4
24.0	24.0	82.9	83.0	84.1	82.9	83.7	83.2
	32.3	80.5	80.6	80.0	79.9	81.2	80.7
	40.6	76.9	77.1	76.9	76.6	77.8	77.9

Table C.12. Compressor Isentropic Efficiency Data

Evaporator Air Temperat. [°C]	Condenser Water Temperat. [°C]	Microfin-Tube Coil				Smooth-tube Coil	
		MO	POE_1	POE_2	POE_3	MO	POE_1
13.0	24.0	49.4	49.6	50.4	49.4	49.8	49.4
	32.3	53.7	54.0	54.6	53.7	53.7	54.0
	40.6	57.5	57.4	57.7	56.9	57.1	57.2
18.5	24.0	47.7	49.1	48.6	48.4	47.9	48.2
	32.3	53.8	53.4	53.9	53.6	53.3	53.4
	40.6	56.9	57.3	57.2	57.4	57.0	57.0
24.0	24.0	46.6	47.3	47.9	48.0	46.4	46.9
	32.3	52.8	53.5	52.1	52.5	52.3	52.9
	40.6	57.2	57.1	56.0	55.7	56.3	56.9

REFERENCES

ASHRAE Refrigeration Handbook, 1998, American Society for Heating Air-Conditioning Engineers, Inc. Atlanta, Georgia. Ch. 7: 7.1-7.24.

Baustian, J. J., M. B. Pate, and A. E. Bergles. 1988a. Measuring the concentration of flowing oil-refrigerant mixture with a vibrating U-tube densimeter. ASHRAE Transactions 94 (2). 571:587.

Baustian, J. J., M. B. Pate, and A. E. Bergles. 1988b. Measuring the concentration of flowing oil-refrigerant mixture with a bypass viscometer. *ASHRAE Transactions* 94(2). 588-601.

Baustian, J. J., M. B. Pate, and A. E. Bergles. 1988c. Measuring the concentration of flowing oil-refrigerant mixture with an acoustic velocity sensor. *ASHRAE Transactions* 94 (2). 602-615

Bayani, A., J.R. Thome, and D. Favrat. 1995. Online measurement of oil concentrations of R-134a/Oil mixtures with a density flowmeter. *HVAC&R Research* 1(3): 232-241.

Byrne, J. J., M. Shows, and M. W. Abel. 1996. *Investigation of flushing and clean-out methods for refrigeration equipment to ensure system compatibility.* Final report. ARTI MCLR Project Number 660-52502.

Carey, V. P. 1992. *Liquid-vapor phase-change phenomena: An introduction to the thermophysics of vaporization and condensation processes in heat transfer equipment.* Washington. Hemisphere Publishing Corporation.

Carpenter, N. E. 1992. Retrofitting HFC134a into existing CFC12 systems. *International Journal of Refrigeration* 15(6): 332-339

Cavestri, R.C., J. Munk, and M. Menning. 1994. Solubility, viscosity, and density measurments of refrigerant-lubricant mixtures - part I: Branched acid pentaerythritol polyolesters with R-134a. *ASHRAE Transactions* 100(2): 221-230.

Chang, Y. N., and A. Nagashima. 1993. Effect of dissolved lubricating oils on the viscosity of alternative refrigerants. *International journal of thermophysics* 14: 1007.

Collins, M. S. 1994. *An experimental study of the performance of R32/134a, R-32/125/134a, and R134a as drop-in replacements for R-22 in air-conditioning applications.* Master of Science Thesis. Ames: Iowa State University.

Cooper, W. D. 1971. Influence of oil-refrigerant relationship on oil return. *ASHRAE Symposium Bulletin PH71*(2): 6-10

Crown, S.W., H.N. Shapiro, and M.B. Pate. 1992. A comparison study of the thermal performance of R-12 and R-134a. *International Refrigeration Conference - Energy Efficiency and New Refrigerants* (1): 187-196.

Damasceno, G.S., P.A. Domanski, S.P. Rooke, and V.W. Goldsmith. 1991. Refrigerant charge effects on heat pump performance. *ASHRAE Transactions* 97: 304-310.

Eckels, S. J., T. M. Doerr, and M. B. Pate. 1993. *Heat transfer and pressure drop during condensation and evaporation of R-134a/Oil mixtures in smooth and micro-fin tubes.* ASHRAE Report RP-630. Iowa State University.

Eckels, S. J., and M. B. Pate. 1991. An experimental comparison of evaporation and condensation heat transfer coefficient for HFC-134a and CFC-12. *International Journal of Refrigeration* 14: 70-77.

Farzad, M. and D.L O'Neal. 1991. System performance characteristics of an air conditioner over a range of charging conditions. *International Journal of Refrigeration* 14: 321-328

Gray, D. L., and R. L. Webb. 1986. Heat transfer and friction correlations for plate finned-tube heat exchangers having plain fins. *Proceedings of 8th International Heat Transfer Conference* 6: 2745-2750.

Grebner, J.J., and R.R. Crawford. 1993. The effects of lubricant on evaporator capacity for systems using mixtures of R-12/mineral oil and R-134a/synthetic oil. *ASHRAE Transactions* 99(1): 380-386.

Hewitt, N. J. and J. T. McMullan. 1997. The replacement of CFCS in refrigeration equipment by environmentally benign alternatives. *Applied Thermal Engineering* 17: 955-972.

Hou, H., J. C. Holste, B. E. Gammon, and K. N. Marsh. 1992. Experimental densities for compressed R-134a. *International Journal of Refrigeration* 15(6): 365-371.

Hughes, D. W., J. T. McMullan, K. A. Mawhiney, and R. Morgan. 1982. Pressure-enthalpy charts for mixtures of oil and refrigerant R-12. *International Journal of Refrigeration* 5 (4): 201.

Incorpera, F. P., and D. P. DeWitt. 1990. *Fundamentals of heat and mass transfer*, third edition. New York: John Wiley & Sons.

Kandlikar, S. S. 1987. A general correlation for saturated two-phase flow and boiling heat transfer inside horizontal and vertical tubes. *ASME Winter Annual Meeting held in Boston*: 9-19.

Kays, W.M. and A. L. London. 1984. *Compact heat exchangers*. Third edition. New York: McGraw-Hill Book Company

Kruse, H. H. and M. Schroeder. 1985. Fundamentals of lubrication in refrigeration and heat pumps. *International Journal of Refrigeration* 8(11): 347-355.

Linton, J.W., W.K. Snelson, and P.F. Hearty. 1992. Effect of condenser liquid subcooling on system performance for refrigerants CFC-12, HFC-134a, and HFC-152a. *ASHRAE Transactions* 98: 160-166.

Leung, M., C. K. Jotsi, D. Y. Goswami, D. O. Shah, and A. Gregory. 1998. Measurements of absorption rates of HFC single and blended refrigerants in POE oils. *International Journal of Heating, Air-Conditioning and Refrigeration* 4(2): 141-151

Martz, W. L., C. M. Burton, and A. M. Jacobi. 1996a. Vapor-liquid equilibria for R-22, R-134a, R-125, and R-32/125 with a polyol ester lubricant: measurements and departure from ideality. *ASHRAE Transactions* 102(1): 367-374.

Martz, W. L., C. M. Burton, and A. M. Jacobi. 1996b. Local modeling of the thermodynamic properties of refrigerant and oil mixtures. *International Journal of Refrigeration* 19(1): 25-33.

McQuiston, F. C., and J. D. Parker. 1994. *Heating, ventilating and air conditioning analysis and design*, Fourth edition. New York: John Wiley & Sons

Meyer, J. J., and J. M. S. Jabardo. 1994. An ultrasonic device for measuring the oil concentration in flowing liquid refrigerant. *International Journal of Refrigeration* 17(7): 481-486.

Moran, M. J., and H. N. Shapiro. 1996. *Fundamentals of engineering thermodynamics*. Third Edition. New York: John Wiley & Sons

Nagel, M., and K. Bier. 1996. Vapour-liquid equilibrium of ternary mixtures of the refrigerants R125, R143a and R134a. *International Journal of Refrigeration* 19(4): 264-271.

Newell, T.A. 1996. In situ refractomery for concentration measurments in refrigeration systems. *HVAC&R Research* 2(3): 247-256.

Pate, M. B. 1992. *Impact of new non-CFC refrigerants on HVAC & R industry*. Iowa State University.

Pate, M. B. 1988. Design consideration for air-conditioning evaporator and condenser coil. *Two-phase flow heat exchangers: thermal-hydraulic fundamentals and design.* edited by: Kakac, A. , A. E. Bergles, and E. O. Fernandes. NATO ASI Series, Series E: Applied Sciences vol. 143: 849-884.

Popovic, P., and H. N. Shapiro. 1995. A semi empirical method for modeling a reciprocating compressor in refrigeration systems. *ASHRAE Transactions* 101(2): 367-382.

Reyes-Gavilan, J. L., T. G. Flak, T. R. Tritcak, and C. B. Barbour. 1997. Enhanced naphthenic refrigeration oils for household refrigerator systems. *ASHRAE Transactions* 103(1): 95-106.

Reyes-Gavilan, J. L., T. G. Flak, and T. R. Tritcak. 1996. Lubricant return comparison on naphthenic and polyol ester oils in R-134a household refrigeration applications. *ASHRAE Transactions* 102(1): 180-185.

Reyes-Gavilan, J. L. 1993. Performance evaluation of naphthenic and synthetic oils in reciprocating compressors employing HFC-134a as the refrigerant. *ASHRAE Transactions* 99(1): 349-360.

Shimon, R. L., 1997. Private communication.

Short, G. D. 1990. Synthetic lubricants and their refrigeration applications. *Lubrication Engineering* 46(4): 239-247.

Short, G. D., and T. E. Rajewski. 1996. Lubricants for use with HFC based refrigerants – the current state of the art. *Proceeding of the International Conference on Energy and Environment*: 321-330.

Short, G. D., T. E. Rajewski, and J. E. Oberle. 1996. Refrigeration lubricants current practice and future development. *Proceedings of Purdue Refrigeration Conference*: 265-271.

Spauschus, H. O. 1988. HFC-134a as a substitute refrigerant for CFC-12. *International Journal of Refrigeration* 11(11): 389-392.

Sunami, M., K. Takigawa, S. Suda, and U. Sasaki. 1995. New immiscible refrigeration lubricant for HFC's. *ASHRAE Transactions* 101(2): 941-946.

Sundaresan, S. G., J. Judge, W. Chu, and R. Radermacher. 1996. Comparison of R-22/Mineral oil and its HFC alternatives (R407C & R-410A) with mineral oil and POE in a residential heat pump. *Proceedings of Purdue Refrigeration Conference*: 297:302.

Sundaresan, S. G., and R. Radermacher. 1996. Oil return characteristics of refrigerant oils in split heat pump systems. *ASHRAE Journal* 38(8): 57-61.

Suzuki, S., Y. Fujisawa, S. Nakazawa, and M. Matsuoka. 1993. Measuring method of oil circulating ratio using light absorption. *ASHRAE Transactions* 99(1): 413-421.

Swallow, A.P., A.M. Smith, and B. Greig. 1995. Control of refrigerant vapor release from polyol ester/ halocarbon working fluids. *ASHRAE Transactions* 101(2): 929-934.

Thome, J.R. 1995. Comprehensive thermodynamic approach to modeling refrigerant-lubricating oil mixtures. *HVAC&R Research* 1(4): 110-126.

Wu, W., and R. Thomas. 1997. Miscibility and stability of synthetic lubricant with HFC refrigerants. *Journal of Synthetic Lubrication* 14(2): 115-127.

Yanagisawa, T., T. Shimizu, and M. Fukuta. 1991. Foaming characteristics of an oil-refrigerant mixture. *International Journal of Refrigeration* 14: 132-136.

Yoon, H. K., C. H. Poppe, and C. Custano. 1996. Predicting lubricant performance in refrigerant compressors: a comparison between component testing and benchtesters. *ASHRAE Transactions 102(1)*: 86-95.

Zoz, S. Z. 1991. *Measurement of solubility, density, and viscosity of lubricant/refrigerant mixtures for HCFC-22 and HFC-134a.* Master of Science Thesis. Ames: Iowa State University.